Influence of Bridge Deck Concrete Parameters on the Reinforcing Steel Corrosion

Soundar S. G. Balakumaran

Thesis submitted to the faculty of the Virginia Polytechnic Institute and State University in partial fulfillment of the requirements for the degree of

Master of Science

In

Civil Engineering

Richard E. Weyers, Chair

Michael C. Brown

Cristopher D. Moen

William J. Wright

April 28, 2010

Blacksburg, VA

Keywords: Corrosion, Reinforced Concrete, Chloride Diffusion, Macrocell Corrosion, Resistivity

Influence of Bridge Deck Concrete Parameters on the Reinforcing Steel Corrosion

Soundar S. G. Balakumaran

Abstract

Chloride induced corrosion of steel in concrete is one of the major forms of deterioration mechanisms found in reinforced concrete bridges. Early age corrosion damage reduces the lifespan of the bridges, which results in heavy economic losses. Research has been conducted to identify economic solutions for significantly delaying and/or preventing corrosion damage. Considering the amount of steel reinforcement used in bridge decks, the influence of as constructed parameters including clear spacing between top and bottom reinforcement bars, ratio of cathode to anode areas, and presence of stay-in-place forms on corrosion activity needs to be evaluated.

The influence of the as constructed parameters have been studied using different corrosion assessment methods including resistivity, half-cell potential, linear polarization, chloride content, moisture content, and visual inspection. This study included the clear spacing distances between the anode and cathode of 51, 76, and 102 mm (2, 3, and 4-inch), number of cathodes as 1 and 2, and the presence and absence of stay-in-place forms. Data up to 15 months were taken from a previous study by Smolinski and integrated into the current study period of 35 to 45 months. A trend line may be established to illustrate the changes which took place over the missing time period, from approximately 15 to 35 months, since the specimens were maintained in controlled environment.

Analysis of the data showed that there is a significant difference between the spacing values (2, 3, and 4-inch) through all forms of evaluations. Regarding the other parameters, no significant difference was identified. Variations in resistivity with increasing spacing, even when the water-cement ratio was kept at 0.50, maybe the result of the difference in unit consolidation between the clear spacing specimens. Thus, the corrosion mechanism observed in this study may be resistivity-controlled. Also, autopsy showed that corrosion on the top bars was in general agreement with the measured corrosion activity. The bottom bars had no visible corrosion and the chloride had not penetrated to the bottom bars, regardless of the separation distance between the top and bottom bars. For this laboratory study, the measurements showed that macrocell corrosion influence on the total corrosion was insignificant.

ACKNOWLEDMENTS

I am thankful for the guidance and encouragement of Dr. Richard Weyers from the initial to the final stage of my research. I am also grateful to Dr. Weyers for giving me this opportunity to learn. Guidance and support from Dr. Michael Brown, Dr. Cristopher Moen, and Dr. William Wright, who have served on my committee, are much appreciated.

I would like to thank Dr. Andrei Ramniceanu for being my mentor and a support throughout the research. I could not have completed this study without your patient guidance and companionship. I am grateful to Sean Weyers for the hours of assistance provided in the laboratory testing. Appreciation is owed to Dr. David Mokarem for his assistance during the critical times in the laboratory. I am also indebted to Brett farmer and Dennis Huffman for their essential help, when equipments do not work as planned.

Most importantly, I would like to thank my parents Balakumaran and Chandra Balakumaran as well as my sister Uma Swaminathan for their constant love, and moral support throughout my hardships. Without your motivation and much needed affection, I would not have completed the research. I am also grateful to my friends for their support and sense of humor in the times of stress.

TABLE OF CONTENTS

LIST OF TABLES

LIST OF FIGURES

INTRODUCTION

Corrosion is a natural process which involves the oxidizing of metals that are refined from naturally occurring ores. Bridges constructed using steel, whether they are reinforced concrete bridges or steel bridges, suffer corrosion eventually. The collapse of Silver Bridge in 1967 has led to a closer inquiry into the corrosion problem in bridges. The collapse resulted in the founding of the National Bridge Inspection Standards under the Federal-Aid Highway Act of 1968 and the Special Bridge Replacement Program under the Federal-Aid Highway Act of 1970 (Weingroff, R.F. 1996).

Corrosion damage in bridges may result in high expenditures for repair and rehabilitation and may even result in loss of lives in extreme cases. The winter maintenance activities, mainly consisting of using chloride containing deicing salts on road surfaces, increase exposure to chloride which promotes steel corrosion. Corrosion of reinforced concrete bridges is considered to be one of the largest maintenance, repair, and rehabilitation problems. The United States of America uses over 15 million tons of chloride-based deicing salts per year as winter maintenance on highway roads (Salt Institute). The state highway agencies spend about $750 million per year on all the winter maintenance activities, of which about 20% or $150 million is spent for deicing salts (Transportation Research Board 1991).

A large number of research studies have been conducted in the past 40 years on controlling of damage to concrete bridge decks due to chloride induced corrosion. But little information is available on the influence of bridge deck construction parameters that affect the rate of corrosion. This study addresses the effects of clear concrete spacing between the anode and cathode, cathode area in concrete bridge decks, and presence of stay-in-place forms on overall corrosion of the bridge decks. The rate of chloride penetration into concrete will also be evaluated. The study will include the contribution of macrocells and microcells to the total corrosion. An attempt at writing new user-friendly software for calculating corrosion current, polarization resistance, and other interpretations of data obtained from 3LP instrument will be made.

LITERATURE REVIEW

Reinforced Concrete Corrosion

Reinforced concrete is an economic, versatile and very widely used material in construction works throughout the world. Yet, corrosion of the reinforced concrete can be considered one of the major problems faced by civil engineers (Broomfield, J.P. 2007). Corrosion damage can result in heavy economical loss and, in extreme cases, even in loss of lives. There is a need for research studies on significantly delaying and/or preventing corrosion damages. Many structures with an expectant life of 120 years were experiencing heavy corrosion damage as early as 20 years (Berke, N.S. and Hicks, M.C. 1996). Such early age damage results in significant economic losses. General causes for the corrosion of steel in concrete are credited to chlorination and carbonation. The increase in corrosion related damages has resulted in the need to develop and implement economic solutions.

Corrosion Mechanism in Concrete

Alkalinity of concrete forms a passive layer on the surface of the steel, protecting it from corrosion. The breakdown of the passive layer results in active corrosion of reinforced steel. The two main conditions that can break down the passive layer in concrete are carbonation and chloride attack (Broomfield, J.P. 2007).

Corrosion of steel in concrete starts with the breakdown of the passive layer on the steel surface. The chemical reactions are the same for corrosion by carbonation or by chloride attack (Broomfield, J.P. 2007). Beyond initial conditions, the corrosion process involves two separate and coupled chemical reactions that take place at different places on the surface of the steel. These electrochemical reactions are called anodic and cathodic reactions, occurring at the anodic and cathodic areas of steel (Bentur, A., Diamond, S. and Berke, N.S. 1997).

The anodic reaction is an oxidation reaction that occurs at the anode sites. Metallic ions are formed at the anode with the removal of electrons from the metal resulting in the loss of metal occurs at the anode areas. The anodic reaction is represented by the following equation.

$$Fe \rightarrow Fe^{2+} + 2e^{-} \quad \text{(Equation 1)}$$

The electrons flow through the steel towards lower potential areas of the steel surface. The electrons collect on the steel surface and increase the electrical potential of the area (Bentur, A., Diamond, S. and Berke, N.S. 1997). The ferrous ions, formed in the anodic reaction, dissolve in the water at the steel surface and produce an acidic condition.

$$Fe^{2+} + 2H_2O \rightarrow Fe(OH)_2 + 2H^+ \quad \text{(Equation 2)}$$

The electrons lost in the anode flow towards the lower potential area called as cathode and are consumed in the cathodic reaction to maintain the electrical neutrality. The reduction reaction at cathode results in the formation of hydroxyl ions, as shown in Equation 3.

$$2e^- + H_2O + \frac{1}{2}O_2 \rightarrow 2OH^- \quad \text{(Equation 3)}$$

The above reactions at anode and cathode result in an internal current flow from anode to cathode. This current flow lowers the potential of the anode and raises the potential at the cathode. The positively charged ferrous ions, produced in the anodic reaction, dissolve in the concrete pore water and flow towards the cathode. Likewise, the negatively charged hydroxyl ions, produced in the cathodic reaction, flow towards the anode forming a closed loop of ionic current (Bentur, A., Diamond, S. and Berke, N.S. 1997). The presence of pore water and a continuous pore system in the concrete is essential for the ionic current to flow.

The cathode and anode reactions must occur at the same rate. Thus the number of electrons lost at the anode must be equal to the number of electrons consumed at the cathode during the corrosion process (Bentur, A., Diamond, S. and Berke, N.S. 1997).

The above mentioned processes initiate the forming of rust on the steel surface. The formation of rust occurs by several processes which follow the ionic flow and electronic current flow as follows.

$$Fe^{2+} + 2OH^- \rightarrow Fe(OH)_2 \quad \text{(Equation 4)}$$

The ferrous ions, formed by anodic reaction (Equation 4), flow towards the cathode, where they react with hydroxyl ions, formed by cathodic reaction, to form ferrous hydroxide (Equation 5).

$$4Fe(OH)_2 + O_2 + 2H_2O \rightarrow 4Fe(OH)_3 \quad \text{(Equation 5)}$$

The ferrous hydroxide reacts with oxygen and concrete pore water to form hydrated ferric oxide (Equation 6).

$$2Fe(OH)_3 \rightarrow Fe_2O_3H_2O + 2H_2O \quad \text{(Equation 6)}$$

Figure 1 summarizes the corrosion process for steel in concrete.

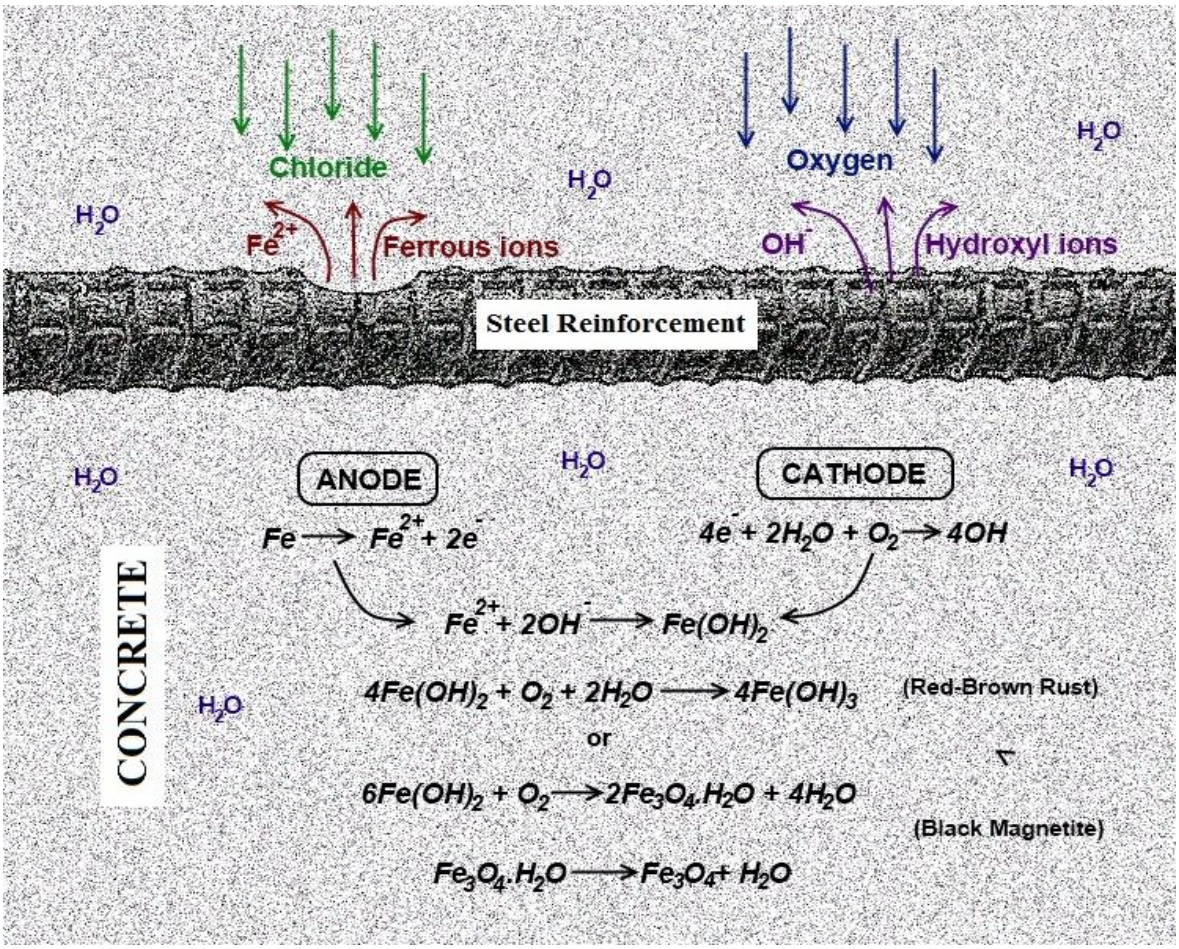

Figure 1 – Electrochemical process of Steel Corrosion in Concrete

The unhydrated ferric hydroxide has a volume twice that of ferrous hydroxide, while the hydrated ferric oxide swells even more to result in a volume increase of six to ten times the ferrous hydroxide (Broomfield, J.P. 2007). Thus the eventual increase in the volume will create an internal pressure great enough to surpass the tensile strength of concrete, which leads to cracking, spalling, and delamination of the concrete cover (Berkeley, K. and Pathmanaban, S. 1990).

Carbonation

Carbonation is a simple process which occurs due to the interaction of atmospheric carbon dioxide gas and the alkaline hydroxides present in the concrete pore water.

Carbon dioxide is a commonly occurring gas, especially near bridge structures because of vehicular exhaust, which can penetrate concrete and dissolve in the pore water to form carbonic acid. The carbonic acid reacts with the alkaline hydroxides in the concrete to form carbonates. Calcium hydroxides present in large amount in concrete pores maintain the pH around 12-13. The intrusion of carbon dioxide and formation of carbonic acid with calcium hydroxides, result in solid carbonates, reduces the pH which results in the steel corrosion (Broomfield, J.P. 2007). The reactions are represented by the following equations.

$$CO_2 + H_2O \rightarrow H_2CO_3 \quad \text{(Equation 7)}$$

$$H_2CO_3 + Ca(OH)_2 \rightarrow CaCO_3 + 2H_2O \quad \text{(Equation 8)}$$

Carbonation will attack the concrete surface and penetrate into the concrete gradually. Steel starts corroding at a pH level at or below 11, while the carbonation reduces the pH from 12-13 to 8. The passive layer formed by the alkalinity of concrete cannot be sustained at lower pH levels, (Revie, R.W. 2000).

The time to carbonation induced corrosion is related to the concrete cover, concrete quality, moisture content, consolidation, and age of concrete (Revie, R.W. 2000). It also depends on the environmental factors such as humidity, temperature, and the carbon dioxide concentration (Bertolini, L. 2004). Carbonation depth is related to the age of concrete as:

$$d = A.t^{0.5} \quad \text{(Equation 9)}$$

Where, d = carbonation depth (mm)

t = time (years)

A = carbonation coefficient (mm/year$^{1/2}$)

Chlorination

Chlorination is a process by which the excess presence of chloride in the concrete damages the passive layer on the reinforcement steel. Unlike carbonation, chlorination does not affect the pH of the concrete pore water. Chloride acts as a catalyst to corrosion without being consumed in the process (Broomfield, J.P. 2007). Chlorides in the pore water react with the passive layer (γ-Fe_2O_3) and break it down for the corrosion to proceed (Bertolini, L. 2004).

Chlorides can be cast into the concrete by deliberate addition of chloride-based accelerators, by use of sea water in the mix, or by use of chloride-contaminated aggregates. Chlorides can also diffuse into the hardened concrete due to the contact with seawater, use of deicing salts, or use of other chemicals (Broomfield, J.P. 2007).

Chlorination begins with the penetration of chlorides into the concrete to the surface of the reinforcing steel. Presence of a small quantity of chloride will not initiate corrosion. Even though the threshold values for the chloride content in concrete is determined using experimental evidence, the actual numbers are a function of practical observation of the structures (Broomfield, J.P. 2007). Once the chloride content exceeds a threshold value, corrosion will initiate.

Electrical Potential

An amount of chloride required for corrosion initiation, referred to as the critical chloride content or threshold value, has been reported to be between 0.6 to 1.2 kilograms of chloride per cubic meter of concrete (Berke, N.S. 1996). However, there is no single value for chloride initiation of steel in concrete but a range of values dependent upon many factors.

As stated earlier, the electrons are removed at the anode and react at the cathode. This deposition results in the increase of potential in the cathode and, likewise in the decrease of potential in the anode. With the increase in the flow of electrons from anode to cathode the potential difference between the anode and cathode increases. Thus the potential difference can be used to predict the likeliness of corrosion occurring in the system. ASTM C 876-91 provides a method to measure the electrical potential difference and to interpret the values to predict the probability of corrosion. In this method, a standard copper-copper sulfate half-cell is used as a reference electrode.

The half-cell potential values do not represent the rates of corrosion, but indicate the probability of corrosion. The interpretation of the half-cell potential ($Cu/CuSO_4$) values suggested in ASTM C 876-91 is as follows.

Potential Value (mV)	Corrosion Probability
$x > -200$	Low, less than 10%
$-200 > x > -350$	Uncertain
$x \leq -350$	High, greater than 90%

Influence of Micro and Macrocell Corrosion

Based on the different spatial locations of anode and cathode, the corrosion in steel occurs in different forms (Elsener, B. 2002). Two important forms of corrosion are microcell and macrocell corrosions.

Microcell Corrosion

Microcell corrosion can take place when the anodic and cathodic reactions are adjacent to each other (Elsener, B. 2002). This leads to uniform iron dissolution over the whole steel surface (Elsener, B. 2002). This uniform corrosion is generally caused by carbonation or by chlorination with very high chloride contents in the proximity of steel bar (Elsener, B. 2002 and Raupach, M 1996). Microcell corrosion is localized and occurs at isolated conditions as pitting corrosion. Since the microcell is microscopic in size, they appear to produce uniform loss of metal (Raupach, M 1996). Knowledge about the mechanism of the microcell corrosion is vital for understanding their effects on the overall corrosion.

Macrocell Corrosion

Macrocell corrosion occurs due to chlorination, when a large amount of chlorides accumulate in the anodic areas (Elsener, B. 2002 and Raupach, M 1996). Macrocells are formed in the presence of large anodic reinforcement areas that are in electrical contact with the cathodic areas. For the electrochemical cell to complete, the water in the concrete acts as the electrolyte. The macrocell corrosion maybe augmented by the effects of the individual microcells, so they should not be neglected (Elsener, B. 2002 and Raupach, M 1996). The total corrosion in the steel is the sum of

the corrosions due to the macrocells and microcells. Thus, to accurately reproduce the corrosion occurring in a given structure, the effects of the microcells should be included with that of the macrocells (Andrade, C. et al 1991).

There are many difficulties in accurately measuring the total corrosion because of the various factors that influence it. The simplest way to analyze the total corrosion is by using the polarization resistance technique which involves the polarization resistance and the size of the steel area under study.

$$I_{corr} = \frac{B}{R_p.s} \quad \text{(Equation 10)}$$

Where, I_{corr} = corrosion current

B = constant depends on whether corrosion is active or not

R_p = polarization resistance

s = exposed steel area to corrosion

The polarization resistance (R_p) is the ratio of the change in potential to the change in polarizing electrical current. The corrosion current (I_{corr}) represents the overall corrosion mechanism including microcell and macrocell corrosion, while the galvanic current (I_g) provides information on macrocell corrosion.

Interpretation for macrocell currents is given as when the average macrocell current reach 10 μA and at least half the total number of samples show macrocell currents more than 10 μA, it is considered as the time to failure (ASTM G 109-99a).

Clear Spacing differences on Macrocell Corrosion

If the resistivity of the concrete is high, the macrocell would not produce a significant increase of the corrosion rate over that of the microcell, since high resistivity will significantly reduce the ionic conduction for long distances. Thus lower resistivity of the concrete will allow the cathodic current to travel to the distant anode (Bertolini, L. 2004). According to Bertolini, the cathodic current can travel distances in range of meters to the anode.

Increased Cathode Area on Macrocell Corrosion

It is a popular belief among corrosion experts that the ratio of cathode to the anode area has significant effects on the rate of corrosion. In small samples of reinforced concrete, the corrosion is entirely due to microcells (Andrade, C. et al 1991). It is also believed that when the structural dimensions increase, the effects of macrocell corrosion must not be neglected but must be added to the effects of microcell corrosion. Large structural dimensions will result in a condition where the outer surface will be penetrated by chlorides and the inner surface will remain chloride-free and passive. With the increase in the dimensions of the structure, it is possible that the passive areas are much larger than the active outer areas. The contribution of the macrocell corrosion to the overall corrosion increases with the increase in the ratio of cathode to the anode area. It is possible that large macrocells may occur in the system. Such large macrocells would accelerate the rate of corrosion, making macrocell an important concern for corrosion researchers (Elsener, B 2002).

Experimentation has shown that when the cathodic area is around 41 times greater than the anodic area, the macrocell corrosion current is three to six times greater than that of microcell corrosion (Andrade, et al, 1991). These experimental results support the popular belief that macrocell corrosion contributes more to the overall corrosion in large structures that have very large cathodic or passive areas compared to that of anode areas.

Stay-in-Place Forms on Macrocell Corrosion

Stay-in-place forms in a bridge deck will limit the bottom concrete deck surface exposure to air, and thus oxygen. Without stay-in-forms, both the surfaces of a bridge deck are exposed to the atmosphere. According to Raupach, bridge decks without stay-in-forms will experience increased effects of macrocell corrosion, since one side of the deck will be exposed to chlorides from deicing salts and the other side will be exposed to the atmosphere. Macrocell corrosion occurs when the anode has a very low potential because of the presence of higher amount of chlorides and high water content, and when the cathode has a very high potential because of the exposure to high oxygen content in the atmosphere. The higher potential difference between an anode and a cathode with some distance between them will result in the formation of macrocell. Thus, the stay-in-place forms are expected to affect macrocell corrosion in the system.

Methods used to measure corrosion activity

With the availability of a number of methods to measure corrosion activity, the choice depends upon the speed and cost at which a method can be operated (Berkeley, K. and Pathmanaban, S. 1990). Also, the corrosion activity should be analyzed by a combination of methodologies to minimize the probability of errors. The three most prominent testing methods are discussed below.

Resistivity

The rate of corrosion depends upon the ease with which the corrosion current can flow inside the concrete and, thus, depends upon the electrical resistivity of the concrete (Berkeley, K. and Pathmanaban, S. 1990). The flow of charged ions in the concrete pore water, known as the ionic current, will be affected by the electrical resistance of the concrete, thus affecting the corrosion activity (Broomfield, J.P. 2007). Factors that influence the structural composition of the concrete such as the moisture content, and size and continuity of the pore system determine the resistivity of the concrete (Berkeley, K. and Pathmanaban, S. 1990).

Different measurement techniques such as single electrode system, two-probe system and four-probe system can be employed to measure the concrete resistivity. The most preferred system to measure resistivity is the four-probe system, as shown in Figure 2. The Wenner 4-Probe was originally designed to measure soil resistivity. The device adapted for concrete testing is a spring loaded instrument to avoid drilling holes in the concrete surface. The inner probes sense the potential difference, while the outer probes pass a current through the concrete. Sometimes wetted wooden plugs are placed at the end of the probes to increase conductivity (Broomfield, J.P. 2007). The probes are to be placed on the surface of concrete while avoiding contact with reinforcement, exposed aggregates and concrete edges so as to prevent errors in the readings. When the steel reinforcement cannot be avoided, the probes are to be placed perpendicular to the reinforcement such that steel is not aligned with and not parallel with the conductive path of electrical current.

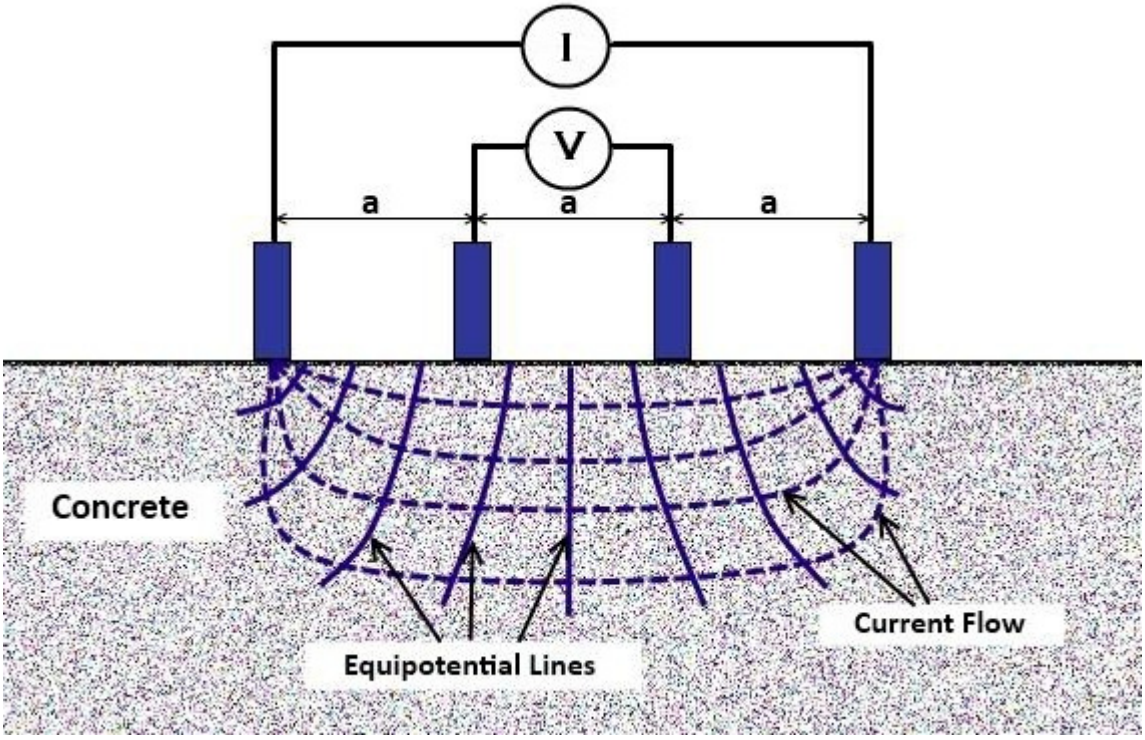

Figure 2 – Wenner Probe or Four-probe Resistivity Meter

Though the two probe system is cheaper, it is considered less accurate than the four-probe system. Holes are to be drilled into the concrete for the probes to be inserted so as to avoid contact with minor carbonation and other impurities (Broomfield, J.P. 2007).

A single electrode system works by placing the electrode on the concrete surface and by using the rebar network to measure resistivity. This method can be operated using the corrosion rate measuring device with two electrodes. It measures only the resistivity of the concrete cover. The contact resistance problem can be considered the disadvantage of this instrument.

Wenner four-probe system will be used all through the project study and the resistivity is calculated as follows.

$$\rho = 2\pi aR$$ (Berkeley, K. and Pathmanaban, S. 1990) (Equation 11)

Where, ρ = resistivity (ohm - cm)

a = spacing between the electrodes (cm)

R = resistance obtained from Wenner Probe (ohm)

The resistivity value is used to predict the capacity of the concrete to resist corrosion, but cannot be used to determine the corrosion rate or even the presence of corrosion. The interpretations of the resistivity values are empirical and are listed in Table 1.

Table 1 – Interpretation of Concrete Resistivity Values (Langford and Broomfield, 1987)

Concrete Resistivity (ohm – m)	Empirical Corrosion Rate
> 200	Negligible
$100 - 200$	Low
$50 - 100$	High
< 50	Very High

Half-Cell Potential

The measurement of the corrosion potential is the simplest and the most commonly used method to determine the presence of corrosion in the steel reinforcement of concrete structures (Bentur, A., Diamond, S. and Berke, N.S. 1997). Since it is quick and cheap, half cell potential testing is more commonly used for field measurements (Mehta, K.P. 2005).

Half cell potential testing consists of a standard half cell as the copper/copper sulfate electrode (CSE) with a porous plug that is kept moist by capillary action. An electrical junction device such as a sponge is used to provide a low electrical resistance bridge between half cell and concrete (ASTM C 876-91-2004). There are standard half cells other than copper/copper sulfate that may be used, such as silver/silver chloride and mercury/mercury oxide (Broomfield, J.P. 2007). The CSE half cell consists of a dielectric container inside which a copper rod is immersed in a saturated solution of copper sulfate. One end of the lead wire is electrically connected to the half cell and the other end of the wire to the negative terminal of the voltmeter (ASTM C 876-91-2004). The positive terminal is connected directly to the reinforcement, which must be electrically continuous. The half cell is placed upon a sponge wetted with an electrolyte which acts as an electrical junction device to provide a low electrical resistance bridge between half cell and concrete. The half cell is moved over the concrete or an embedded reinforcement to take potential readings.

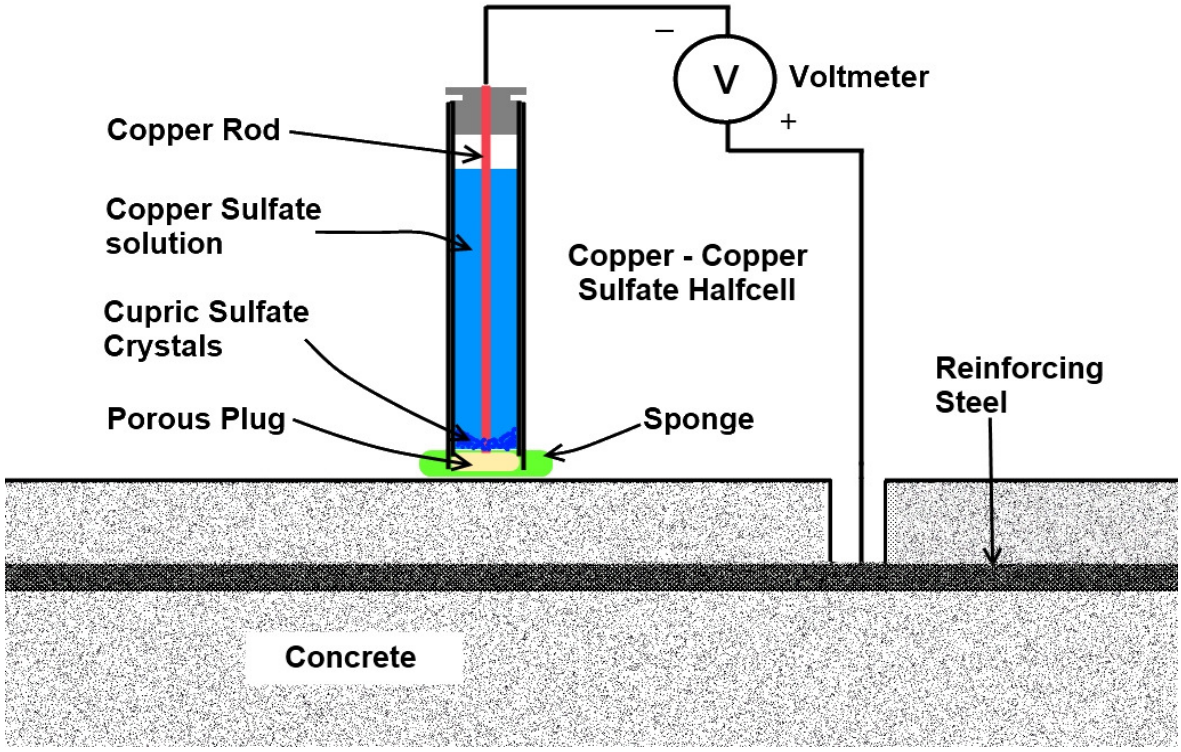

Figure 3 – Half-Cell Potential Apparatus

The voltmeter measures the potential difference between the reference electrode and the embedded steel reinforcement. The potential value can be used to assess the probability of active corrosion. The interpretation of potential values is listed in Table 2.

Table 2 – Interpretation for Corrosion of Reinforced Steel for a Copper/Copper Sulfate Half-cell (ASTM C 876-91)

Measured Potential (mV vs. CSE)	Corrosion Probability
> -200	Low, less than 10%
$-200\ to -350$	Uncertain
< -350	High, greater than 90%

Linear Polarization

To measure the rate of corrosion of the reinforcement steel in concrete, linear polarization can be utilized. One of the fastest and most commonly used methods to measure rate of corrosion is the three-electrode polarization method (3LP method), as shown in Figure 4. Though this method is

a physically non-destructive method, this may not be considered non-destructive since it accelerates the corrosion rate when current is passed through the concrete.

The 3LP test method is based on the Stern-Geary characterization of a polarization curve for corrosion. The method utilizes three electrodes. The steel bar which is tested for corrosion rate is called "working electrode" (Clear, K.C. 1989). The "reference electrode" is a standard half-cell, usually CSE electrode, which is used to measure the potential changes in the steel bar (Clear, K.C. 1989). The third electrode is called a "counter electrode", which is a conductive metallic mesh, used to introduce current into the concrete and reinforcement (Clear, K.C. 1989). The counter electrode is placed over a sponge on the surface of the concrete directly above the reinforcing steel. A current is applied through the counter electrode into the concrete reinforcement and the corresponding potential change is sensed by standard half cell and recorded. Using the Stern and Geary equation, the corrosion current (Icorr) is calculated.

Stern-Geary equation is as follows.

$$I_{corr} = \frac{\Delta I_{appl}}{2.3\Delta\emptyset} . \frac{(\beta_a . \beta_c)}{(\beta_a + \beta_c)} \quad \text{(Equation 12)}$$

Where,

I_{corr} = corrosion current in mA

I_{appl} = current required to polarize the rebar by different potential values from static potential

$\Delta\emptyset$ = absolute value of polarization potential minus the natural electrical half cell potential

β_a = anodic tafel slope

β_c = cathodic tafel slope

$$R_p = \frac{B}{i_{corr}} \quad \text{(Equation 13)}$$

$$B = \frac{\beta_a . \beta_c}{2.3(\beta_a + \beta_c)} \quad \text{(Equation 14)}$$

Where,

R_p = polarization resistance in ohms

i_{corr} = corrosion current density in $\mu A/cm^2$

B = constant value between 26 and 52 (mV), a value of 40 is used in the unguarded 3LP device (Clear, K.C. 1989)

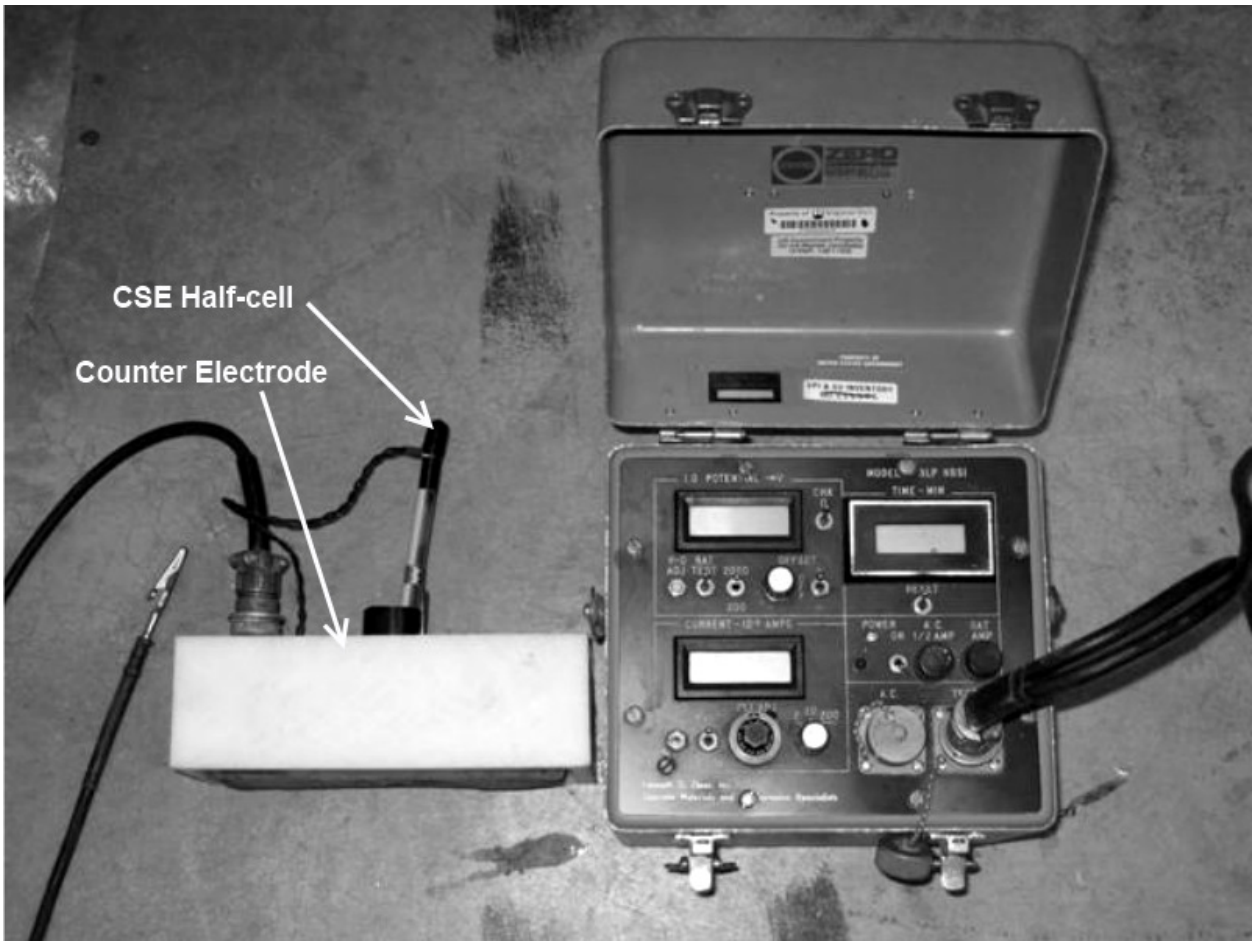

Figure 4 – Three Linear Polarization Apparatus

Corrosion current is represented by I_{corr} while corrosion current density is represented as i_{corr}. The i_{corr} is calculated from the corrosion current (I_{corr}) and the polarized area of steel. It is assumed in the calculation that the whole surface area of the steel bar beneath the probe becomes polarized during the measurement. The measured corrosion current value is for the instant of time the measurement is done and is not considered constant times. However, assuming the corrosion current is constant over time, I_{corr} can be converted to MDD (milligrams per square decimeter per year) and to MPY (mils of penetration per year) as different interpretations (Clear, K.C. 1989). The interpretations for the unguarded corrosion 3LP current values are listed in Table 3.

Table 3 – Interpretation of Corrosion Current Density Values (Clear, K.E. 1989)

Corrosion Current Density ($\mu A/cm^2$)	Expected time for corrosion
$i_{corr} < 0.2$	No corrosion damage expected
$\boldsymbol{i_{corr} = 0.2\ to\ 1.0}$	Corrosion damage possible in 10-15 years
$\boldsymbol{i_{corr} = 1.0\ to\ 10}$	Corrosion damage expected in 2-10 years
$i_{corr} > 10$	Corrosion damage expected in 2 years or less

Chloride Content

Chloride content is measured either by using acid-soluble method or by water- soluble method. Out of the two methods, the acid-soluble method is recommended for routine analysis (Bertolini, L. 2004). The amount of acid-soluble chloride in a hydraulic-cement system is equal to the total amount of chloride in the system, except some initially insoluble organic matter (ASTM C 1152/C 1152M). For the chloride content measurement, concrete cores or drilled concrete powder samples are taken. The concrete cores are dry cut and powdered (< #30 sieve).

Chloride concentration of the powdered sample from each depth will be determined using potentiometric titration. According to ASTM C 1152/C 1152M, a 10-gram powdered concrete sample is dissolved in 1:1 nitric acid solution and then brought to a rapid boil for not more than a few seconds. Then it is cooled and filtered using a coarse-textured filter paper. Finally 2 ml of standard 0.05N NaCl solution is added to the filtered solution. The filtrate is titrated against 0.05N $AgNO_3$.

The percent of chloride by mass of the concrete can be found as:

$$Cl, \% = \frac{3.545\ [(V1-V2)N]}{W} \quad \text{(Equation 15)}$$

Where, V1 = milliliters of 0.05 N $AgNO_3$ solution used for sample titration (equivalence point)

V2 = milliliters of 0.05 N $AgNO_3$ solution used for blank titration (equivalence point)

N = exact normality of 0.05 N $AgNO_3$ solution

W = mass of sample, g

For calculating kilograms of chloride per cubic metre (pounds of chloride per cubic yard) of concrete, multiply percent chloride by D1/100 or D2/100 to the nearest 0.1 kg/m^3 (lb/yd^3).

Where, D1 = oven dry density of concrete

D2 = saturated-surface-dry density of concrete

It is important to prevent any cross-contamination among the samples. Interpretation of the chloride concentration required to initiate corrosion can be conservatively taken as 0.7 kg/m^3 (1.2 lb/yd^3), though the actual interpretation is a range of values. The criteria for corrosion risk due to chloride contents in Europe are given in Table 4.

Table 4 – Corrosion Risk at given Chloride Contents (Broomfield, J.P 2007)

% Chloride by mass of cement	% Chloride by mass of sample (concrete)	Risk
< 0.20	< 0.03	Negligible
0.2 – 0.4	0.03 – 0.06	Low
0.4 – 1.0	0.06 – 0.14	Moderate
> 1.0	> 0.14	High

In order to measure the penetration rate of chloride into the concrete, diffusion coefficient is used. Using a solution of Fick's second law, one-dimensional penetration of chloride through the concrete medium can be estimated by:

$$C_{(x,t)} = C_0\left(1 - \text{erf}\frac{x}{2\sqrt{D_c t}}\right) \quad \text{(Equation 16)}$$

Where, $C_{(x,t)}$ = concentration at depth x at time t

C_0 = surface chloride concentration

D_c = diffusion coefficient

x = distance over which chloride has diffused

t = time for diffusion

erf = statistical error function

Moisture Content

Moisture content in concrete is an important factor in the deterioration mechanism. Moisture plays a vital role in the deterioration mechanisms such as spalling caused by corrosion and deterioration caused by freezing and thawing (Cady, P.D. and Carrier, R.E. 1971).

Corrosion can occur only if the ionic conduction is possible between anode and cathode, which in turn requires moisture and continuous pores to move. Thus moisture content is an essential parameter when corrosion is concerned. Concrete with very low moisture content will have very slow or no ionic conduction, which will result in low corrosion rate. When concrete is saturated or has very high moisture content, the absence of oxygen will contribute to low corrosion rate. Thus, moderate amount of moisture content will allow high rate of corrosion.

Purpose & Scope of Work

The scope of this study involves the testing and recording of data on resistivities, half-cell potentials, corrosion current densities, and macrocell currents from reinforced concrete specimens. The concrete specimens used are from a previous study by Smolinski, L., conducted in the similar manner as this study. Twenty seven concrete specimens are used in the testing program, which were made from nine batches of concrete, three specimens per batch. Integration of data from the previous study is done with the current data into a timeline and thus the long term effects are studied. The scope also involves the identification of any inconsistencies in the previous data and correcting them by comparing the raw data of the previous study. Analysis of the corrected data will be done using JMP Statistical Analysis Software. The scope also included the writing of new software with easier interface, using MS Visual Basic .NET (2008 version) for calculating and analyzing the data obtained from the 3LP instrument.

Purposes of this study are to determine the following using previous data available and from the continuation of the testing program:

- ✓ Influence of clear spacing between anode and cathode on corrosion.
- ✓ Influence of the number of cathode bars (cathodic area) on corrosion.
- ✓ Influence of the presence of stay-in-place forms on corrosion.
- ✓ The contribution of the macrocells and microcells on the total observed corrosion.
- ✓ The critical chloride concentration in the concrete that can initiate corrosion.

MATERIALS & METHODS

Concrete Specimens

The concrete specimens were 356 mm (14.0 inch) in breadth, 318 mm (12.5 inch) in length and with depths of 152, 178, and 203 mm (6, 7, and 8 inch) to vary the spacing between the top and bottom bars, see Figure 5. To simulate the presence of SIP forms, specimens with SIP forms were coated with a low viscosity epoxy on all the sides except the top surface within the ponding dyke, whereas, the specimens without SIP forms were only coated on the four sides with epoxy. In total, the study used 9 specimens without SIP and 18 specimens with SIP. To prevent the occurrence of subsidence cracking over the top reinforcing bars, the specimens were casted in an inverted position. Casting in the inverted position also reduces the effects caused by hand finishing on the top surface.

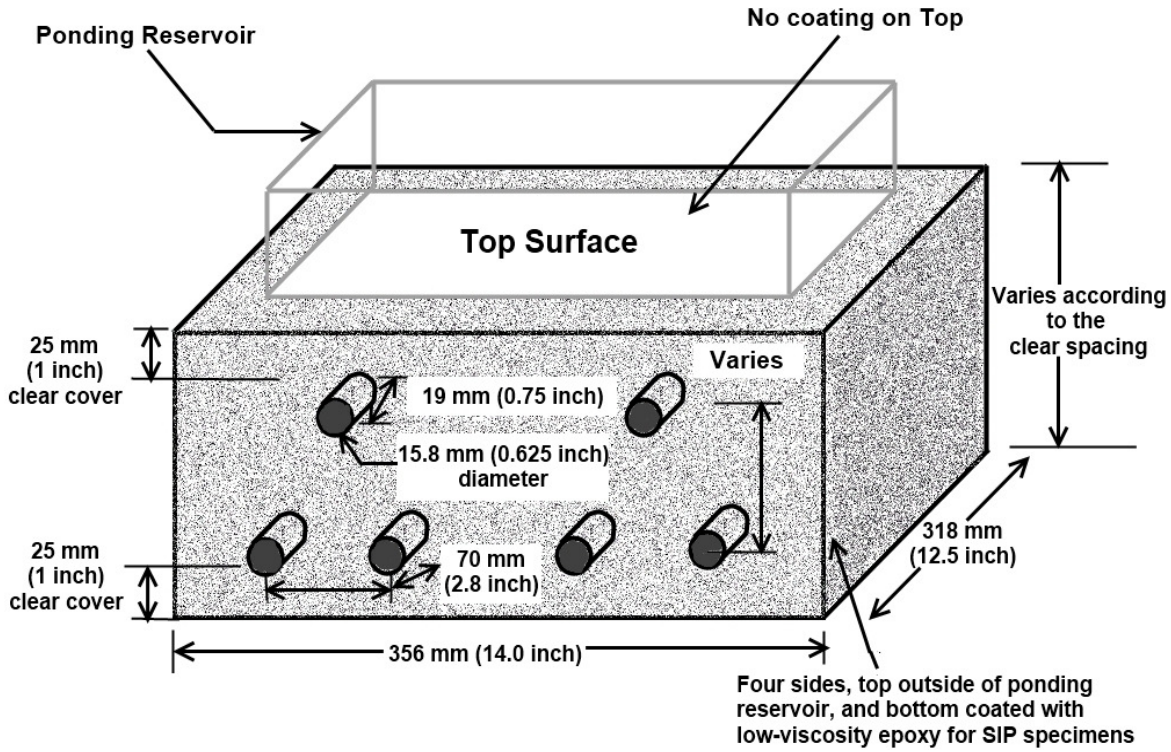

Figure 5 – Modified ASTM G 109-99a Concrete Prism Dimensions

Figure 5 shows a specimen with 2 cathodes (bottom bars), while the specimens with 1 cathode bar would has one bottom reinforcement bar. The two conditions, 1 cathode and 2 cathodes, are to represent every other truss bars configuration as in constructed bridge decks. The 2 cathode specimens represent the portions of the bridge where the truss bar is in the bottom mat and the 1

cathode specimens represent the portions of the bridge where the truss bar is in the top mat. The reinforcing steel bars used in the study were 356 mm (14.0 in) in length and 15.9 mm (0.625 in) in diameter (#5 Rebar).

The concrete prism has dimensions modified from the dimensions listed in ASTM G 109-99a, so that to accommodate two sets of anode-cathode groups in each specimen. Two anode-cathode groups in each specimen will allow for the comparison of within-batch variations (Brown, M.C. 1999). While multiple batches, three, include the variability between batches. Together, the specimens represent the total variability, sum of the variance between and within specimens. Clear spacing between the anode and cathode was 50.8 mm, 76.2 mm, and 101.6 mm (2, 3, and 4-inch) to represent the possible spacing between the mats in actual bridge decks. Clear cover concrete over the top bars and bottom bars is set as 25 mm (1 inch). The bottom 25 mm (1 inch) clear concrete cover represents bridge deck construction while the top cover was reduced to 25 mm (1 inch) to reduce the time for chloride corrosion initiation.

The specimens that represent the truss bars in the bottom were cast with the triad arrangement listed in ASTM G 109-99a, while the specimens representing the truss bars at the top mat were cast with 4 reinforcing steel bars. The 4 bar specimens consist of a pair of top reinforcing bars (anode) and a pair of bottom reinforcing bars (cathode), while the 6 bar specimens have a pair of reinforcing bars at the top (anode) and 4 reinforcing bars at the bottom (cathode). All the specimens had a 100 ohm resistor connecting the anode and cathode. The connection configuration is used to compare the connected and unconnected states. The wire with known resistance is used to calculate the macro-cell current with the potential reading obtained from the voltmeter. In the case of the double cathode bar specimen, the 2 cathodes are connected by a zero ohm jumper. The resistor arrangement is shown in Figure 6.

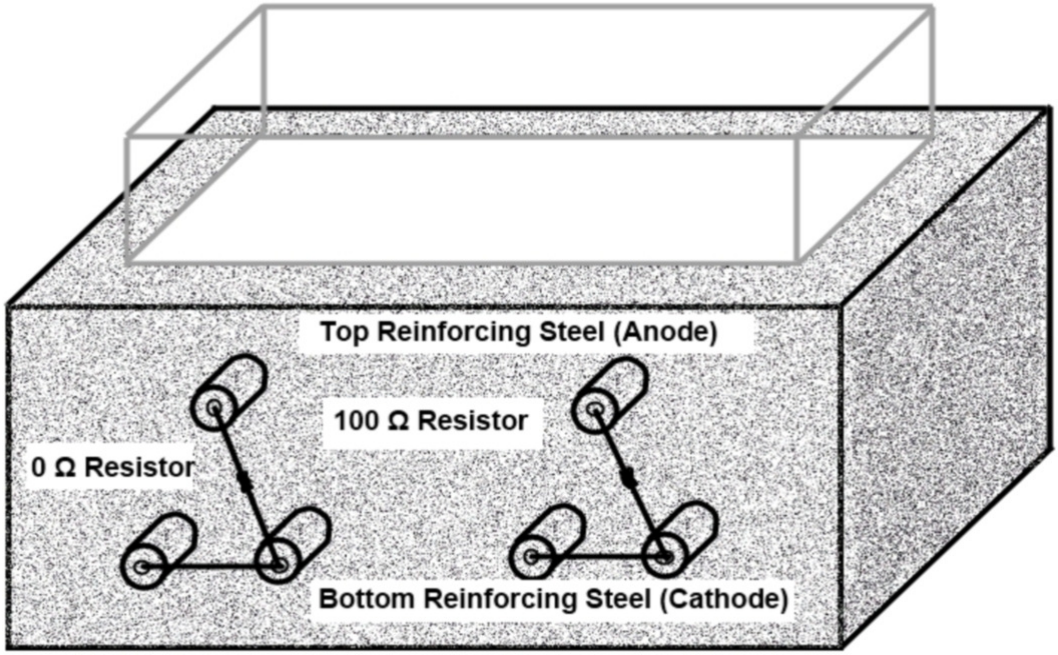

Figure 6 – Resistor Configuration of Concrete Specimen

As shown in Figure 6, a ponding reservoir was adhered to the top surface. To simulate the actual bridge conditions during winter maintenance and to initiate corrosion, saline water was kept stagnant on the top surface and removed as a ponding cycle. A ponding cycle is two weeks of 3% sodium chloride solution by mass, followed by removal and let dry for two weeks.

Test Matrix

The study test matrix is presented in Table 5.

Table 5 – Test Matrix for the Study (Smolinski, L 2007)

Clear Spacing mm (inch)	Number of Specimens without SIP	Number of Specimens with SIP	
	Cathodes-2	Cathodes-2	Cathode-1
50.8 (2)	3	3	3
76.2 (3)	3	3	3
101.6 (4)	3	3	3
Total	9	9	9

The three specimens without SIP were cast with 2 cathodes in each of the spacing differences and the remaining 18 specimens were cast with SIP. Of the 18 specimens with SIP, nine were cast with 1 cathode (bottom bar) and the other nine were cast with 2 cathodes (bottom bar). Figure 7 represents a specimen with one cathode. The clear spacing between the top bar and the bottom bar also varied, 50.8 mm, 76.2 mm, and 101.6 mm (2, 3, and 4-inch).

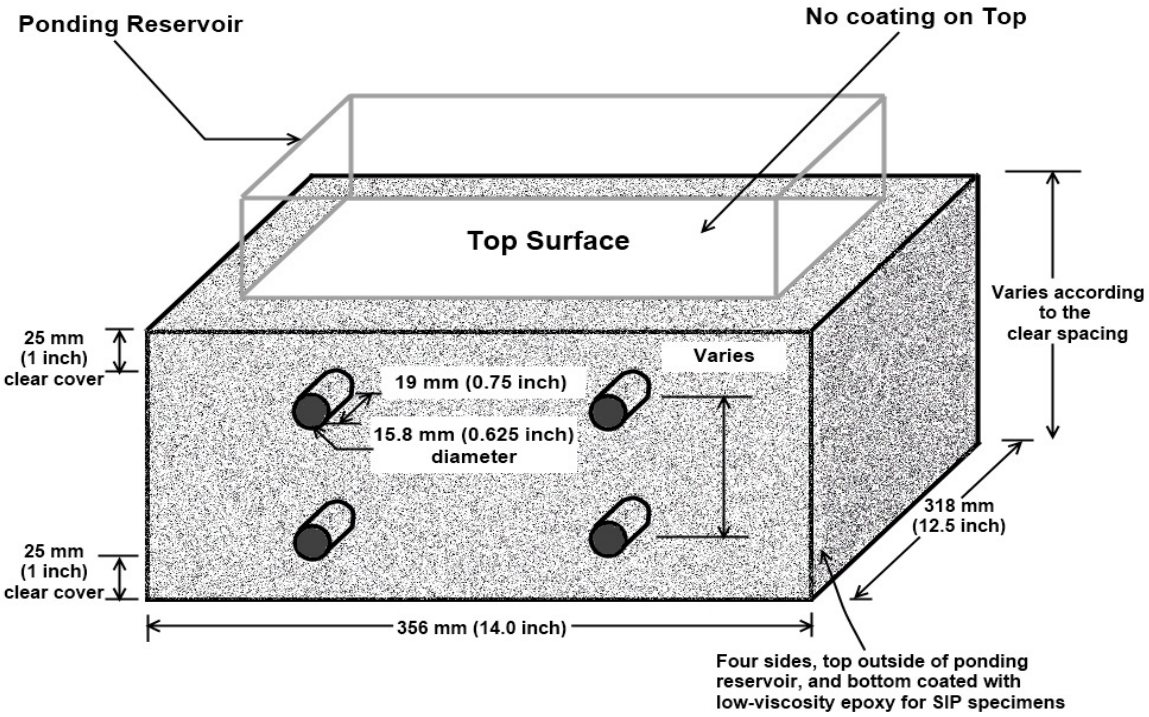

Figure 7 – Modified ASTM G 109-99a Concrete Prism Dimensions with One Cathode

Procedures

The concrete specimens used in this study were cast in a previous study by Smolinski (Smolinski, L 2007). Details from Smolinski's study are summarized here for completeness and as an aid to the reader.

Concrete Specimen

Nine batches of concrete were mixed with three specimens cast from each batch. The mixing of concrete for all the batches was performed in accordance with ASTM C 192/C 192 M: "Standard practice for making and curing concrete test specimens in the laboratory". The water to cement (w/c) ratio was kept constant at 0.5 with a cement content of 426 kg/m^3 (600 lb per cy) of concrete. The concrete mixture included approximately 26 mL of high range water reducer. The

design slump was a minimum of 50 mm (2-inch) and ranged from 76 mm (3-inch) to 197 mm (7.75 inch). Also, the mixture included about 9 mL of air entraining admixtures. Air content of concrete ranged from 5.5 to 6.9 percent.

Steel Reinforcement and Forms

Bare steel bars were utilized for the reinforcement in the specimens, which were obtained from the local building materials supply center. Some of the reinforcement bars were thin ribbed and some were thick ribbed. So reinforcement bars of the same rib size were used in a single specimen to reduce variations.

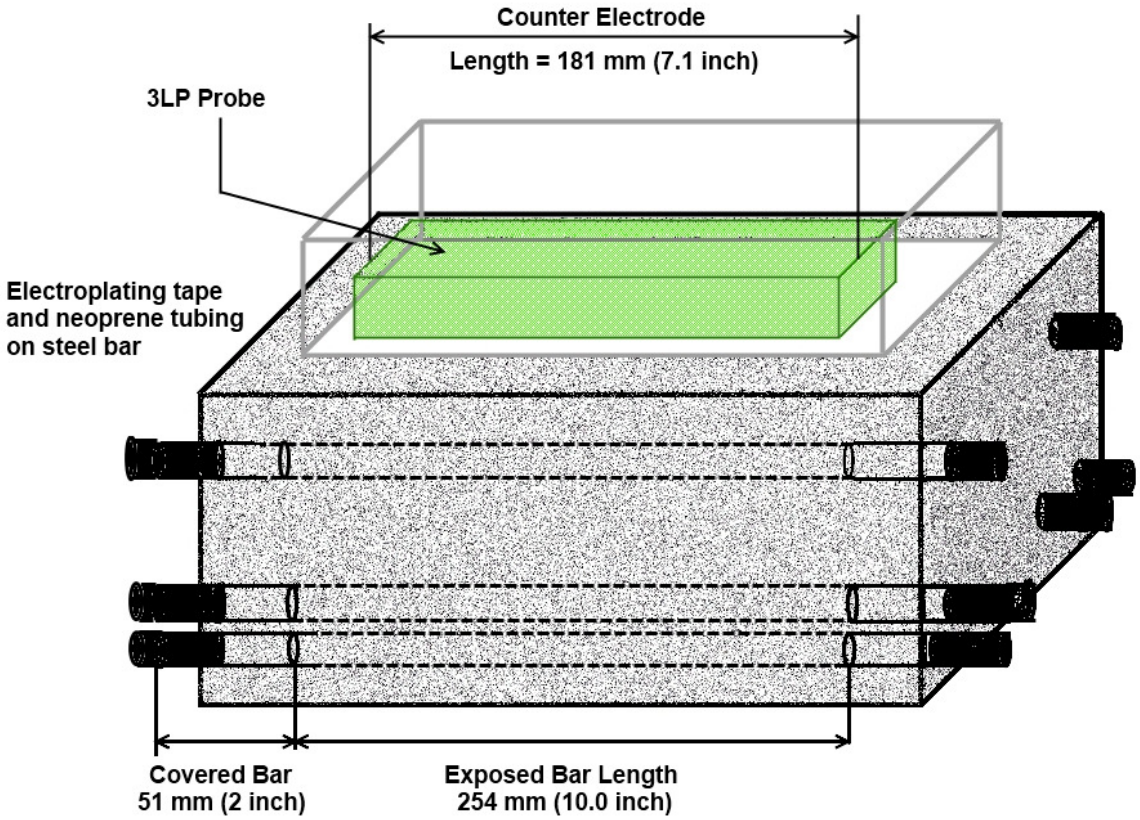

Figure 8 – Configuration of the Reinforcement Bar

According to the dimensions of the specimen, each reinforcement bar was cut to a length of 356 mm (14-inch) in the laboratory. And one side of the bars was drilled and tapped for a stainless steel screw. Surface rust was cleaned using wire brush and then the bars were soaked in hexane after which they were dried with a lint free cloth. As shown in Figure 8, both bar ends for a distance of 51 mm (2-inch) were covered. Thus, 254 mm (10 inch) of exposed steel was directly

exposed to concrete. The cover was used to expose a predetermined length of steel bar for the linear polarization measurements and to prevent corrosion at the corrosion air interface, see Figure 8. Bar end covering consisted of electroplaters, neoprene rubber with the annular space filled with epoxy, see Figure 9. The isolation and covering procedure is in accordance with ASTM C 109-99a.

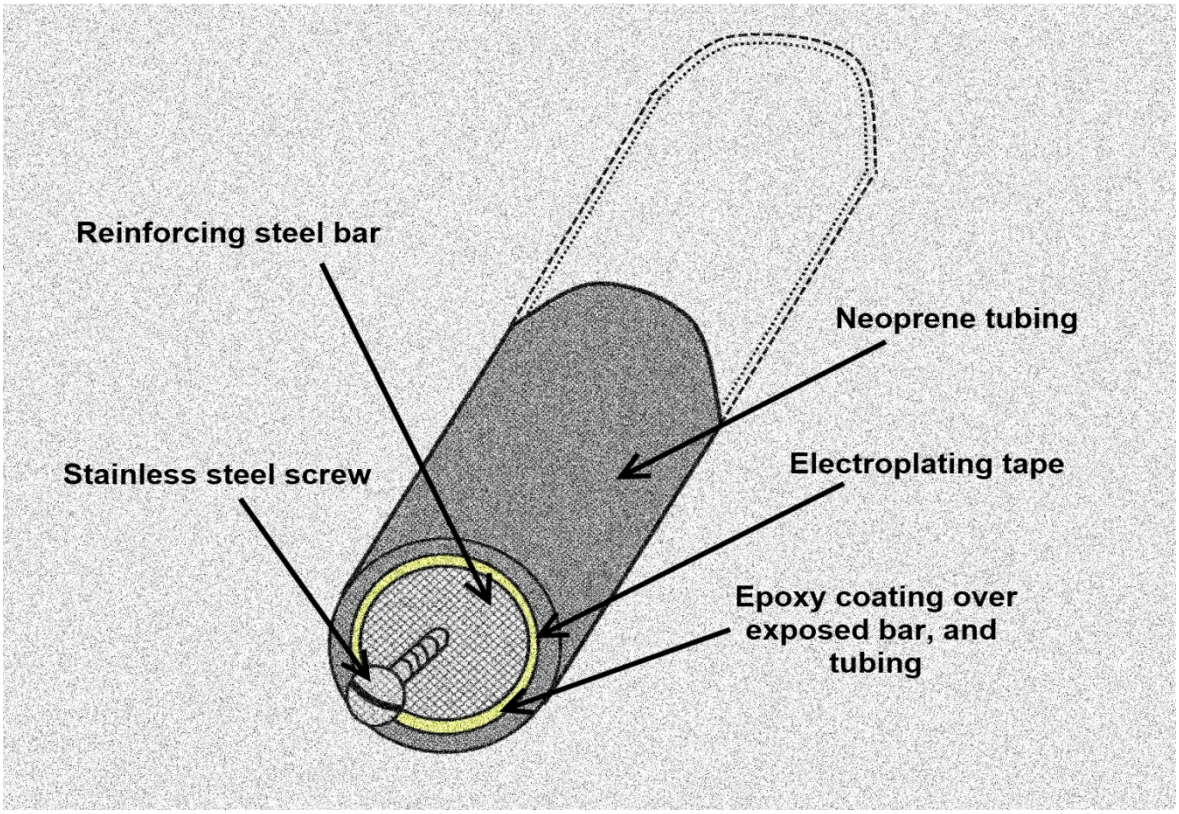

Figure 9 – Reinforcement Connection Details

After the resistor and jumper were fastened with the stainless steel screws, a two part commercial epoxy was applied over the bare steel ends. The epoxy coating was applied to prevent the exposed steel from corroding, which may affect the corrosion measurements.

Materials Preparation

The coarse limestone aggregate was obtained from the CON-Rock ready-mix plant in Blacksburg, Virginia and the fine aggregate was the local natural sand from Wytheville, Virginia (Smolinski, L 2007). Maximum coarse aggregate size was 12.5 mm (0.5 inch). The specific gravity and absorption for the coarse aggregate were 2.82 and 0.30% respectively and for the fine aggregate were 2.61 and 0.80% respectively.

The aggregates used in each batch were oven dried at 110 degrees Celsius (230 degrees F) for at least 8 hours and then allowed to cool to room temperature prior to mixing to better maintain a constant water-to-cement ratio of 0.50 between batches.

Concrete casting

The details of concrete casting are also presented by Smolinski. The casting steps of the reinforced concrete specimens described by Smolinski are only summarized here.

Taking into account the capacity of the laboratory mixing equipments six specimens were cast in one day, two batches of three specimens. Batching of the materials was done on a digital scale to the nearest 0.01 kilogram. The concrete was mixed in a tub-type mixer with a capacity of approximately 0.07 cubic meters (2.5 cu. ft). To test the compressive strengths of the concrete, three test cylinders of diameter 102 mm (4.0 inch) and of length 204 mm (8.0 inch) were cast in accordance with ASTM C 192-95 and tested in accordance with ASTM C 39-96.

Concrete specimens were moist cured with wet burlap and covered by a polyethylene sheet, for 72 hours. After moist curing, the specimens were removed from the form and inverted upon a non-conducting base and air dried in a temperature and humidity controlled room. After 72 hours the specimens were coated with epoxy. The ponding dams were placed on the top after 24 hours after the epoxy cured. The ponding commenced on the 7^{th} day with a saline solution of 3% sodium chloride by mass (ASTM G 109-99a).

After ponding for 7 days, the specimen was allowed to surface dry for 24 hours and the first set of corrosion measurements were taken on the 15^{th} day.

Corrosion Testing

After allowing the specimens to surface dry for 24 hours after the ponding solution was removed, the following corrosion measurements were taken.

Macro-Cell Corrosion Measurement

Macro-cell corrosion current was measured by using a high impedance voltmeter across the 100 ohm resistor between anode and cathode. The measurement is the potential difference between the top reinforcement bar and the bottom reinforcement bar. Ohm's law states that the current through a conductor between two points is directly proportional to the potential difference across two points and inversely proportional to the resistance between them.

$$V = IR \quad \text{(Equation 17)}$$

Where, V = Potential Difference across the resistor (Volt)

I = Electrical Current (Ampere)

R = Electrical Resistance (Ohm)

Using the Ohm's law, with a known resistance, the macrocell corrosion current was calculated. According to ASTM G 109-99a, the time to failure is considered as the time for the average macrocell current to reach 10 μA and at least half the total number of samples showing a macrocell current more than 10 μA.

Resistivity

The resistivity measurement was conducted using the Wenner four-probe resistivity meter, since it is considered to be more accurate than the other ways of measuring resistivity. The measurements were taken by placing the probes on the surface of the concrete specimen between the reinforcement steel bars, in order to measure the resistivity of concrete without interference from the steel bars. The spacing between the four probes was set at 50.8 mm (2-inch), thus, measuring the average resistivity of the top 50.8 (2-inch) of concrete.

Half-Cell Potential Test

Half-cell potential test was performed in accordance to the ASTM C 876-91 standard procedure, 'Standard Test Method for Half-Cell Potentials of Uncoated Reinforcing Steel in Concrete'. The measurement of potential difference indicated the possibility of corrosive activity in the specimens. A CSE was used to compare the magnitude of the electrical potential of the reinforcing steel, as recommended by the ASTM standard procedure. The steel rebar acts as the electrode and the pore water in concrete acts as the electrolyte. A voltmeter is attached to the

anode (top bar) and the probe, which is kept on a moistened sponge, thus completing the electrical circuit. The sponge moistened with an electrolytic solution acts as a low resistance connection between the half-cell and the concrete surface.

The half-cell potential value was read while the top reinforcement bar was connected to the bottom reinforcement bar through a 100 ohm resistor, to obtain the total corrosion activity. Then, the half-cell potentials were read while the top and bottom bars are left unconnected, to determine the contribution of microcells to the overall corrosion. The unconnected readings represent the microcell corrosion values and the connected readings represent the total corrosion including microcells and macrocells. The unconnected potentials can be subtracted from the connected potentials to determine the contribution of the macrocell currents to the total corrosion. Care was taken so that sufficient time was permitted between the connected and unconnected readings, to allow the corrosion cell to come to an equilibrium condition.

Linear Polarization

The linear polarization test was performed to measure the rate of corrosion. Corrosion rate is a measure of the amount of metal loss from the steel bars. The test determines the corrosion current density for a test bar at an instant in time, which is used for predicting the rate of corrosion. The device used in the 3LP test was developed by Kenneth Clear (Clear, K.E. 1989).

The 3LP values were read when the top reinforcement bar and the bottom reinforcement bar were in connected state and in unconnected state. Again in order to determine the contribution of the macrocell corrosion to the total corrosion in the system. The unconnected 3LP readings represent the microcell corrosion current values and the connected 3LP readings represent the total corrosion including microcells and macrocells. The microcell values are subtracted from the total corrosion values to determine the contribution of the macrocell currents. Sufficient time was permitted between the connected and unconnected readings, to minimize errors.

Cleaning of Reinforcement Ends

Corrosion readings were measured, stored, and analyzed by Smolinski up to 273 days (9 months). After this phase was completed, the specimens were maintained in the temperature and humidity controlled room. The ponding cycle of 2 weeks was also continued. The current study

was commenced in March, 2009 (age of specimen ~ 35 months) when the testing program was started again.

The specimens were suspected to have corroded at the exposed ends of the steel bars. This external corrosion could affect the corrosion measurements of the specimen itself. Thus, the cleaning of the exposed ends of the steel bars began in June, 2009 (age of specimen ~ 38 months) and was completed in the same month.

The cleaning up of exposed ends involved the removal of the existing neoprene tubing and electroplating tape using wire brush. The resistor wire and the stainless steel screw were removed as well. Polishing the surface of the exposed ends was done using a wire brush in order to remove all corrosion products on the circumference and the tip surface of the bars. When the cleaning up of the exposed ends was complete, the old resistor and jumper wires and stainless steel screws were replaced with new ones. Then the end surface of the exposed bars was cleaned with alcohol to remove any dirt and the ends surface was double coated with epoxy to limit further corrosion from occurring on the exterior end surfaces.

RESULTS, ANALYSIS & DISCUSSION

Concrete Properties

The physical properties of concrete for the nine batches including compressive strength, air content, and slump were taken and reported by Smolinski. The results are summarized here for completeness.

Compressive Strength

ASTM G 109-99a does not set forth a requirement for the compressive strength of concrete, but states the maximum w/c ratio to be 0.50. Thus, w/c ratio was held constant for all batches at 0.50 (Smolinski, L 2007). Compressive strength readings were taken at 7 days and 28 days and are given in Table 6.

Table 6 – Cylinder Compressive Strengths (Smolinski, L 2007)

Batch	Compressive Strength MPa (psi)	
	7-days	28-days
1	27.4 (3980)	35.1 (5090)
2	24.1 (3500)	29.9 (4340)
3	27.4 (3980)	34.0 (4930)
4	26.9 (3900)	34.4 (4990)
5	27.4 (3980)	31.6 (4580)
6	25.8 (3740)	31.4 (4560)
7	27.4 (3980)	34.8 (5050)
8	29.1 (4220)	34.3 (4970)
9	27.4 (3980)	34.7 (5030)
Average Compressive Strength	27.0 (3920)	33.4 (4840)

As shown in Table 6, the compressive strengths of nine batches were relatively consistent within 7 and 28 days.

Air Content

As per ASTM G 109-99a, the air entrainment values must meet 6 ± 1%. The air entrainment values of the nine batches, taken from Smolinksi's work, are given below, see Table 7. As shown, the air contents are within the specified limits.

Table 7 – Air Entrainment Measurements (Smolinski, L 2007)

Batch	Air Entrainment (%)
1	6.4
2	6.2
3	6.4
4	6.4
5	6.6
6	5.5
7	6.4
8	6.9
9	6.4
Average Air Entrainment	6.4

Slump

As per ASTM G 109-99a, the slump value should not be less than 50.8 mm (2-inch). The slump values from Smolinksi's work are shown in Table 8. All the slump values are greater than 50.8 mm (2-inch) satisfying the requirement set forth by the ASTM standard. Although the water-to-cement ratio was kept constant at 0.5, batches 2 and 6 had slumps relatively higher than the other batches.

Table 8 – Slump Test Measurements

Batch	Slump in mm (inch)
1	88.9 (3.5)
2	196.9 (7.75)
3	101.6 (4.0)
4	114.3 (4.5)
5	76.2 (3.0)
6	177.8 (7.0)
7	114.3 (4.5)
8	114.3 (4.5)
9	139.7 (5.5)
Average Slump	127.0 (5.0)

Corrosion Measurements

Corrosion potential and activity tests, including resistivity test, half-cell potential, linear polarization, chloride content, and macrocell current test, were conducted on the specimens to identify which test parameters, including clear spacing between anode and cathode, number of cathodes, and presence of stay-in-place forms, have a significant influence on corrosion activity.

Resistivity

Resistivity measurements were taken using Wenner four-probe resistivity meter. The concrete can support very low corrosion when the resistivity value is more than 200 ohm-m. When the resistivity is less than 50 ohm-m, the concrete can support very high corrosion. The resistivity data up to 15 months were taken from Smolinski's work and integrated with the subsequent data up to 45 months. Corrosion measurements were not taken between the start of the present study and the end of the Smolinski study, time period 15 to 35 months, But since the specimens were maintained in controlled temperature and humidity, and the ponding cycle was maintained, a trend line may be established to illustrate the changes which took place over the 15 to 35 month

time period. The dashed lines in all the following figures represent the trend in the change properties between 15 and 35 months.

Resistivity as a function of time for batch-1 specimens, clear spacing 2-inches is shown in Figure 10. The lowermost dotted horizontal line, parallel to X-axis, denotes the 50 ohm-m value below which the support for corrosion rate is interpreted as very high. Between 50 and 100 ohm-m, a high rate of corrosion may be supported, while between 100 and 200 ohm-m, a low to moderate corrosion rate. Above 200 ohm-m, low corrosion rate is supported by the relatively low moisture (electrolyte) content of the concrete.

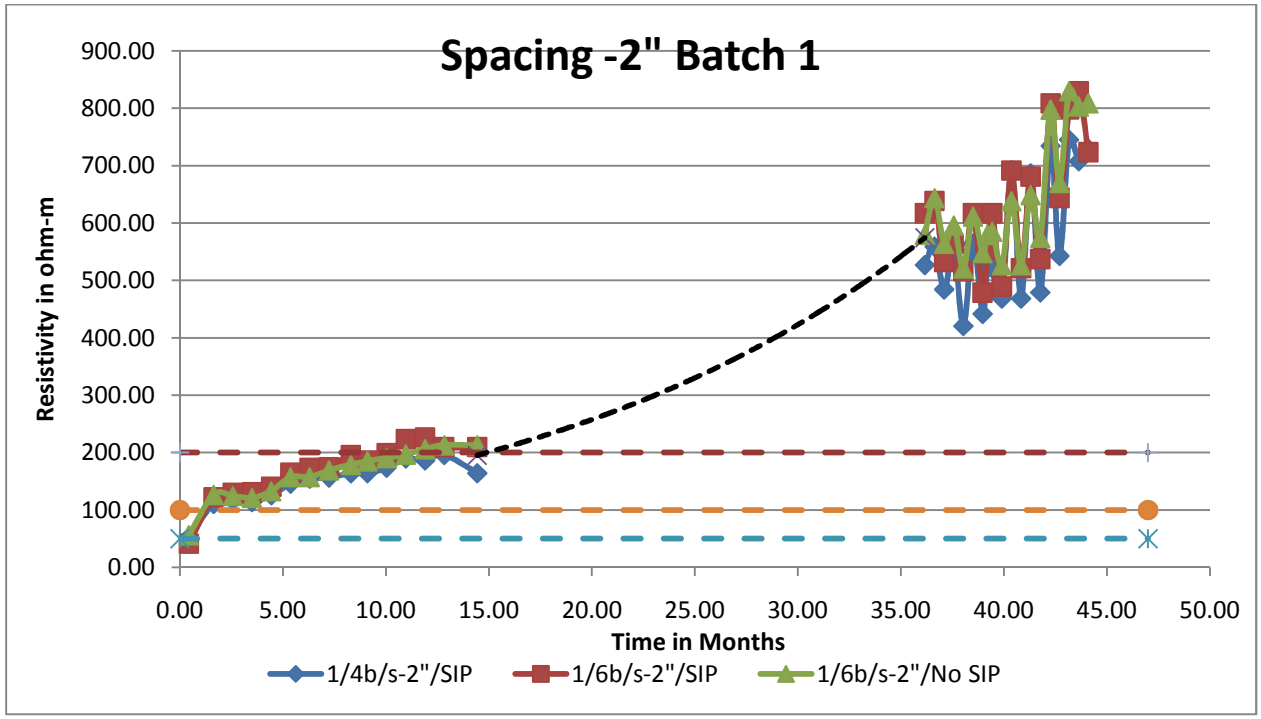

Figure 10 – Resistivity of Batch-1 Specimens with 2" Spacing

As shown in Figure 10, the resistivity is very low (less than 100 ohm-m) in the beginning months, allowing the concrete to support higher corrosion rates. At this point of time the water content in the concrete was higher and the formation of passive layer around the reinforcements was supported by the concrete. The resistivity increased with time as the concrete continued to cure and loss moisture. At 35 months the resistivity increased to greater than 500 ohm-m and at 45 months in excess of 700 ohm-m. The appearance of the variability of the resistivity after 35 months is related to the ponding cycles, decreasing during ponding as the saline water is absorbed and increasing as the water evaporates when the ponding water was removed.

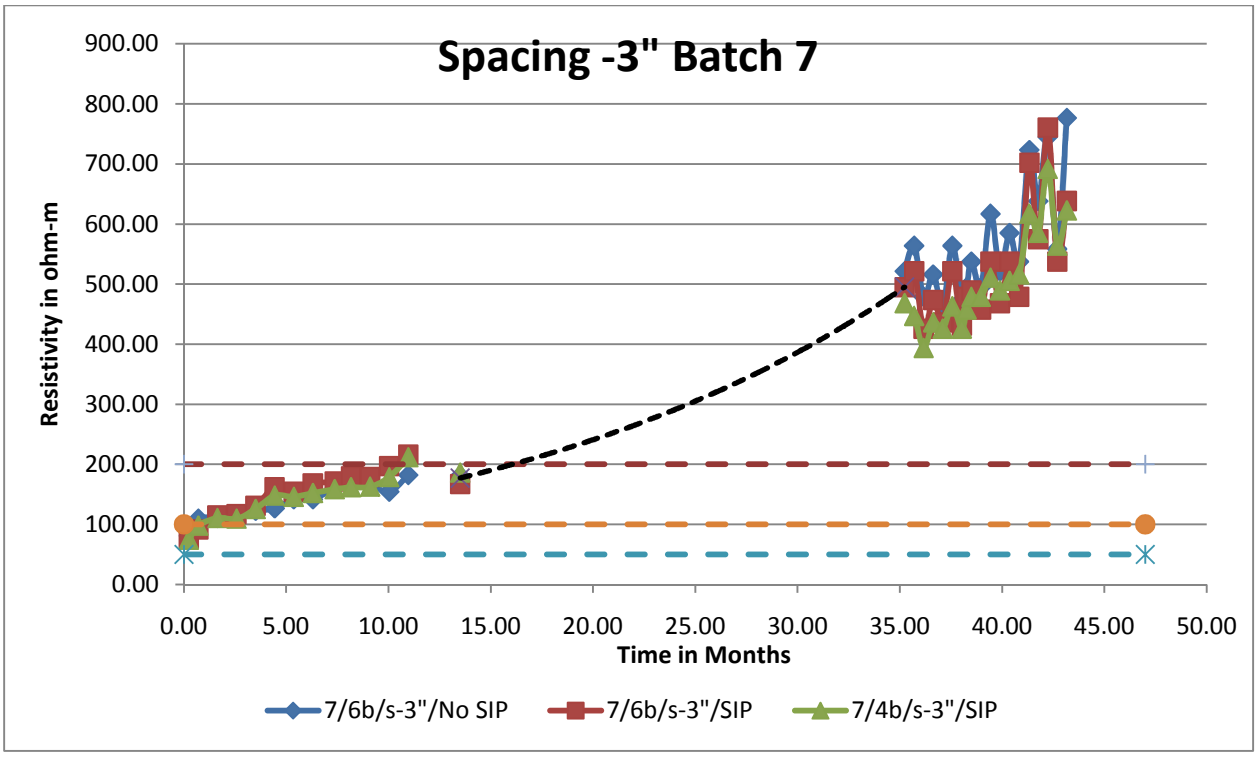

Figure 11 – Resistivity of Batch-7 Specimens with 3" Spacing

Figure 11 represents the resistivity values of batch-7 specimens of 3-inch clear spacing. Similar to the 2-inch spacing specimens, resistivity is very low (less than 100 ohm-m) in the beginning months due to the higher moisture content. Resistivity slowly increases as time increases. At 35 months the resistivity is greater than 500 ohm-m and at 45 months about 700 ohm-m, allowing the concrete to support very low corrosion rate.

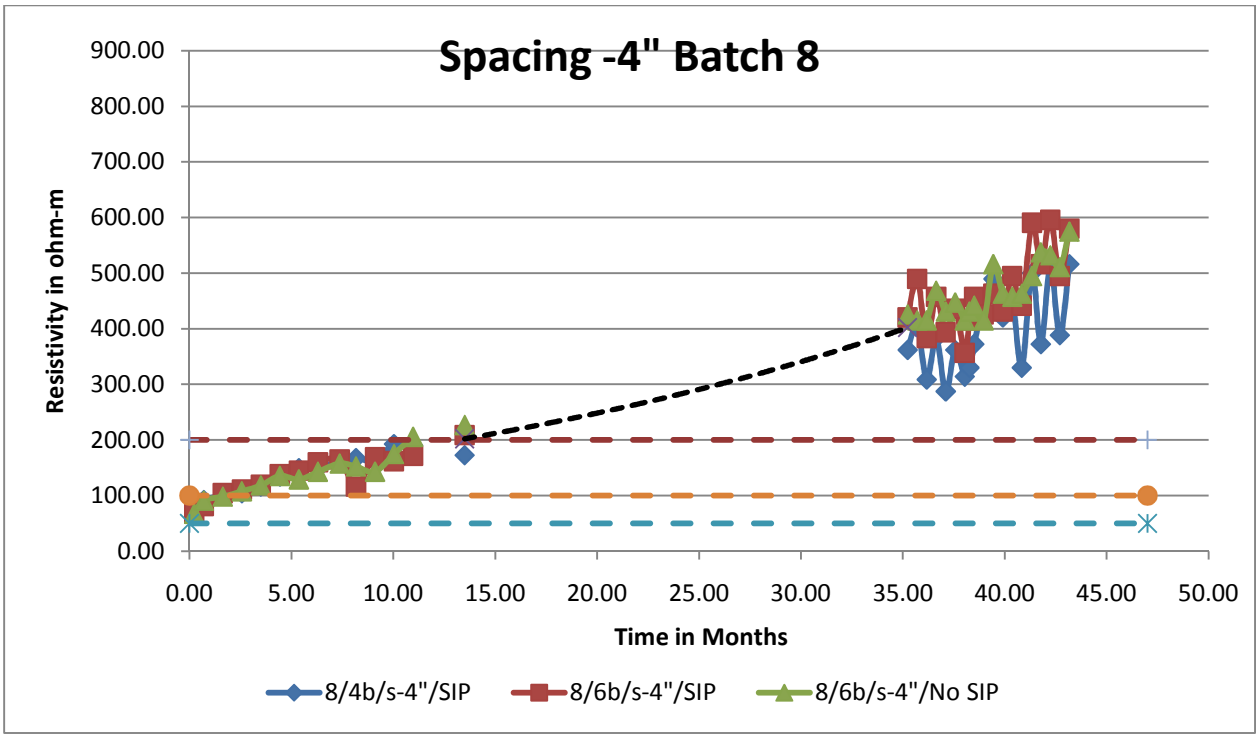

Figure 12 – Resistivity of Batch-8 Specimens with 4" Spacing

Figure 12 presents resistivity change with time for batch-8 specimens of clear spacing 4-inches. Similar to the 2-inch and 3-inch spacing specimens, resistivity is very low (less than 100 ohm-m) in the beginning months. Resistivity gradually increases with time. At 35 months the resistivity has increased to about 400 ohm-m and at 45 months it is about 600 ohm-m. the 2, 3, and 4-inch spacing specimens follow the same trend with time.

The influence of the differences in the clear spacing, number of cathodes and the presence of stay-in-forms on the resistivity can be studied by rearranging the data according to the comparison factors. The comparisons are done by taking into account the values from the first month to the latest measurements to study the trend of variations in the resistivities. The trend may aid in the explanation of the corrosion activity that has taken place throughout the study period.

Clear Spacing Differences

To identify the influence of the clear spacing between the top reinforcement mat and the bottom reinforcement mat on the corrosion activity, the average of the resistivities among the spacing groups are compared. The comparison is shown as a scatter plot resistivity versus time in months.

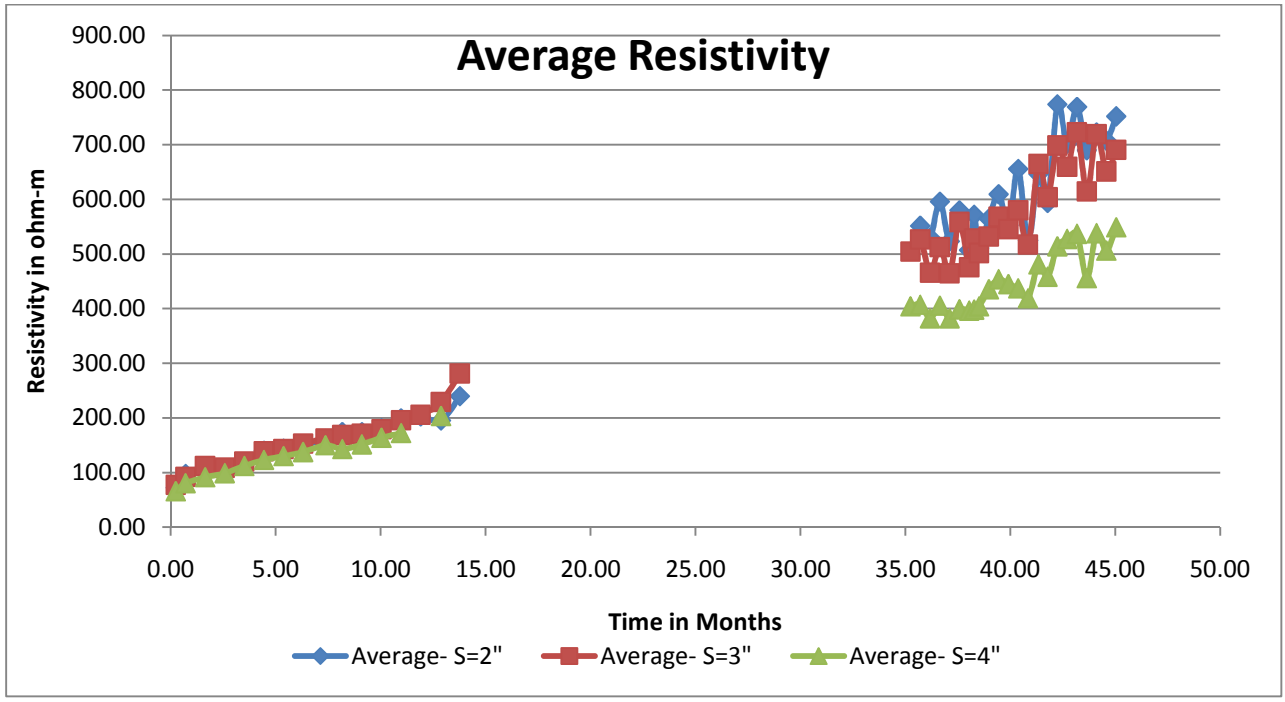

Figure 13 – Average Resistivity of Specimens with 2", 3" and 4" Spacing

The average of the resistivity values from 9 specimens of clear spacing 2, 3, and 4-inches were compared. Comparison includes the specimens with 1 and 2 cathodes and also specimens with and without stay-in-place forms as the only difference should be the variations between concrete batches, as resistivity is a measured concrete parameter.

As shown in Figure 13, it can be noted that the resistivity values up to about 14 months appear to have little differences between them, irrespective of the spacing differences, which agrees with Smolinski's inference. But the values after 35 months show a consistent difference between the different spacing values. Of the three spacings, the 4-inch spacing appears to have lower resistivity than the other two spacings beyond 35 months. Also, the 2-inch and 3-inch spacings

appear to have little difference between them. Statistical analyses of the results are presented later.

Number of Cathodes

To identify the influence of the number of cathodes or the number of bottom reinforcement bars for every top reinforcement bar on the corrosion activity, the average of the resistivities among the cathode groups are compared. The comparison is shown as a normal scatter plot between resistivity and time in months.

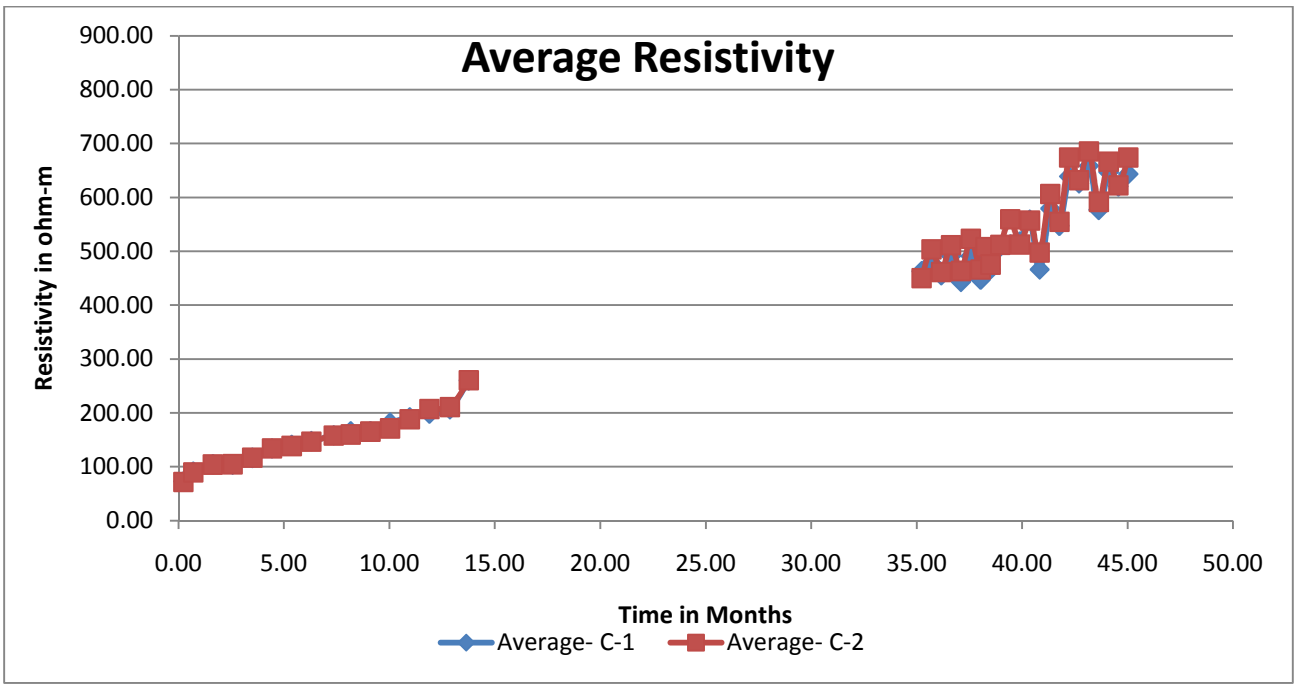

Figure 14 – Average Resistivity of Specimens with 1 and 2 Cathodes

The average of the resistivity values from 9 specimens with one cathode and 18 specimens with two cathodes are compared. The comparison includes the specimens with 2, 3, and 4-inch clear spacings and also specimens with and without stay-in-place forms.

As shown in Figure 14, it can be noted that the resistivity values up to about 14 months appear to have no difference. After 35 months, the resistivities of specimens with one and two cathodes also show little difference. Statistical analyses are presented later to determine if any significant difference exists.

Presence of Stay-In-Place (SIP) forms

To identify the influence of the presence of the stay-in-place (SIP) forms in the corrosion activity, the average of the resistivities among the SIP groups are compared. The comparison is presented using a scatter plot between resistivity and time in months.

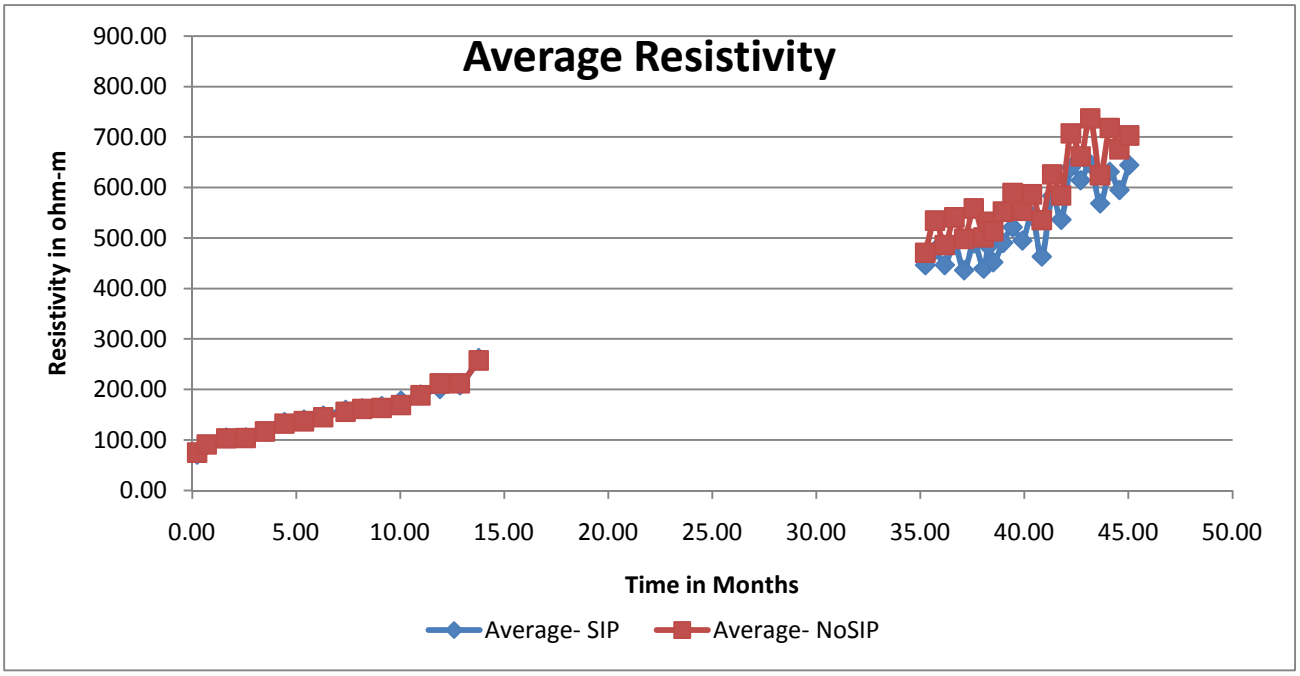

Figure 15 – Average Resistivity of Specimens With and Without SIP

The average of the resistivity values from 18 specimens with stay-in-place forms and 9 specimens without stay-in-place forms are compared. Comparison includes the specimens with 2, 3, and 4-inch clear spacings and also specimens with 1 and 2 cathode bars.

As shown in Figure 15, it can be noted that the resistivity values up to about 14 months spear not be different, irrespective of the presence of SIP, following the same trend as the spacing differences and cathode differences plots, which agrees with Smolinski's inference. After 35 months the specimens with SIP show a small but consistent decrease in resistivity compared to the specimens without SIP. The moisture content of a deck with SIP forms is higher than the deck without SIP forms, because the SIP forms do not allow the moisture to escape from the bottom surface (P.D. Cady and R.E. Carrier 1971). Resistivity is indirectly proportional to the

moisture content. Thus, the observations of this study agree with the findings of P.D. Cady and R.E. Carrier. However, statistical analyses are required to identify any significant difference.

Statistical Analysis

Statistical analyses were conducted to identify significant differences in resistivity exist between clear spacing, cathode bar, and stay-in-place forms. The analyses, an one-way ANOVA of the means and student's t-test to determine significant differences.

Clear Spacing Differences

ANOVA one-way analysis was conducted for the 2, 3, and 4-inch spacings as the nominal terms and resistivities at 35, 40, and 45 months.

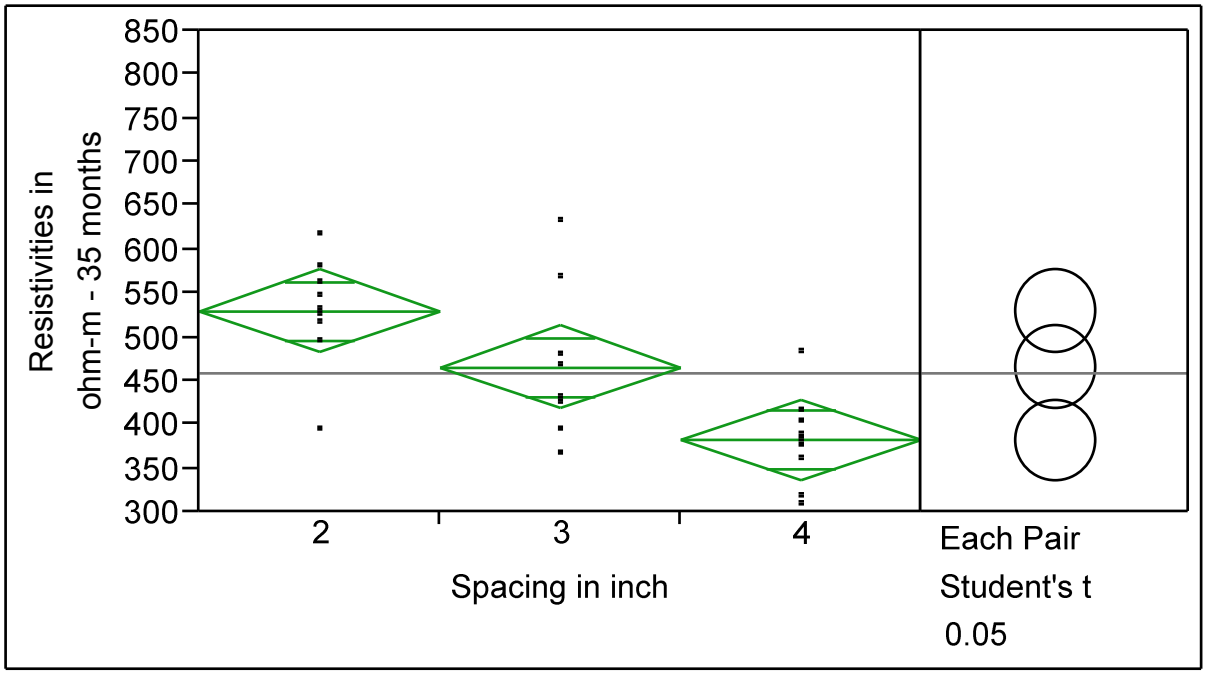

Figure 16 – Statistical Analysis – Resistivity of 2", 3" and 4" Spacing Specimens at 35 Months

The analysis plot (Figure 16) of resistivities at 35 months illustrates a decrease in resistivity with an increase in spacing from 2, 3, and 4-inch spacings. The student's t-test at the 95% confidence level shows that the 2 and 3-inch spacing values are more in common than 4-inch spacing as noted by the degree of overlap of the circles. However, since the circles do overlap, there is no significant difference between the spacings.

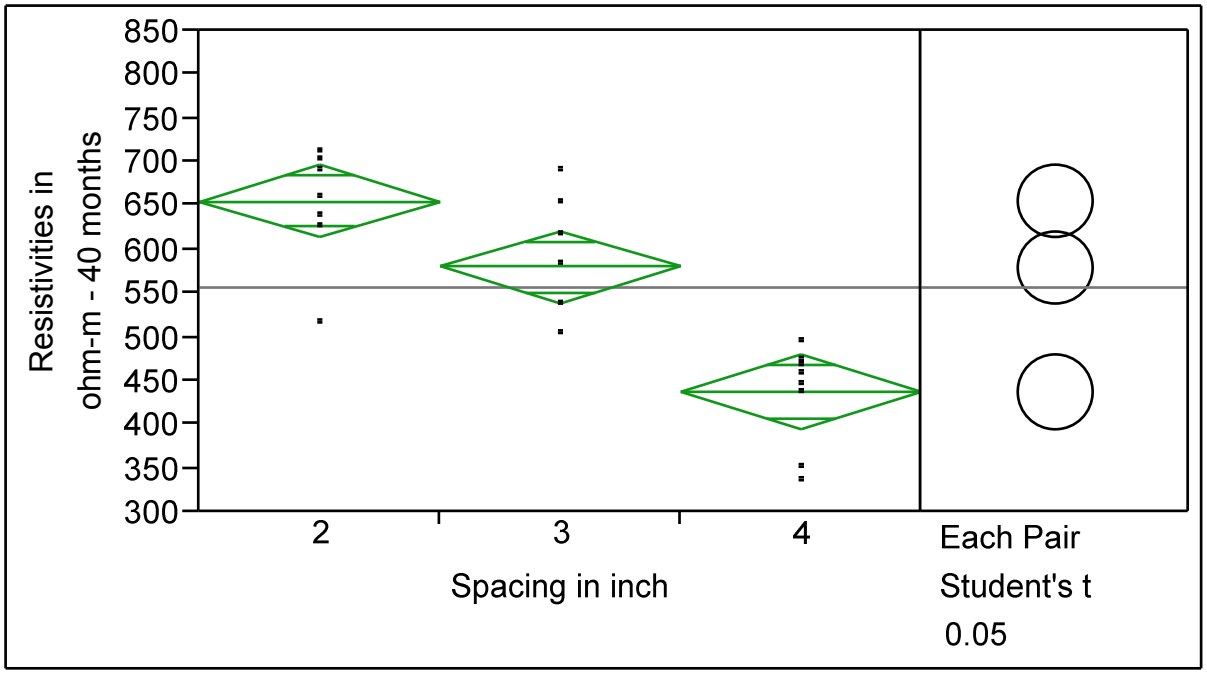

Figure 17 – Statistical Analysis – Resistivity of 2", 3" and 4" Spacing Specimens at 40 Months

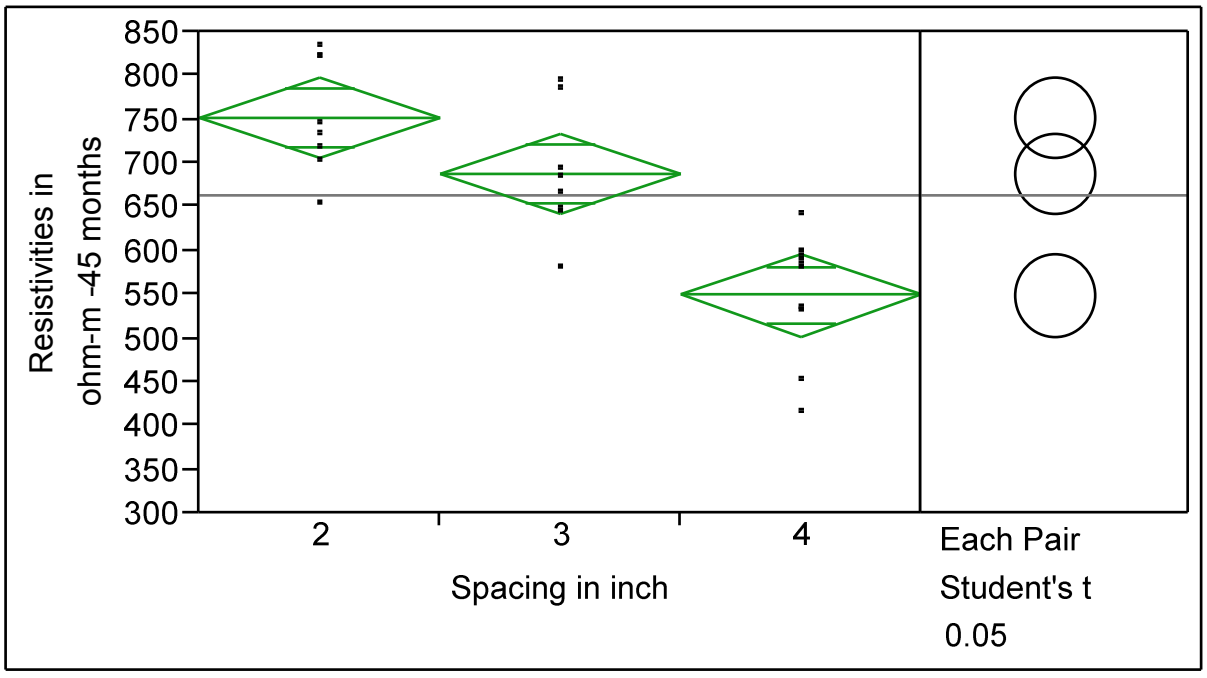

Figure 18 – Statistical Analysis – Resistivity of 2", 3" and 4" Spacing Specimens at 45 Months

As shown in Figures 17 and 18, the resistivities continued to decrease with increasing spacing between anode and cathode bars for both the 40 and 45 month measurements. The 40 (Figure 17)

and 45 month (Figure 18) plots show that the 4-inch spacing values are significantly different (lower) than the 2 and 3-inch spacing, while the 2 and 3-inch spacing resistivities are more in common and not significantly different, as shown by the overlap in the circles.

Even though all the concrete batches had same w/c ratio and similar properties, compressive strength, slump, and air entrainment, there is a difference in resistivity with increasing clear spacings. This could be explained as difference in vibration energy for compaction of specimens with higher spacings. Since the increase in clear spacing between anode and cathode bars also increases the volume of concrete, the amount of vibration energy per unit volume of concrete decreased with increasing spacing factor. Volume of concrete increased by 17 and 34% for the 3 and 4-inch spacing factors over the 2-inch spacing. ACI 222R-01 shows that improper consolidation results in greater amount and deeper depths of chloride penetration (ACI 222R-01). So, conjecture is that similar compaction times for all specimens resulted in relatively lower compaction for the specimens with higher spacings. But, no relative data is available regarding compaction differences from autopsy.

Number of Cathodes

ANOVA one-way analyses conducted with 1, and 2 cathodes as the nominal terms and the resistivities at 35, 40, and 45 months are shown in Figures 19, 20, and 21. This analysis includes the 2, 3, and 4-inch spacings even though significant difference was found between spacings.

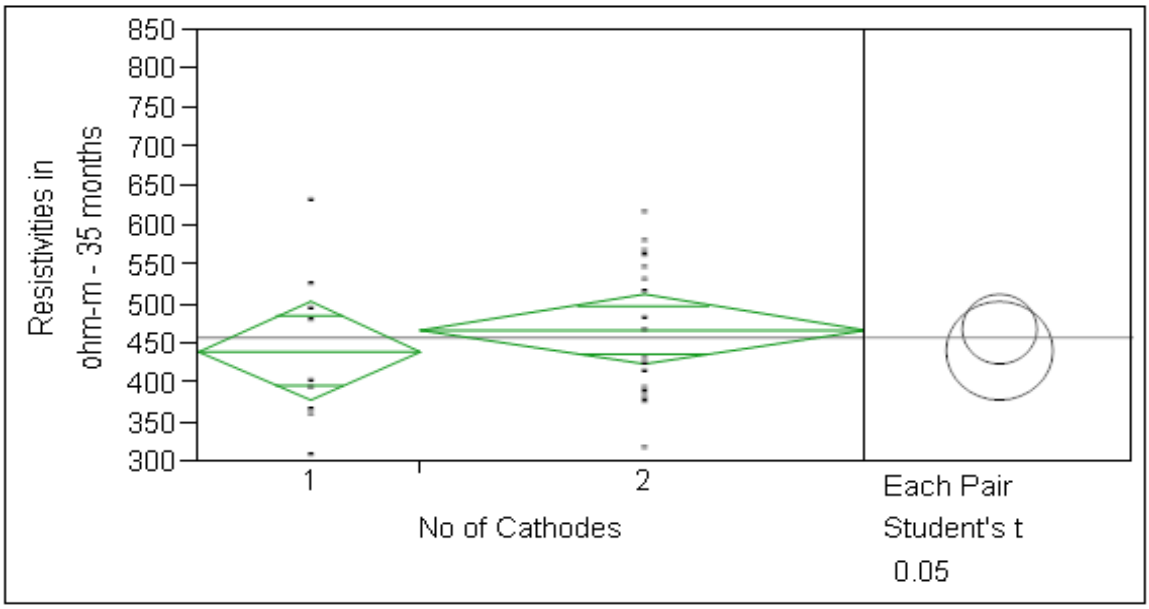

Figure 19 – Statistical Analysis – Resistivity of Specimens with 1 & 2 Cathodes at 35 Months

As illustrated, there is no significant difference in resistivity between 1 and 2 cathodes at 35, 40, and 45 months. As resistivity is a concrete related parameter, the number of bars should not influence resistivity.

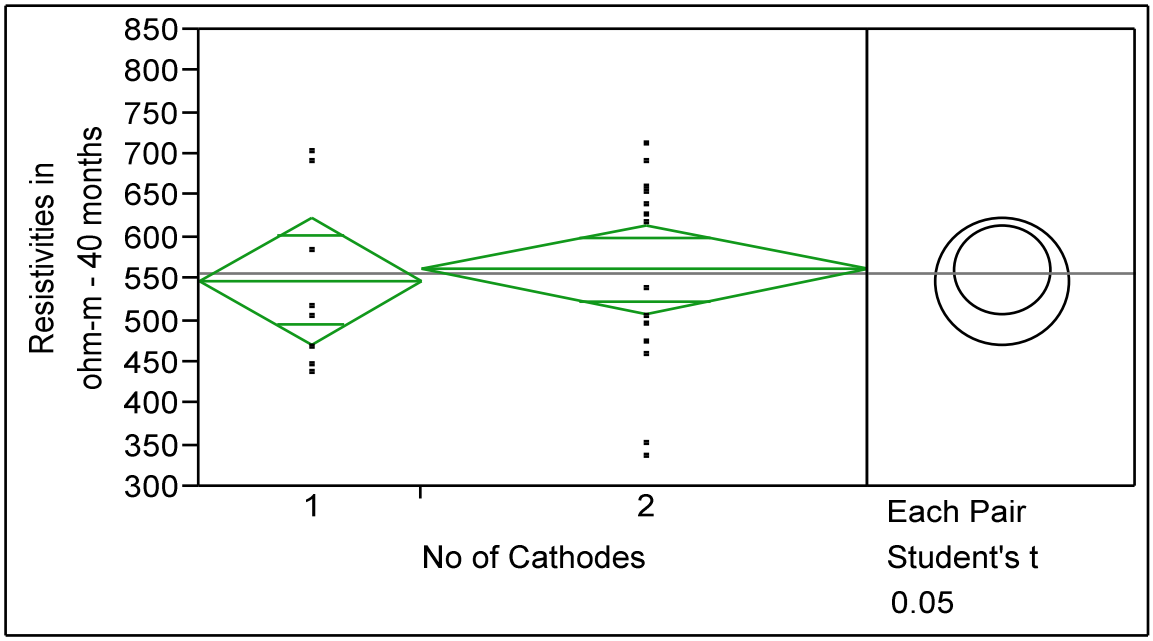

Figure 20 – Statistical Analysis – Resistivity of Specimens with 1 & 2 Cathodes at 40 Months

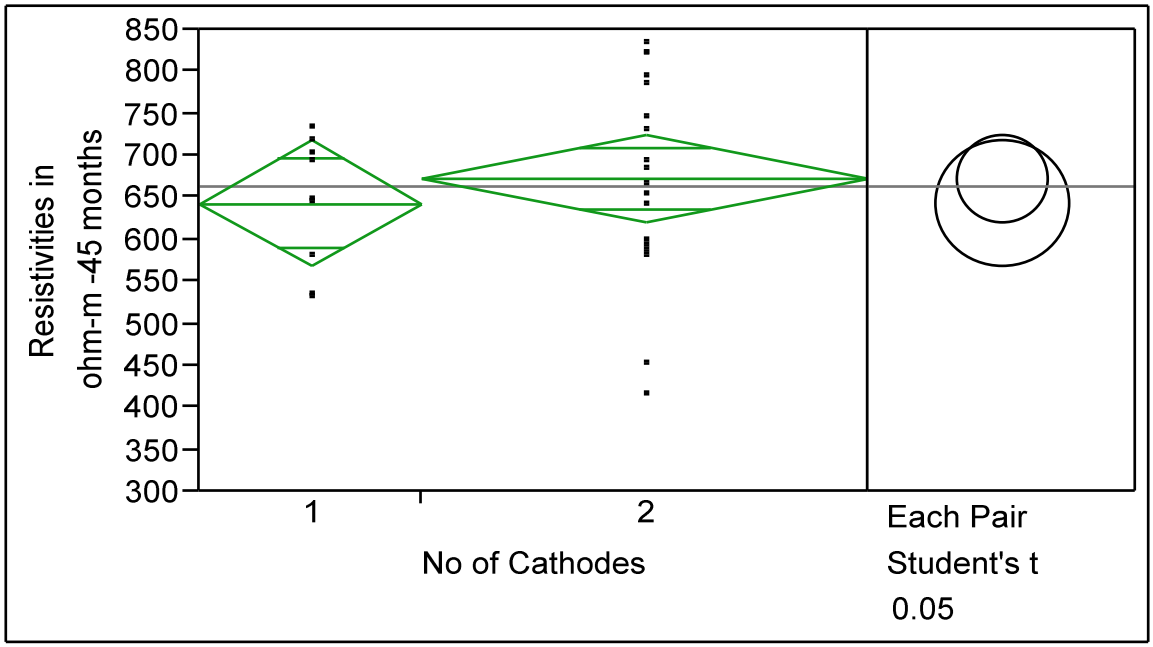

Figure 21 – Statistical Analysis – Resistivity of Specimens with 1 & 2 Cathodes at 45 Months

However, there is a large spread in 2 cathodes because of the greater number of specimens.

By including all the spacing differences in the analyses presented in Figures 19, 20, and 21, the number of cathodes may not be shown. Thus, only the resistivities of specimens with 4-inch spacing at 45 months are considered with the number of cathodes as the nominal term.

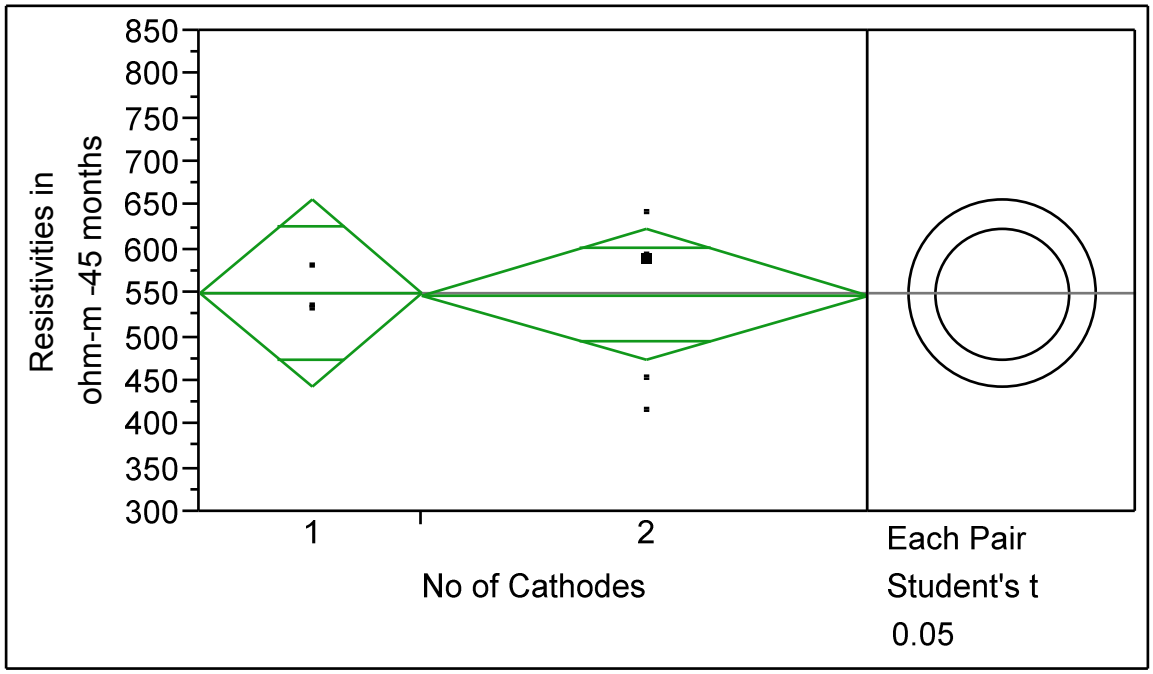

Figure 22 – Statistical Analysis – Resistivity of 4" Spacing Specimens with 1 & 2 Cathodes at 45 Months

In Figure 22, it is shown that the number of cathodes does not influence resistivity, even if the spacing differences are excluded.

Presence of Stay-In-Place (SIP) forms

ANOVA one-way analysis was performed for specimens with SIP (Yes) and without SIP (No) as the nominal terms and the resistivities at 35, 40, and 45 months. The analyses include the 2, 3, and 4-inch spacings even though significant difference was found between the different spacings. Analysis also includes the different number of cathodes, since no significant difference is found between them.

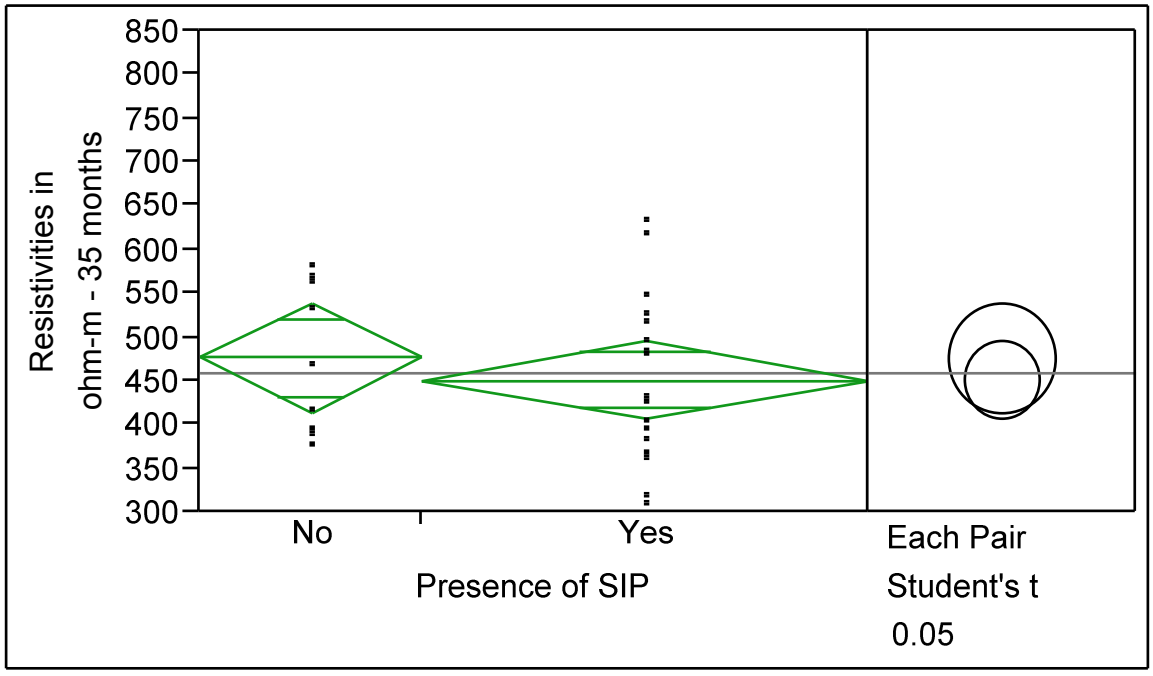

Figure 23 – Statistical Analysis – Resistivity of Specimens With & Without SIP at 35 Months

The one-way analysis and student's t-test of resistivities at 35 months (Figure 23) show that there is no significant difference between resistivities of specimens with SIP (Yes) and without SIP (No). The specimens with SIP (Yes) have slightly lower resistivity mean than specimens without SIP (No). It was expected for resistivity, a concrete parameter, to have no relationship with presence of SIP provided the absence of SIP does not allow the concrete to have significantly different moisture content.

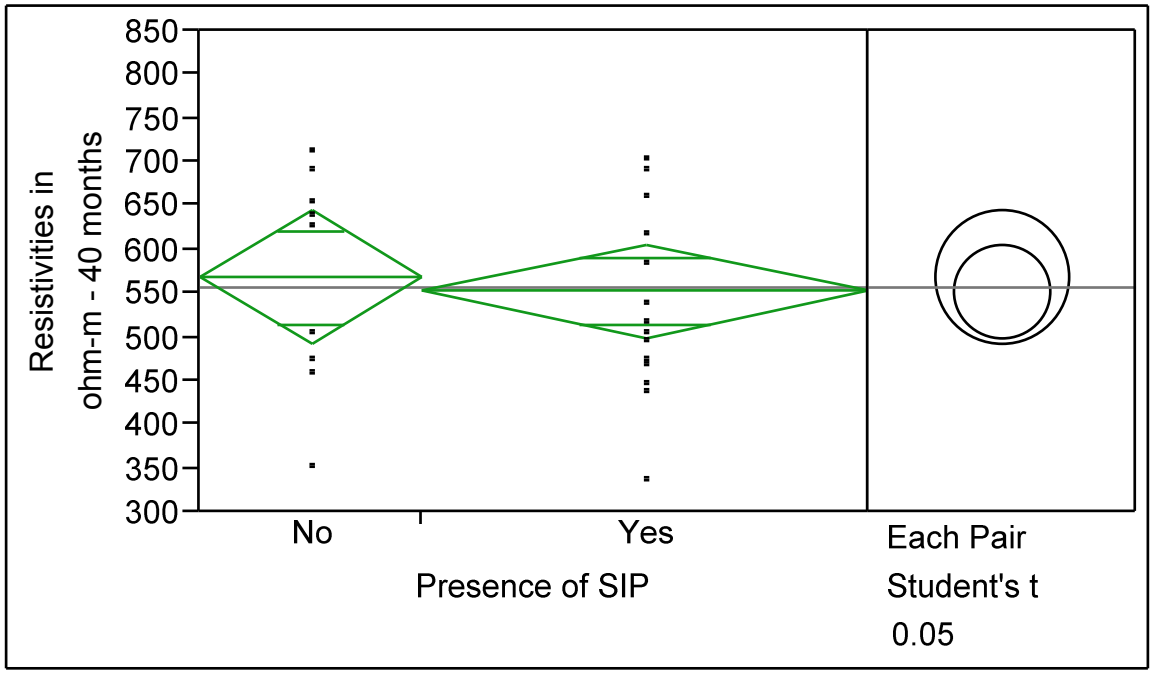

Figure 24 – Statistical Analysis – Resistivity of Specimens With & Without SIP at 40 Months

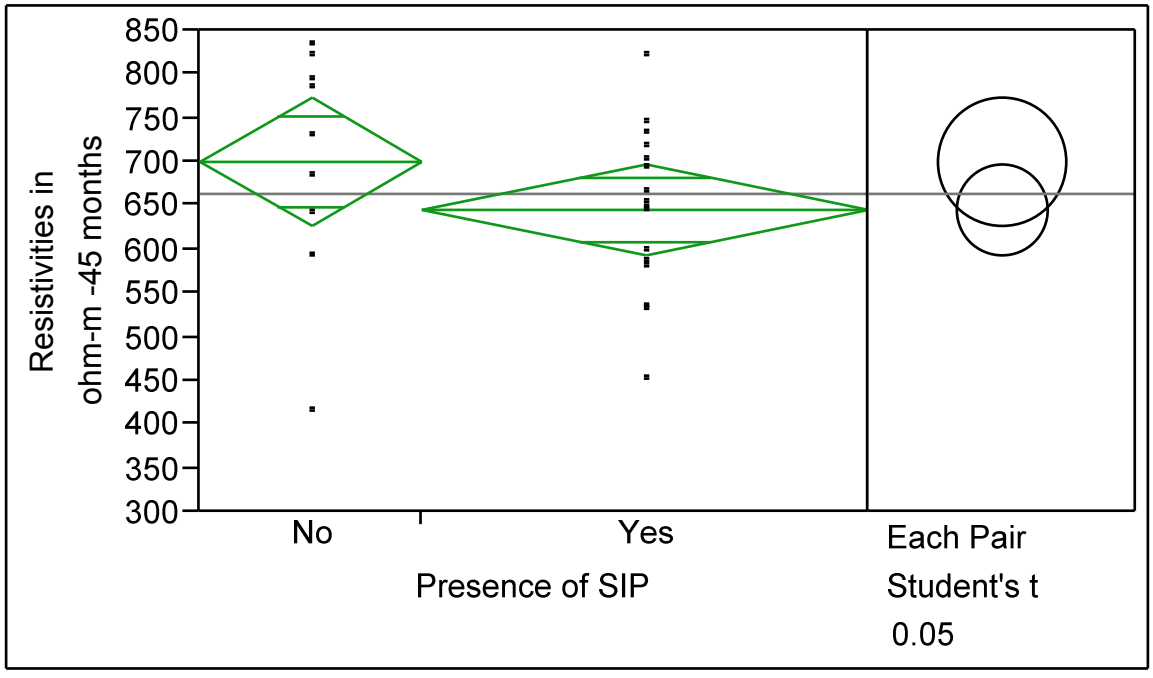

Figure 25 – Statistical Analysis – Resistivity of Specimens With & Without SIP at 45 Months

The statistical analysis also shows that there is no significant difference between the resistivities of specimens with SIP (Yes) and without SIP (No) at 40 (Figure 24) and 45 months (Figure 25). The specimens with SIP (Yes) have a slightly lower resistivity than specimens without SIP (No). There is a larger spread in specimens with SIP (Yes) because of larger number of specimens. But when considering all the spacings, the presence of SIP has no significant influence on resistivity.

However, since the spacing differences are included in the analysis, the presence of SIP may not show any differences because of the larger difference between the 4 inch and the 2 and 3 inch spacing. Thus, only the resistivities of specimens with 4-inch spacing at 45 months are taken and the analysis was performed with presence of SIP as the nominal term.

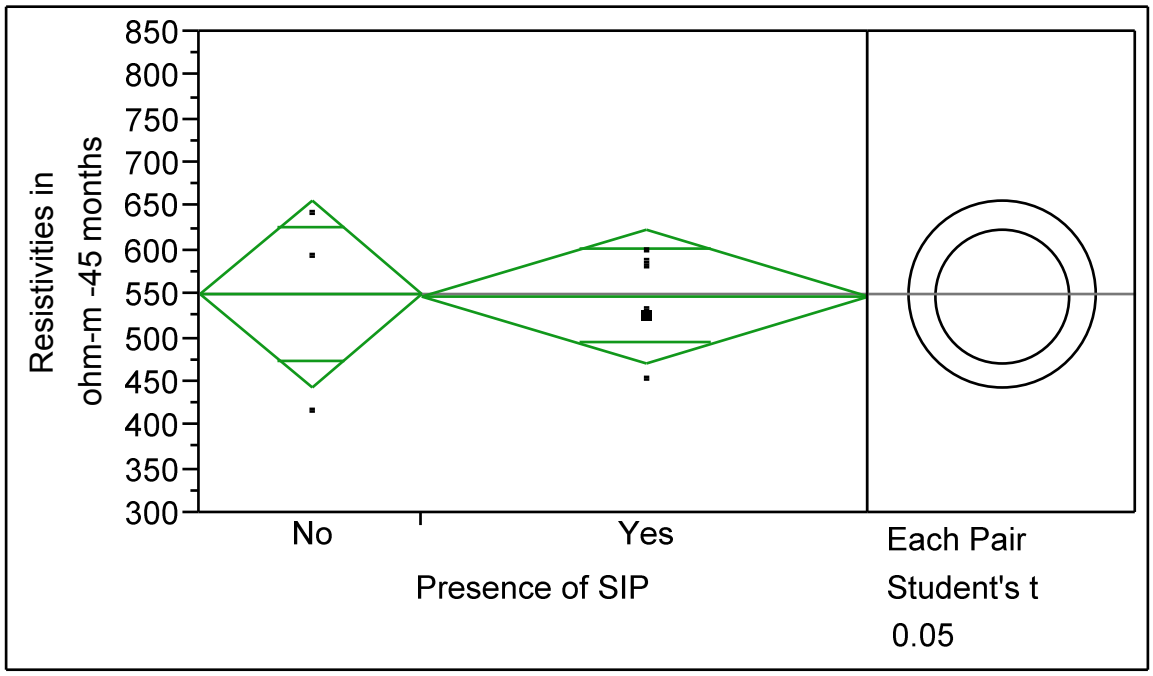

Figure 26 – Statistical Analysis – Resistivity of 4" Spacing Specimens With & Without SIP at 45 Months

As shown in Figure 26, it is again illustrated that the presence of SIP does not have a significant influence on resistivities, even when the spacing differences are neglected.

Half-Cell Potential

Half-cell potential measurements were taken using standard copper/copper sulfate half-cell. There is a corrosion probability of more than 90% when the potential value is more negative than -350 mV. When the potential is more positive than -200 ohm-m, the corrosion probability is 10% or less. The range between -200 mV and -350 mV is called the uncertain range. The half-cell potential data up to 15 months are taken from Smolinski's work and then are integrated with the latest data up to 45 months. Corrosion potentials from approximately 15 to 35 months were not measured. But since the specimens were maintained in controlled temperature and humidity, and the ponding cycle was maintained this time period, a trend can be interpreted with the missing data range.

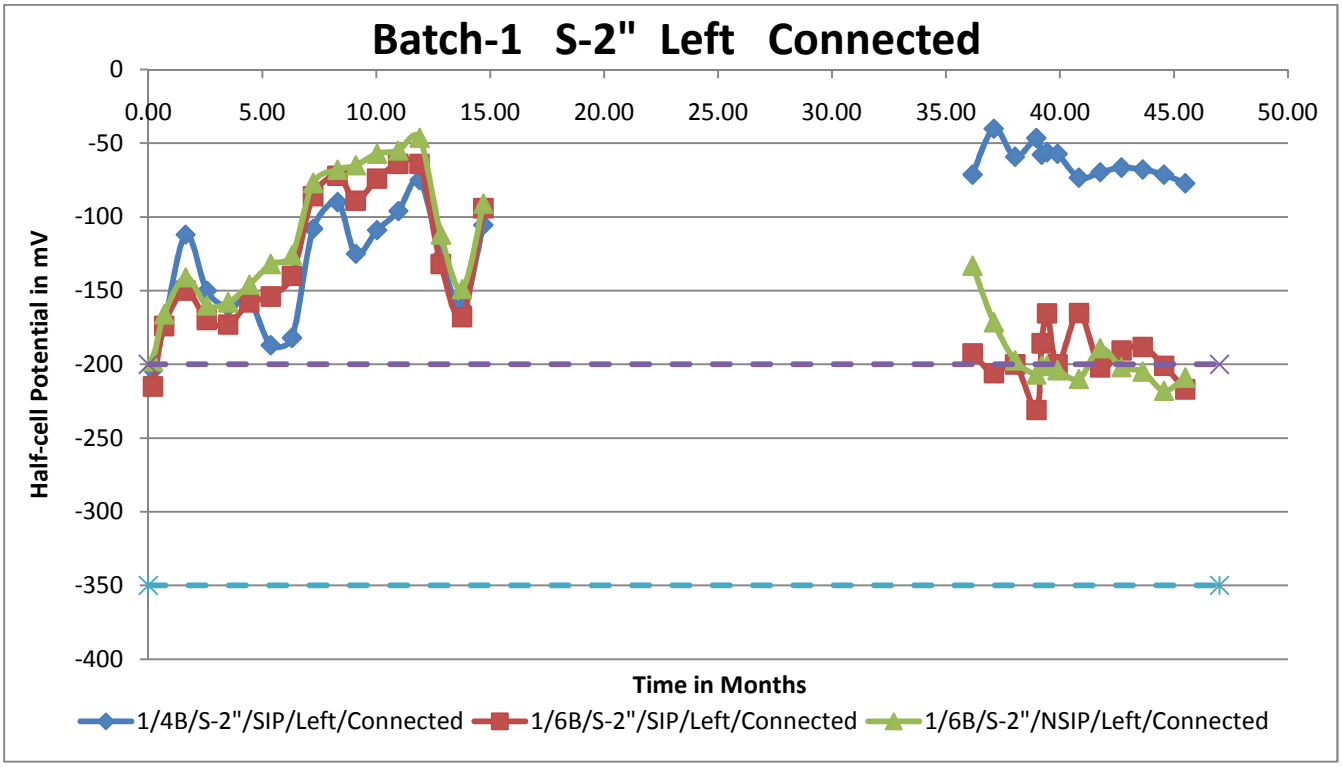

Figure 27 – Connected Half-Cell Potentials – Batch-1 Specimens with 2" Spacing

Potentials as a function of time for batch-1 specimens with clear spacing 2-inches are shown in Figure 27. The sample plot includes values only from the left side triad bars and connected state. In the plots, the lower dotted horizontal line, parallel to X-axis, denotes the critical point below which is interpreted as 90 percent probability of active corrosion. The upper dotted horizontal

line, parallel to X-axis, denotes the point graphically above which is interpreted as 90% probability of no active corrosion. The middle range between the dotted horizontal lines denotes the uncertain range.

As shown in Figure 27, the initial potential values are about -200 mV resulting from the formation of the passive layer. But as time increases, the potential values become more positive at about -100 mV in 14 months. After 35 months some of the specimens have potentials about -200 mV and a few have values at more positive than -100 mV. There is some variation within the values of the same batches may be related to each batch having specimens with 1 and 2 cathodes, and presence & absence of SIP forms. So the variance within the batch can be due to the influence other factors. The potentials of the whole batch with 2-inch spacing lie in the first range where the corrosion probability is less than 10%.

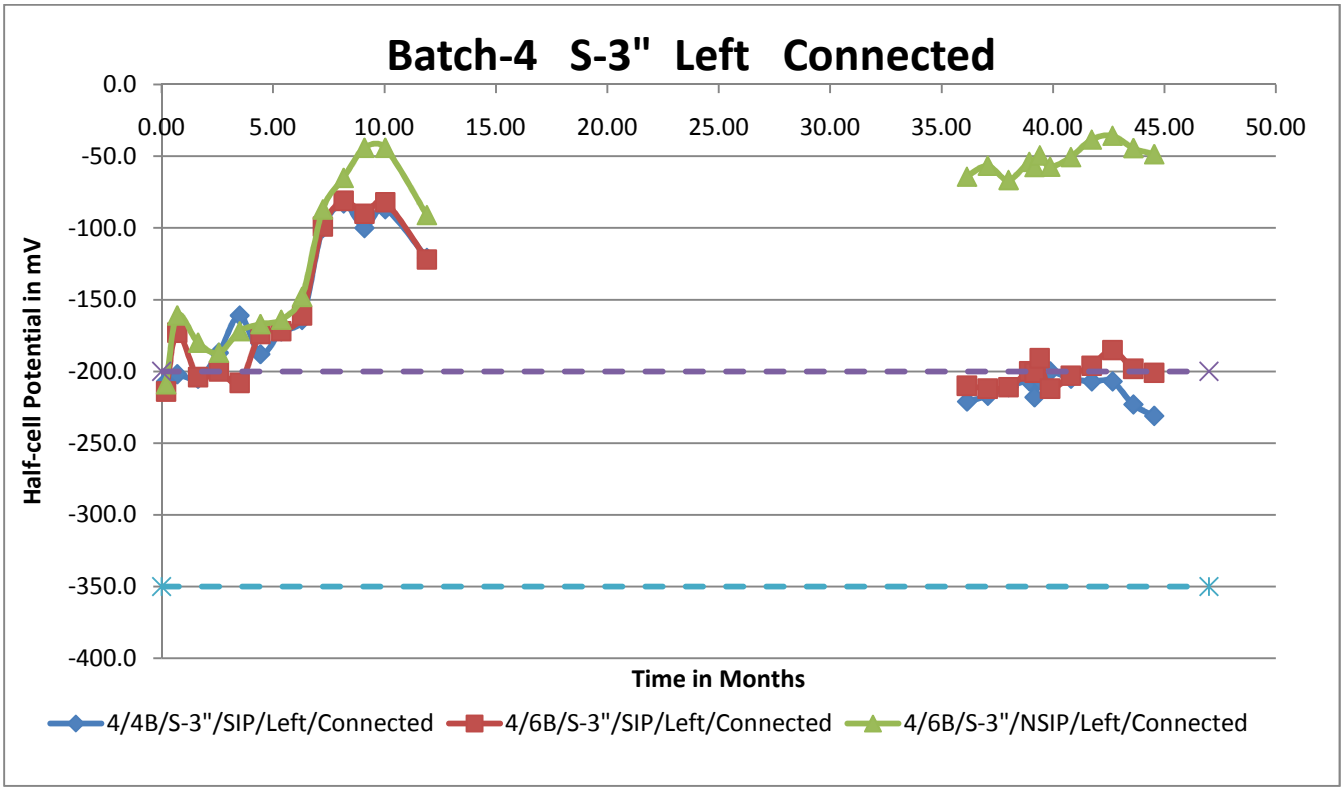

Figure 28 – Connected Half-Cell Potentials – Batch-4 Specimens with 3" Spacing

Figure 28 represents the batch-4 specimens with 3-inch spacing. The sample plot shows values only for the left side triad bars and connected state. Similar to the 2-inch spacing specimens, the half-cell potential values show more negative corrosion potentials at the beginning when the passive layer is forming. As time increases, the potential become more positive to about -100

mV at 14 months. As explained before, the variation observed within the batch could be due to the influence of the different parameters. The potential values after 35 months for two specimens are about -200 mV and for other specimen it is about -50 mV. However, the 3-inch spacing specimens have potentials in the first range representing about 10% probability of corrosion.

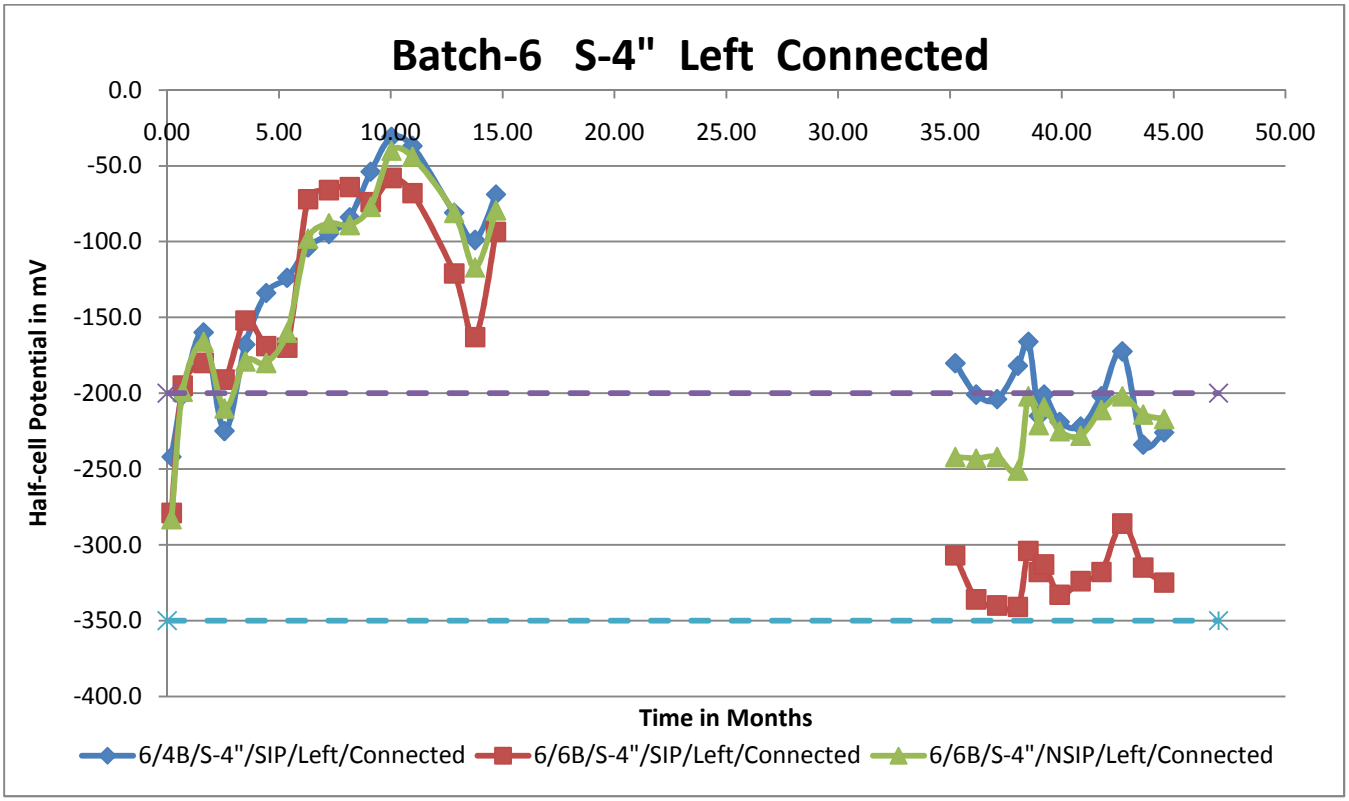

Figure 29 – Connected Half-Cell Potentials – Batch-6 Specimens with 4" Spacing

Figure 29 shows the potential values of batch-6 with a clear spacing of 4-inches. It includes only the left side triad bars and connected state. Similar to the 2-inch and 3-inch spacing specimens, the half-cell potential values show higher corrosion possibility as the passive layer forms. As time increases, the potential values reach more positive potential than -100 mV at 14 months. As explained before, the variation observed within the batch could be due to the influence of the different parameters. The potential values after 35 months for some specimens are more negative than -200 mV and for other specimens it is about -300 mV. Most of the specimens with 4-inch spacing lie in the uncertain range.

The influence of the differences in the clear spacing, number of cathodes and the presence of stay-in-forms on the potential can be evaluated by rearranging the data according. The comparisons were performed considering the values from the first month to the latest

measurements to illustrate the trends in the potentials. The trend may aid in the explanation of the corrosion activity that has been taking place within the specimen groups.

Clear Spacing Differences

To identify the influence of the clear spacing between the top reinforcement mat and the bottom reinforcement mat, the average of the potentials among the spacing groups are compared. The comparison is presented as x-y plot between resistivity and time in months.

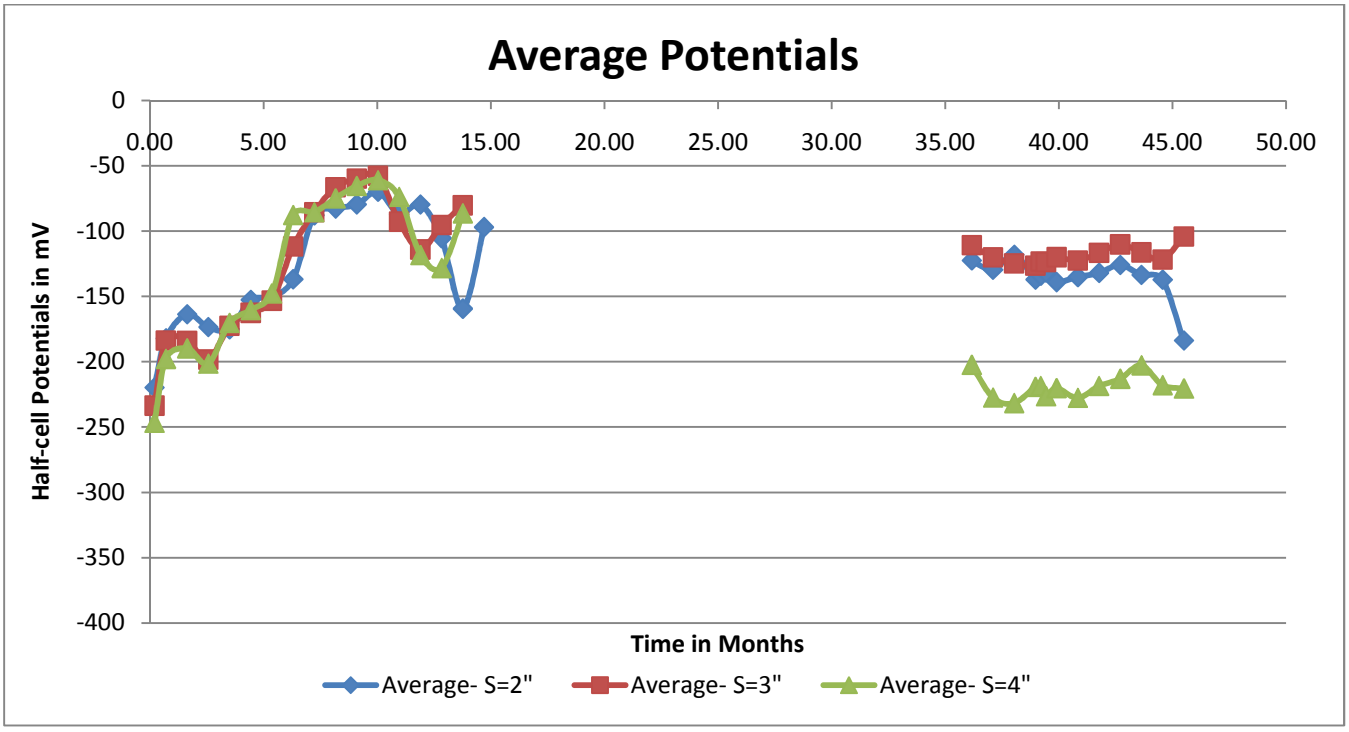

Figure 30 – Average Half-Cell Potentials of Specimens with 2", 3" & 4" Spacing

The average of the half-cell potential values from 9 specimens with clear spacing of 2, 3, and 4-inches are taken for comparison. Comparison includes the specimens with 1 and 2 cathodes and also specimens with and without stay-in-place forms for the connected condition.

As shown in Figure 30, it can be noted that the half-cell potential values up to about 14 months do not have visible differences between them, irrespective of the spacing differences, which agrees with Smolinski's inference. But the values after 35 months show a consistent difference between the 4-inch and 2 & 3-inch spacing values. Out of the three spacings, the 4-inch spacing appears as a more negative potential than the other two spacings. Also, the 2-inch and 3-inch

spacings do not have visible differences between them. Statistical analysis of the results is presented later.

Number of Cathodes

To identify the influence of the number of cathodes, or the number of bottom reinforcement bars per top reinforcement bar, the averages of the half-cell potentials among the cathode groups are compared. The comparison is shown as x-y plot between half-cell potential and time in months.

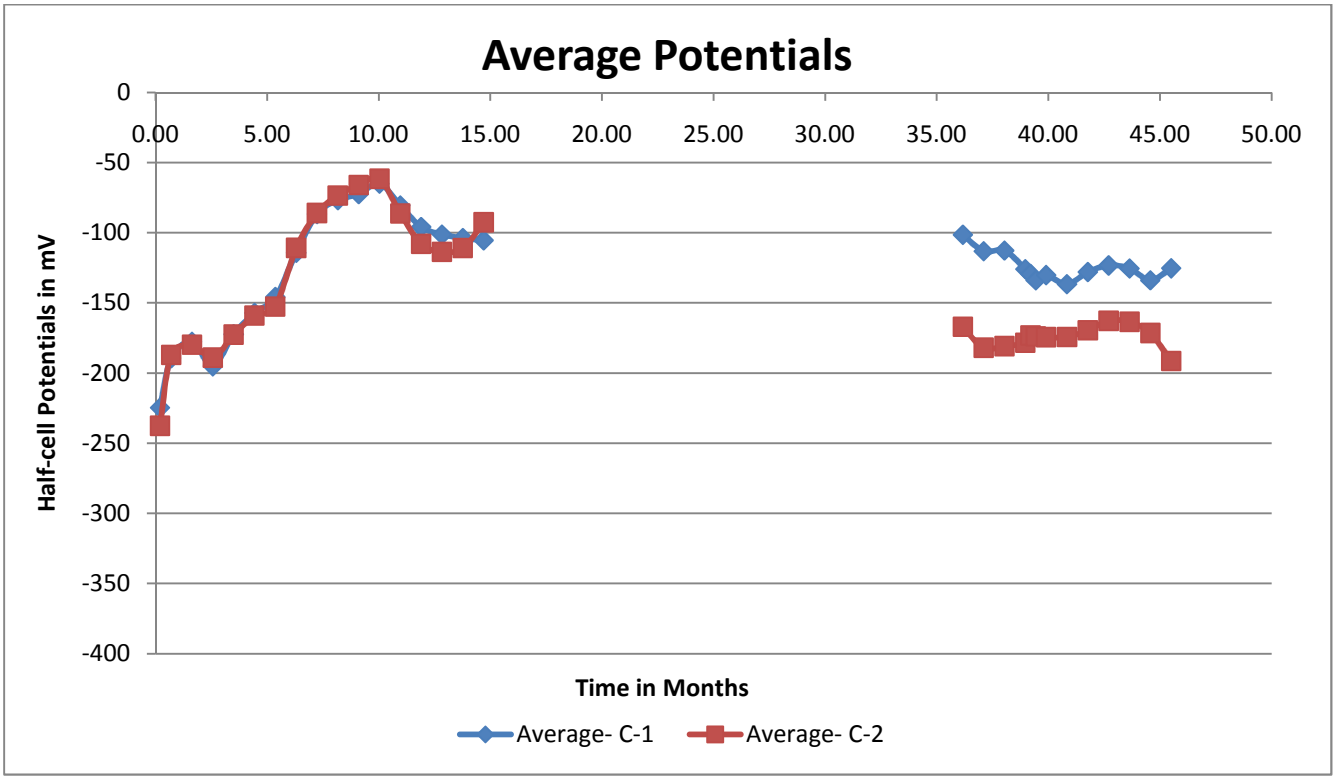

Figure 31 – Average Half-Cell Potentials of Specimens with 1 & 2 Cathodes

The averages of the half-cell potential values from 9 specimens with one cathode and 18 specimens with two cathodes are used for comparison. The comparison includes the specimens with 2, 3, and 4-inch clear spacings and also specimens with and without stay-in-place forms.

As shown in Figure 31, the potential values up to about 14 months show little differences between them irrespective of the number of cathodes following the same trend as the spacing differences plot, which agrees with Smolinski's inference. But after 35 months, the potentials of specimens with two cathodes have more negative potentials than specimens with 1 cathode. However, both one and two-cathode specimens are in the same range of less than a 10%

probability of active corrosion. Statistical analysis are presented later to illustrate any difference between 1 and 2 cathodes.

Presence of Stay-In-Place (SIP) forms

To identify the influence of the presence of the stay-in-place (SIP) forms on the corrosion activity, the averages of the half-cell potentials among the SIP groups are compared in the connected configuration. The comparison is shown as a x-y plot between half-cell potential and time in months.

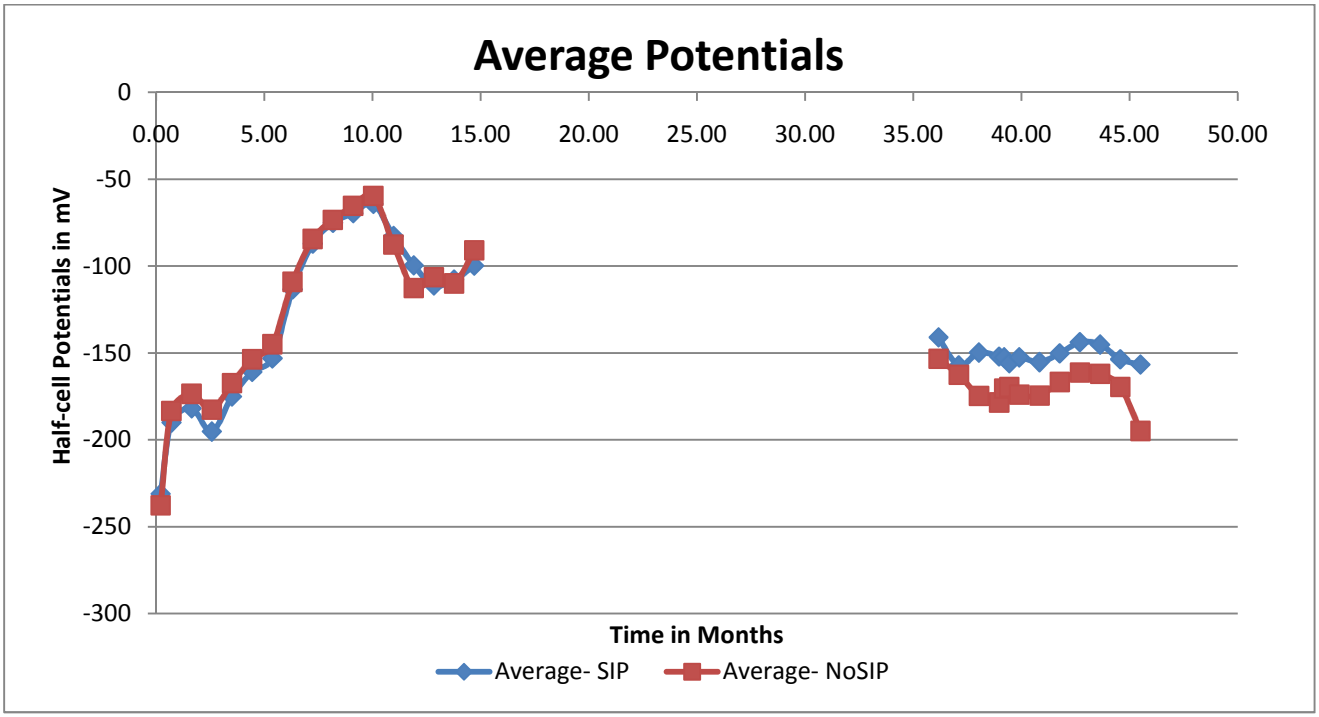

Figure 32 – Average Half-Cell Potentials of Specimens With & Without SIP

The averages of the potential values from 18 specimens with stay-in-place forms and 9 specimens without stay-in-place forms are taken for comparison. Comparison includes the specimens with 2, 3, and 4-inch clear spacings and also specimens with 1 and 2 cathode bars.

As shown in Figure 32, the potential values up to about 14 months are approximately the same, irrespective of the presence of SIP, following the same trend as the spacing differences and cathode results, which agree with Smolinski's inference. After 35 months, the specimens with SIP show a little, but consistent, difference in potential compared to the specimens without SIP.

Statistical analysis was conducted to determine if there is a significant difference between the presence and absence of SIP on potentials and is presented later.

Connection State

The measurements were performed for two conditions – connected and unconnected. To identify the influence of the macrocell corrosion in the total corrosion activity, the average of the half-cell potentials among the connected and unconnected groups is compared. The comparison is shown as x-y plot between half-cell potential and time in months.

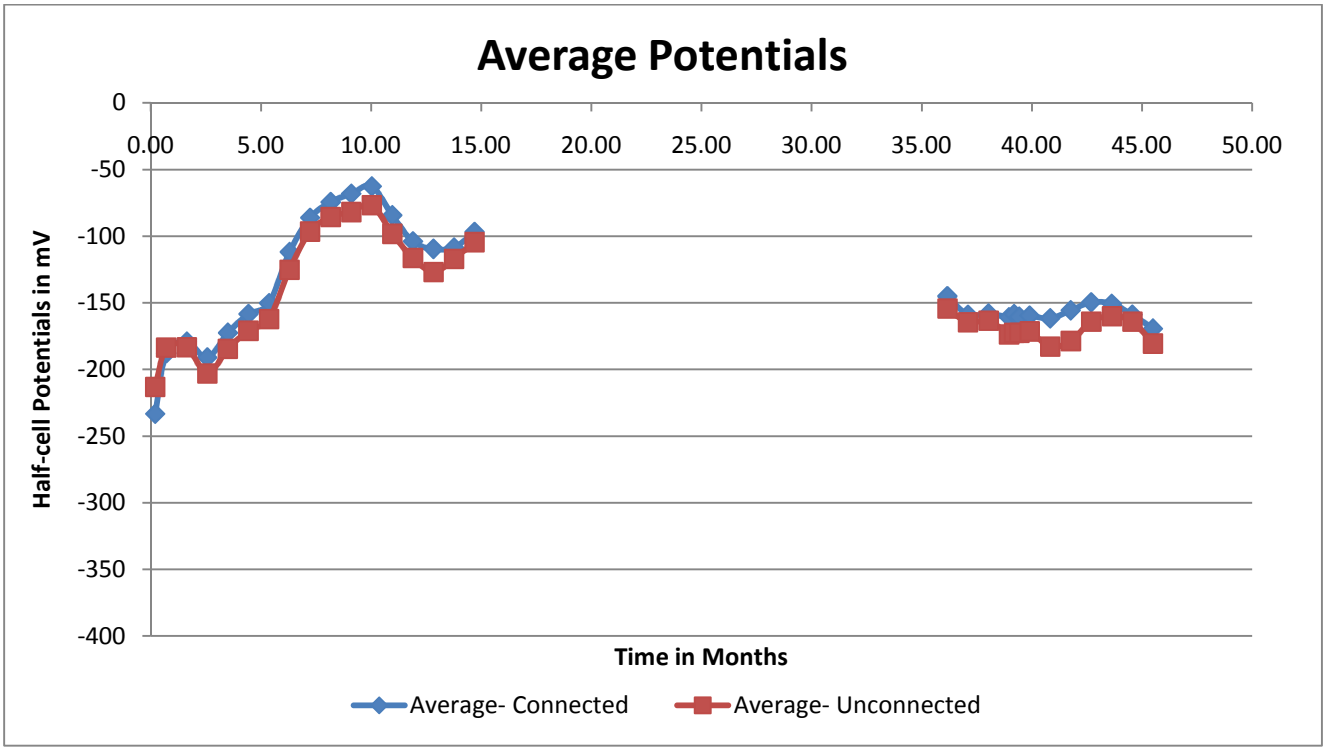

Figure 33 – Connected and Unconnected – Average Half-Cell Potentials

The average of the potential values from all 27 specimens at connected and unconnected are compared. Comparison includes the specimens with 2, 3, and 4-inch clear spacings, specimens with 1 & 2 cathodes and also specimens with and without SIP forms.

As illustrated in Figure 33, there is little difference between the connected and unconnected potentials. Since the connected values represent the total corrosion and the unconnected values represent the microcell corrosion, the difference between the connected and unconnected values represent the influence of the macrocell currents in the overall corrosion. As shown, there is little

difference between the connected and unconnected potentials. Thus, there appears to be little influence from the macrocell corrosion on the corrosion potential.

Statistical Analysis

Statistical analyses were performed to identify the influence of spacing differences, cathode bar differences, and stay-in-place forms differences on half-cell potential. The analyses include the ANOVA one-way analysis of the means and student's t-test to determine significant differences.

Clear Spacing Differences

ANOVA one-way analysis was performed with 2, 3, and 4-inch spacings as the nominal terms and potentials at 35, 40, and 45 months.

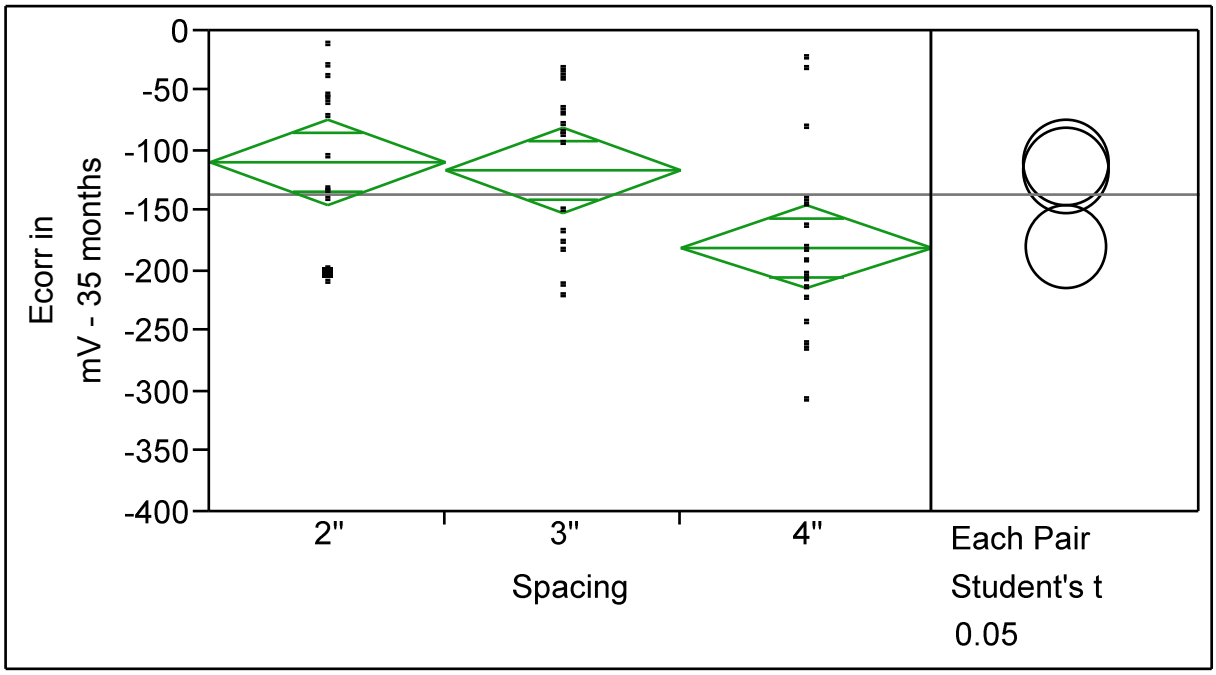

Figure 34 – Statistical Analysis – Half-Cell Potentials of 2", 3" & 4" Spacing at 35 Months

The analysis plot (Figure 34) with potentials at 35 months shows that there is significant difference between the 2, 3, and 4-inch spacings. The student's t-test shows that for the 4-inch spacing, even though the student's t-test circle very slightly overlaps 3-inch spacing, is significantly different from 2 and 3-inch spacings. The cleaning of connections was performed at about 38 months, which is later than the 35 months. Whereas, the 40 and 45 month plots represent the potentials after the connection were cleaned. It may be expected that the cleaning of

the connections would have an effect on the corrosion measurements.

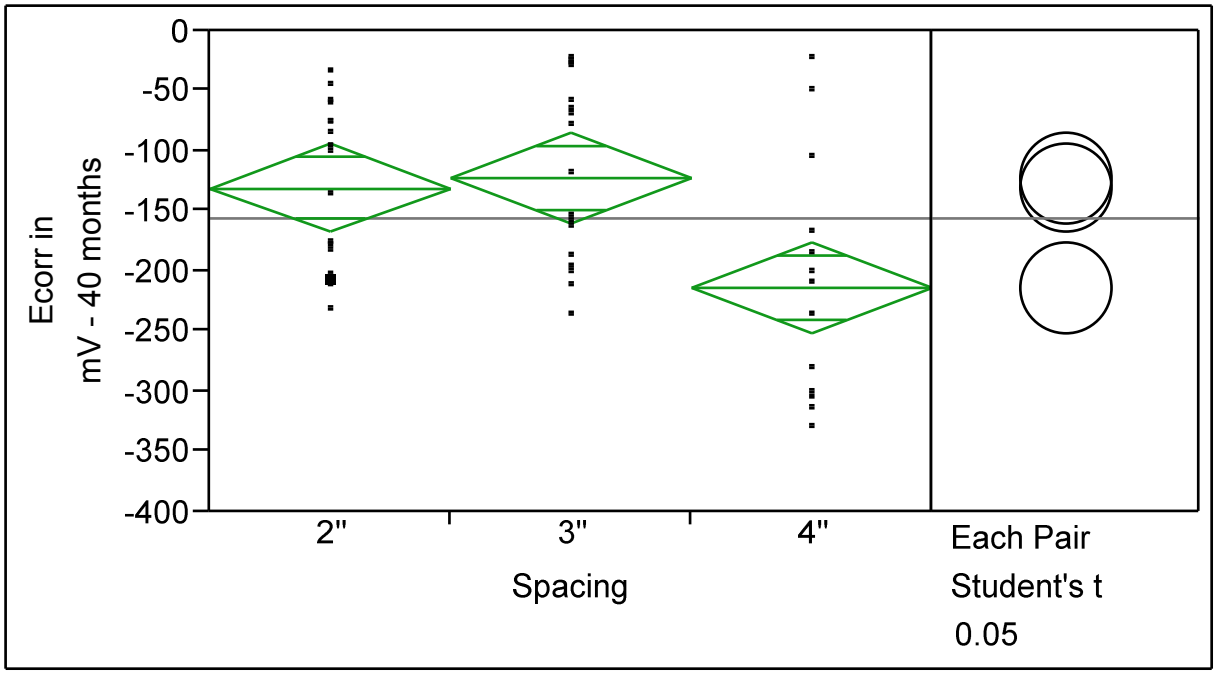

Figure 35 – Statistical Analysis – Half-Cell Potentials of 2", 3" & 4" Spacing at 40 Months

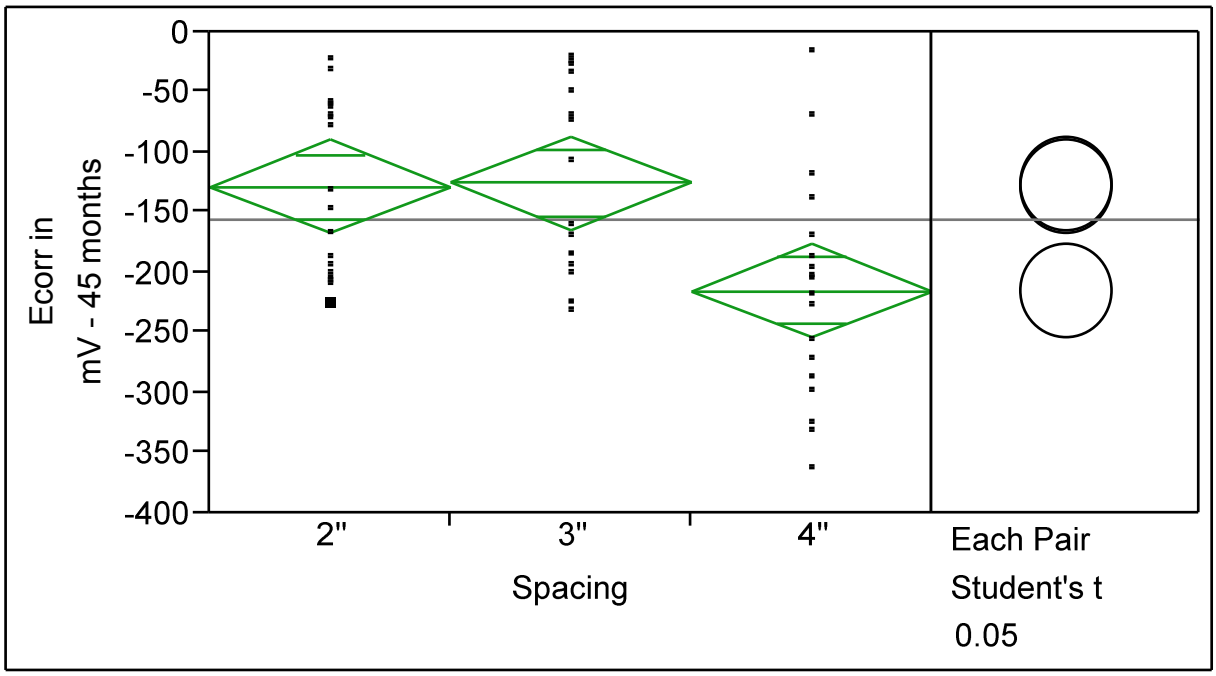

Figure 36 – Statistical Analysis – Half-Cell Potentials of 2", 3" & 4" Spacing Specimens at 45 Months

As shown in Figures 35 and 36, the potentials of 2 and 3-inch spacings are more positive than 4-inch spacing specimens. The 40 (Figure 35) and 45 month (Figure 36) potentials of the 4-inch spacing values are significantly different from the 2 and 3-inch spacing specimens, while the 2 and 3-inch spacings are almost identical.

Number of Cathodes

ANOVA one-way analysis is conducted with 1, and 2 cathodes as the nominal terms and the potentials at 35, 40, and 45 months are taken to identify the significant differences. This analysis includes the 2, 3, and 4-inch spacings even though significant difference was found between the different spacings for resistivities and potentials.

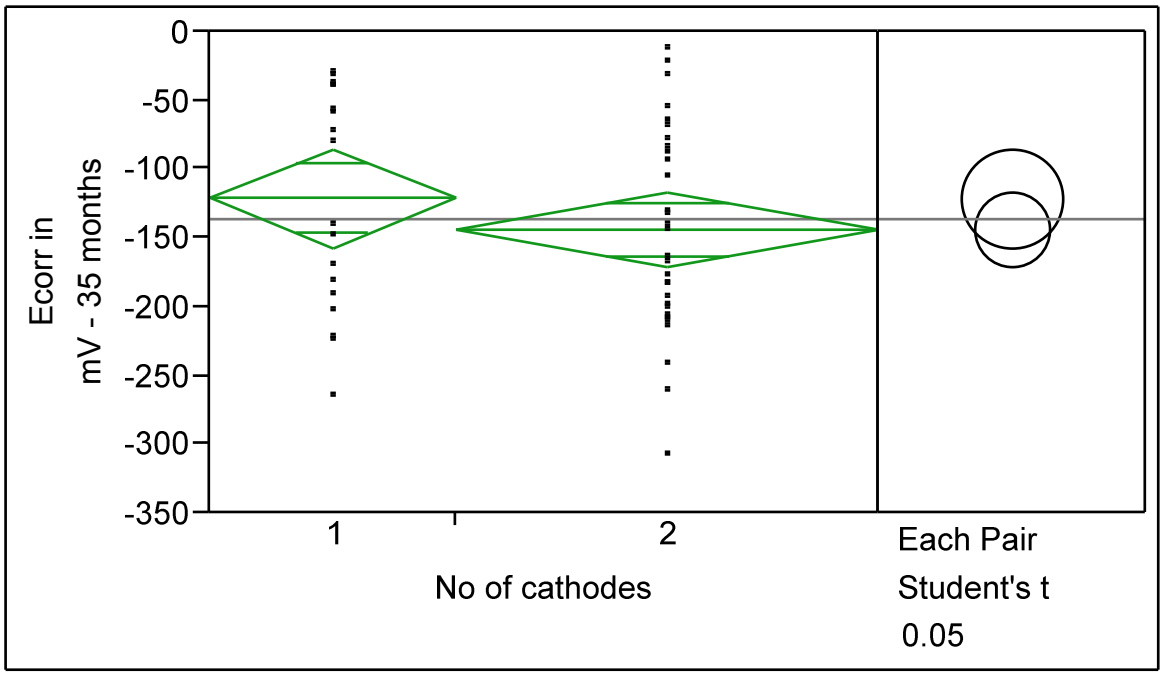

Figure 37 – Statistical Analysis – Half-Cell Potentials of 1 & 2 Cathodes at 35 Months

The one-way analysis and student's t-test of potentials at 35 months (Figure 37) show that there is no significant difference between the 1, and 2 cathodes. The cleaning up of the specimens was completed at about 38 months, which is after 35 months analysis. Thus the 40 and 45 month plots represent the potentials after the connection cleaning. It was expected that the connection would affect the potentials, because of influence from corrosion at the bar ends.

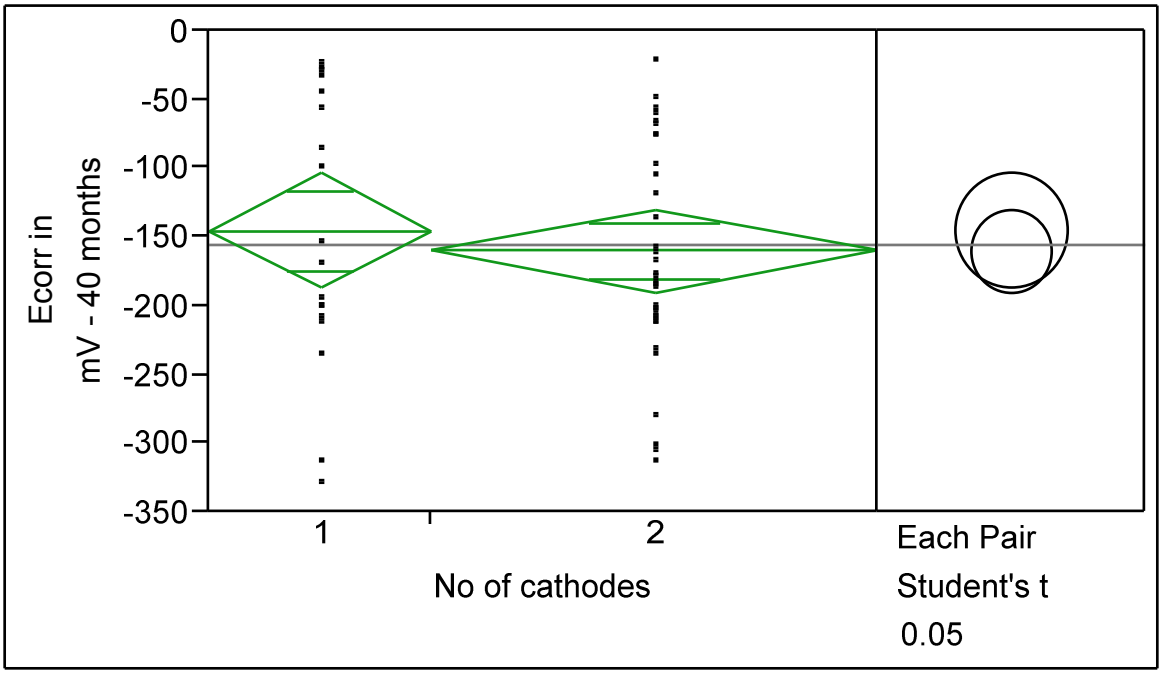

Figure 38 – Statistical Analysis – Half-Cell Potentials of 1 & 2 Cathodes at 40 Months

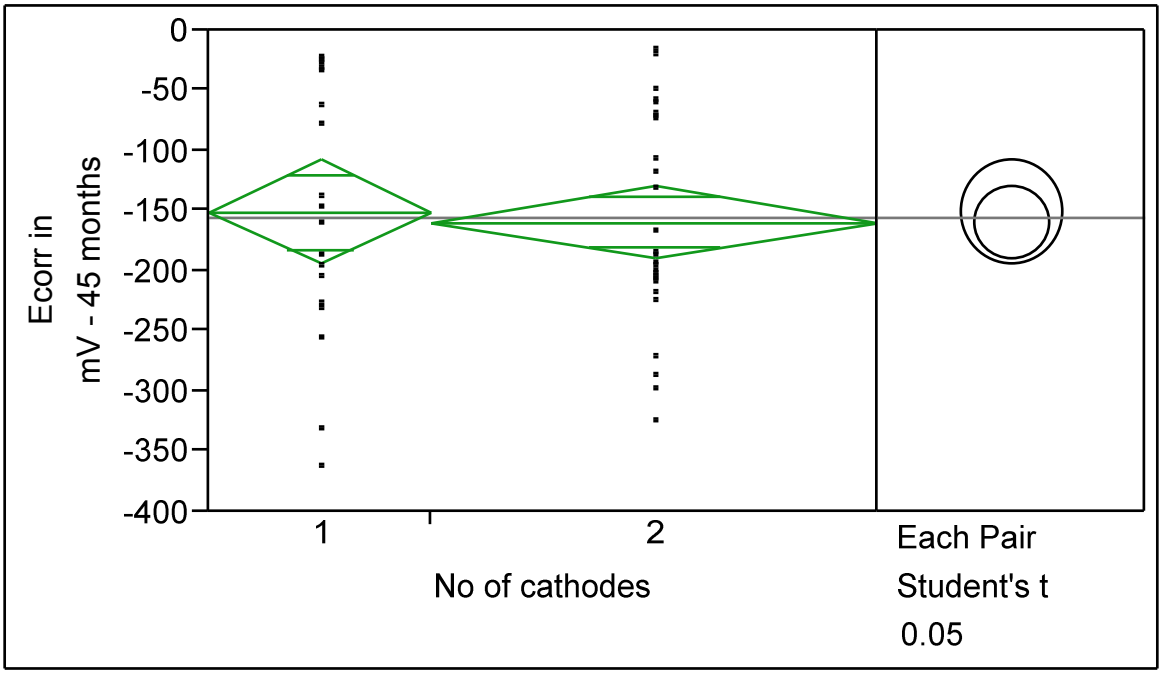

Figure 39 – Statistical Analysis – Half-Cell Potentials of 1 & 2 Cathodes at 45 Months

The analysis shows that there is no significant difference between the 1 and 2 cathodes at 40 (Figure 38) and 45 months (Figure 39). Thus, even considering the spacing factor, the number of cathodes has no significant influence on half-cell potentials.

When including the spacing differences, the number of cathodes may not show any differences. Thus, only the potentials of specimens with 4-inch spacing at 45 months are taken and the analysis was performed by taking number of cathodes as the nominal term.

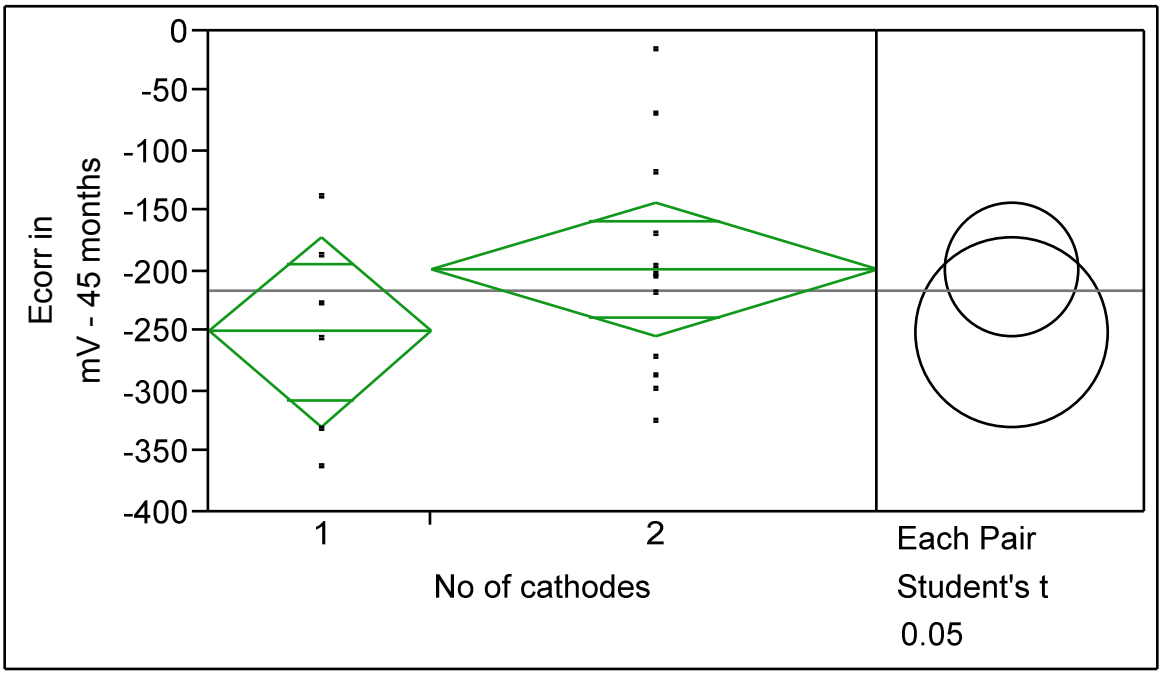

Figure 40 – Statistical Analysis – Half-Cell Potentials of 4" Spacing Specimens with 1 & 2 Cathodes at 45 Months

As shown in Figure 40, the specimens with two cathodes have potentials which are slightly more positive than the specimens with one cathode. Anyhow, there is no statistical significance between the 1 and 2 cathode specimens when it comes to potentials.

Presence of Stay-In-Place (SIP) forms

ANOVA one-way analysis was performed using specimens with SIP (Yes) and without SIP (No) as the nominal terms and the potentials at 35, 40, and 45 months to identify significant differences. The analysis includes the 2, 3, and 4-inch spacings even though significant difference was found between the different spacings for both resistivity and potentials. Analysis

also includes the different number of cathodes, since no significant difference was found between them.

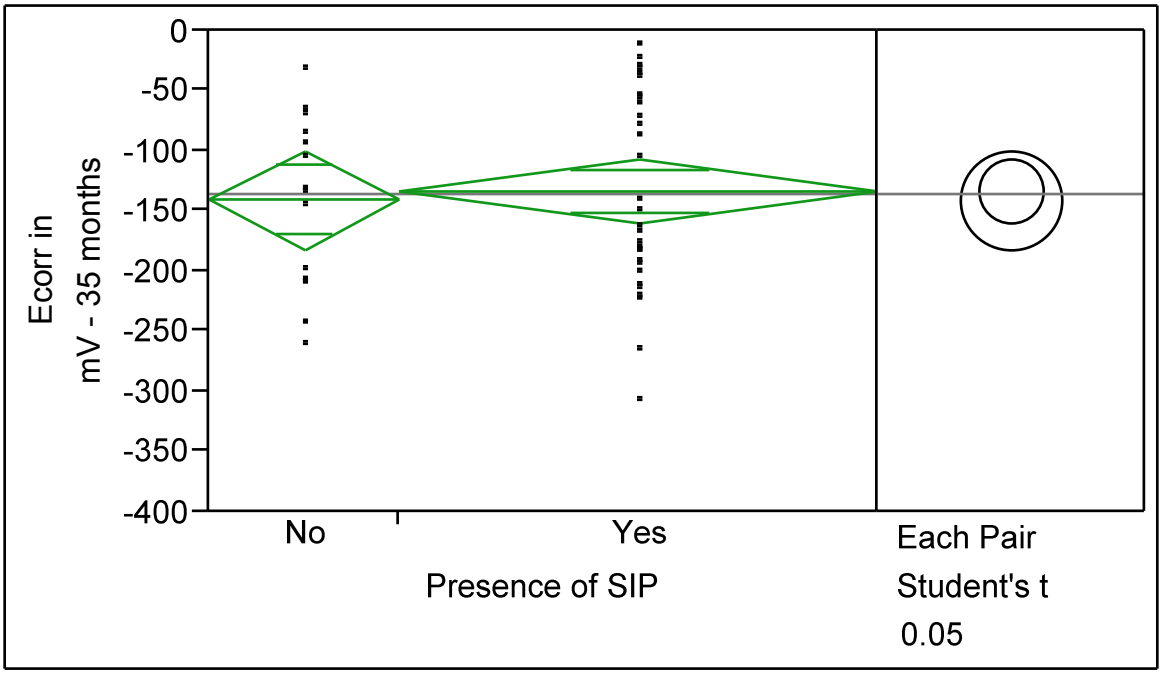

Figure 41 – Statistical Analysis – Half-Cell Potentials of With & Without SIP at 35 Months

The one-way analysis and student's t-test of potentials at 35 months (Figure 41) show that there is no significant difference between potentials of specimens with SIP (Yes) and without SIP (No). The cleaning up of the specimens was completed at approximately at 38 months, which is after than the 35 months. Thus the 40 and 45 month plots represent the potentials after the cleaning up was completed. It was expected for the cleaning would have an effect on the potentials, because of influence of corrosion at the ends of the bar.

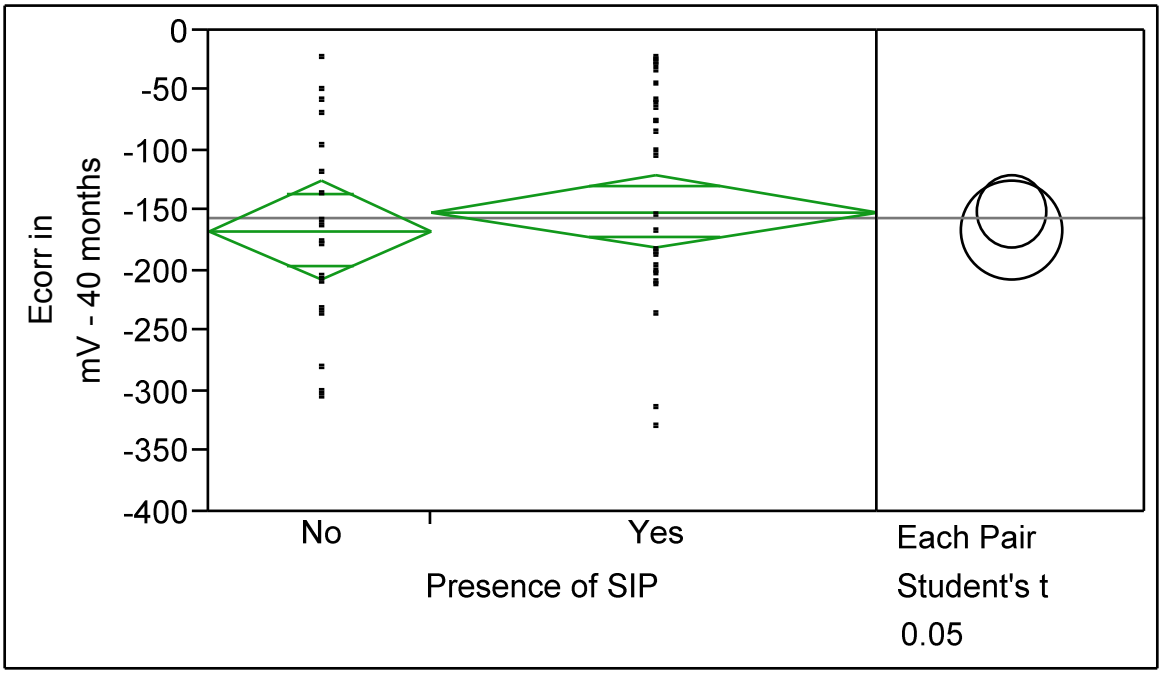

Figure 42 – Statistical Analysis – Half-Cell Potentials of With & Without SIP at 40 Months

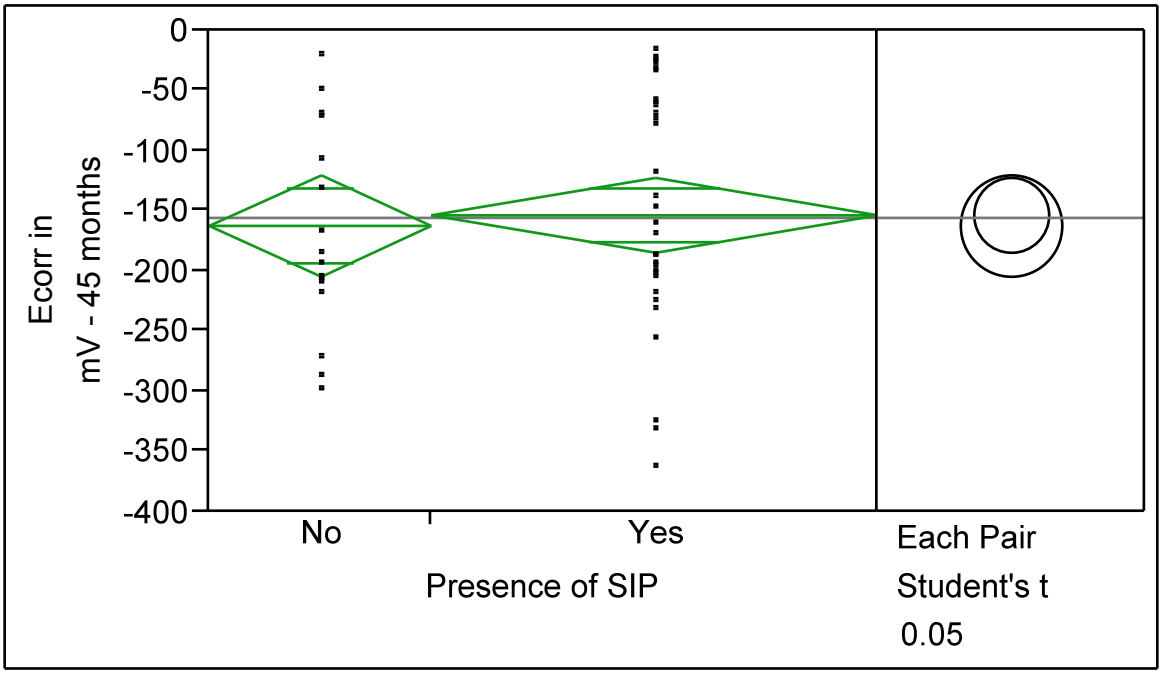

Figure 43 – Statistical Analysis – Half-Cell Potentials of With & Without SIP at 45 Months

The analysis shows that there is no significant difference between the potentials of specimens with SIP (Yes) and without SIP (No) at 40 (Figure 42) and 45 months (Figure 43). The specimens with SIP (Yes) are slightly less negative than specimens without SIP (No). There is a large spread in specimens with SIP (Yes) because of more number of specimens. But when taking into account of all the spacings, the presence of SIP have no significant influence on potentials.

If the spacing differences are included in the analysis, the influence of SIP may not be identified. Thus, only the potentials of specimens with 4-inch spacing at 45 months were used in an analysis of SIP as the nominal term.

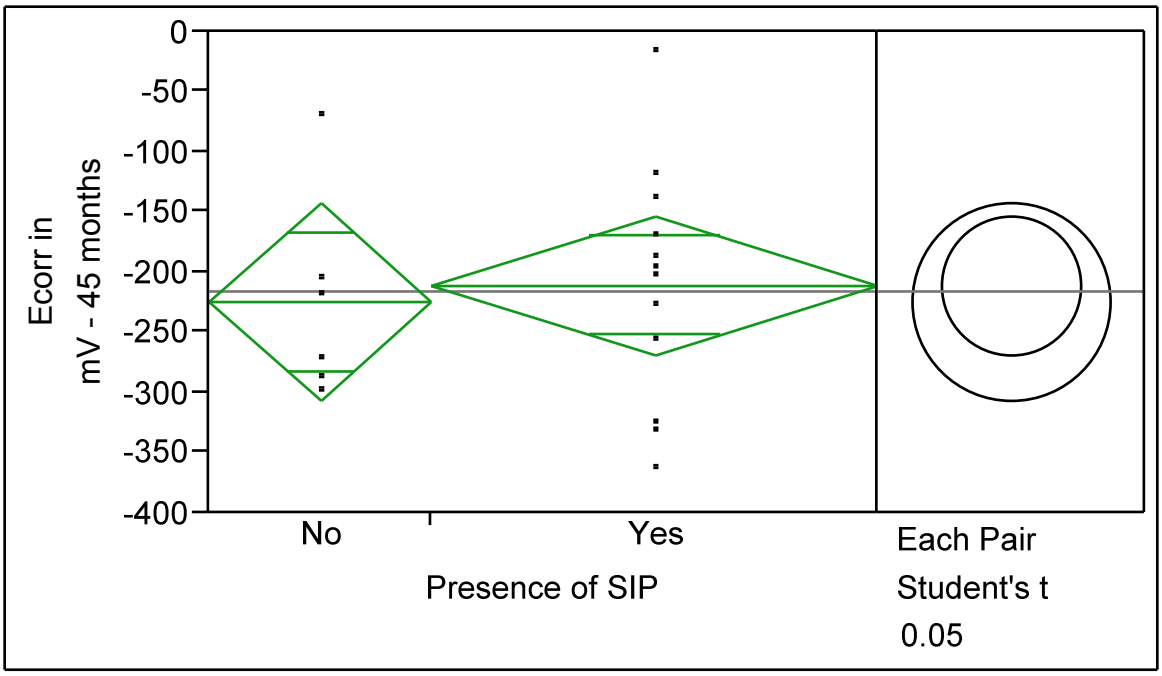

Figure 44 – Statistical Analysis – Half-Cell Potentials of 4" Spacing Specimens With & Without SIP at 45 Months

As shown in Figure 44, the presence of SIP does not have any influence on potential even if the spacing differences are taken into account.

Connection State

To find if the macrocell corrosion has large influence on the total corrosion, statistical analysis was performed with the connected (CON) and unconnected (UNCON) states as the nominal terms. The analysis was performed for 35, 40, and 45 months to identify significant differences. After the connected readings were taken, the connecting wire was disconnected and then allowed to stabilize for a minimum of 20 minutes. Then the unconnected readings were taken.

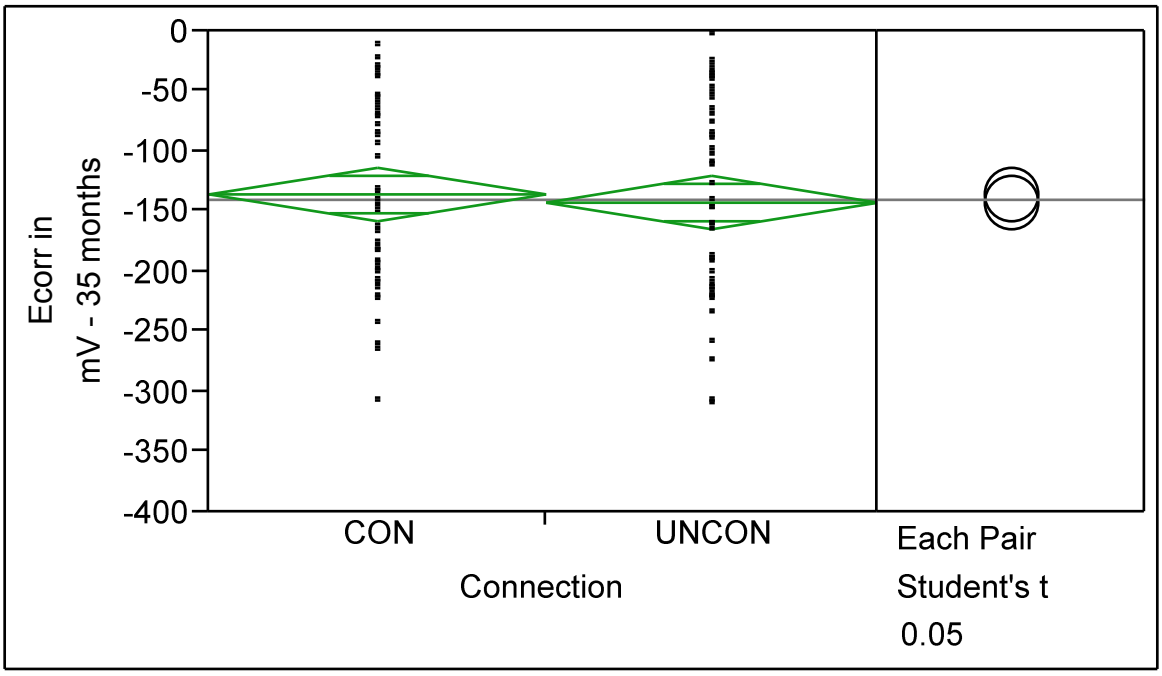

Figure 45 – Statistical Analysis – Connected & Unconnected Half-Cell Potentials at 35 Months

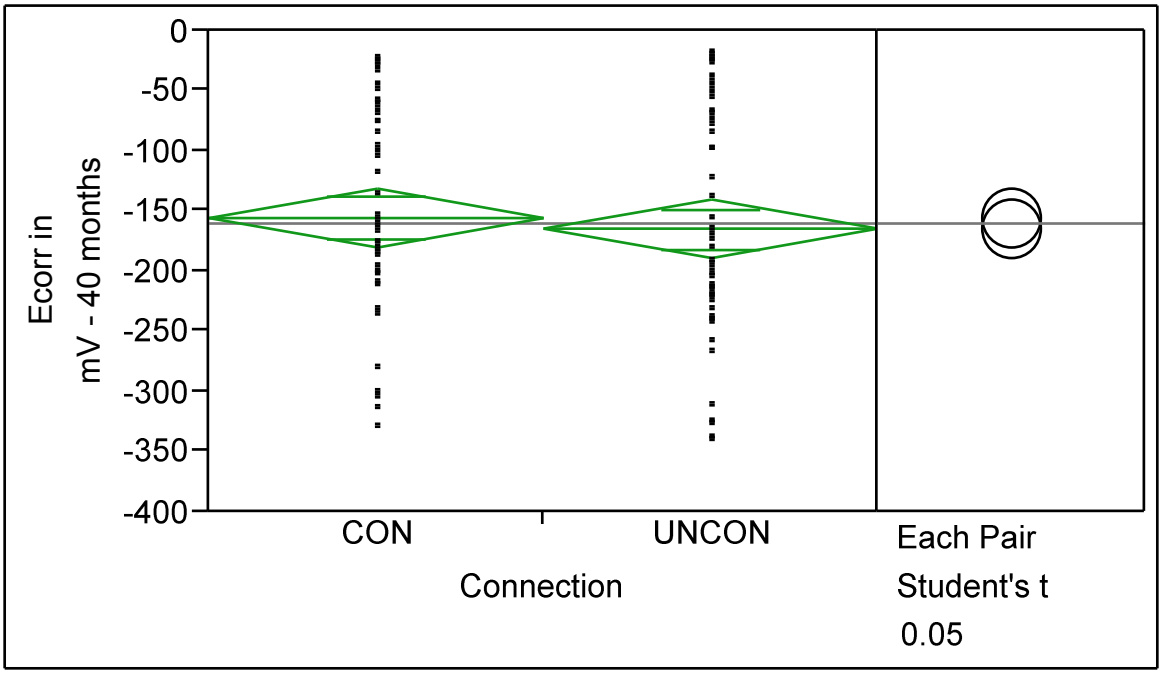

Figure 46 – Statistical Analysis – Connected & Unconnected Half-Cell Potentials at 40 Months

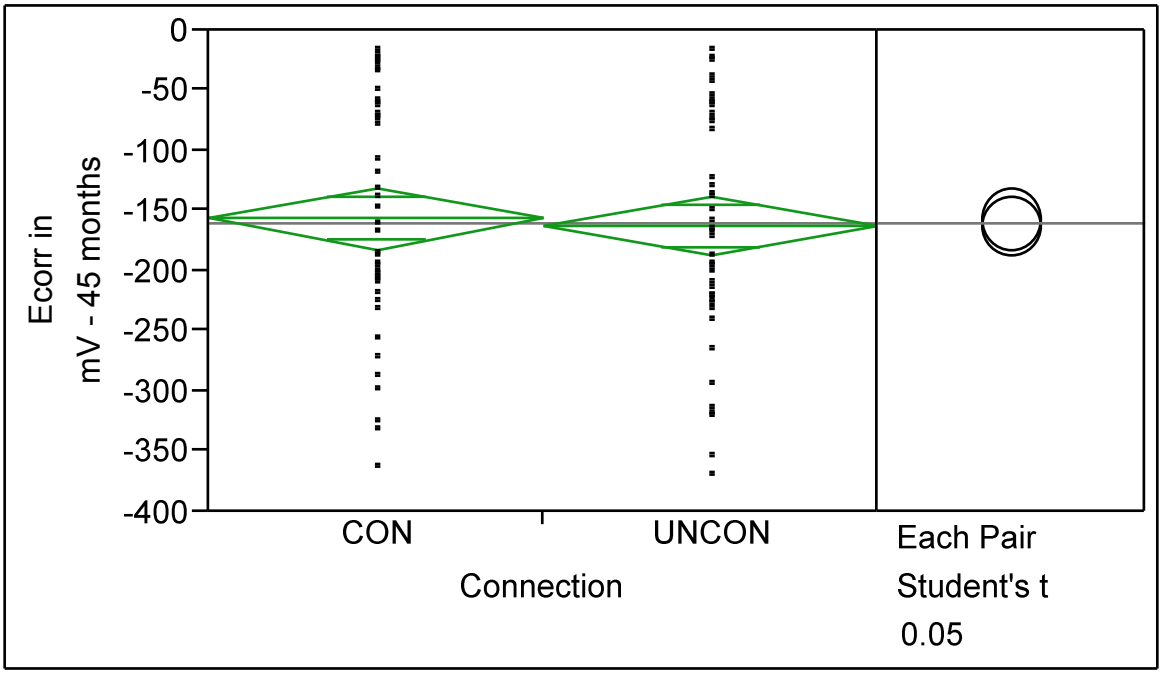

Figure 47 – Statistical Analysis – Connected & Unconnected Half-Cell Potentials at 45 Months

As shown in Figures 45, 46, and 47, it can be stated that there is no significant difference between connected and unconnected potential values. Thus, the macrocell corrosion appears less significant compared to microcell corrosion on the corrosion potential.

Corrosion Current Density

The 3LP device, an unguarded linear polarization instrument, developed by Kenneth C. Clear, was used to measure the corrosion current density. According if the corrosion current value is greater than 10 $\mu A/cm^2$, then the corrosion damage can be expected in 2 years or less. No corrosion damage can be expected if the corrosion current value is lesser than 0.2 $\mu A/cm^2$. The measurements were performed in both connected and unconnected states. The corrosion current density data up to 15 months were taken from Smolinski's work and integrated with the results of this study. The measurements from approximately 15 to 35 months are not available. But since the specimens were maintained in controlled temperature and humidity, and the ponding cycles continued, a trend can be illustrated for 15 to 35 month time period.

For illustration purposes, corrosion current density of 2-inch spacing is presented in Figure 48.

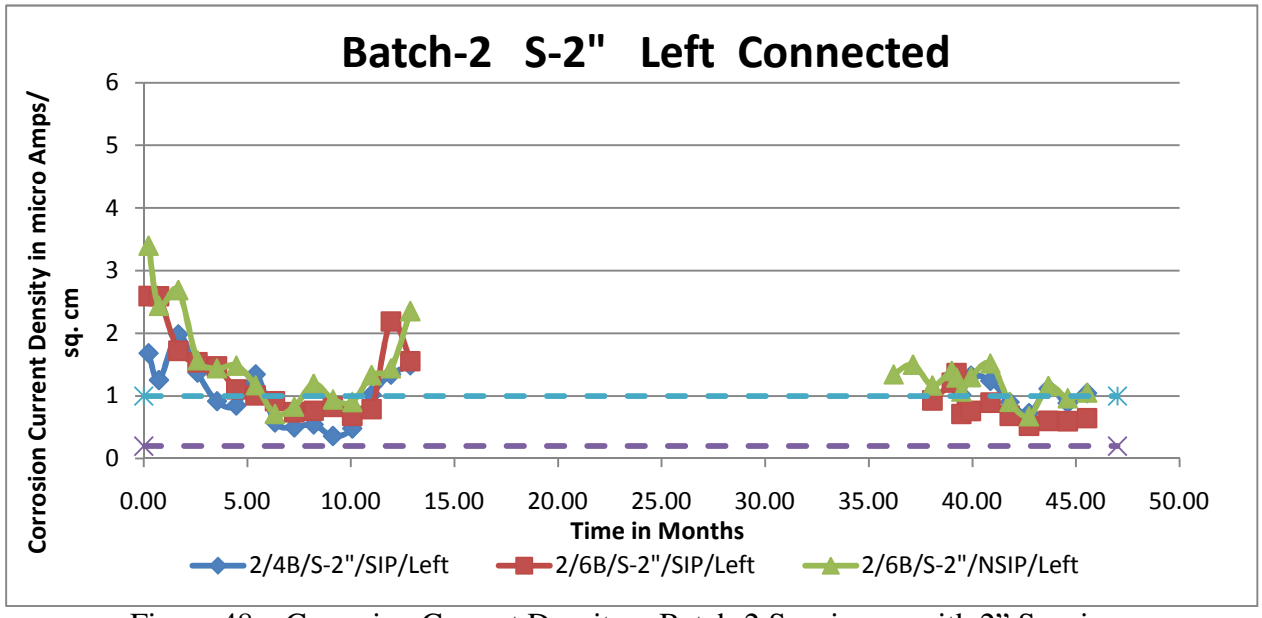

Figure 48 – Corrosion Current Density – Batch-2 Specimens with 2" Spacing

In the plots, the lower dotted horizontal line, parallel to X-axis, denotes the critical point below which there is no corrosion damage. The upper dotted horizontal line, parallel to X-axis, denotes the critical point above which the corrosion damage is expected in 2 to 10 years. The middle

region between the two horizontal lines, parallel to X-axis, denotes that the corrosion damage can be expected in 10 to 15 years.

For the remainder of this study the following relative terms will be used for the corrosion current density readings.

- Less than 0.2 µA/cm^2 no active corrosion
- 0.2 to 1.0 µA/cm^2 low active corrosion
- 1.0 to 10.0 µA/cm^2 moderate active corrosion
- Greater than 10 µA/cm^2 high active corrosion

As shown in Figure 48, the initial *icorr* values are higher and about 1.5 µA/cm^2 as a result of the formation of the passive layer. The drcrease to below 0.5 µA/cm$^{2\ \text{at about}}$ 10 months followed by an increase to above 1.0 µA/cm^2 may also be related to the continuing formation of the passive layer. From 35 to 45 months, the *icorr* was about 0.75 µA/cm^2, which is a low rate of corrosion.

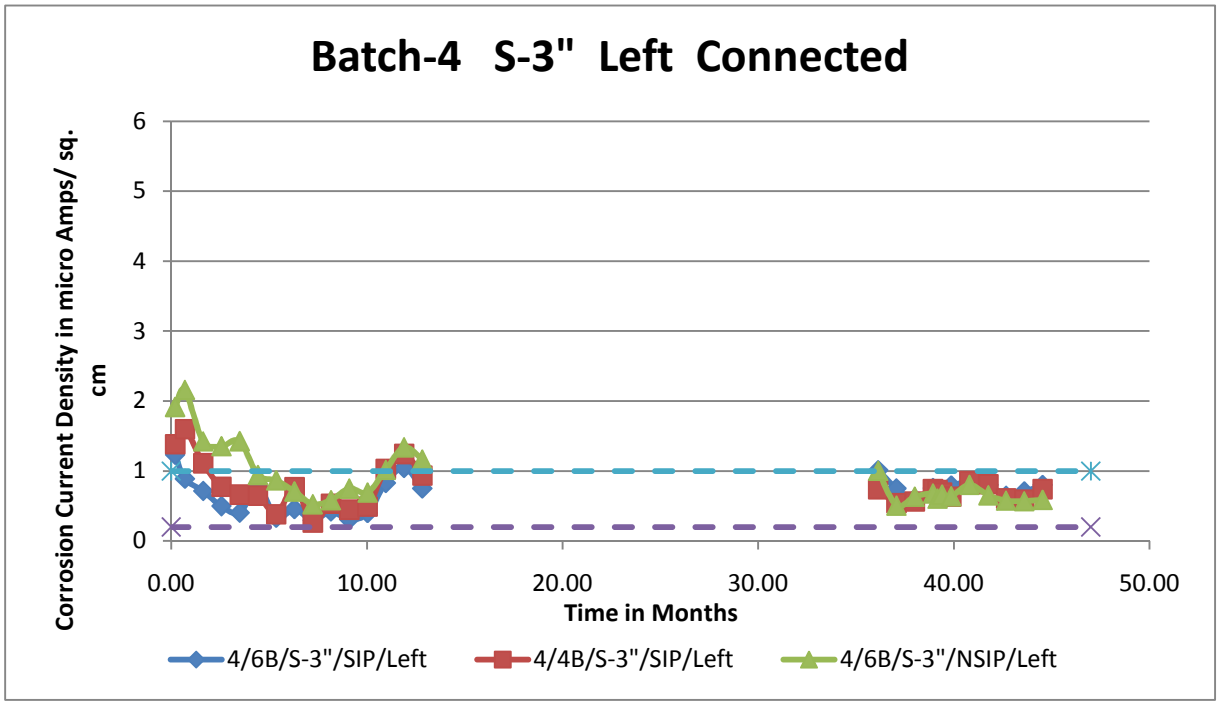

Figure 49 – Corrosion Current Density – Batch-4 Specimens with 3" Spacing

Figure 49 represents the batch-4 specimens with 3-inch spacing. The presented values are only for the left side triad bars and connected state. Similar to the 2-inch spacing specimens, *icorr* values are higher at the beginning then decrease to about 1 µA/cm^2 at 14 months. The *icorr*

measurements after 35 months are about 0.75 µA/cm^2 for all the specimens in this batch. The *icorr* values of 3-inch spacing specimens are within the low corrosion rate.

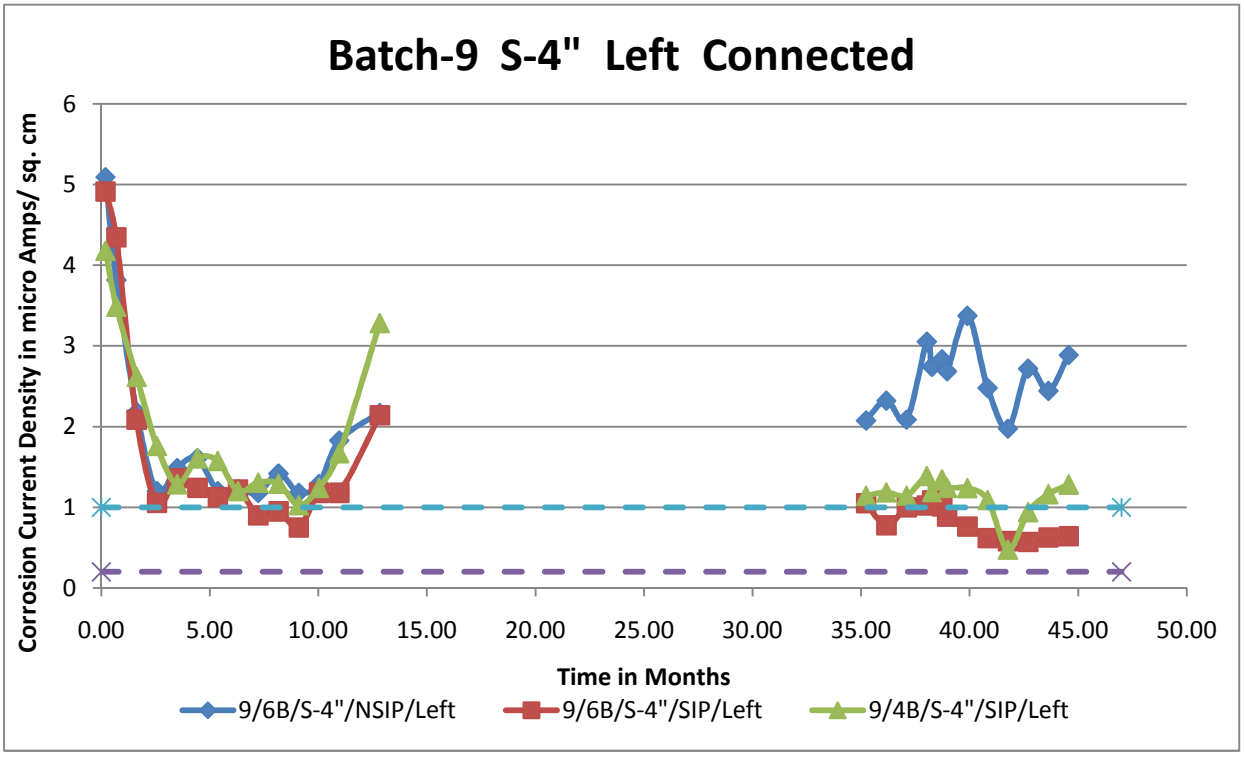

Figure 50 – Corrosion Current Density – Batch-9 Specimens with 4" Spacing

Figure 50 presents the *icorr* values of batch-9 with a clear spacing of 4-inches for the left side triad bars and connected state. Similar to the 2-inch and 3-inch spacing specimens, moderate corrosion rates are exhibited in the beginning. It is possibly the formation of passive layer. With time, the corrosion continues to decrease to10 months and then increases to about 2 µA/cm^2 at about 14 months. Some of the specimens have *icorr* values over 2 µA/cm^2, while some *icorr* values are about 1 µA/cm^2. The variability within the 4 inch batch may be related to the presence of SIP forms, as the NoSIP is greater than the two SIP specimens.

The influence of the differences in the clear spacing, number of cathodes and the presence of stay-in-forms on the corrosion current density can be assessed by rearranging the data according to the conditions to be compared. The illustrated comparisons included early and later measurements to idenify the trend of variations in the *icorr* values. The trend may aid in the explanation of the corrosion activity that has been taking place in the specimens.

Clear Spacing Differences

To identify the influence of the clear spacing between the top reinforcement mat and the bottom reinforcement, the average of the *icorr* values among the spacing groups are compared. The comparison is shown as a normal x-y plot between *icorr* and time in months.

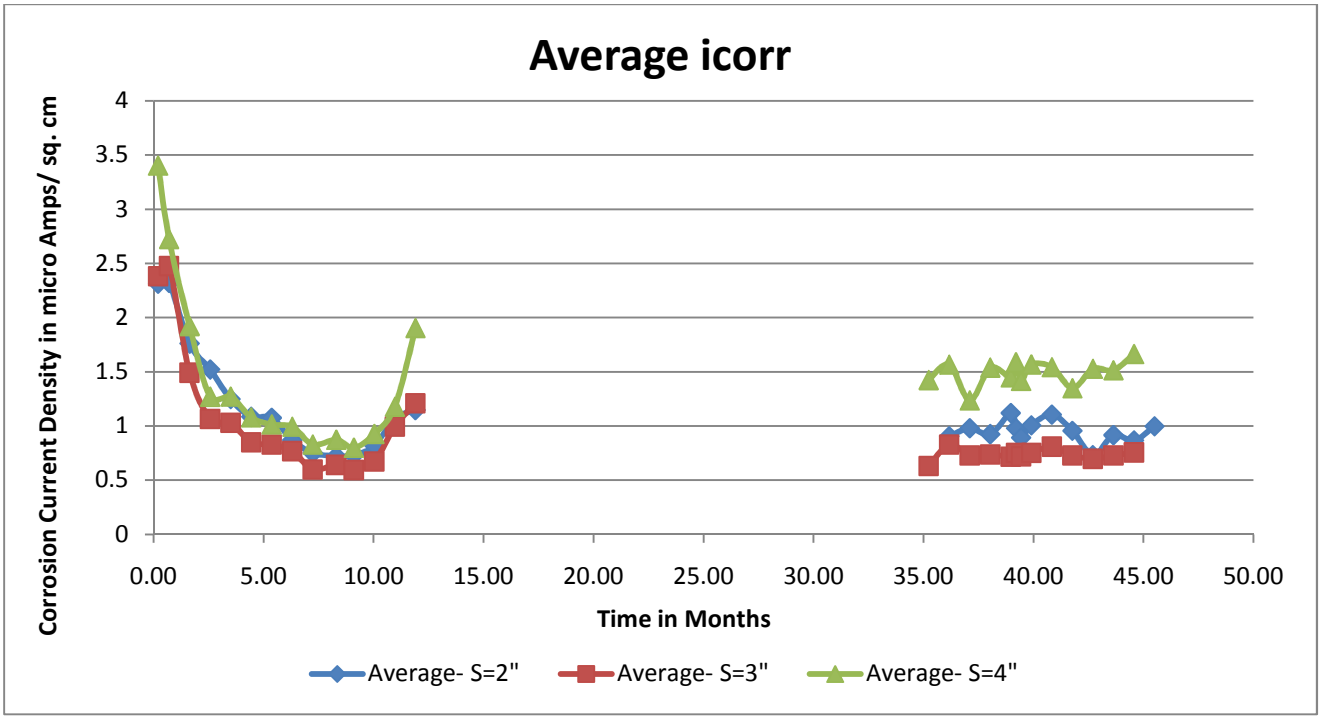

Figure 51 – Average Corrosion Current Density of 2", 3" & 4" Spacing Specimens

The average of the corrosion current density values from 9 specimens of clear spacing 2, 3, and 4-inches are taken for comparison. Comparison includes the specimens with 1 and 2 cathodes and also specimens with and without stay-in-place forms.

As shown in Figure 51, the *icorr* values up to about 14 months there is little difference between the spacing factors, which agrees with Smolinski's inference. But after 35 months, there is a consistent difference between the 4-inch and 2 & 3-inch spacing values. Out of the three spacings, the 4-inch spacing has a moderate corrosion rate. Whereas, the 2 and 3-inch spacings generally have a low corrosion rate with little differences between the *icorr* values. Statistical analyses of the results are presented later.

Number of Cathodes

To identify the influence of the number of cathodes or the number of bottom reinforcement bars for every top reinforcement bar on the corrosion rate, the average of the *icorr* values among the cathode groups are compared, see Figure 52.

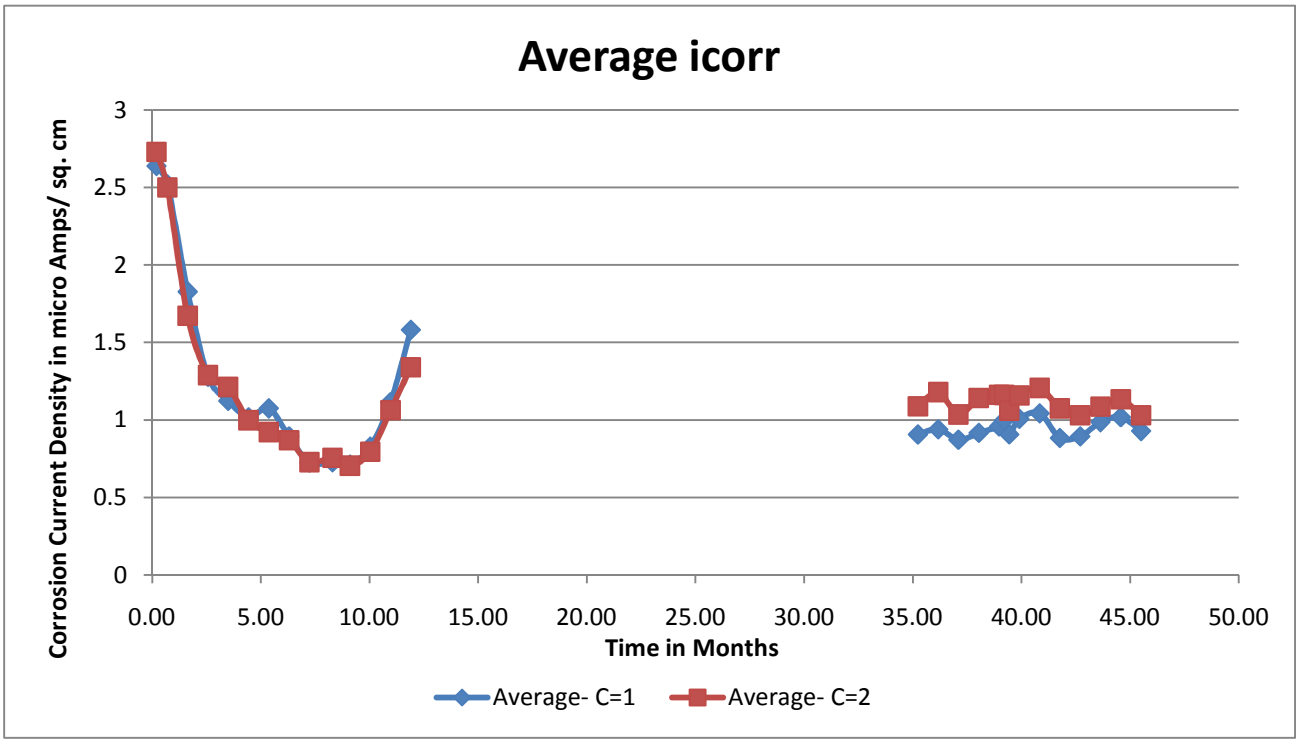

Figure 52 – Average Corrosion Current Density of 1 & 2 Cathodes

The averages of the *icorr* values from 9 specimens with one cathode and 18 specimens with two cathodes are taken for comparison. Comparison includes the specimens with 2, 3, and 4-inch clear spacings and also specimens with and without stay-in-place forms.

As shown in Figure 52, it can be noted that the *icorr* values up to about 14 months have little differences between them, irrespective of the number of cathodes, following the same trend as the spacing differences plot, which agrees with Smolinski's inference. But after 35 months, the *icorr* of specimens with two cathodes is slightly higher than the specimens with one cathode. However, both one and two cathode specimens are generally in the low corrosion rate. Statistical analysis is presented later to identify difference between 1 and 2 cathodes.

Presence of Stay-In-Place (SIP) forms

Figure 53 presents the icorr values versus time for the SIP and NoSIP cases.

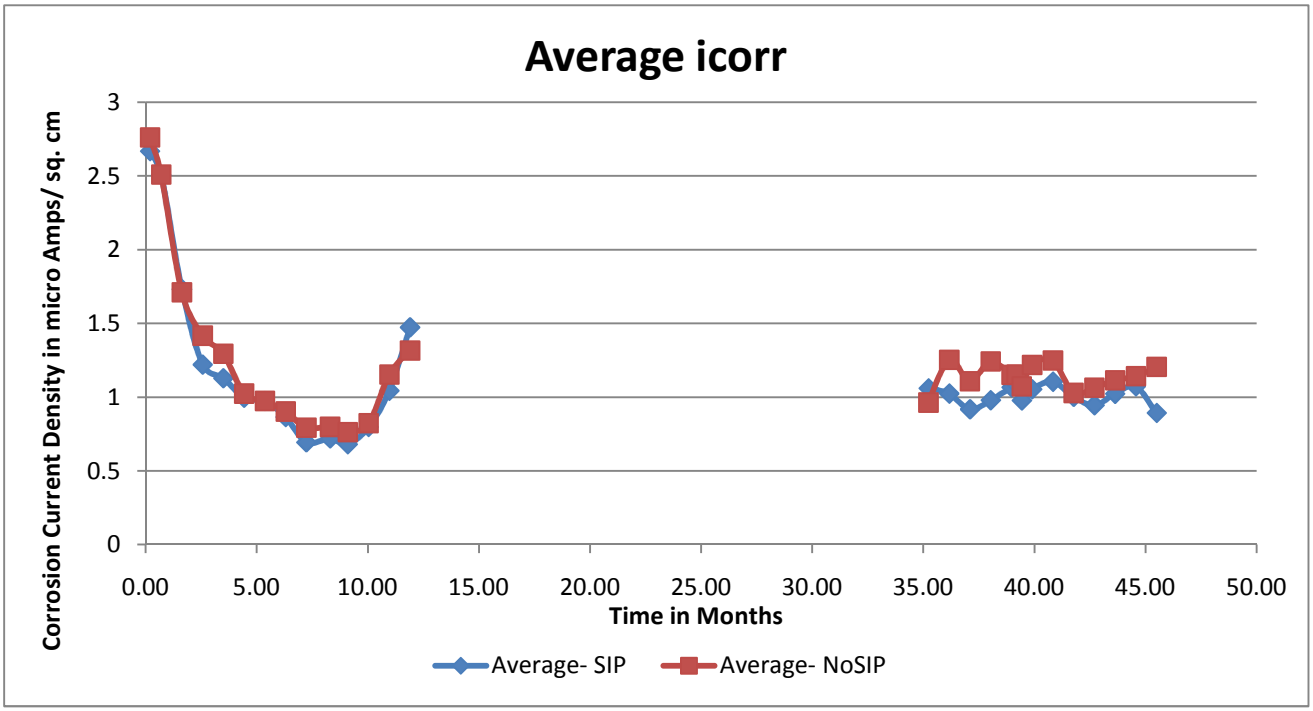

Figure 53 – Average Corrosion Current Density of Specimens With & Without SIP

The averages in the connected condition *icorr* values are for 18 specimens with stay-in-place forms and 9 specimens without stay-in-place forms for comparison purposes. Comparison includes the specimens with 2, 3, and 4-inch clear spacings and also specimens with 1 and 2 cathode bars.

As shown in Figure 53, *icorr* values up to about 14 months are nearly identical irrespective of the presence of SIP and follow the same trend as the spacing differences and cathode differences plots, which agrees with Smolinski's inference. After 35 months the specimens with NoSIP have a slightly higher *icorr* values compared to the specimens with SIP. Statistical analysis is presented later to identify significant difference between the presence and absence of SIP on *icorr*.

Connection State

The measurements were conducted in the – connected and unconnected state. To identify the influence of the macrocell corrosion in the total corrosion activity, the averages of the *icorr* values among the connected and unconnected groups is compared. The comparison is shown as a x-y plot of *icorr* and time in months.

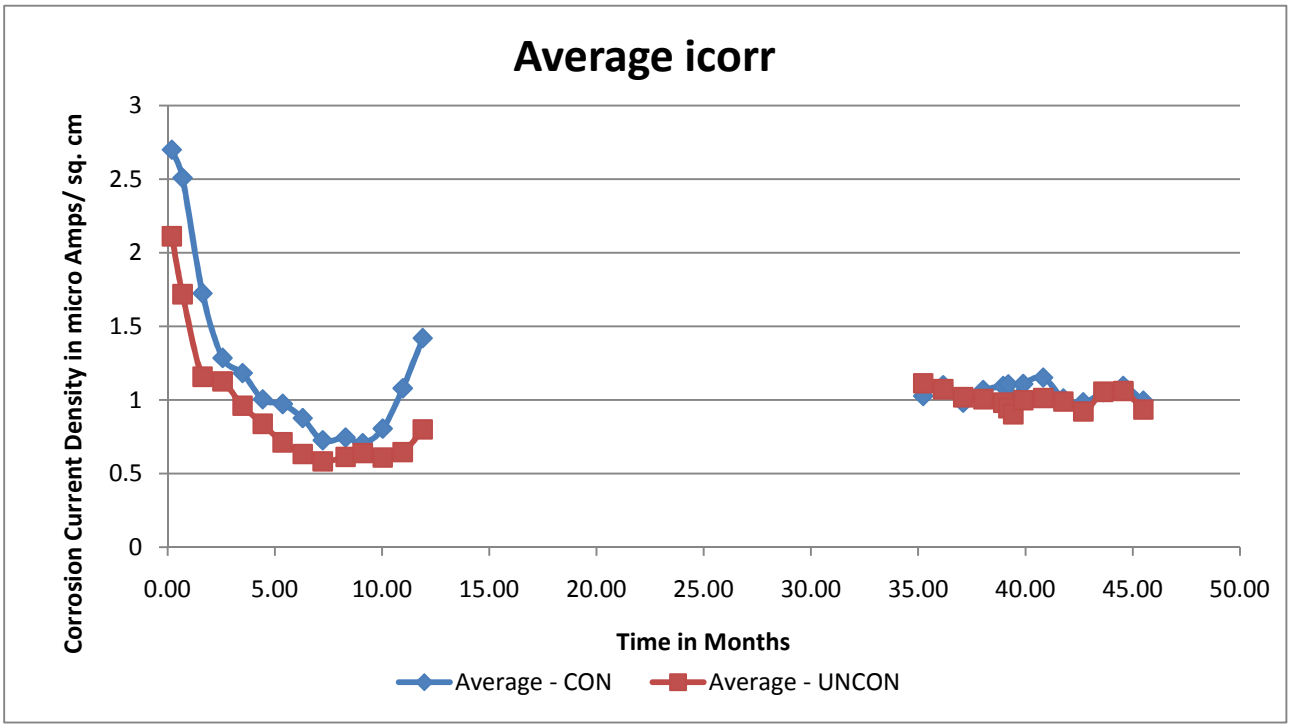

Figure 54 – Connected & Unconnected - Average Corrosion Current Density

The averages of the *icorr* values from all 27 specimens at connected and unconnected state are shown see Figure 54. Comparison includes the specimens with 2, 3, and 4-inch clear spacings, specimens with 1 & 2 cathodes and also specimens with and without SIP forms.

From the simple x-y plot between the connected and unconnected icorr (Figure 54), there appears to be little difference between connected and unconnected values. Since the connected values represent the total corrosion and the unconnected values represent the microcell corrosion, the difference between the connected and unconnected values should represent the influence of the macrocell currents in the overall corrosion. Figure 54 illustrates the difference between the connected and unconnected *icorr* is not notable, thus it can be inferred that macrocell corrosion is not the dominant form of corrosion. Statistical analysis of comparison is presented later.

Statistical Analysis

Statistical analyses are conducted to identify any significant differences between clear spacing differences, cathode bar differences, and stay-in-place forms on corrosion current density. The analyses include the ANOVA one-way analysis of the means and student's t-test to identify significant difference.

Clear Spacing Differences

ANOVA one-way analysis is presented for 2, 3, and 4-inch spacings as the nominal terms and *icorr* values at 35, 40, and 45 months, see Figures 55, 56, and 57.

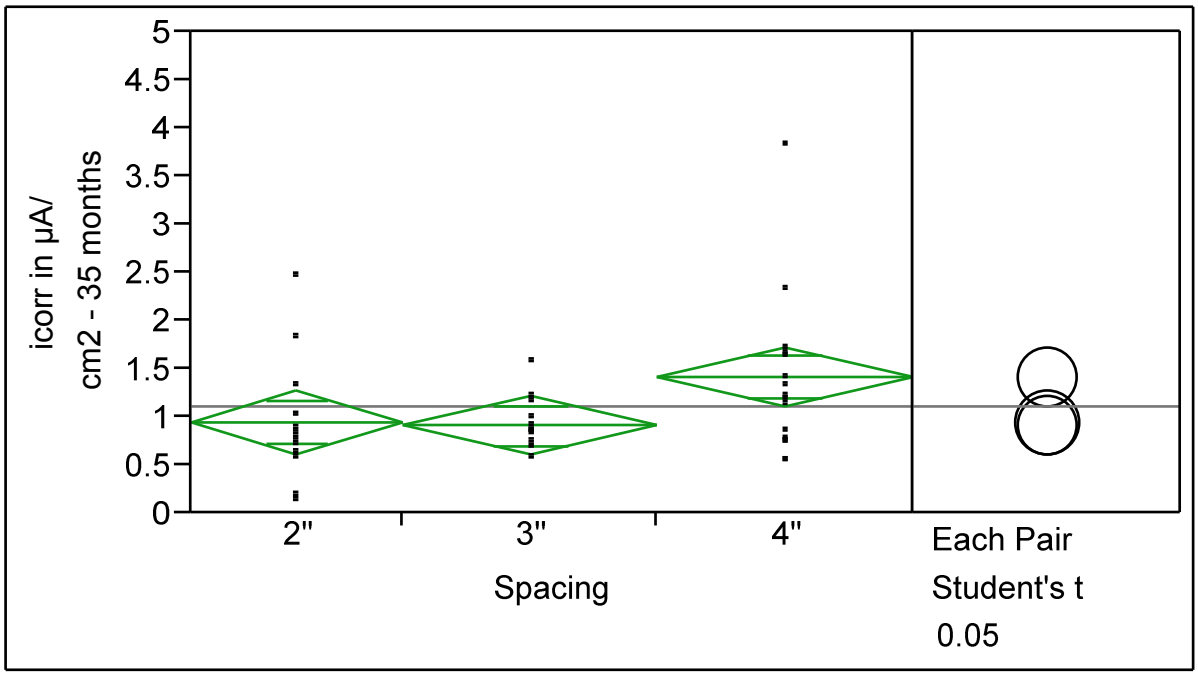

Figure 55 – Statistical Analysis – Corrosion Current Density of 2", 3" & 4" Spacings at 35 months

One-way analysis of *icorr* at 35 months (Figure 55) shows that for 4-inch spacing, even though there is a slight overlap with the other student t-test circles, there is a notable difference for the 4-inch spacings. The student's t-test shows that the 4-inch spacing is significantly different from 2 and 3-inch spacing values. The cleaning of the connections was performed after the 35 month readings, completed at about 38 months. Thus the 40 and 45-month plots represent the *icorr* values after the connections were cleared.

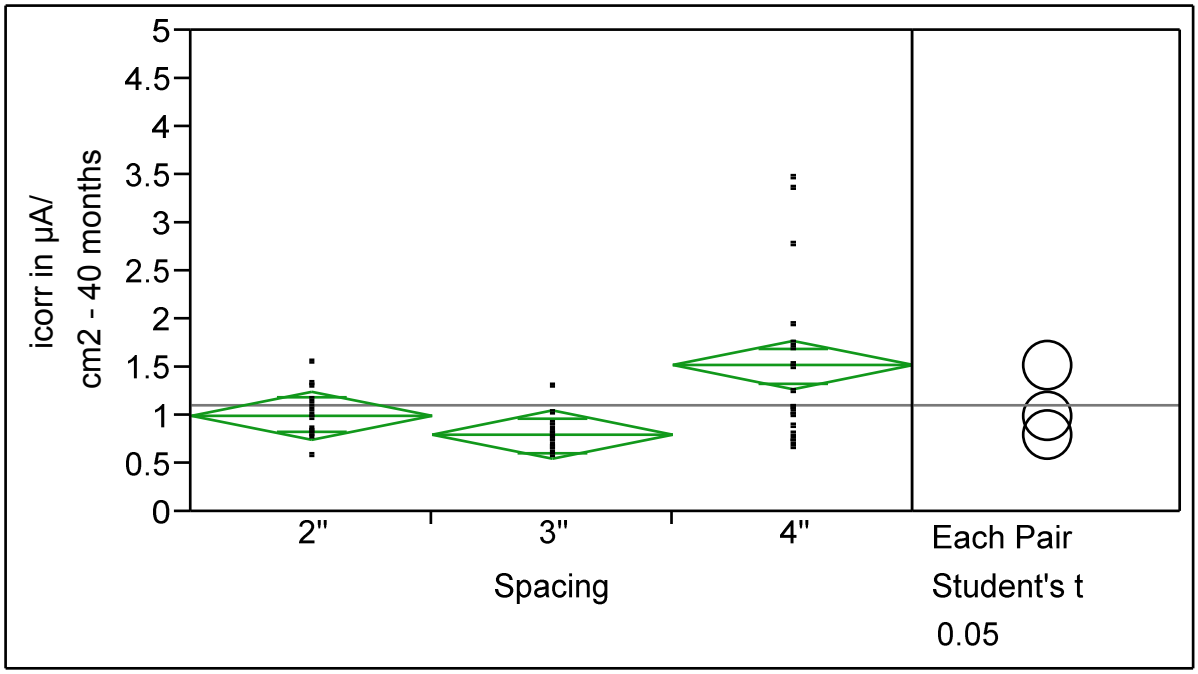

Figure 56 – Statistical Analysis – Corrosion Current Density of 2”, 3” & 4” Spacings at 40 months

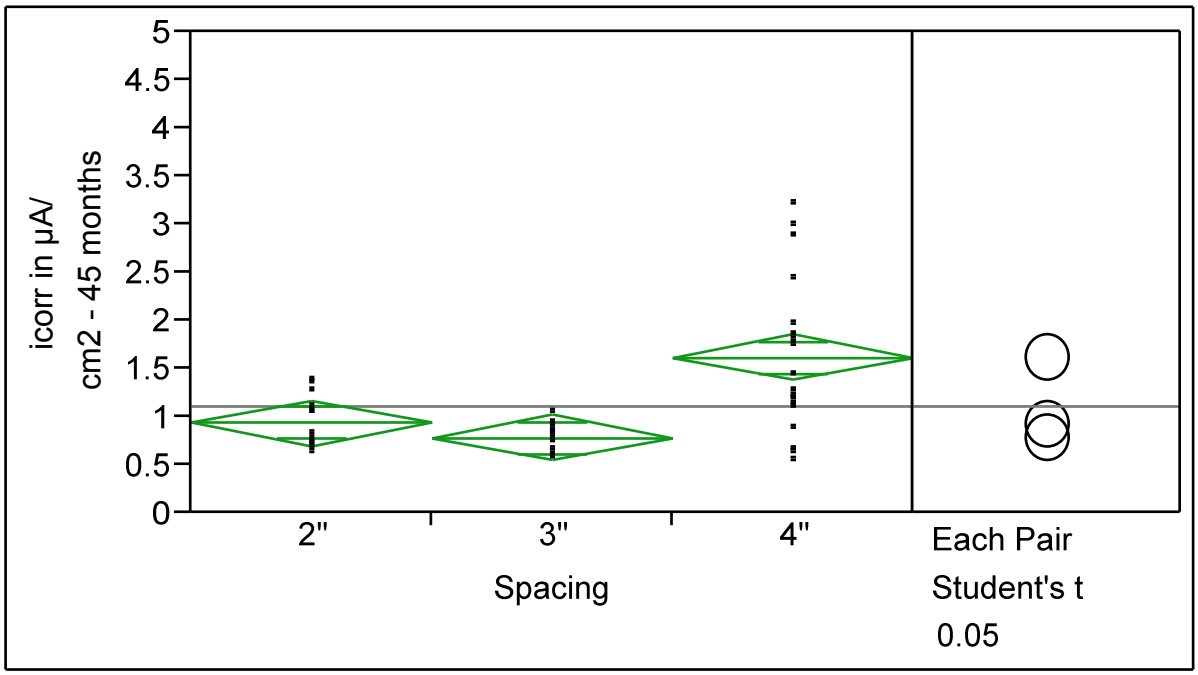

Figure 57 – Statistical Analysis – Corrosion Current Density of 2”, 3” & 4” Spacings at 45 months

As shown in Figures 56 and 57, the icorr values of 2 and 3-inch spacings are lower than 4-inch spacing specimens. The 40 (Figure 56) and 45 month (Figure 57) *icorr* values demonstrate that the 4-inch spacing values are significantly different from the 2 and 3-inch spacing specimens, while the 2 and 3-inch spacings are not statistically different.

Number of Cathodes

ANOVA one-way analysis for the 1 and 2 cathodes as the nominal terms and the *icorr* at 35, 40, and 45 months are shown in Figures 58, 59, and 60. This analysis includes the 2, 3, and 4-inch spacings even though significant difference was found between the different spacings.

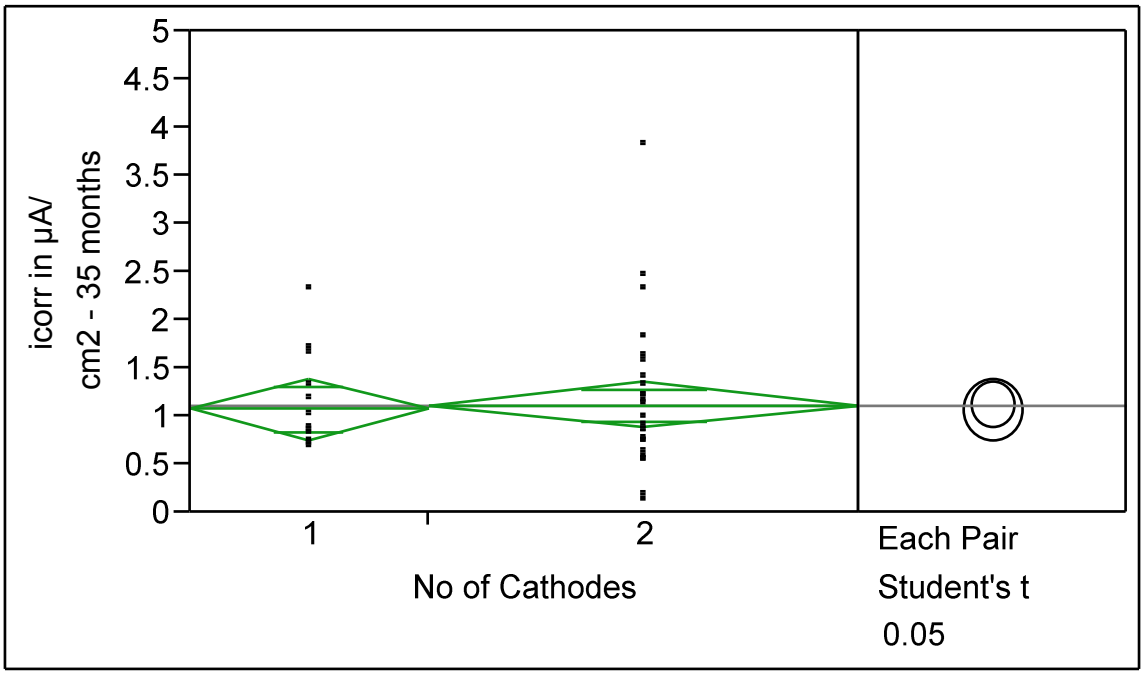

Figure 58 – Statistical Analysis – Corrosion Current Density of 1 & 2 Cathodes at 35 months

The one-way analysis and student's t-test of *icorr* at 35 months (Figure 58) show that there is no significant difference between the 1 and 2 cathodes. Again, the 35 month readings were taken prior to the completion of the cleaning of the connection at 38 months. Thus, the 40 and 45 month measurements represent the *icorr* values after the cleaning.

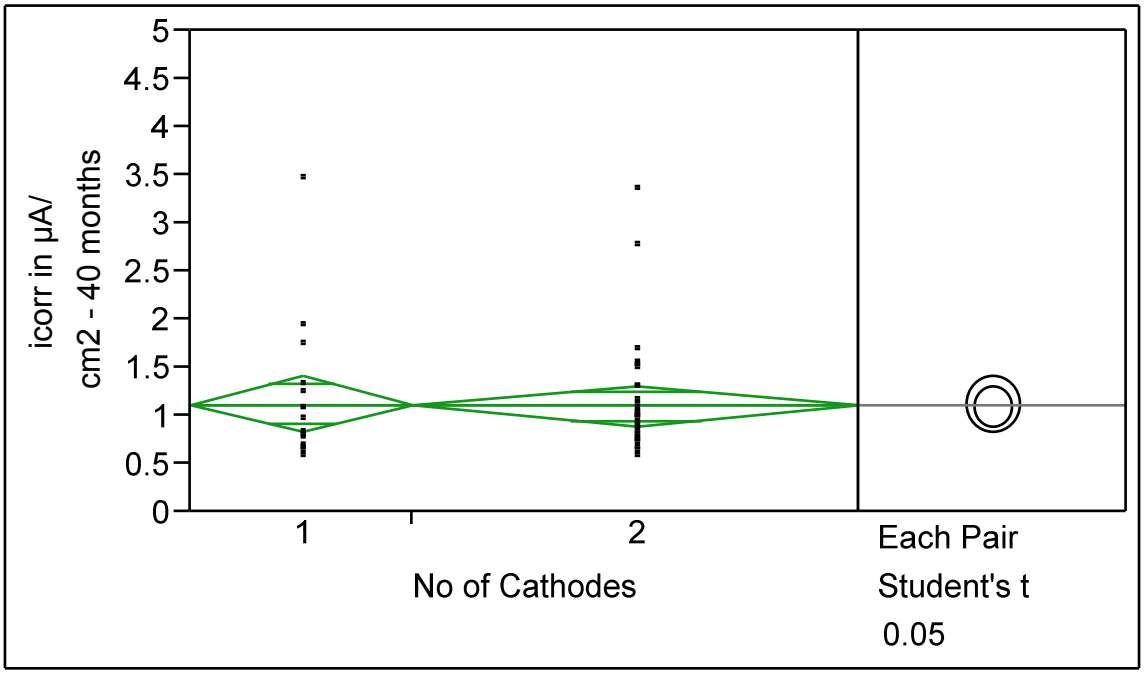

Figure 59 – Statistical Analysis – Corrosion Current Density of 1 & 2 Cathodes at 40 months

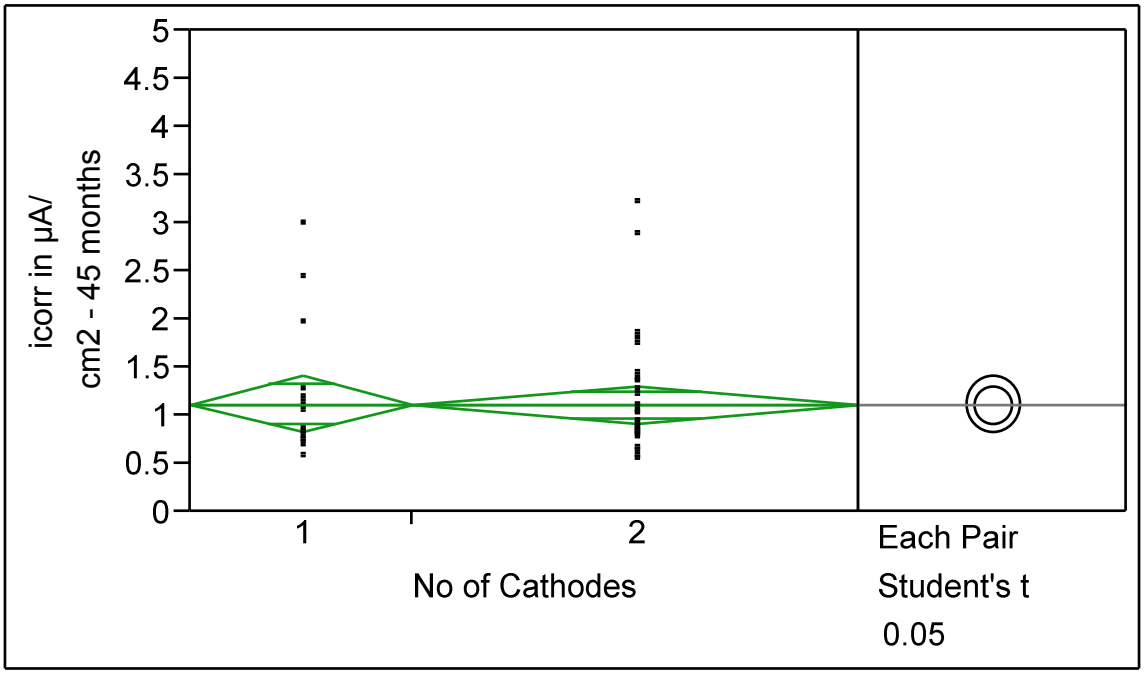

Figure 60 – Statistical Analysis – Corrosion Current Density of 1 & 2 Cathodes at 45 months

The analysis shows that there is no significant difference between the 1 and 2 cathodes at 40 (Figure 59) and 45 months (Figure 60). Thus, when considering all the spacings, the number of cathodes has no significant influence on corrosion current densities.

If all the spacing differences are included in the analysis, the number of cathodes analyses may not show any significant difference because of the inclusion of the 4-inch spacing. Thus, only the *icorr* values of specimens with 4-inch spacing at 45 months were included in the analysis of the number of cathodes as the nominal term shown in Figure 61.

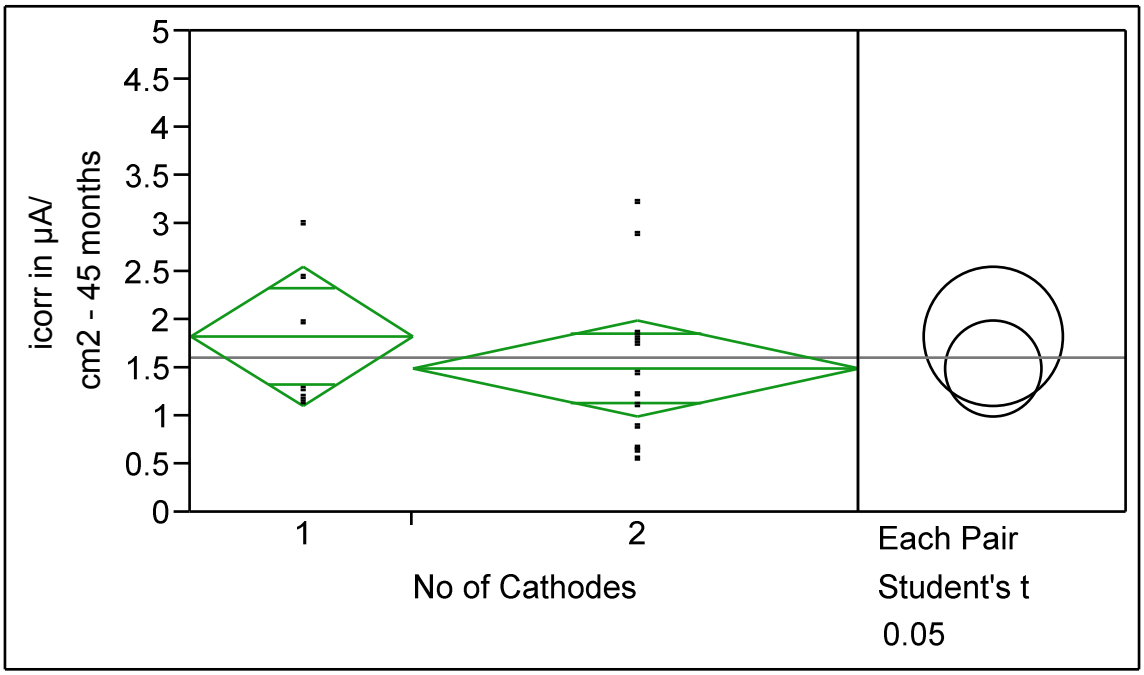

Figure 61 – Statistical Analysis – Corrosion Current Density of 4" Spacing with 1 & 2 Cathodes at 45 months

As shown in Figure 61, the specimens with two cathodes have *icorr* values that are slightly less than those specimens with one cathode. However, there is no statistical difference in the *icorr* measurements between the 1 and 2 cathode specimens at 45 months.

Presence of Stay-In-Place (SIP) forms

ANOVA one-way analysis was performed for specimens with SIP (Yes) and without SIP (No) as the nominal terms and *icorr* at 35, 40, and 45 months, see Figures 62, 63, and 64. This analysis includes the 2, 3, and 4-inch spacings, even though significant difference was found for the 4-inch spacing. Analysis also includes the number of cathodes, since no significant difference is found between them.

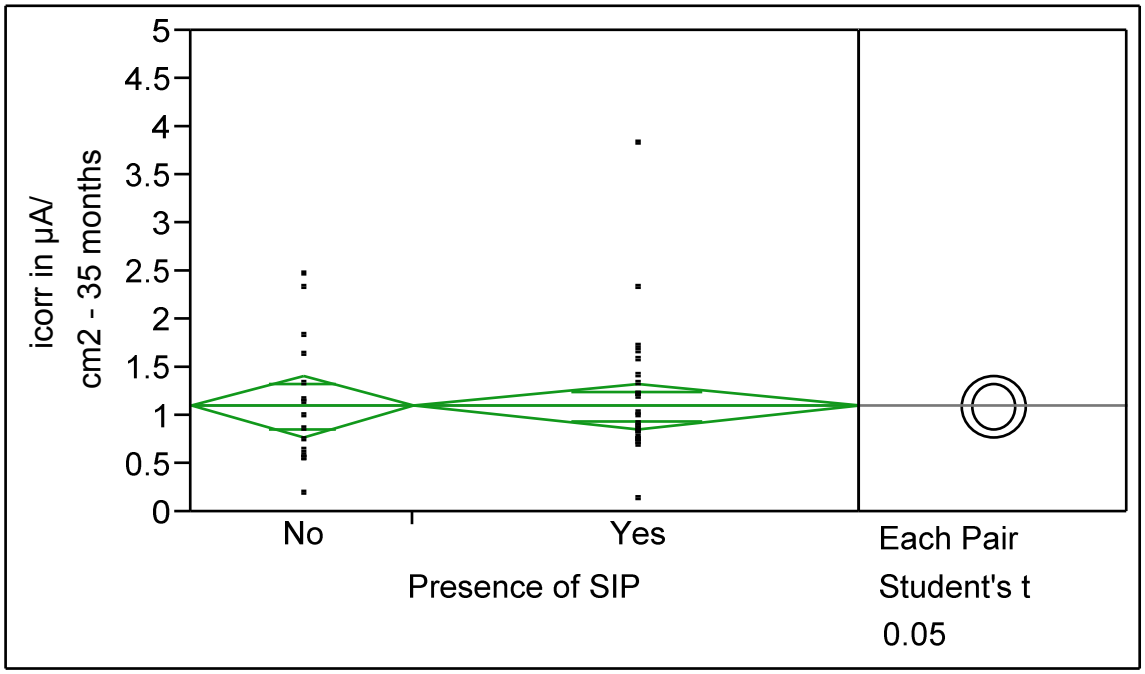

Figure 62 – Statistical Analysis – Corrosion Current Density of With & Without SIP at 35 months

The one-way analysis and student's t-test of *icorr* at 35 months (Figure 62) show that there is no significant difference between *icorr* values of specimens with SIP (Yes) and without SIP (No). The cleaning of connections was completed at 38 months, after the 35 months readings. Thus, the 40 and 45-month plots represent the *icorr* values after the cleaning of the connections was completed.

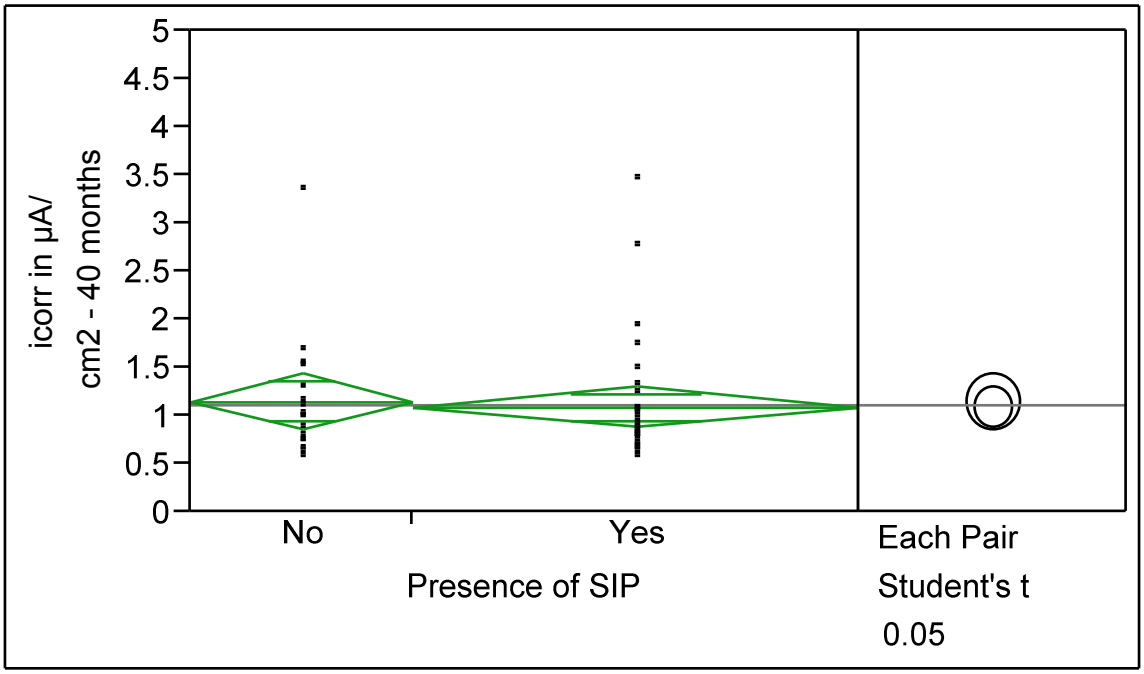

Figure 63 – Statistical Analysis – Corrosion Current Density of With & Without SIP at 40 months

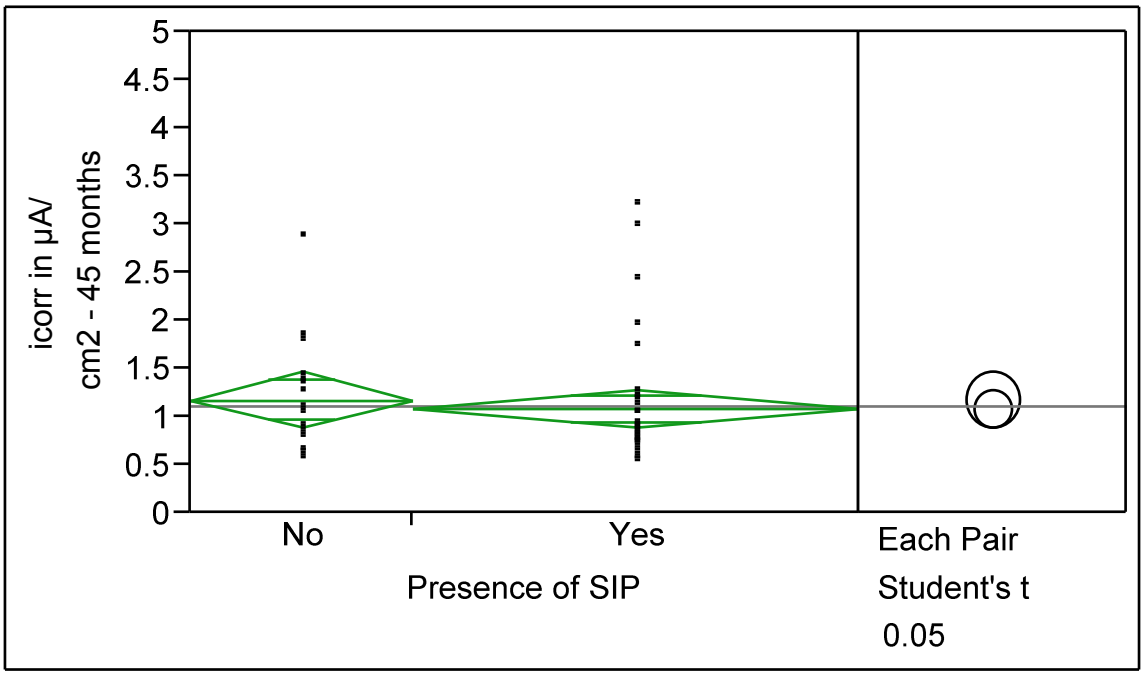

Figure 64 – Statistical Analysis – Corrosion Current Density of With & Without SIP at 45 months

The analysis shows that there is no significant difference between the *icorr* of specimens with SIP (Yes) and without SIP (No) at 40 (Figure 63) and 45 months (Figure 64). The specimens with SIP (Yes) have slightly lower *icorr* than specimens without SIP (No). But, when taking into account of all the spacings, the presence of SIP have no significant influence on corrosion current densities.

If all the spacing differences are included in the analysis the presence of SIP no significant difference may be found because of the 4-inch spacing factor being significantly different than the 2 and 3-inch spacing factor. Thus, only the *icorr* values of specimens with 4-inch spacing at 45 months are included in the following analysis of SIP as the nominal term, see Figure 65.

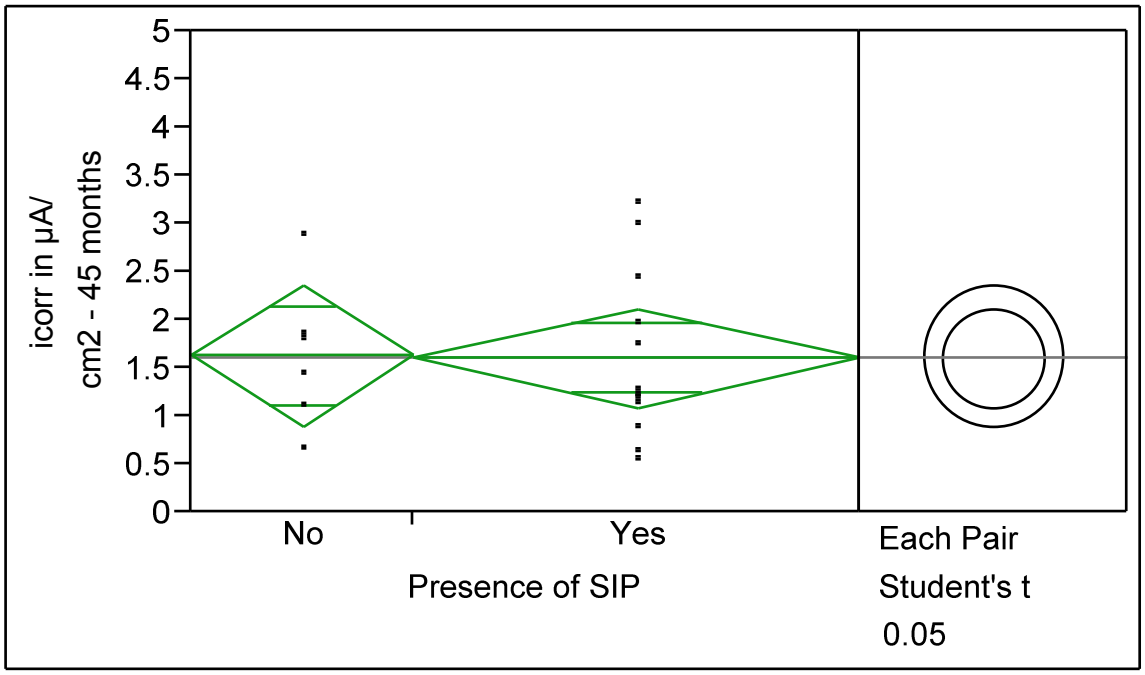

Figure 65 – Statistical Analysis – Corrosion Current Density of 4" Spacing Specimens With & Without SIP at 45 months

As shown in Figure 65, the presence of SIP does not have any significant influence on *icorr* even if the spacing differences are excluded.

Connection State

To determine if the macrocell corrosion has a significant impact on the total corrosion, statistical analysis conducted with the connected (CON) and unconnected (UNCON) states as the nominal

terms. The analysis is performed for 35, 40, and 45 months to identify significant differences.

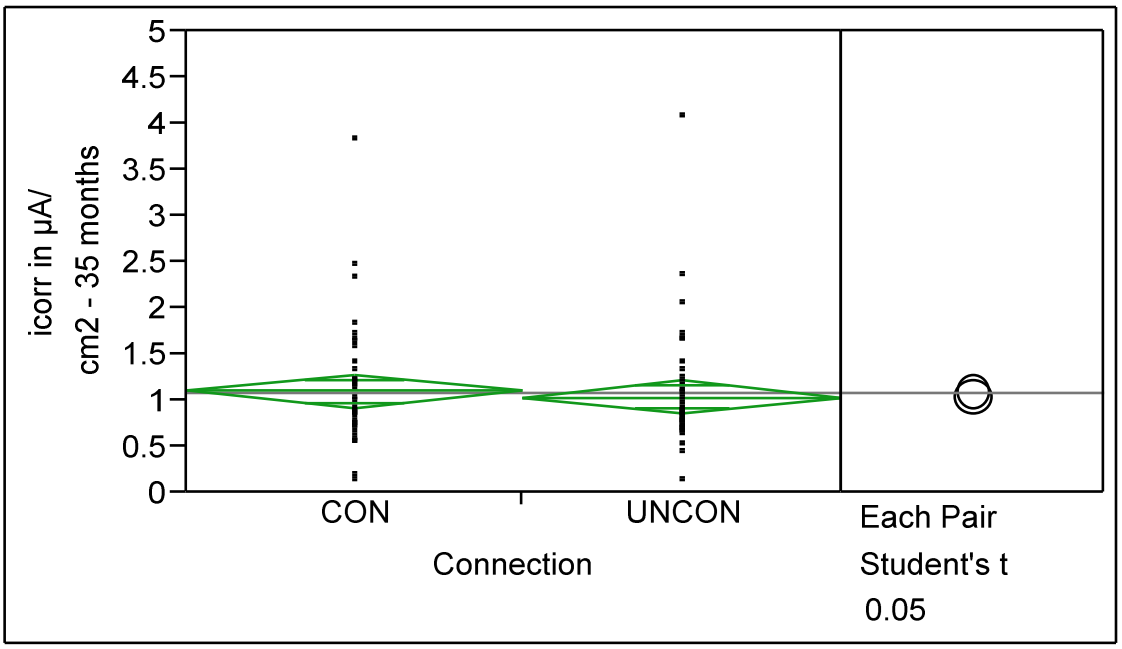

Figure 66 – Statistical Analysis–Connected & Unconnected Corrosion Current Density at 35 months

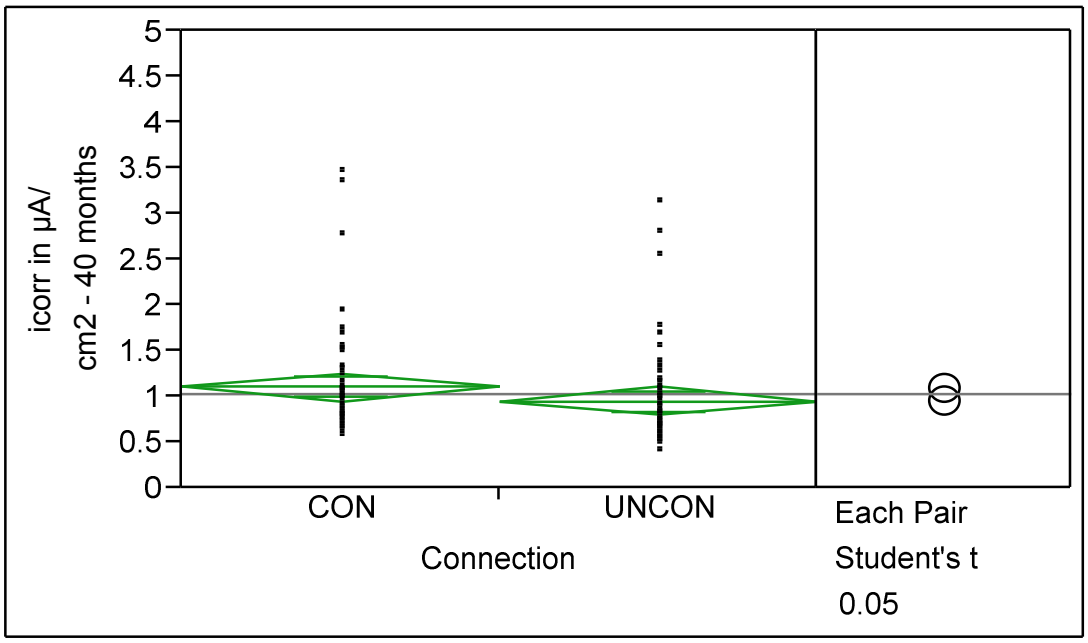

Figure 67 – Statistical Analysis – Connected & Unconnected Corrosion Current Density at 40 months

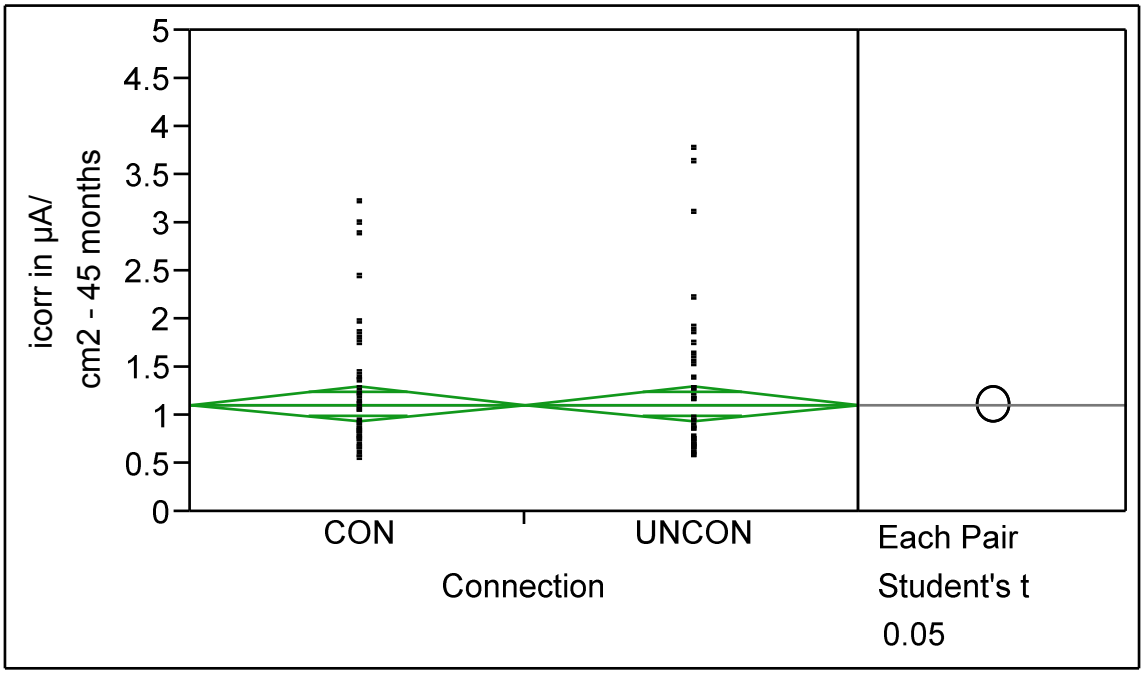

Figure 68 – Statistical Analysis – Connected & Unconnected Corrosion Current Density at 45 months

As shown in Figures 66, 67, and 68, there is no significant difference between connected and unconnected *icorr* values. The implication is that the macrocell corrosion has little influence compared to microcell corrosion on the total corrosion.

Chloride Content and Diffusion

Chloride content was measured by taking powdered concrete samples at three depths from all 27 specimens at 45 months only. Averages depths of the three samples were 0.25 inch, 0.75 inch, and 1.25 inch. Acid soluble chloride content was performed by potentiometric titration in accordance with ASTM C 1152/C 1152M.

Statistical analyses are performed to find if significant differences exist between the influence of clear spacing differences, cathode bar differences, and stay-in-place forms differences on chloride contents. The analyses include the ANOVA one-way analysis of the means and student's t-test to find any significant differences.

Clear Spacing Differences

Since differences were found between clear spacings in case of resistivities, it is expected for the chloride contents to be influenced by the same directly or indirectly. Figure 69 represents the one-way analysis of the chloride contents at 0.25 inch depth (topmost layer) with respect to the clear spacings 2-inch, 3-inch, and 4-inch as the nominal terms.

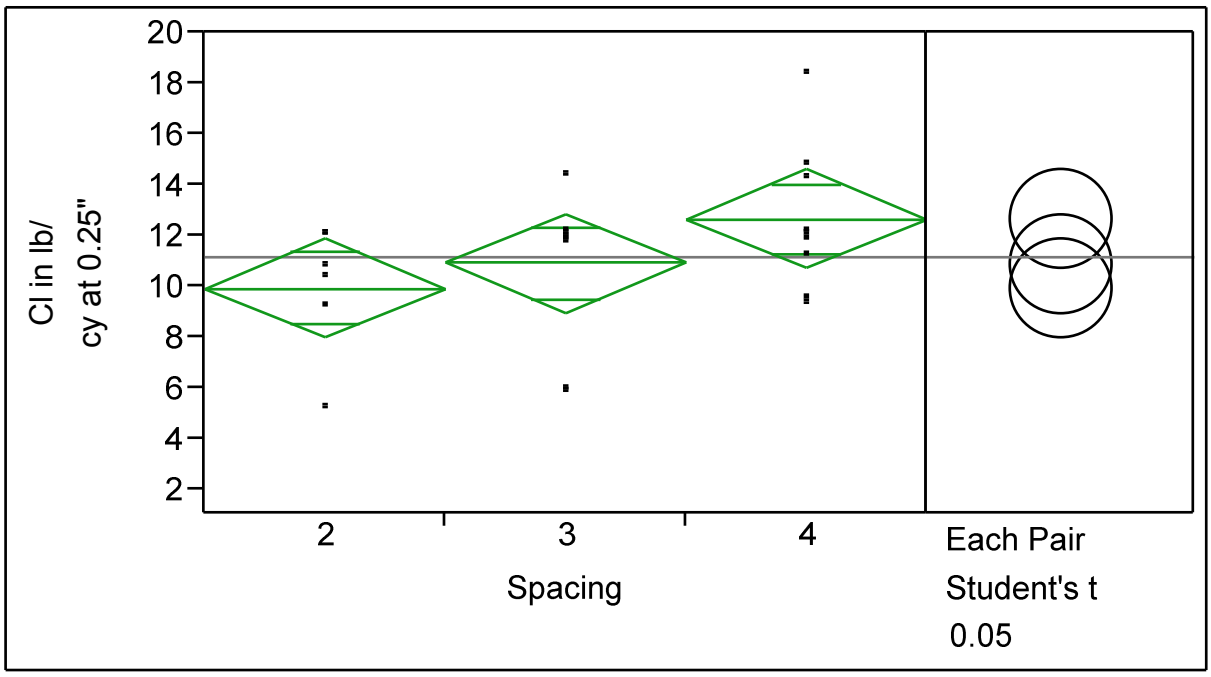

Figure 69 – Chloride Content of 2", 3" & 4" Spacings at 0.25" depth

As shown in Figure 69, the spacings do not have a significant difference among them. As shown, the average chloride content increases with increasing spacing factor from 2 to 4 inches. The influence of resistivity on chloride content at a depth of 0.25 inch can be inferred, as the resistivity decreases with increasing spacing factor.

Figure 70 represents the one-way analysis of the chloride contents at 0.75 inch depth with respect to the clear spacings 2-inch, 3-inch, and 4-inch as the nominal terms.

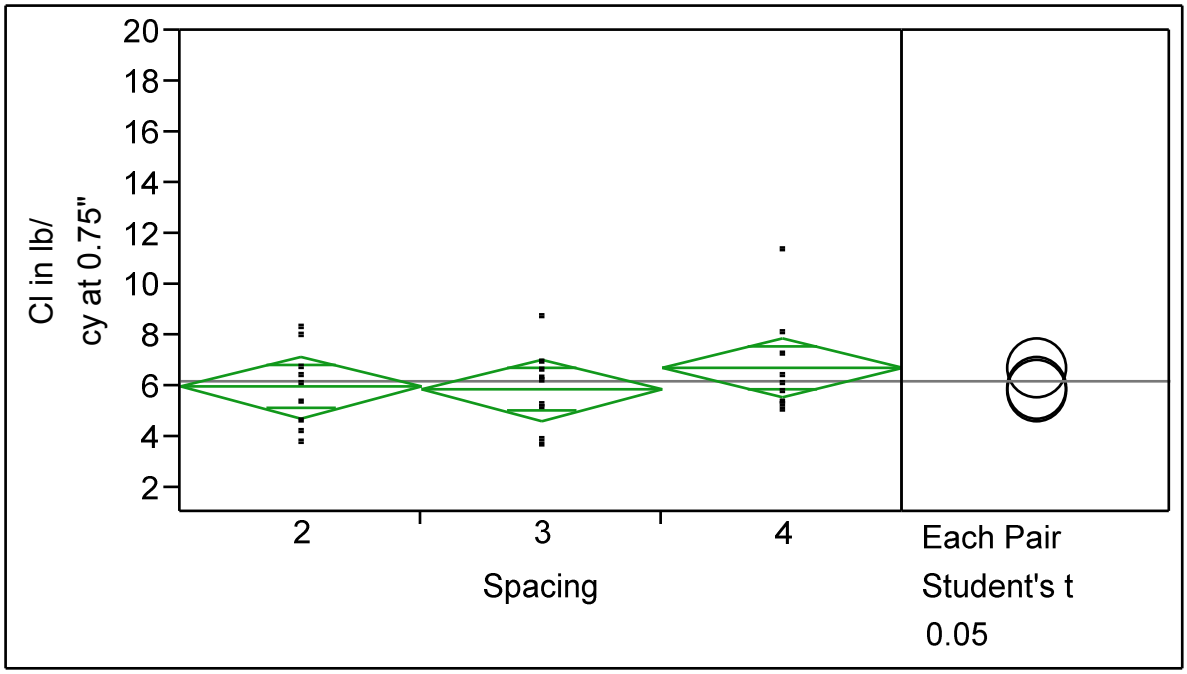

Figure 70 – Chloride Content of 2”, 3” & 4” Spacings at 0.75” depth

As shown in Figure 70, the spacing factors do not have a significant difference between them. The chloride content at 0.75 inch depth for the 2 and 3-inch spacing are approximately the same, but the 4-inch spacing factor is slightly higher.

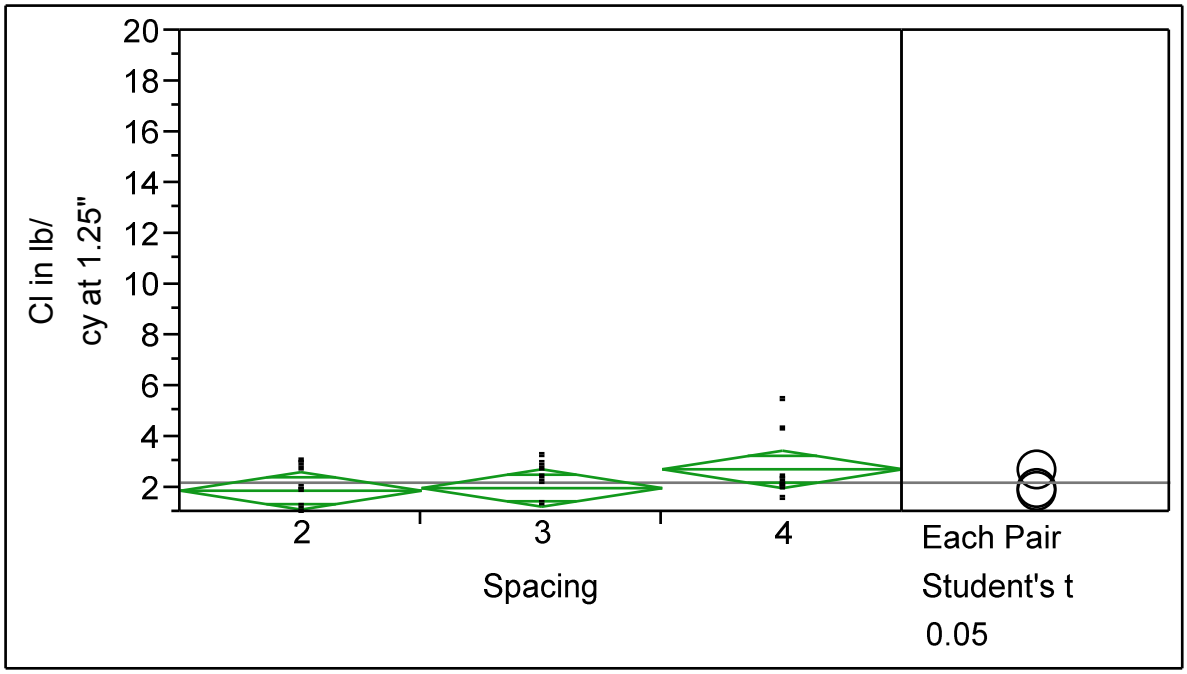

Figure 71 – Chloride Content of 2", 3" & 4" Spacings at 1.25" depth

Figure 71 represents the one-way analysis of the chloride contents at 1.25 inch depth with respect to the clear spacings 2-inch, 3-inch, and 4-inch as the nominal terms. As shown in Figure 71, the spacings do not have a significant difference. Again, the 2 and 3-inch spacing factor are approximately same and the 4-inch spacing is slightly higher.

Number of Cathodes

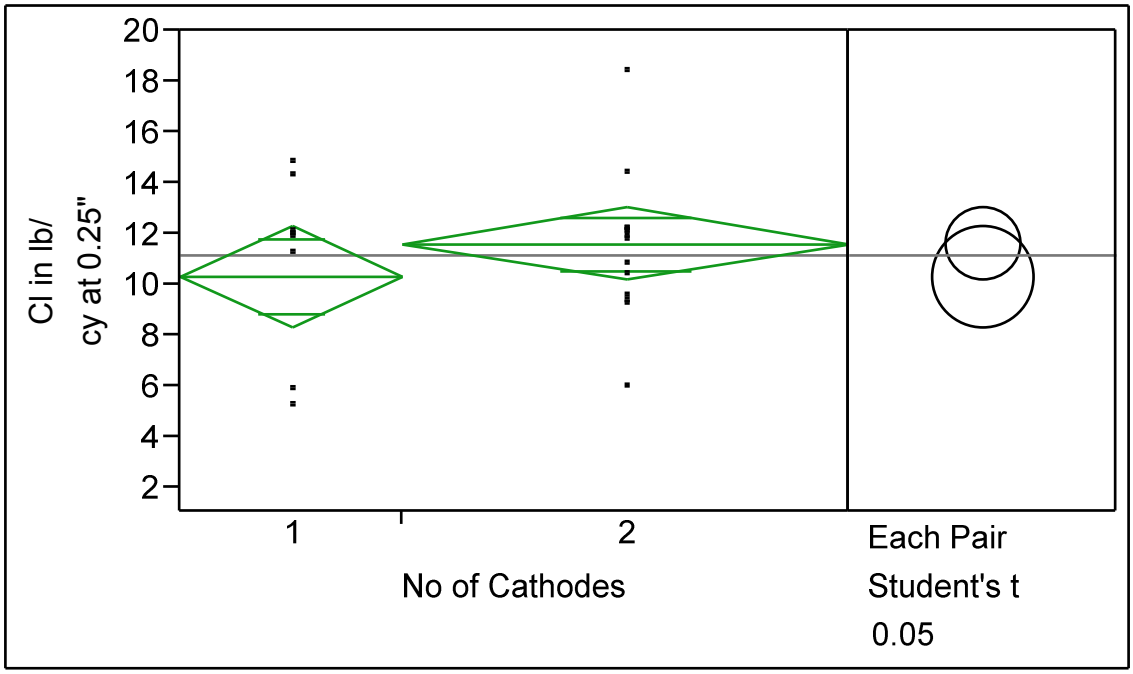

Figure 72 – Chloride Content of 1 & 2 Cathodes at 0.25" depth

Figure 72 represents the one-way analysis of the chloride contents at 0.25 inch depth (topmost layer) with respect to the number of cathodes as the nominal terms. As shown in Figure 72, the number of cathodes does not relate to significant differences between them. However, the two cathode specimens have greater average chloride content at the 0.25 inch depth and the one cathode specimens. There is also a large variation in both data sets.

Figure 73 represents the one-way analysis of the chloride contents at 0.75 inch depth with respect to the number of cathodes as the nominal terms.

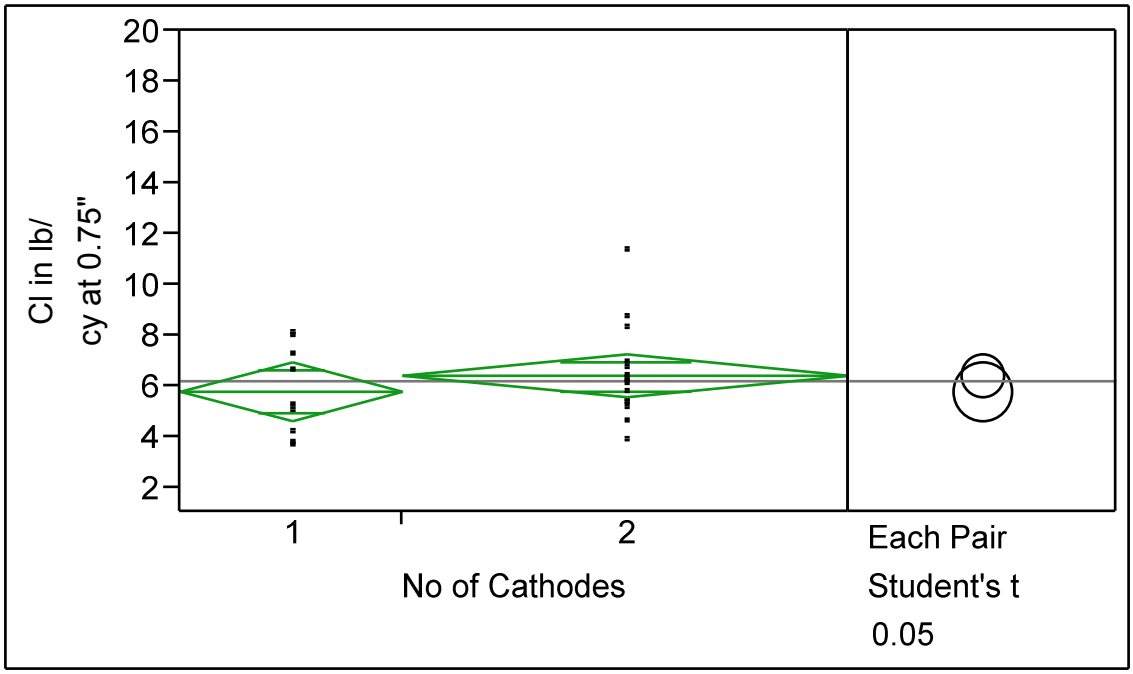

Figure 73 – Chloride Content of 1 & 2 Cathodes at 0.75" depth

As shown in Figure 73, the number of cathodes is not significantly different. The average two cathode specimens have slightly greater average chloride content at the 0.75 inch depth than the one cathode specimens. Also, the variability in chloride contents is greater for the two cathode than the one cathode.

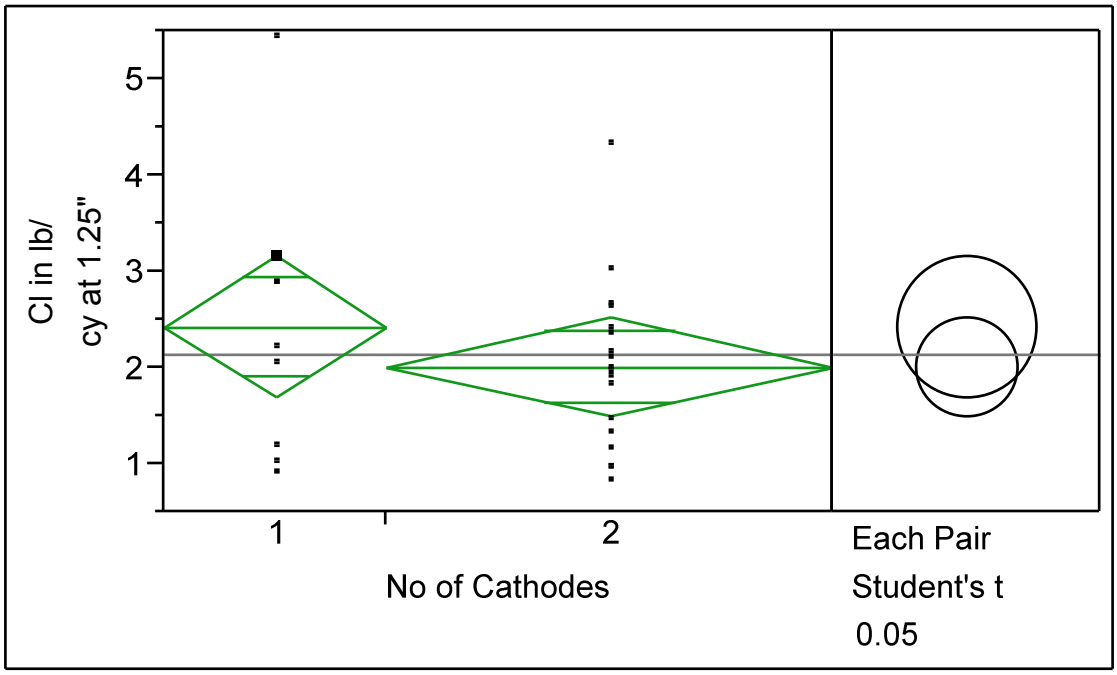

Figure 74 - Chloride Content of 1 & 2 Cathodes at 1.25" depth

Figure 74 represents the one-way analysis of the chloride contents at 1.25 inch depth with respect to the number of cathodes as the nominal terms. As shown in Figure 74, the number of cathodes does not cause a significant difference between chloride concentrations. But it is also clear that the specimens with 2 cathodes have slightly less chloride content than the specimens with 1 cathode.

Presence of Stay-In-Place (SIP) forms

Figure 75 represents the one-way analysis of the chloride contents at 0.25 inch depth (topmost layer) with respect to the presence of stay-in-place forms as the nominal terms. As shown in Figure 75, the presence of SIP does not cause a significant difference between data sets. The one cathode average chloride content is slightly less than the two cathodes and the variability between data sets is about the same.

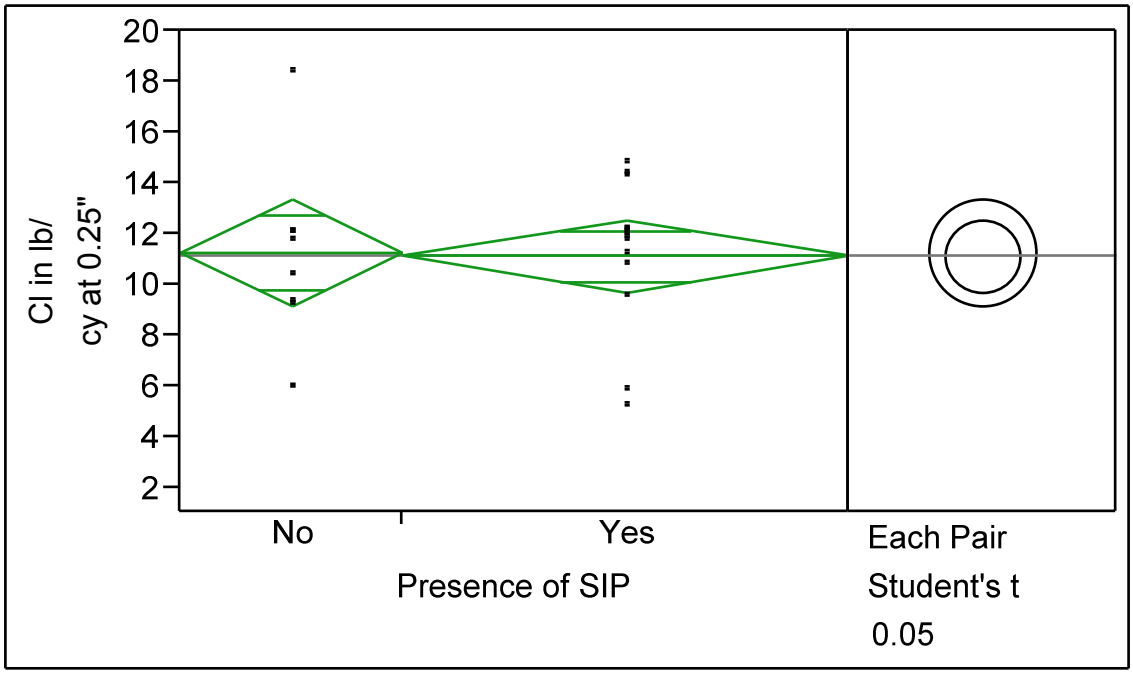

Figure 75 - Chloride Content of Specimens With & Without SIP at 0.25” depth

The condition for the SIP versus NoSIP for the chloride contents at 0.75 and 1.25 inches are the same as the 0.25 inch depth, see Figures 76, and 77.

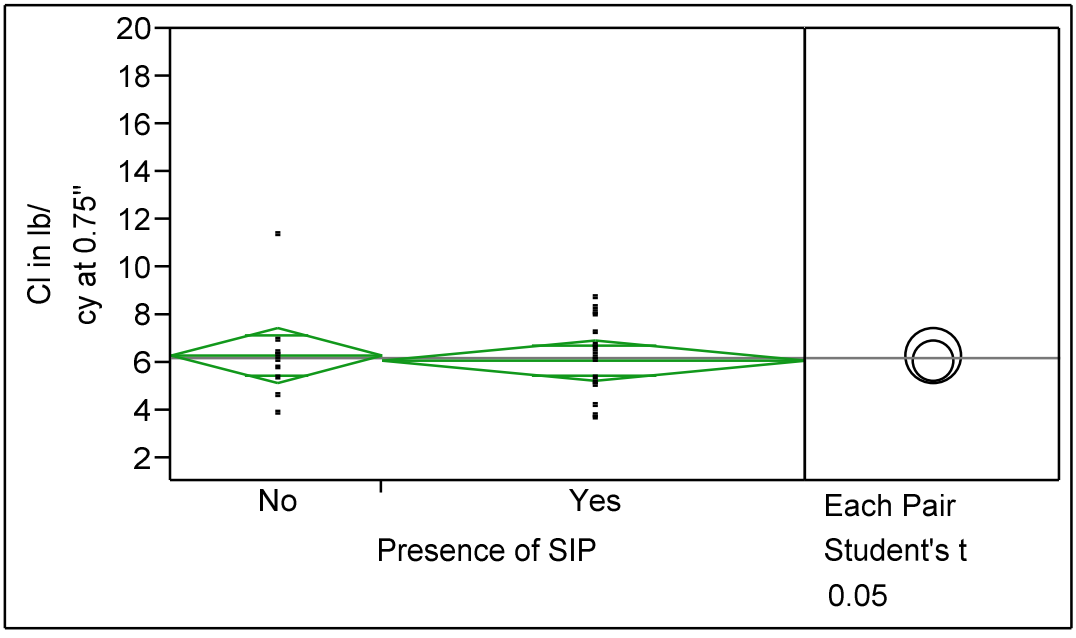

Figure 76 - Chloride Content of Specimens With & Without SIP at 0.75” depth

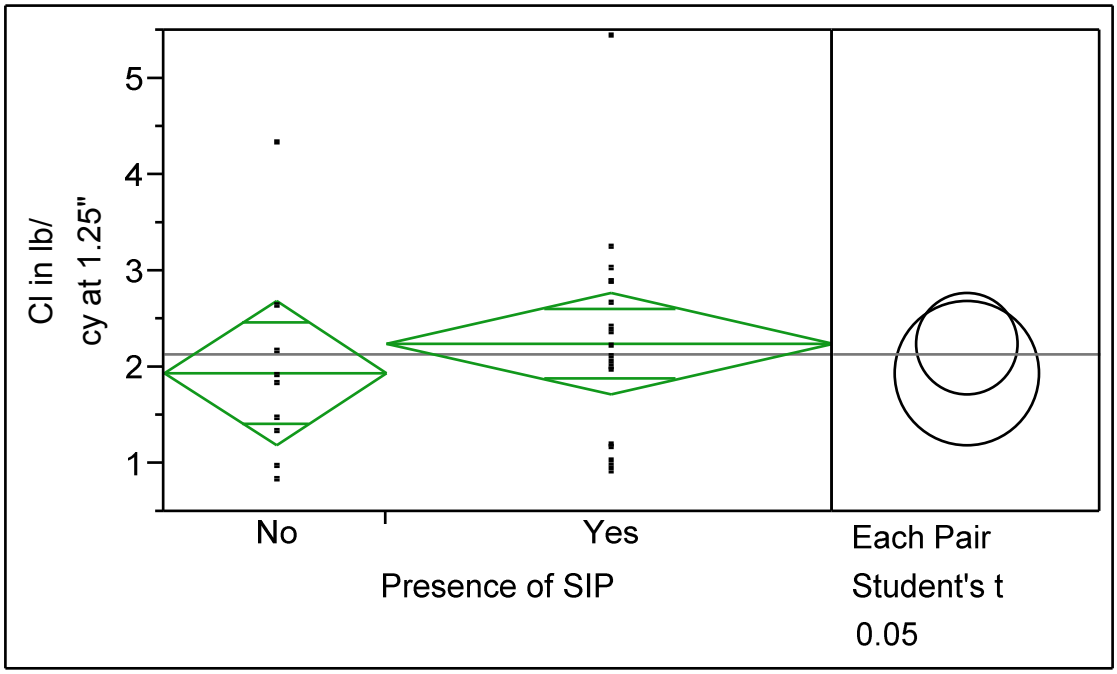

Figure 77 - Chloride Content of Specimens With & Without SIP at 1.25” depth

Chloride Content and Resistivity

Resistivity, being a concrete parameter, is expected to be related to chloride diffusion rate. The statistical analyses showed that the resistivity was influenced by clear spacings. Increase in spacing resulted in the decrease of resistivity. A similar but inverse relationship between the chloride concentrations and resistivity is thus expected.

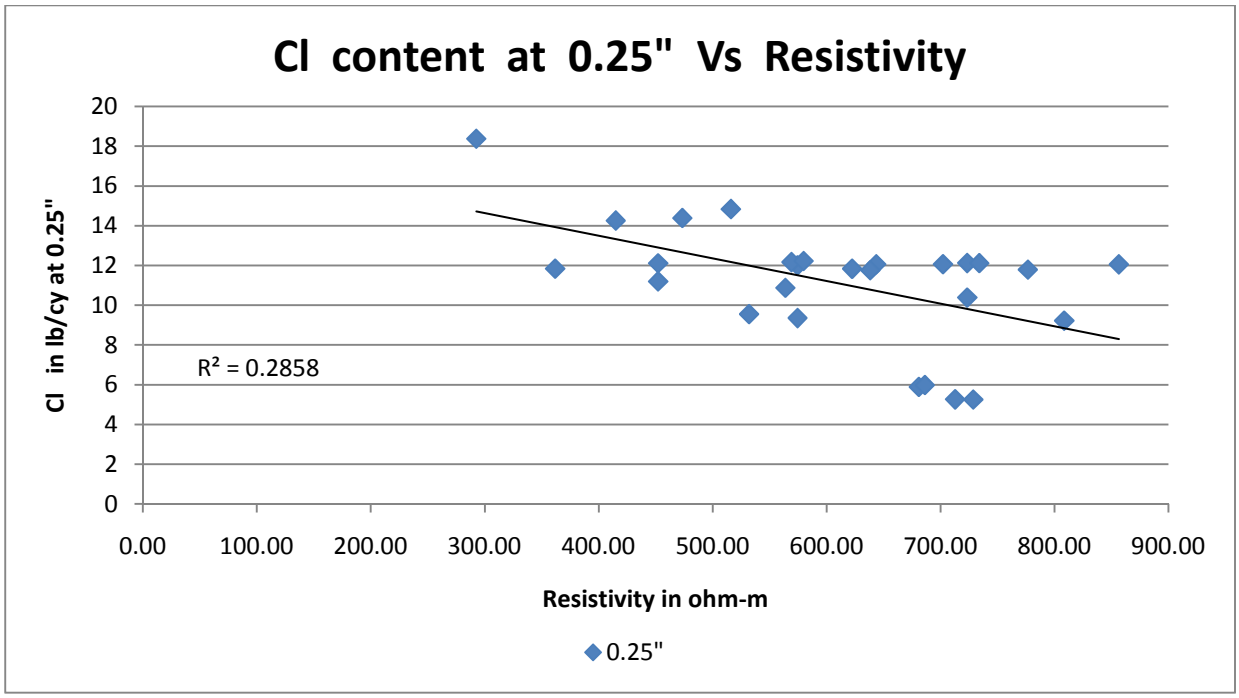

Figure 78 – Chloride Content at 0.25" Depth Vs Resistivity

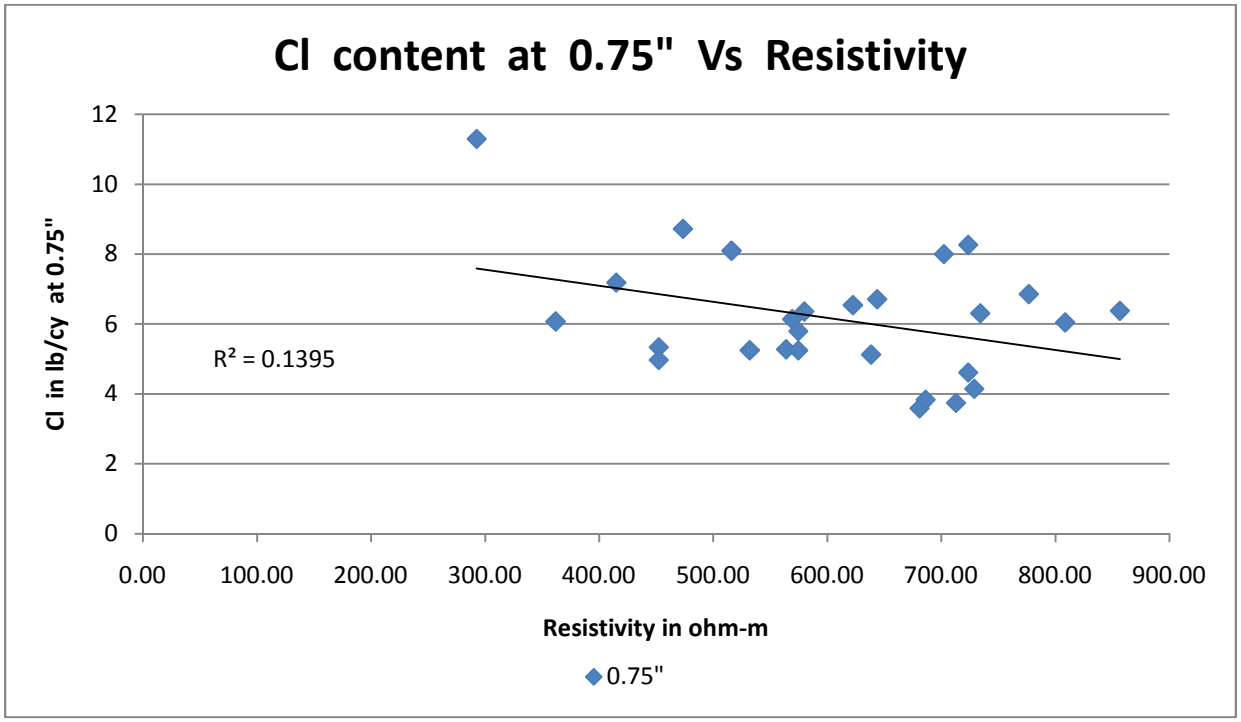

Figure 79 – Chloride Content at 0.75" Depth Vs Resistivity

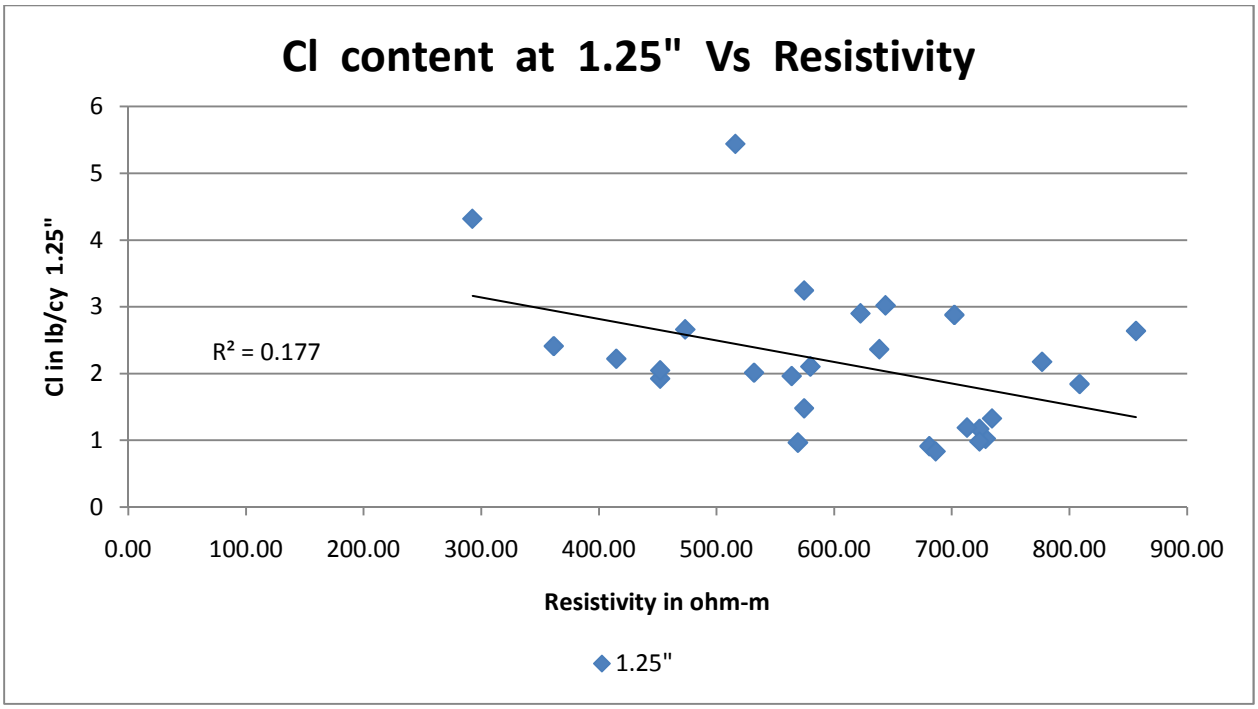

Figure 80 – Chloride Content at 1.25" Depth Vs Resistivity

As shown in Figures 78, 79, and 80, the chloride contents at 6.3 mm, 19 mm, and 31.7 mm (0.25, 0.75, and 1.25 inch), are inversely related to resistivity. However, the relationship are poor and became more so with depth. The results indicate that resistivity may not be constant with depth. As the resistivity values are an average of the top two inches of the concrete. That is the spacing distance between probes.

Diffusion Coefficient (Dc)

The diffusion coefficient represents the penetration rate of chloride into the concrete. It is calculated by a solution to Fick's second law of diffusion, equation 16. The diffusion coefficient values are presented in Table 9.

Table 9 – Diffusion Coefficient Calculated Values

Diffusion Coefficient *mm^2/year*	Number of Cathodes	Presence of SIP	Clear Spacing *inch*	
81	1	Yes	2	
72	1	Yes	2	
76	1	Yes	2	
54	2	Yes	2	Mean = 60
60	2	Yes	2	σ_{n-1} = 16
43	2	Yes	2	CV = 27%
65	2	No	2	
52	2	No	2	
32	2	No	2	
48	1	Yes	3	
53	1	Yes	3	
59	1	Yes	3	
57	2	Yes	3	Mean = 49
36	2	Yes	3	σ_{n-1} = 8
40	2	Yes	3	CV = 17%
40	2	No	3	
55	2	No	3	
54	2	No	3	
43	1	Yes	4	
80	1	Yes	4	
39	1	Yes	4	
49	2	Yes	4	Mean = 52
46	2	Yes	4	σ_{n-1} = 14
54	2	Yes	4	CV = 26%
37	2	No	4	
55	2	No	4	
65	2	No	4	

The diffusion coefficient may be related to the resistivity of concrete, since resistivity depends on the volume of pores, connection of pores, and the moisture content of the concrete as does the diffusion constant. As shown in Table 9, the average diffusion constants are approximately the same, 49 to 60 mm^2/year, whereas the average resistivities decrease with increasing spacing factor. The diffusion constants are highly variable as illustrated by the coefficient of variation (CV) of 17 to 27%.

Diffusion Coefficient & Resistivity

Diffusion coefficient indicates the rate with which the ions penetrate through the concrete. Resistivity, as a parameter of concrete, can indicate the resistance of concrete to the penetration of ions. Thus, an inverse relationship is expected between chloride diffusion coefficients and resistivities.

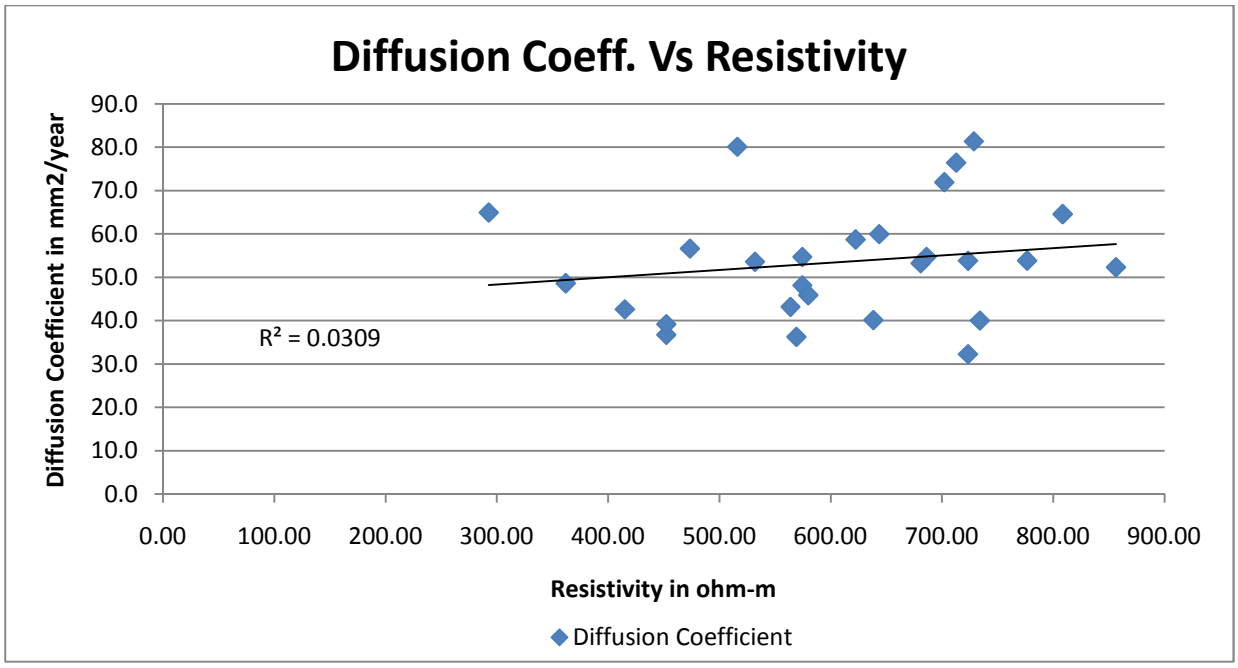

Figure 81 – Diffusion Coefficient Vs Resistivity

As shown in Figure 81, the diffusion coefficients form extremely poor relationship with resistivity. Thus, the relationship between the two parameters could not be established from the data available. The lack of correlations is most likely related to the extreme variability of both the diffusion constant and resistivity data sets.

Moisture Content

Table 10 – Relative Humidity Values

Relative Humidity *%*	Number of Cathodes	Presence of SIP	Clear Spacing *inch*	
91	1	Yes	2	
76	1	Yes	2	
73	1	Yes	2	
73	2	Yes	2	Mean = 78
73	2	Yes	2	σ_{n-1} = 8.2
71	2	Yes	2	CV = 11%
76	2	No	2	
93	2	No	2	
74	2	No	2	
78	1	Yes	3	
82	1	Yes	3	
82	1	Yes	3	
76	2	Yes	3	Mean = 81
77	2	Yes	3	σ_{n-1} = 6.4
77	2	Yes	3	CV = 8%
97	2	No	3	
79	2	No	3	
79	2	No	3	
82	1	Yes	4	
82	1	Yes	4	
78	1	Yes	4	
79	2	Yes	4	Mean = 80
83	2	Yes	4	σ_{n-1} = 2.2
78	2	Yes	4	CV = 3%
80	2	No	4	
78	2	No	4	
77	2	No	4	

The Table 10 presents the relative humidity values measured from all the specimens at the bar level at 45 months. The average temperature of the specimens when the relative humidity measurements were recorded was 68 ˚F and the temperature was relatively constant between specimens. Since moisture content requires destructive methods, the relative humidity was measured.

The average relative humidity are approximately same between spacing factors, see Table 10. The relative humidity measurements are somewhat less variable than the resistivity and diffusion constant. Thus, no relationship was found.

Macrocell Current

To determine the contribution of the macrocell current to the total corrosion, a high-impedance voltmeter was connected across the 10 ohm resistor. The macrocell potential obtained from the measurement was used to calculate the macrocell current using Ohm's law, since the resistance between the top and bottom bar. Figure 82 shows a sample macrocell current plot for the 45-month time.

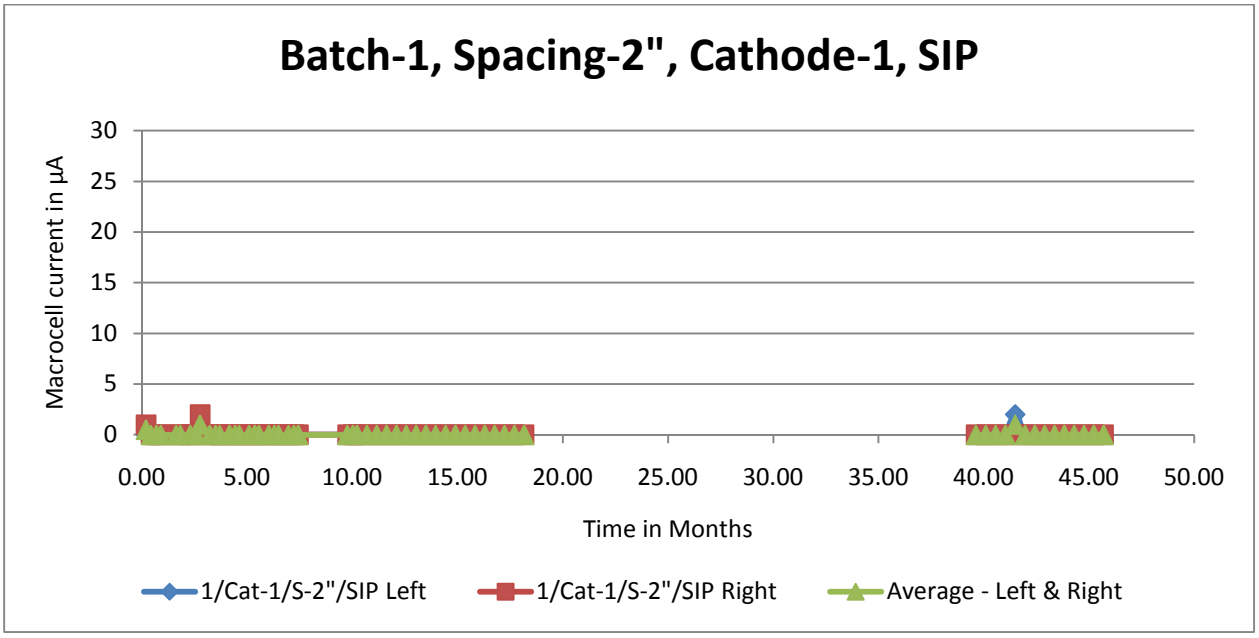

Figure 82 – Macrocell Currents of Batch-1, Spacing-2", Cathode-1, SIP

The macrocell currents for most of the specimens were less than 5 µA at the beginning. But as time passed, the macrocell current values decreased to 0 µA. After 35 months, the measurements showed greater macrocell current values. But after the cleaning up of the exposed steel surfaces, the macrocell values dropped to below 10 µA in most of the specimens. Thus, the measurements were influenced by the corrosion products at the exterior bar ends. Since the macrocell currents of more than half the specimens were less than 10 µA, the macrocells were not high enough to designate failure under the test method. The failure in this case is considered to be the

destruction of the protective passive layer. The macrocell corrosions are presented in Appendix D.

Autopsy

The 3LP relative corrosion rates were assessed by autopsy of select samples. Six specimens were selected, based on the different corrosion measurements, see Table 11.

Table 11 – Visual Inspection Data

Specimen ID	Predicted Corrosion	Top Bar	Bottom Bar
6 – C-2 – 4" – SIP – Left	High	Length of Corrosion = 8"	No Visible Corrosion
8 – C-1- 4" – SIP – Right	High	Length of Corrosion = 7"	No Visible Corrosion
9 – C-2 – 4" – NSIP – Right	Moderate	Length of Corrosion = 5.25"	No Visible Corrosion
3 – C-2 – 2" – NSIP – Right	Moderate	Length of Corrosion = 2"	No Visible Corrosion
4 – C-1- 3" – SIP – Right	Low	Length of Corrosion = 1.5"	No Visible Corrosion
9 – C-2 – 4" – SIP – Right	Low	No Visible Corrosion	No Visible Corrosion

Selection of six was such that two of six bars had a high corrosion rate, two moderate corrosion rate, and remaining two specimens low. Then the specimens were cut using a rotating saw to separate the required slice of concrete containing the selected bar. The visual inspection results of the six specimens are presented in Table 11.

As shown in Table 11, the length of corrosion observed in the specimens can be related to the predicted corrosion activity. All the corrosion was confined to the top half of the bar as the bottom side of the top bars did not exhibit any corrosion products. Also, note that the bottom bars did not have visible corrosion activity. Thus the bottom bar could have acted as the macrocell cathode, but does not appear that its influence was significant. The photographs of the top and bottom bars are included in the Appendix E.

Table 12 presents the measured resistivity and corrosion activity and literature interpretation of resistivities for the autopsied specimens.

Table 12 – Comparison of Observed and Interpreting Resistivity

Specimen	Resistivity in Ω-m	Measured Corrosion Activity	Literature Interpretation	
			Resistivity in Ω-m	Corrosion Rate
6 – C-2 – 4” – SIP – Left	452	High	50 – 100	High
8 – C-1- 4” – SIP – Right	532	High	50 – 100	High
9 – C-2 – 4” – NSIP – Right	416	Moderate	100 – 200	Low to Moderate
3 – C-2 – 2” – NSIP – Right	732	Moderate	100 – 200	Low to Moderate
4 – C-1- 3” – SIP – Right	643	Low	> 200	Low
9 – C-2 – 4” – SIP – Right	588	Low	> 200	Low

The measured resistivity and corrosion activity are compared to the resistivity interpretations presented in the literature, see Table 12. Note that the measured resistivities much higher than those presented in the literature, have corroded. Resistivities of greater than 400 Ω-m have been observed with high and moderate corrosion activity, where the interpretations specify that

resistivities greater than 200 Ω-m will support negligible corrosion rates. It is implied that the observed corrosion activity does not follow the interpretations. The corrosion activity devices used in this study and reported literature may have been different devices and thus the reason for the differences in interpretations.

3LP Calculation Software

For calculating the corrosion current density (*icorr*) and other necessary values from the data obtained from 3LP instrument, software called "Corrate2" was used. The "Corrate2" software works in DOS environment. The results are to be manually entered into spreadsheet for various analyses and plotting graphs, since the software does not export data to other analyzing software. Since a huge number of 3LP data had to be entered and the results had to be stored for analysis and plotting graphs, code was written for new improved software. Microsoft Visual Basic 2008 (.NET) was used to write the codes for this software. The new software "3LP Calc" has been written as a part of this study.

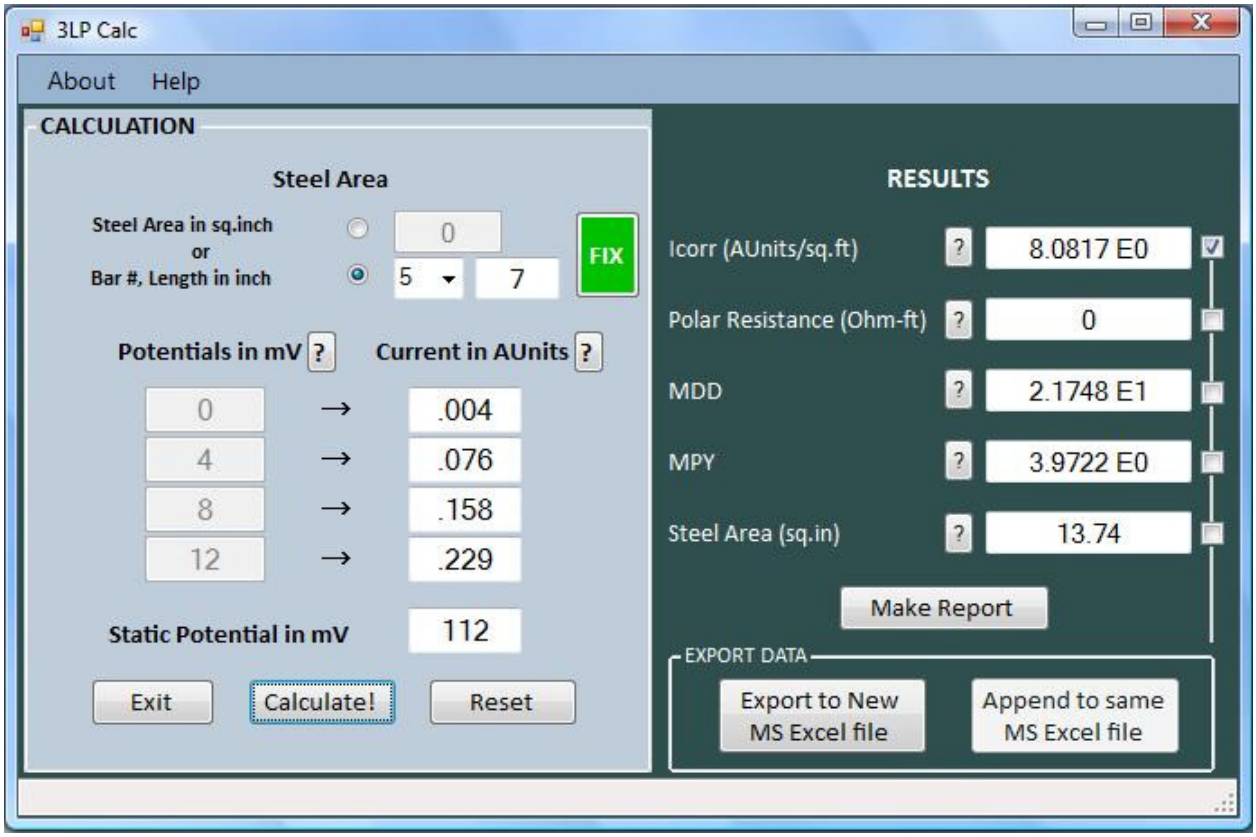

Figure 83 – 3LP Calc Software – Main Interface

Figure 83 shows the main window where the calculation is done. Input of data and display of results are designed in the same view to avoid confusions. One click calculation makes it simpler than calculation using “Corrate2” software.

The results can be stored in two ways. If the user’s computer has MS Excel installed, then the necessary results can be exported to MS Excel. The exporting action can be done either by opening a new MS Excel window or by appending the new results in the same MS Excel window in use. If the user’s computer does not have MS Excel installed, a report can be made out of the inputs and the results. The report is self-generated and can be saved as a simple text file. A sample report is shown in Figure 84.

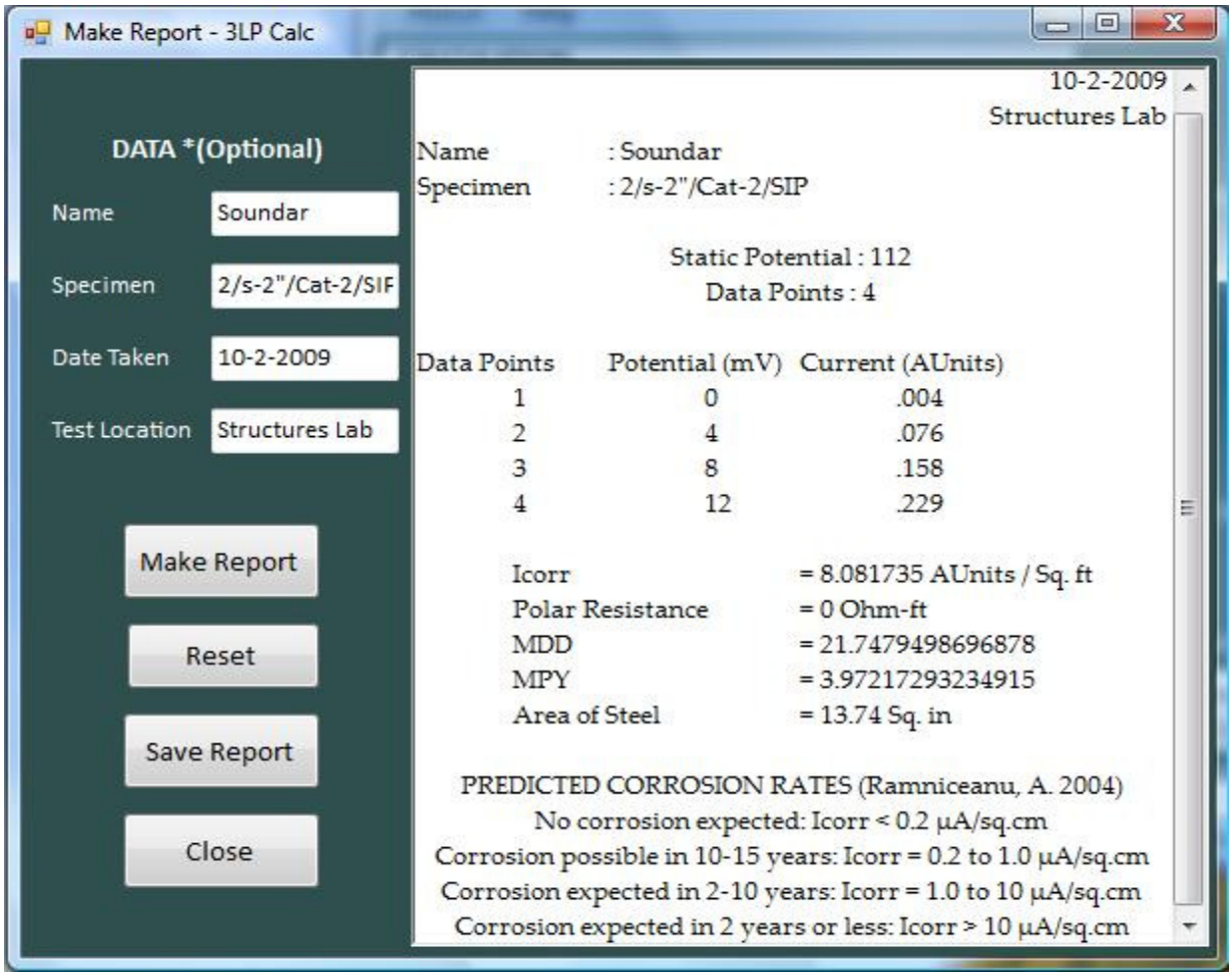

Figure 84 – 3LP Calc Software – Generated Report

CONCLUSIONS

The influence of the parameters such as spacing between top and bottom reinforcement mat, number of cathodes, and the presence of stay-in-place forms was studied using resistivity, half-cell potential test, linear polarization, and chloride content.

Resistivity

Resistivity of all specimens were measured and analyzed to find if the parameters have any influence on corrosion activity. Significant differences of the clear spacing groups between the anode and cathode on the resistivity were observed from the statistical analysis. Regarding the other parameters, no significant influence was observed.

The results of the autopsied specimens, and associated corrosion current density, and resistivities are not in agreement with the resistivity interpretations presented in the literature. Higher corrosion rates are observed in much higher resistivities than the values presented in the literature.

Half-Cell Potentials

Half-cell potentials of all specimens were measured and analyzed to find if the parameters have any influence on corrosion activity. Significant influence of clear spacing groups between the anode and cathode on the potentials was observed from statistical analysis. Regarding the other parameters, no significant influence was observed. Measurements were conducted in both connected and unconnected state to find the contribution of macrocell corrosion on the total corrosion. The contribution of macrocell corrosion to the total corrosion was found to be insignificant.

Corrosion Current Density

Corrosion Current density of all specimens was calculated and analyzed to find if the parameters have any influence on corrosion activity. Significant influence of clear spacing groups between the anode and cathode on the corrosion current density was observed from the statistical analysis. Regarding the other parameters, no significant influence was observed. Measurements were conducted in both connected and unconnected state to find the contribution of macrocell

corrosion on the total corrosion. The contribution of macrocell corrosion to the total corrosion was found to be insignificant from the analysis. The corrosion current density values exhibit a relationship with resistivity and half-cell potential in accordance with the generally accepted theory.

Chloride Content

The chloride content was obtained at three depths from the top surface of concrete. Even if no statistically significant influence of clear spacing groups was found on chloride content, there is a definite increase in chloride content for the increase in clear spacing between groups. This supports the observation formed from resistivity measurements and that corrosion activity is resistivity controlled in the observed specimens.

Autopsy

The autopsy of the top and bottom reinforcement bars of the selected specimens showed that the top half of the top steel bars had corrosion. The visually observed amount of corrosion on each specimen agreed with the corrosion activity predicted from instrument corrosion measurements. The bottom half of the top steel bars may be the cathodes in the corrosion reaction.

Macrocell Corrosion

From the different measurements, macrocell corrosion was found insignificant in the total corrosion.

Finally, the instrument corrosion measurements reinforced the literature that, the consolidation of fresh concrete is an important factor in the whole corrosion mechanism. Lower unit consolidation energy, results in greater amount and depth of chloride penetration, per given chloride exposure methods and times.

RECOMMENDATIONS FOR FUTURE RESEARCH

There are many questions that are left unanswered in this study. The supposition that the resistivity is the controlling factor of corrosion activity requires further support. Resistivity could vary with depth, thus measurement at different depths is recommended to form a consistent relationship with diffusion coefficients and chloride contents. The interpretations of resistivity followed in this study must be revised for better predictions.

The influence of the diffusion coefficient or the relationship of diffusion coefficient with resistivity was not established in this study. Also the influence of moisture content on corrosion activity was not defined. More chloride content samples from the same specimens would be useful to check the consistency among the chloride content values, since only one set of chloride cores were obtained from each specimen.

If the study will be repeated, continuous measurements of moisture content at different depths and more chloride samples from each specimen are recommended. Also, a greater number of specimens will be useful to form a better relationship among the testing parameters.

REFERENCES

ACI Manual of Practice Part 1, 2002. American Concrete Institute, Farmington Hills, MI

Andrade, C., I.R. Maribona, S. Feliu, J.A. Gonzalez, and S. Felieu Jr. "The Effect of Macrocells Between Active and Passive Areas of Steel Reinforcements."Corrosion Science 33 (1991): 237-249.

ASTM, American Society for Testing and Materials, "C 876-91, Standard Test Method for Half-Cell Potentials of Uncoated Reinforcing Steel in Concrete," Annual Book of ASTM Standards Vol. 04.02 Concrete and Aggregates (1991).

Bentur, Arnon, Sidney Diamond, and Neal Berke. Steel Corrosion In Concrete. London: E&FN Spon, 1997.

Berke, N. S. and Hicks, M. C., "Predicting Times to Corrosion From Field and Laboratory Chloride Data," Berke, N. S., Escalante, E., Nmai, C. K., Whiting, D. Ed., TECHNIQUE TO ASSESS THE CORROSION ACTIVITY OF STEEL REINFORCED CONCRETE STRUCTURES, 41-57. 1996. W Consohocken, American Society Testing and Materials. AMERICAN SOCIETY FOR TESTING AND MATERIALS SPECIAL TECHNICAL PUBLICATION.

Berkeley, K and S. Pathmanaban. Cathodic Protection of Reinforcement Steel in Concrete. London: Butterworth & Co. Ltd, 1990.

Bertolini, L., B. Elsener, P. Pedeferri, and R. Polder. Corrosion of Steel in Concrete – Prevention, Diagnosis, Repair. Weinheim, Germany: Wiley-VCH Verlag GmbH & Co. KGaA, 2004.

Broomfield, John P. Corrosion of Steel in Concrete. London: E&FN Spon, 2007.

Brown, Michael C. (1999). "Assessment of Commercial Corrosion Inhibiting Admixtures for Reinforced Concrete." Master of Science Thesis in Civil and Environmental Engineering, Virginia Polytechnic Institute and State University.

Cady, P.D. and Carrier, R.E. (1971) Durability of Bridge Deck Concrete, Department of Civil Engineering, The Pennsylvania State University.

Castro, P, E. Pazini, C. Andrade, and C. Alonso. "Macrocell Activity in Slightly Chloride-Contaminated Concrete Induced by Reinforcement Primers." Corrosion 59 (June 2003): 535-545.

Clear, Kenneth C. (1989). "Measuring Rate of Corrosion of Steel in Field Concrete Structures." Kenneth C. Clear, Inc. Concrete Materials and Corrosion Specialists, Sterling, Virginia (1989).

Elsener, B. "Macrocell Corrosion of Steel in Concrete – Implications for Corrosion Monitoring." Cement & Concrete Composites 24 (2002): 65-72.

Feliu, S., J.A. Gonzalez, J.M. Miranda, V. Feliu. “Possibilities and Problems of in Situ Techniques for Measuring Steel Corrosion Rates in Large Reinforced Concrete Structures.” Corrosion Science 47 (2005): 217-238.

Mehta, K.P. Concrete: Microstructure, Properties, and Materials. 3rd Edition, New York: The McGraw-Hill Companies, 2005.

Ramniceanu, Andrei (2004). “Correlation of Corrosion Measurements and Bridge Conditions with NBIS Deck Rating.” Master of Science Thesis in Civil and Environmental Engineering, Virginia Polytechnic Institute and State University.

Raupach, M. “Chlrodie-Induced Macrocell Corrosion of Steel in Concrete – Theoretical Background and Practical Consequences.” Construction and Building Materials 10 (1996): 329-338.

Schiessl, Peter. “Chloride-Induced Corrosion of Steel in Concrete: Development of a Concrete Corrosion Testing Cell.” Concrete Precasting Plant and Technology 52 (1986): 626-635.

Shiessel, Peter. Corrosion of Steel in Concrete. London, New York: Chapman and Hall, 1998.

Smolinski, L. “Influence of Reinforcing Steel Parameters on the Formation of the Passive Layer” Master of Science Thesis in Civil and Environmental Engineering, Virginia Polytechnic Institute and State University.

Weingroff, Richard F., “FHWA By Day: A Look at the History of the Federal Highway Administration.” 1996. www.fhwa.dot.gov/byday/ghbd1215.htm. 2006.

Zemajtis, Jerzy, Modeling the Time to Corrosion Initiation for Concretes with Mineral Admixtures and/or Corrosion Inhibitors in Chloride-Laden Environments, Virginia Polytechnic Institute and State University, (1998).

APPENDICES

Appendix A – Resistivity Measurements

Figure A-1 – Resistivity – 2” Spacing, 1 Cathode Bar, with SIP

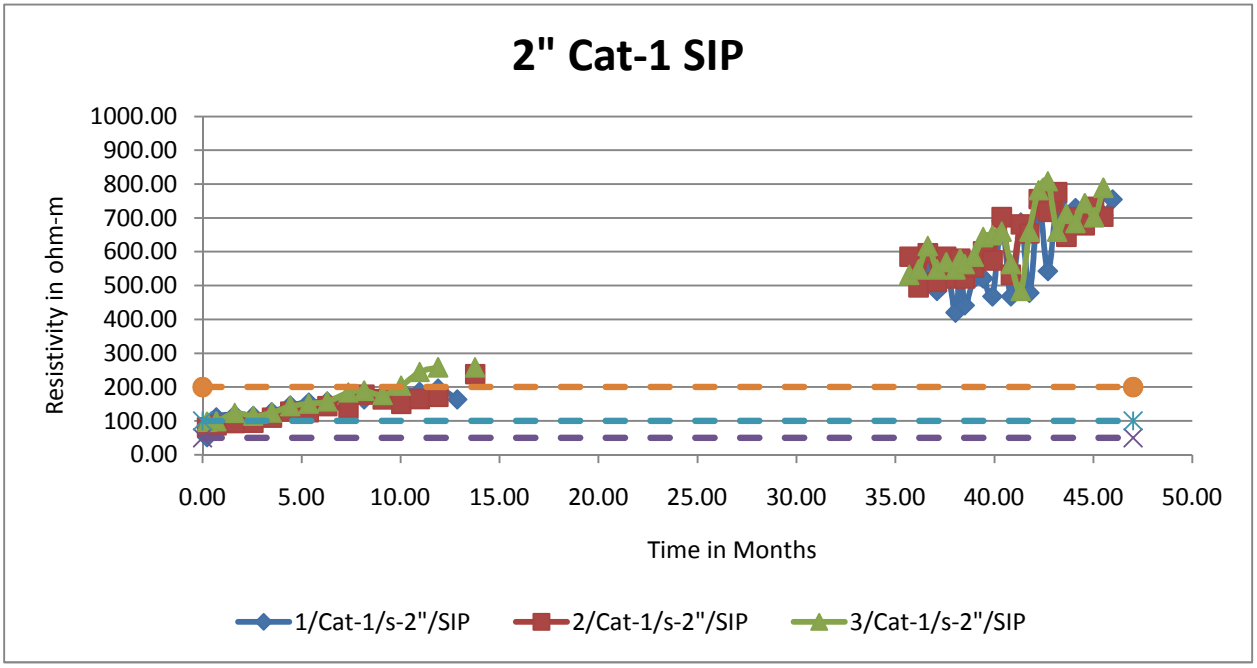

Figure A-2 – Resistivity – 2” Spacing, 2 Cathode Bars, with SIP

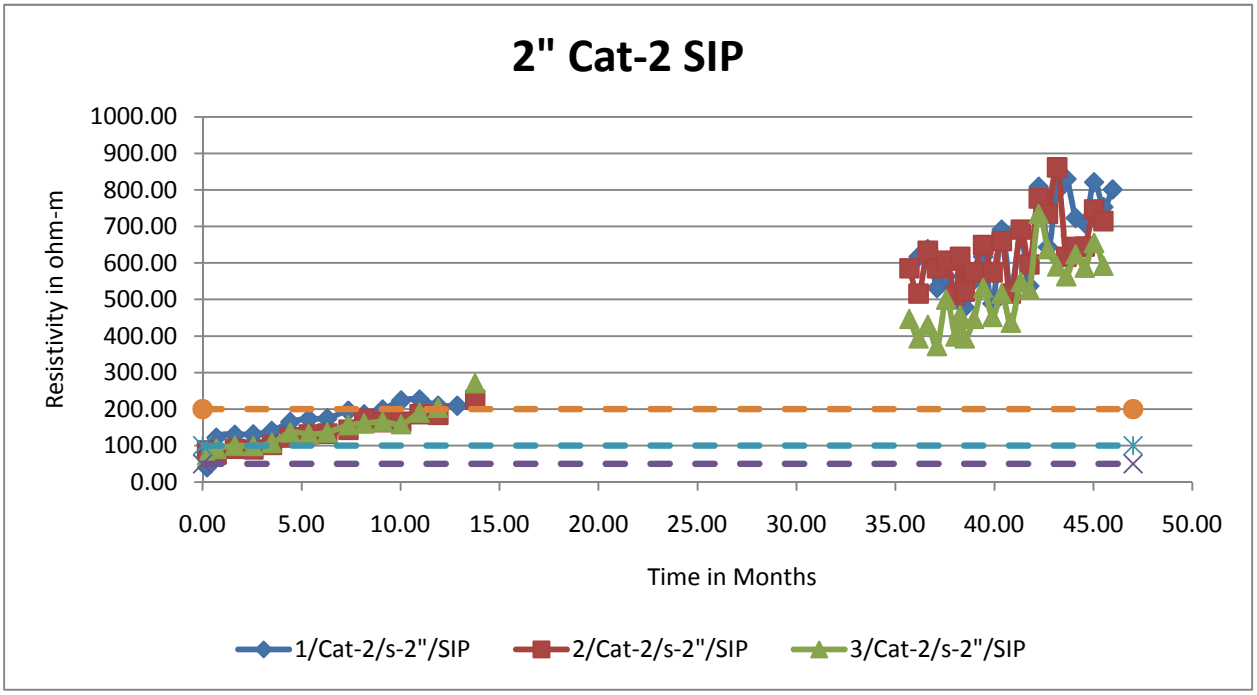

Figure A-3 - Resistivity – 2” Spacing, 2 Cathode Bars, with No SIP

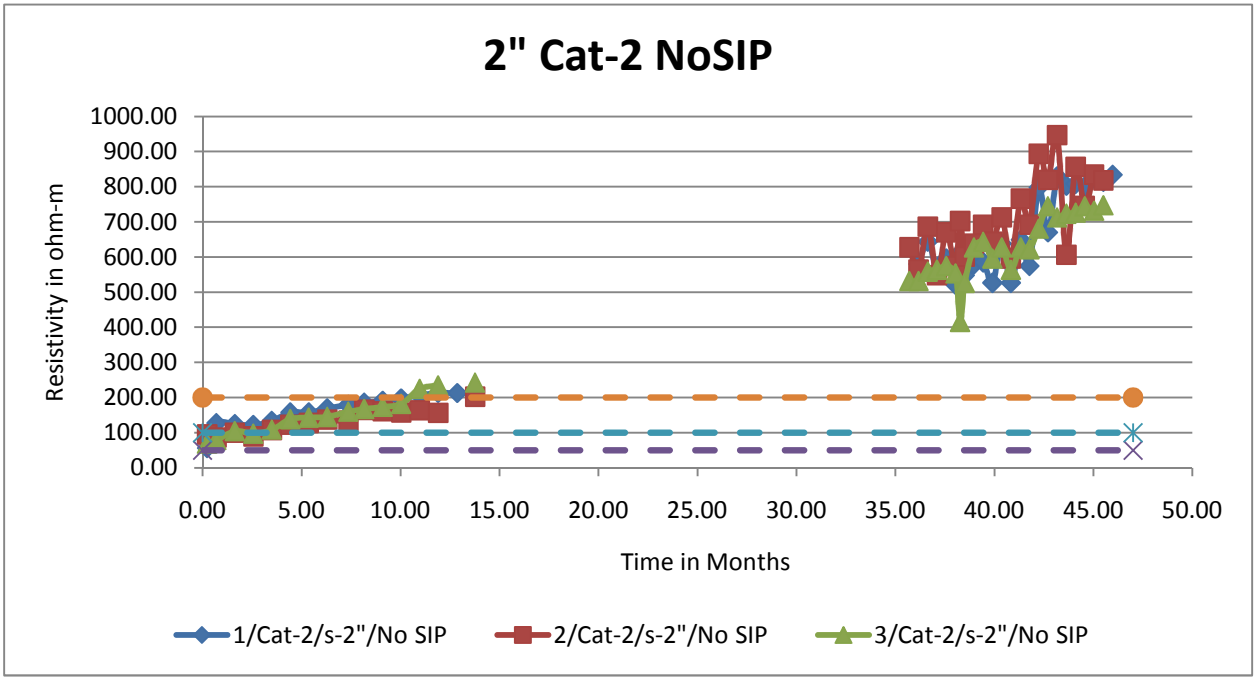

Figure A-4 - Resistivity – 3” Spacing, 1 Cathode Bar, with SIP

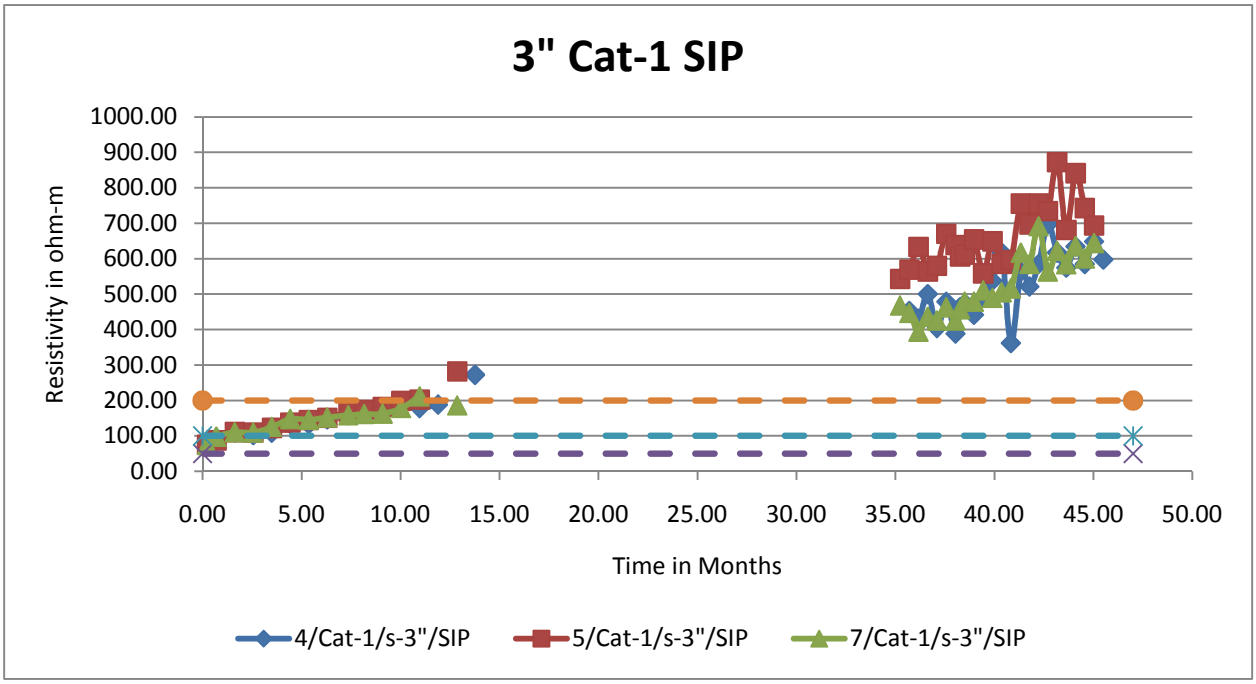

Figure A-5 - Resistivity – 3” Spacing, 2 Cathode Bars, with SIP

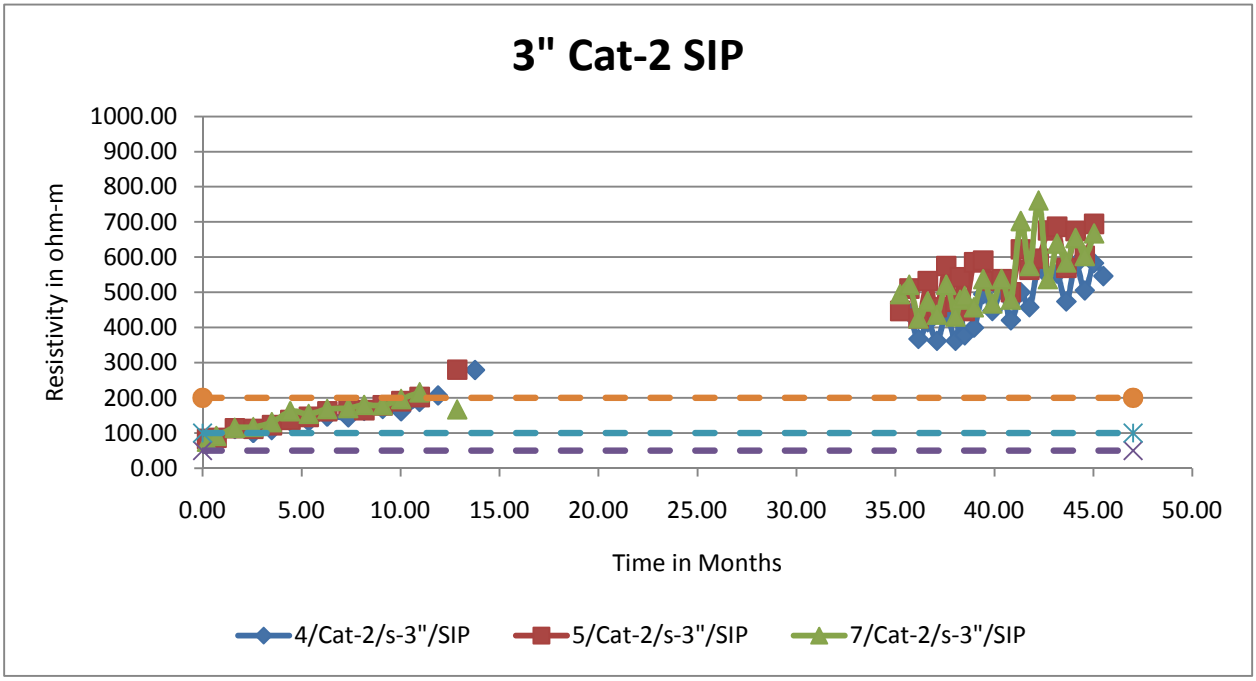

Figure A-6 - Resistivity – 3” Spacing, 2 Cathode Bars, with No SIP

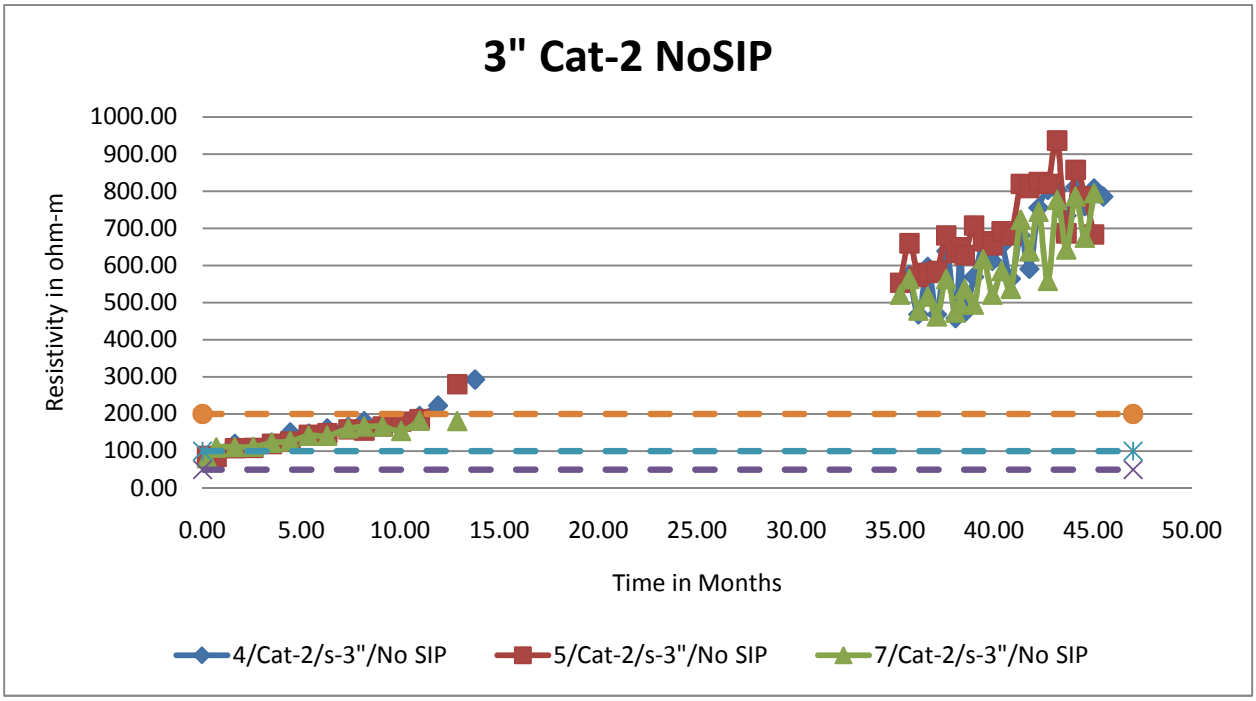

Figure A-7 - Resistivity – 4” Spacing, 1 Cathode Bar, with SIP

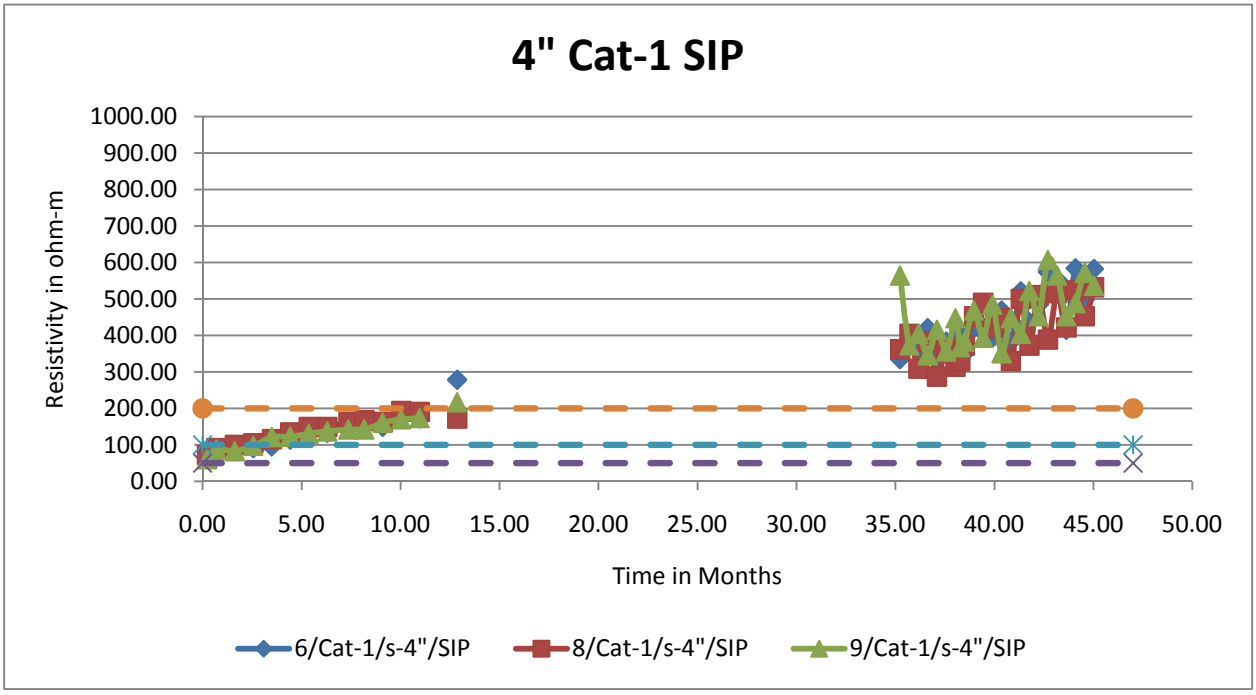

Figure A-8 - Resistivity – 4” Spacing, 2 Cathode Bars, with SIP

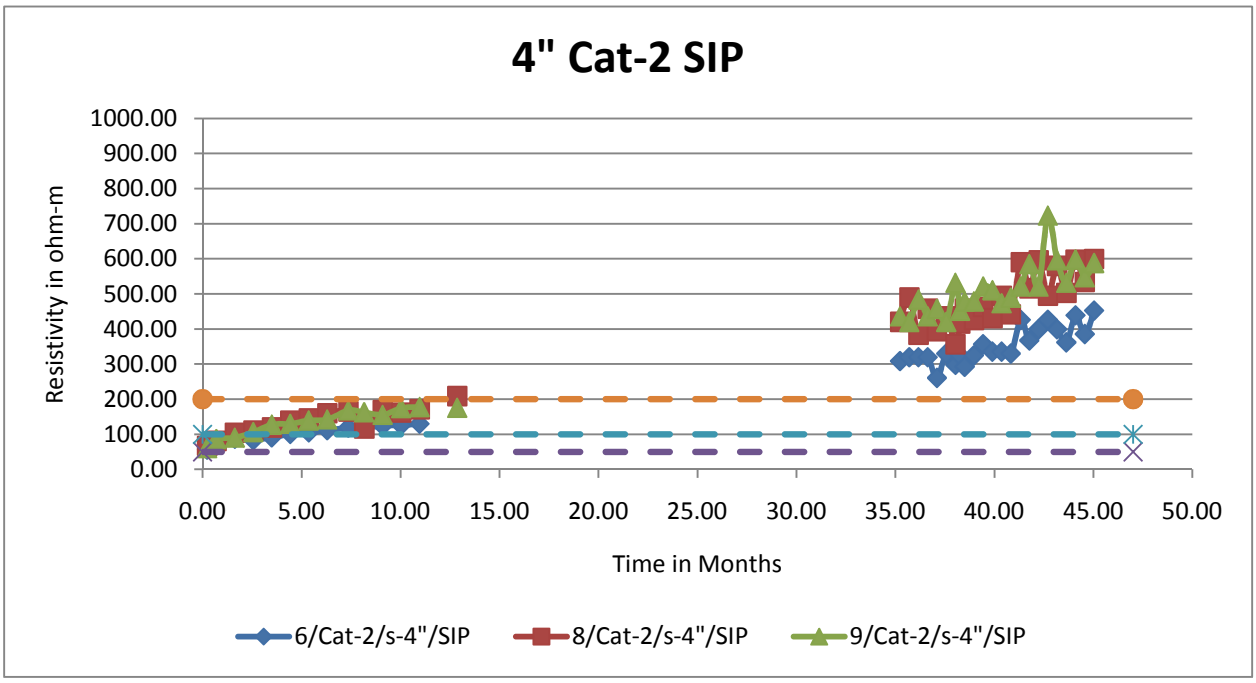

Figure A-9 - Resistivity – 4” Spacing, 2 Cathode Bars, with No SIP

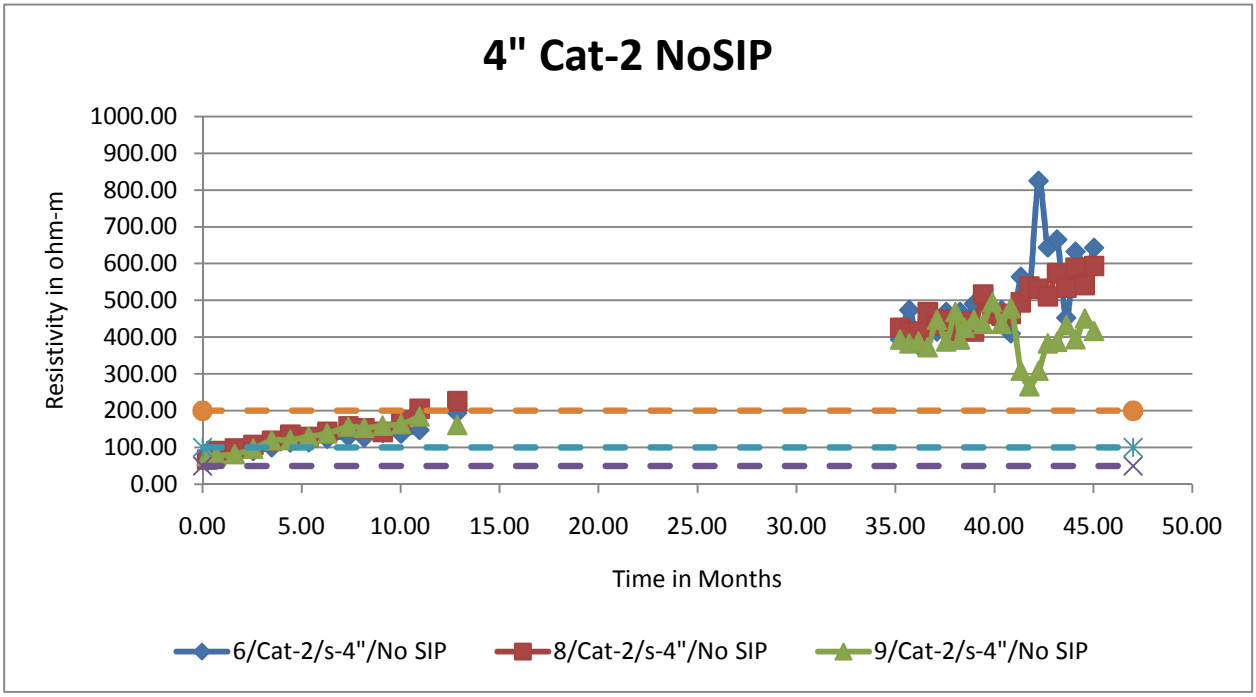

Appendix B – Half-Cell Potential Measurements

Figure B-1 - Half-Cell Potentials - 2” Spacing, 1 Cathode Bar, with SIP, Left Side, Connected

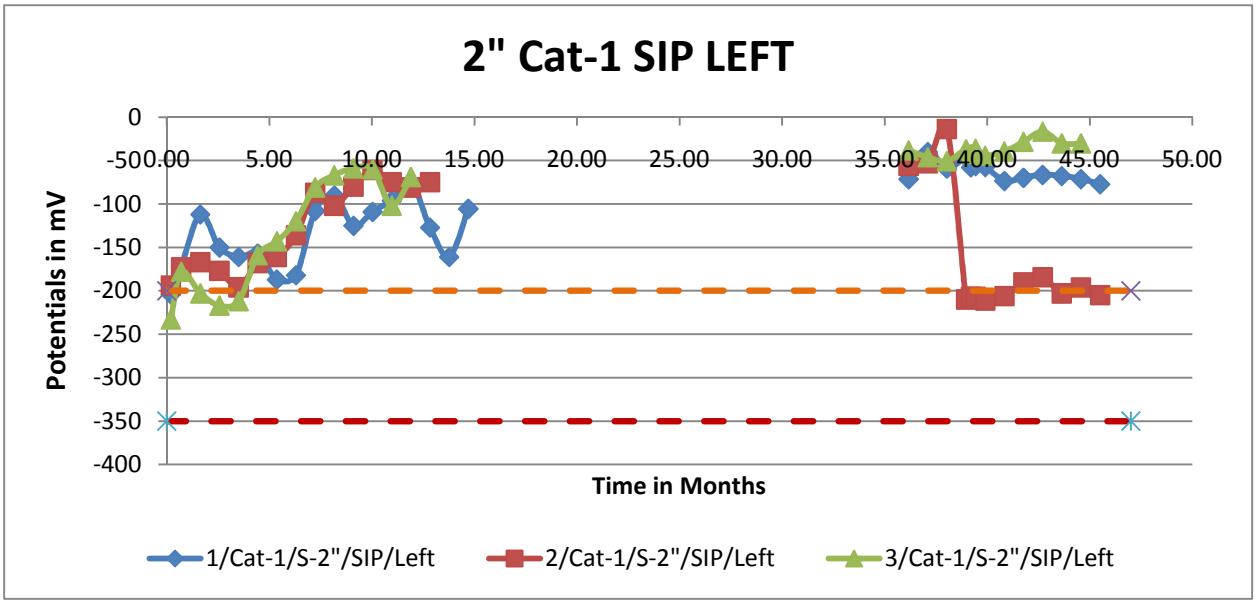

Figure B-2 - Half-Cell Potentials - 2” Spacing, 1 Cathode Bar, with SIP, Left Side, Unconnected

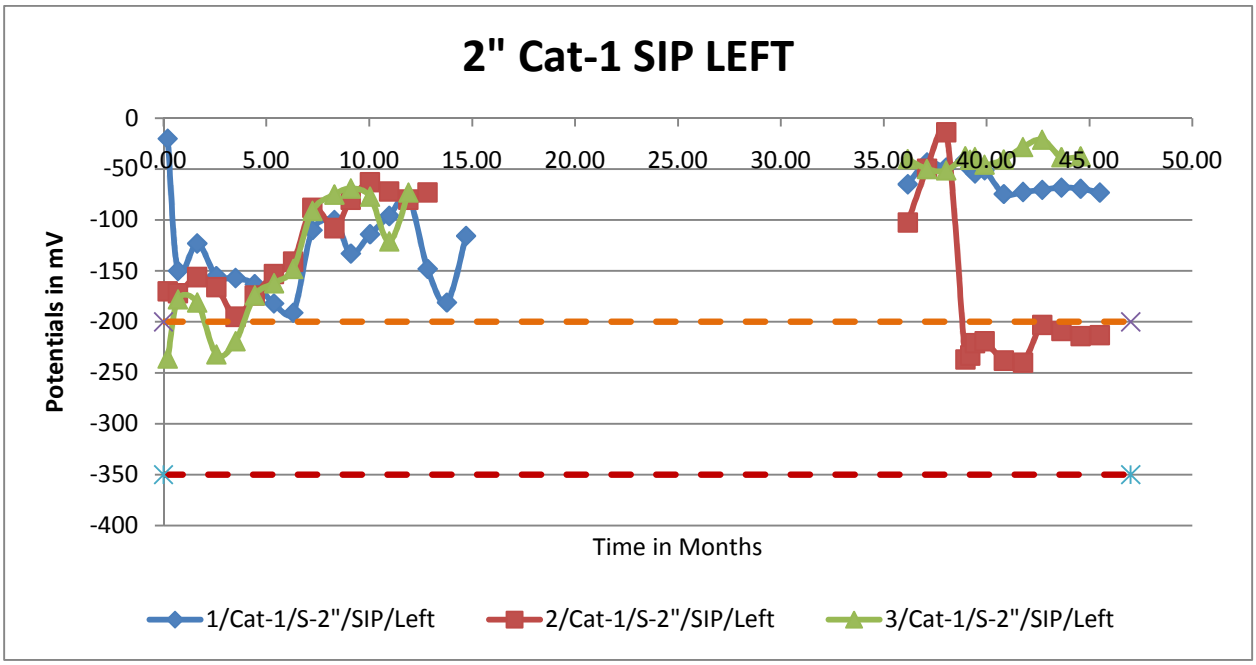

Figure B-3 - Half-Cell Potentials - 2” Spacing, 2 Cathode Bars, with SIP, Left Side, Connected

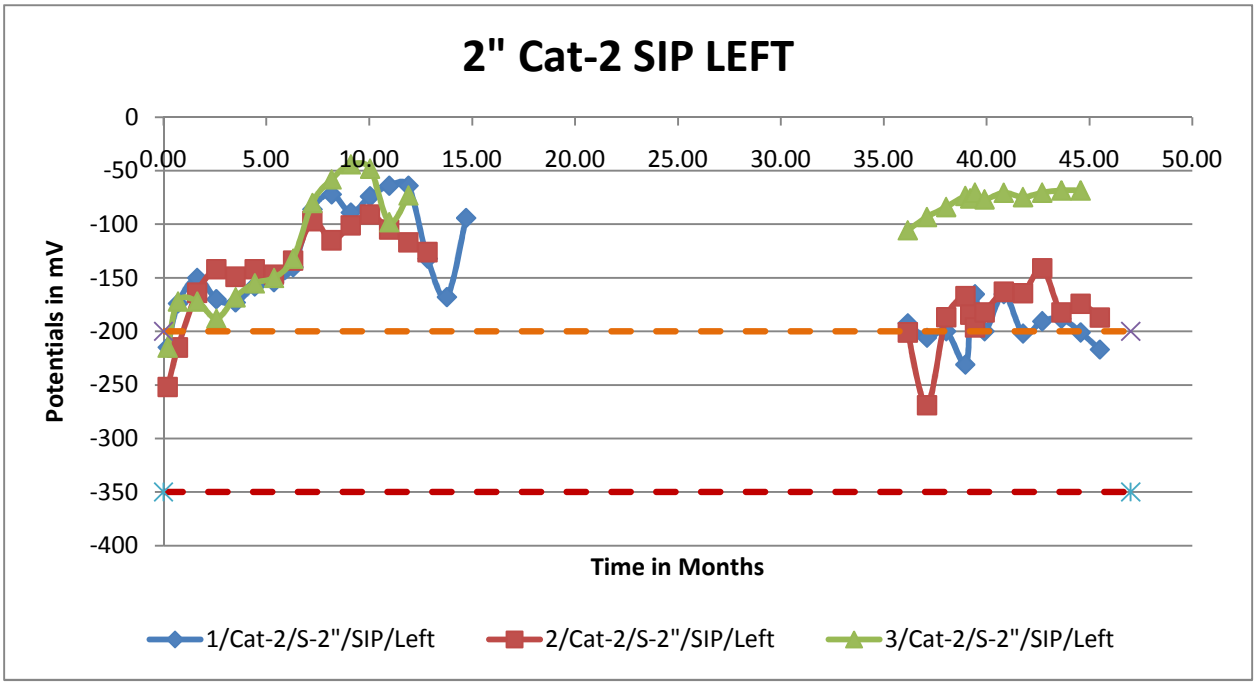

Figure B-4 - Half-Cell Potentials - 2” Spacing, 2 Cathode Bars, with SIP, Left Side, Unconnected

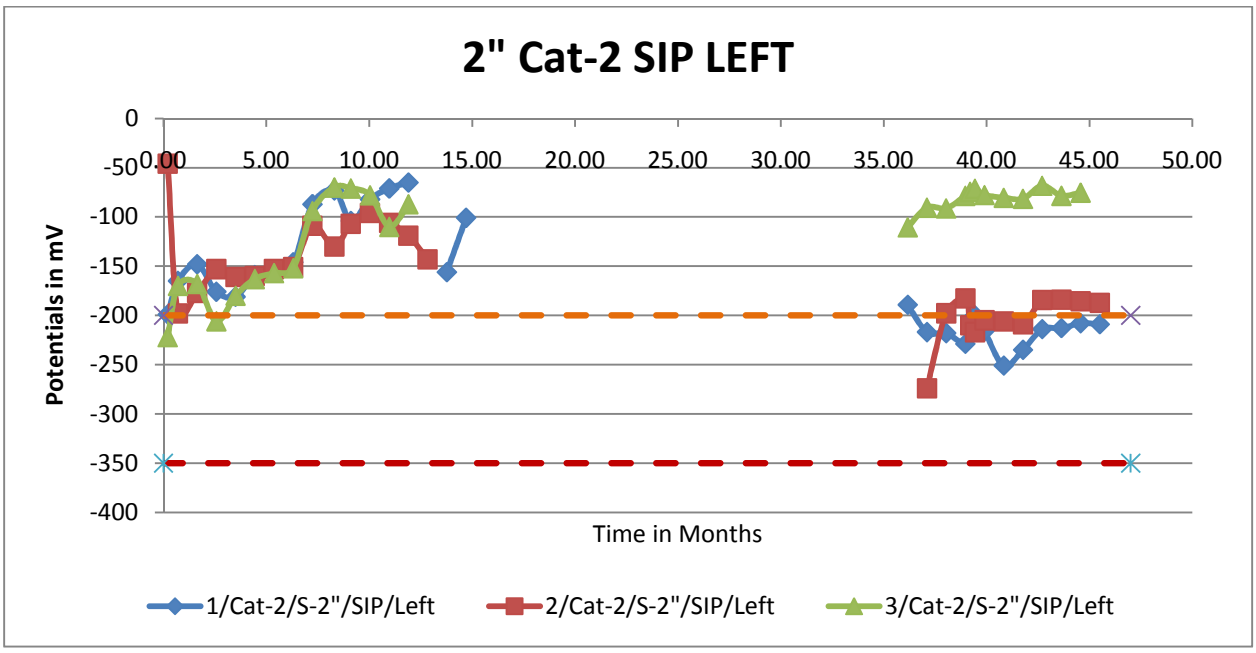

Figure B-5 - Half-Cell Potentials - 2” Spacing, 2 Cathode Bars, with No SIP, Left Side, Connected

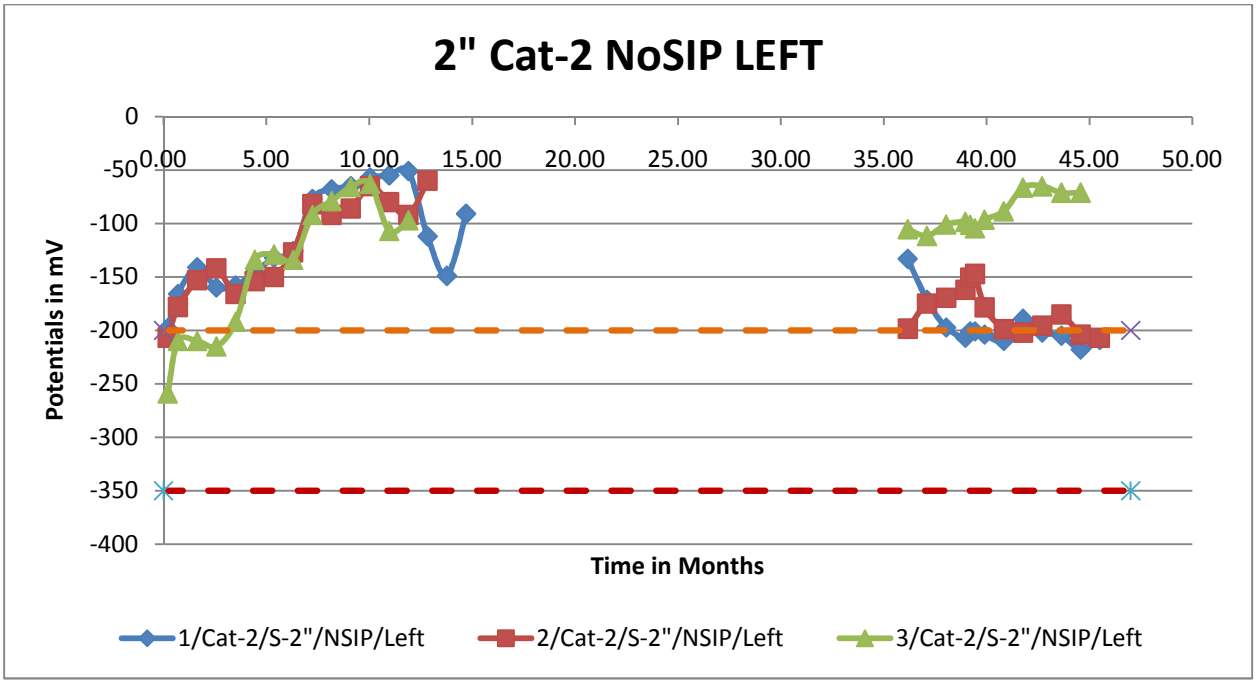

Figure B-6 - Half-Cell Potentials - 2” Spacing, 2 Cathode Bars, with No SIP, Left Side, Unconnected

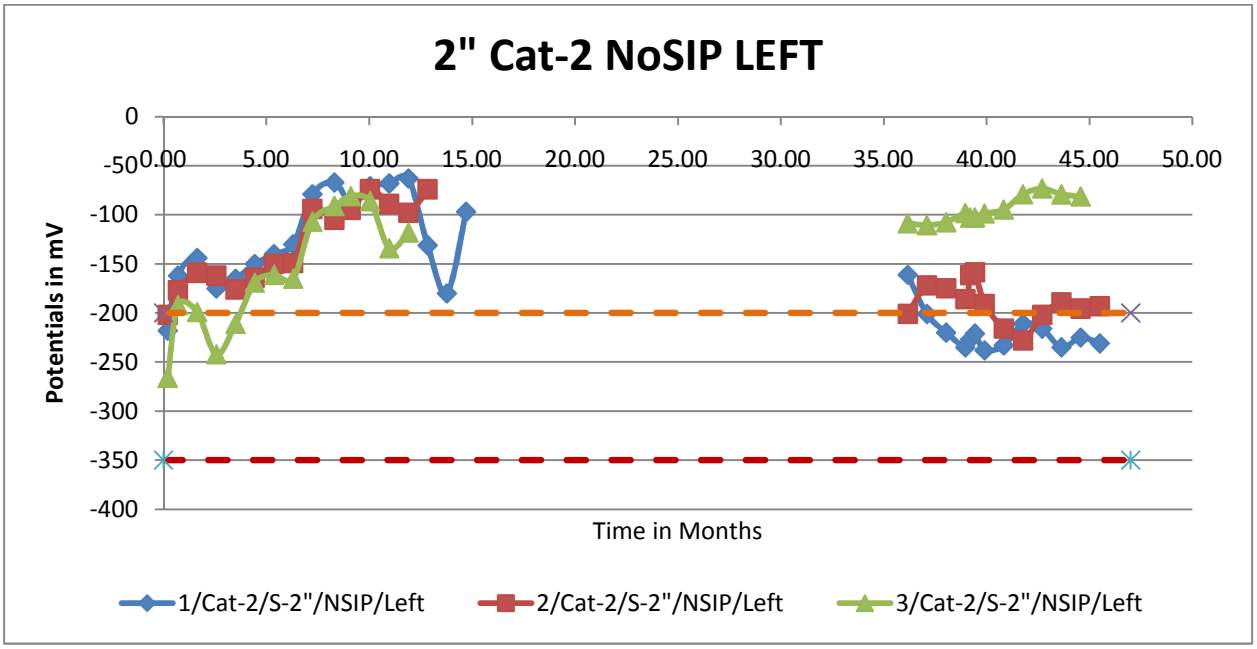

Figure B-7 - Half-Cell Potentials -3" Spacing, 1 Cathode Bar, with SIP, Left Side, Connected

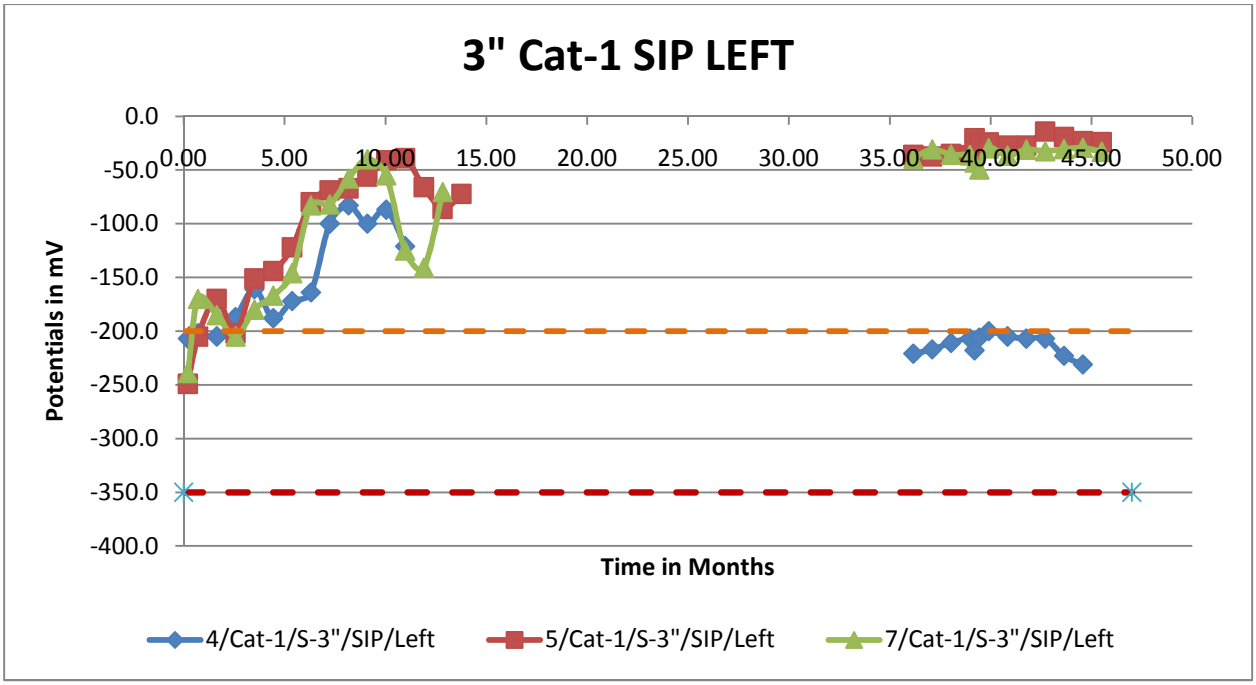

Figure B-8 - Half-Cell Potentials -3" Spacing, 1 Cathode Bar, with SIP, Left Side, Unconnected

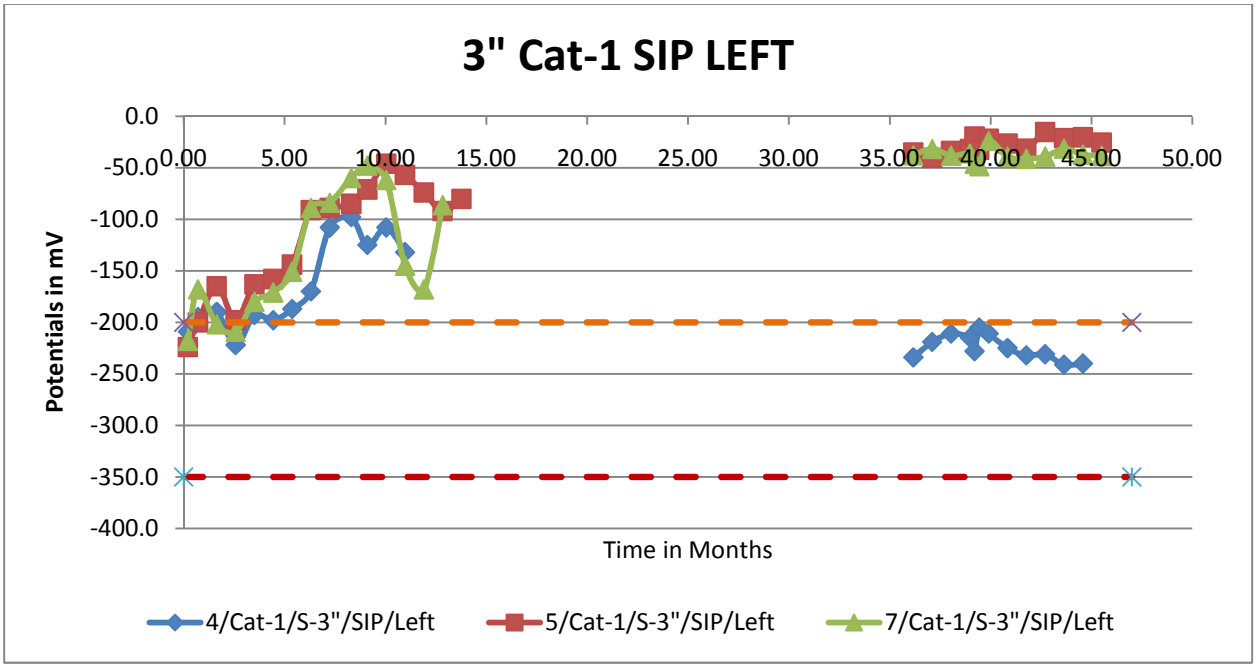

Figure B-9 - Half-Cell Potentials -3" Spacing, 2 Cathode Bars, with SIP, Left Side, Connected

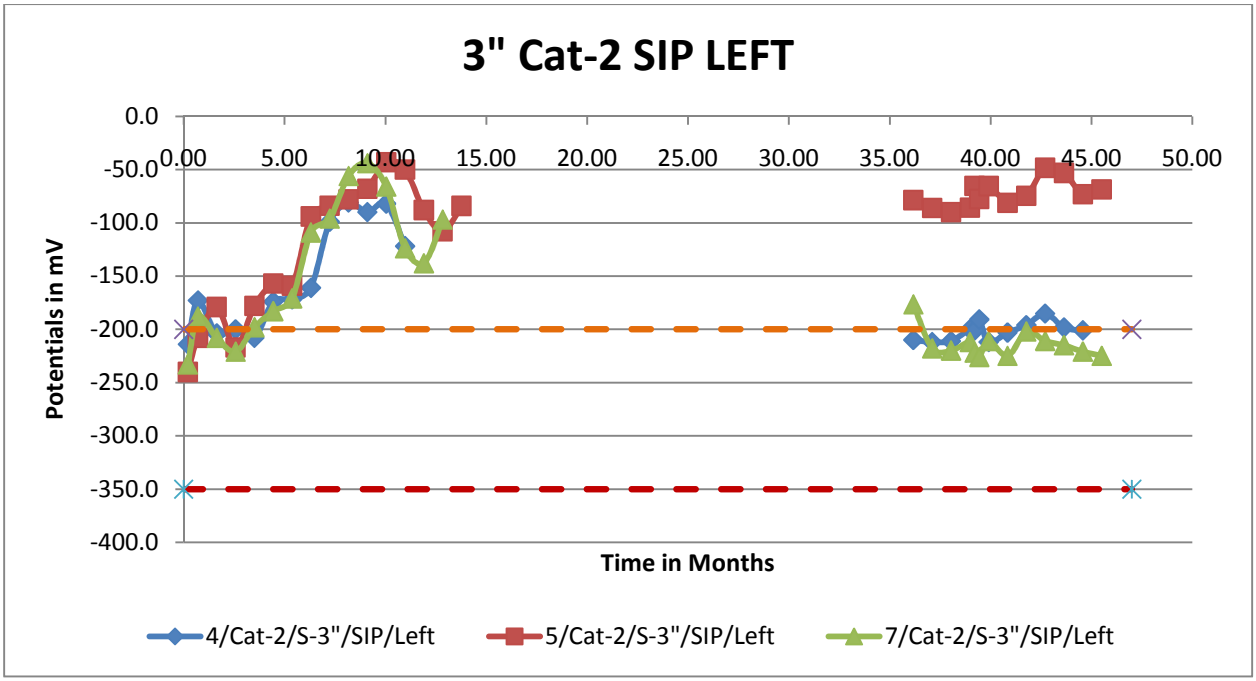

Figure B-10 - Half-Cell Potentials -3" Spacing, 2 Cathode Bars, with SIP, Left Side, Unconnected

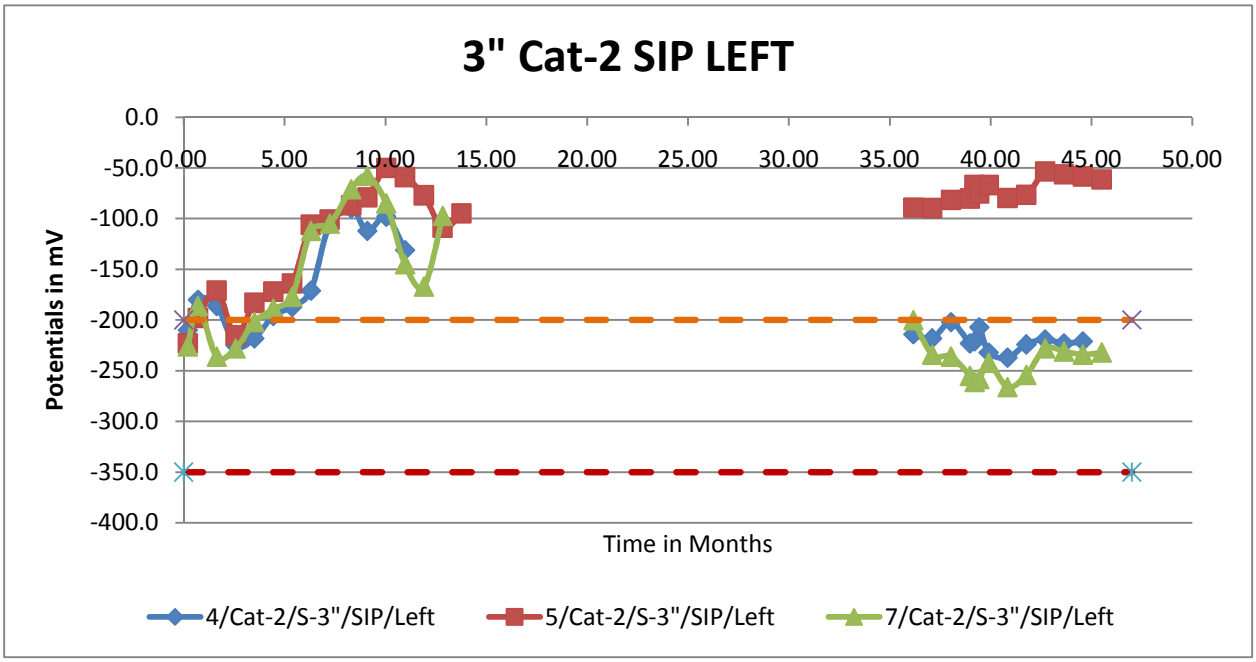

Figure B-11 - Half-Cell Potentials -3" Spacing, 2 Cathode Bars, with No SIP, Left Side, Connected

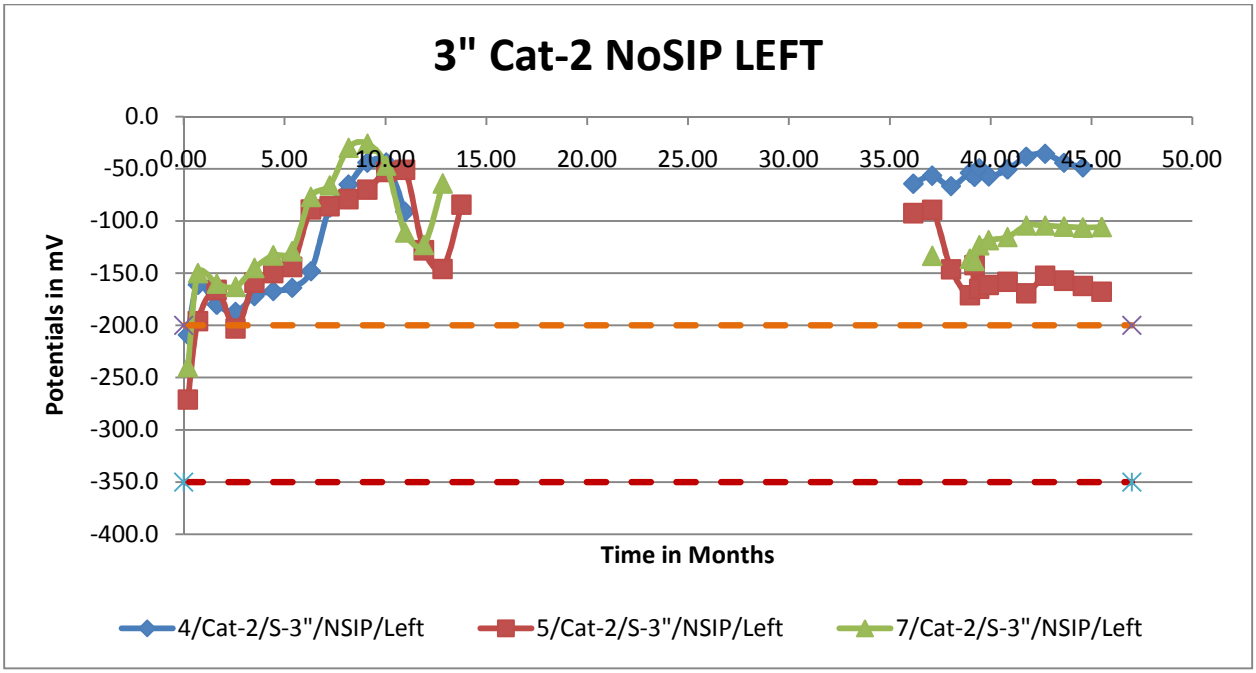

Figure B-12 - Half-Cell Potentials -3" Spacing, 2 Cathode Bars, with No SIP, Left Side, Unconnected

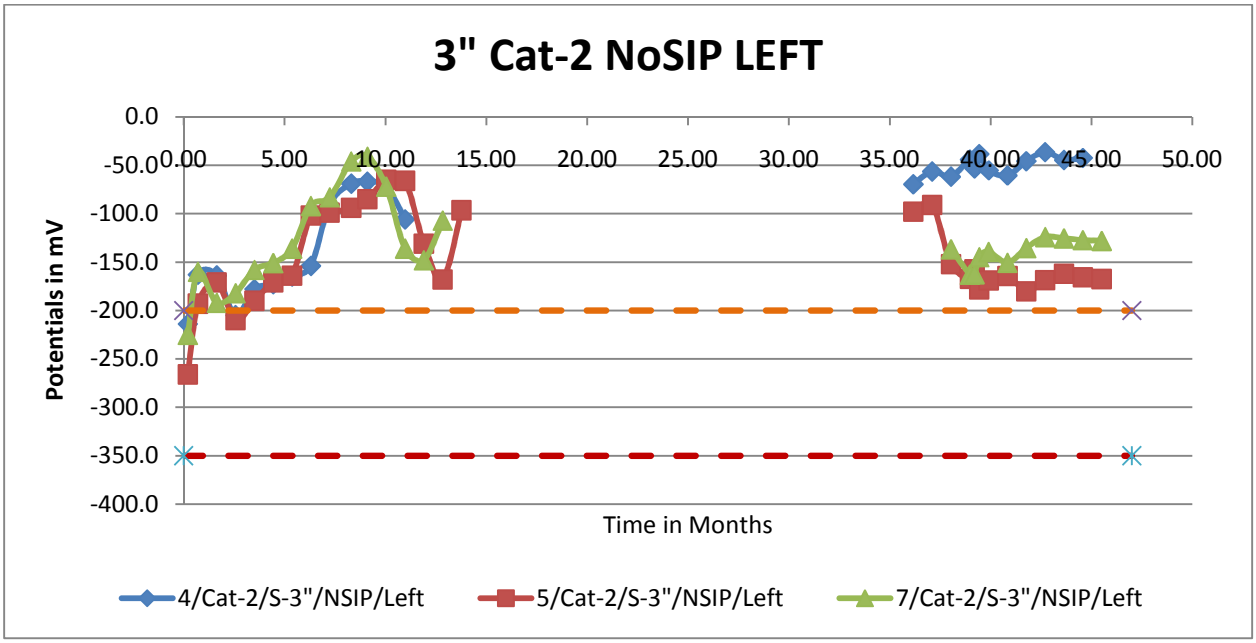

Figure B-13 - Half-Cell Potentials -4" Spacing, 1 Cathode Bar, with SIP, Left Side, Connected

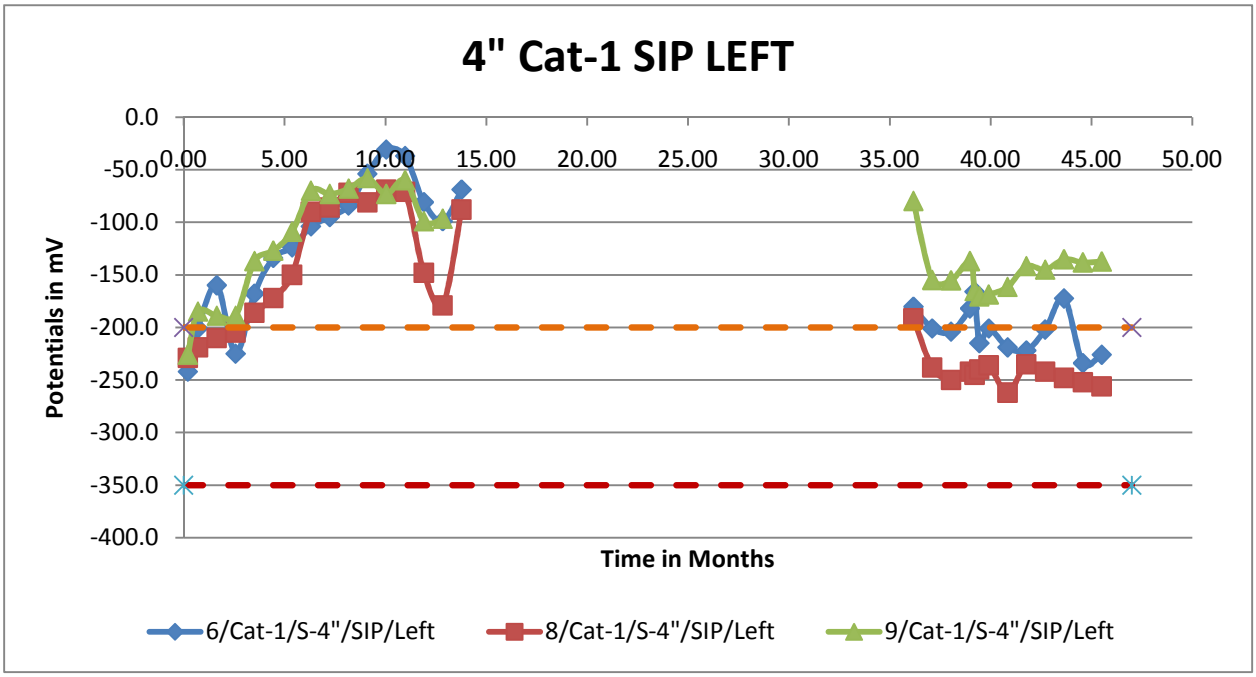

Figure B-14 - Half-Cell Potentials -4" Spacing, 1 Cathode Bar, with SIP, Left Side, Unconnected

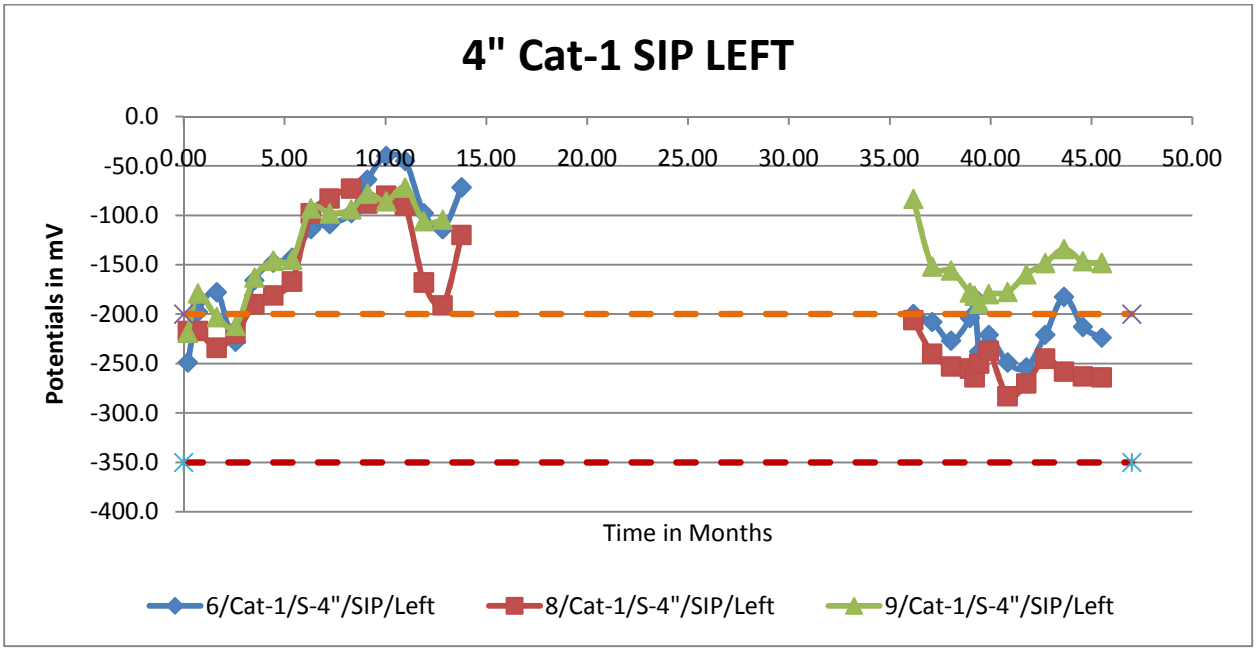

Figure B-15 - Half-Cell Potentials -4" Spacing, 2 Cathode Bars, with SIP, Left Side, Connected

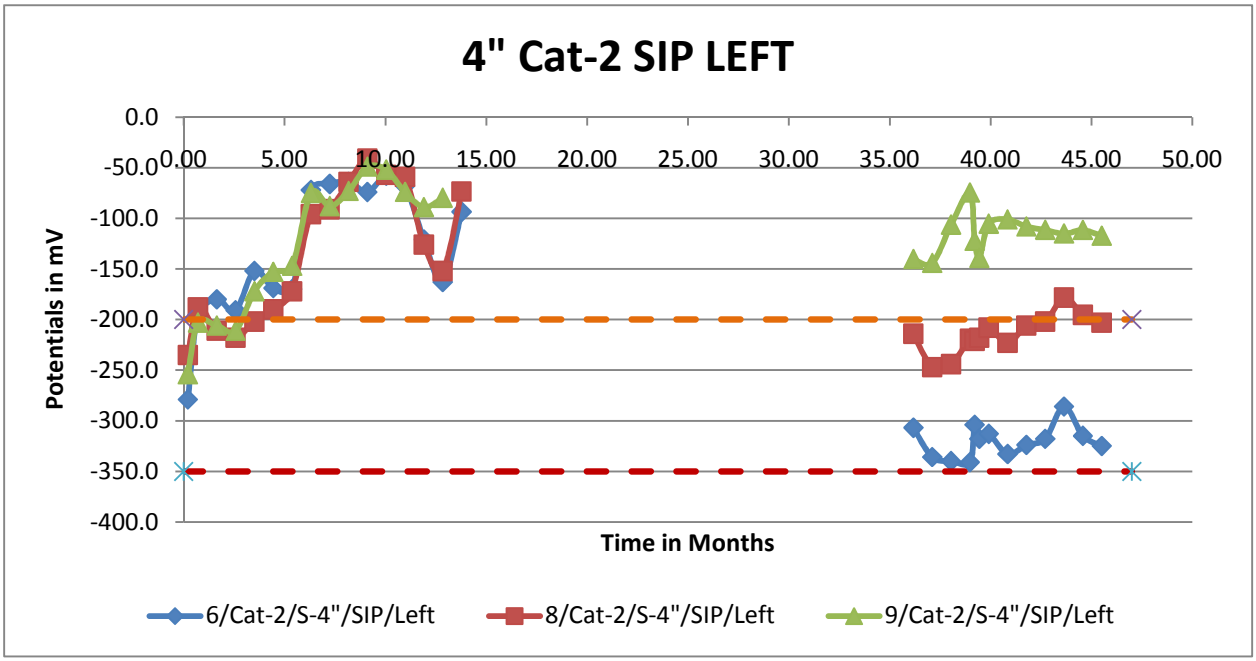

Figure B-16 - Half-Cell Potentials -4" Spacing, 2 Cathode Bars, with SIP, Left Side, Unconnected

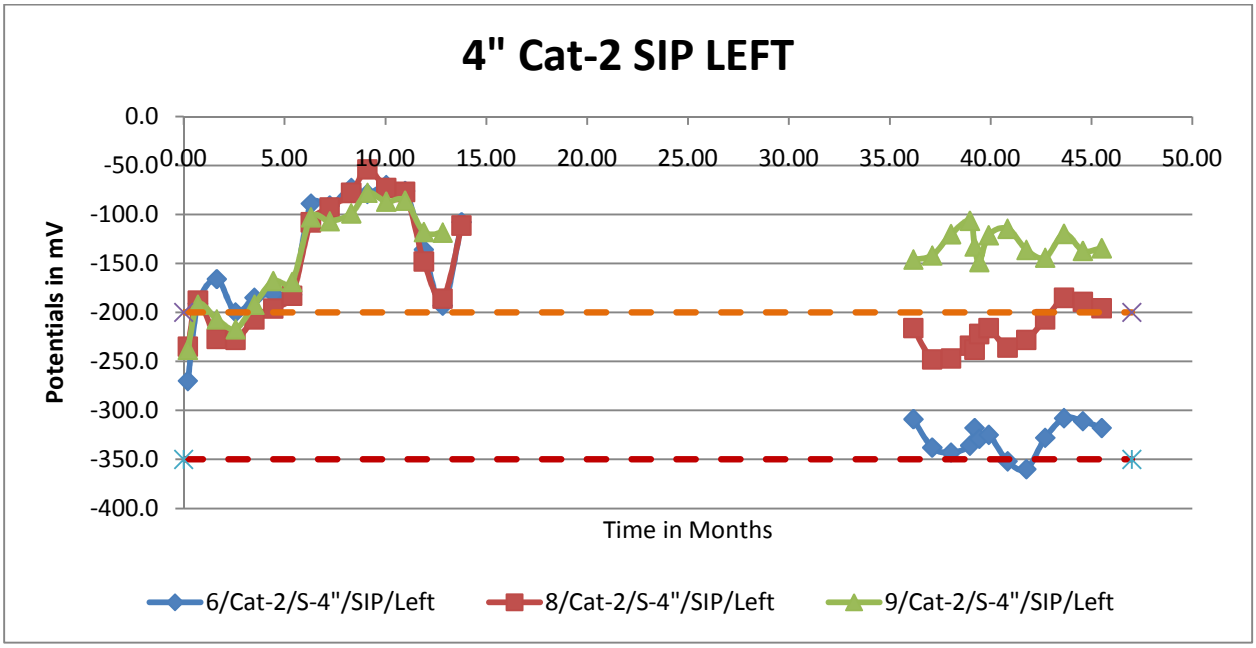

Figure B-17 - Half-Cell Potentials -4" Spacing, 2 Cathode Bars, with No SIP, Left Side, Connected

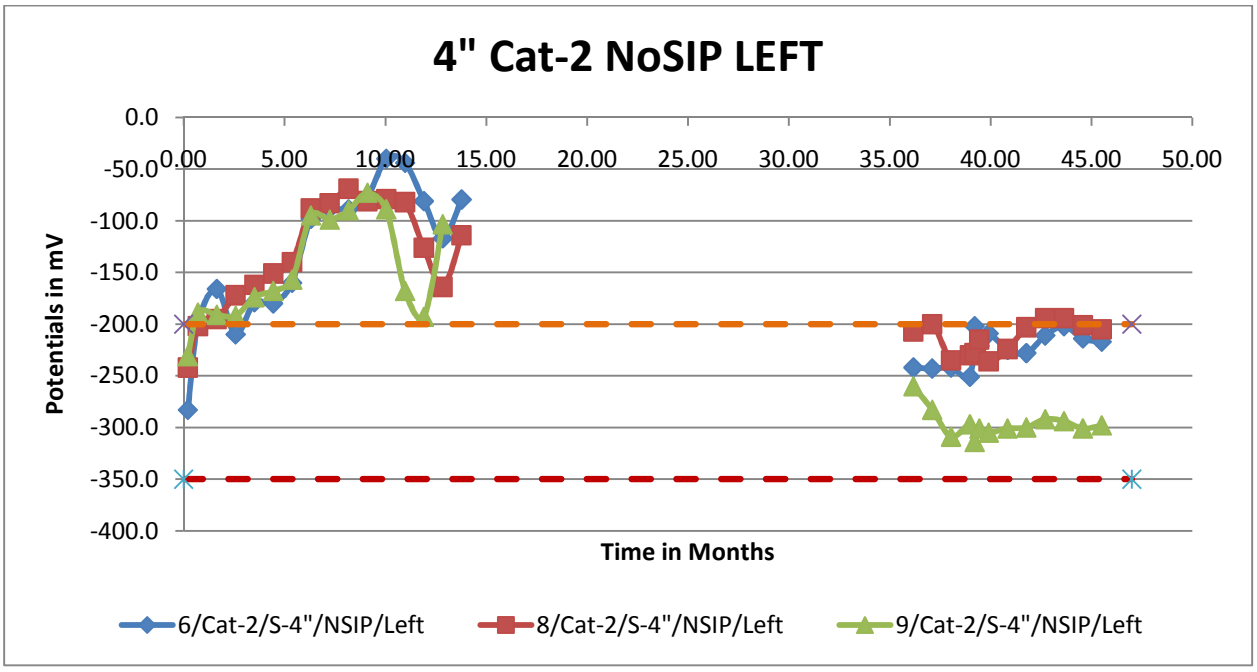

Figure B-18 - Half-Cell Potentials -4" Spacing, 2 Cathode Bars, with No SIP, Left Side, Unconnected

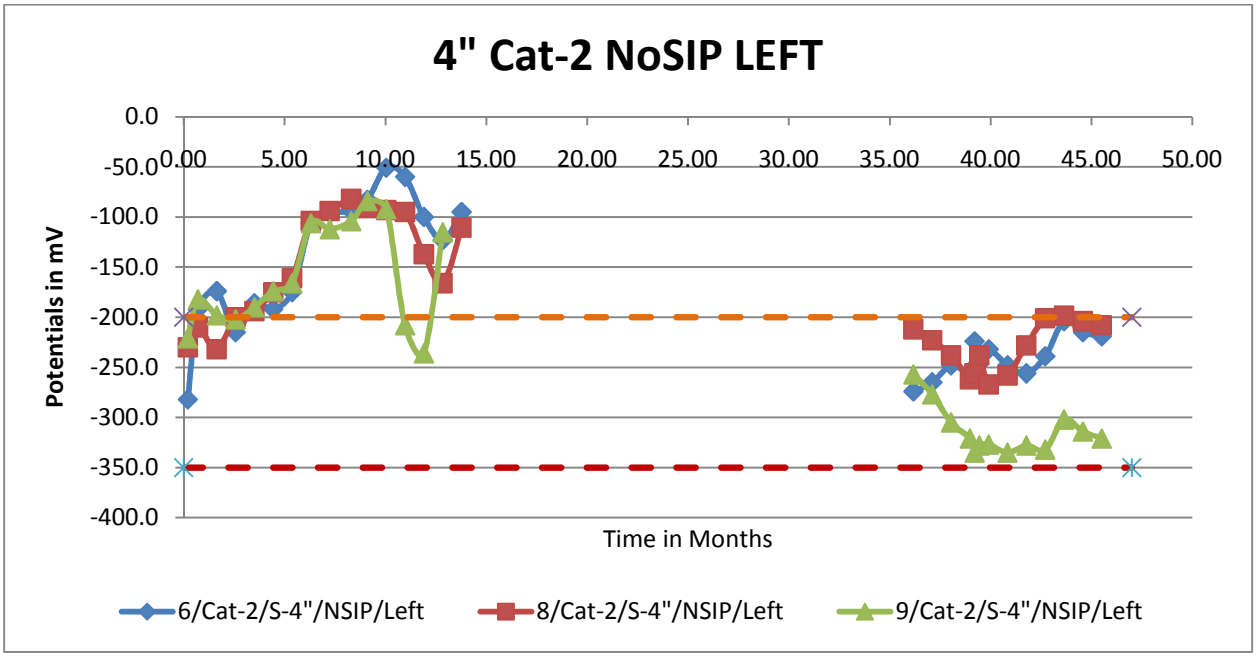

Figure B-19 - Half-Cell Potentials -2” Spacing, 1 Cathode Bar, with SIP, Right Side, Connected

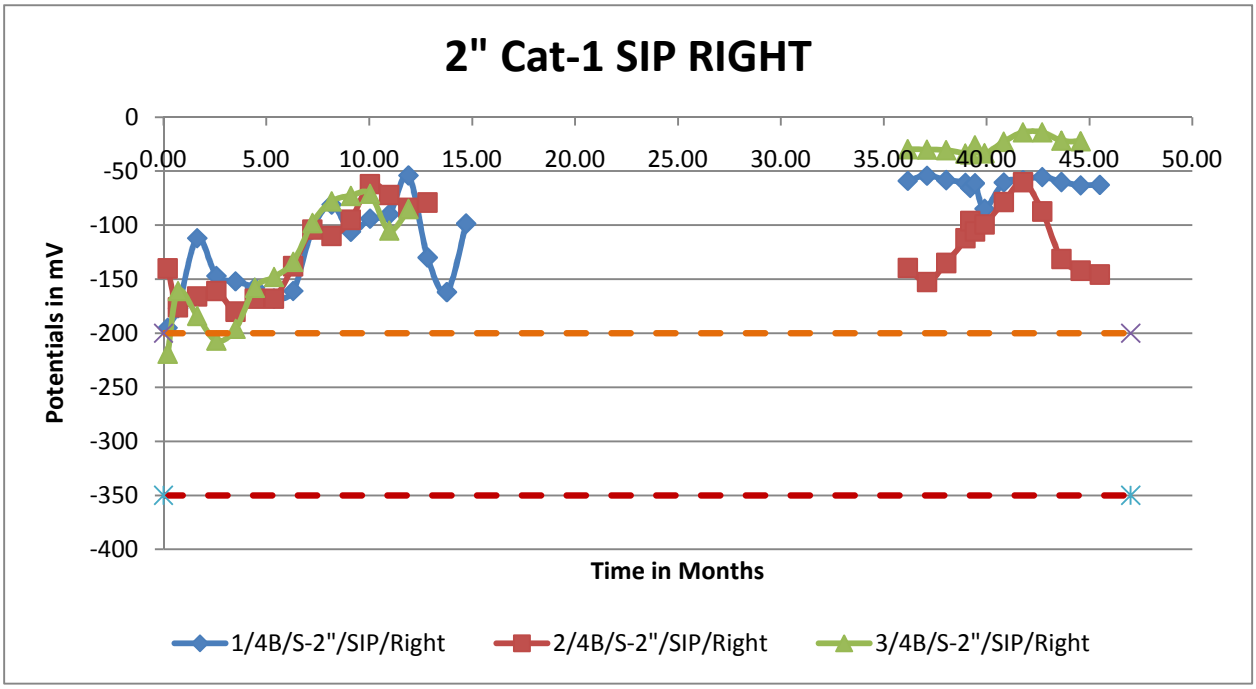

Figure B-20 - Half-Cell Potentials -2” Spacing, 1 Cathode Bar, with SIP, Right Side, Unconnected

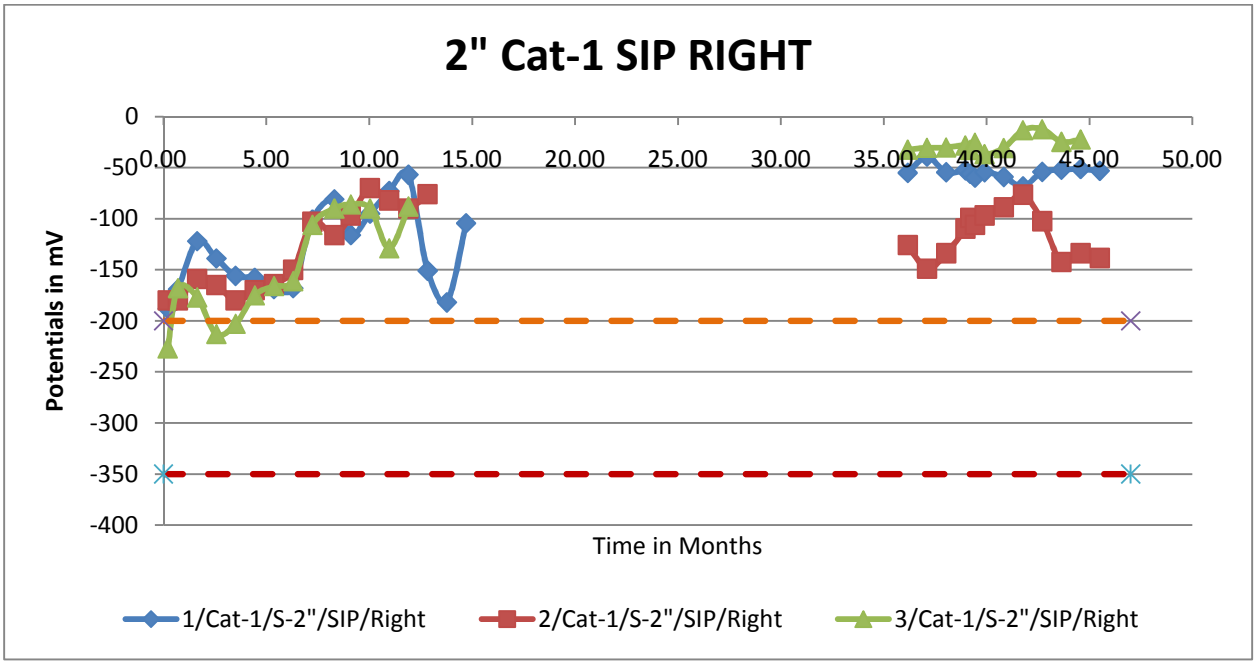

Figure B-21 - Half-Cell Potentials -2" Spacing, 2 Cathode Bars, with SIP, Right Side, Connected

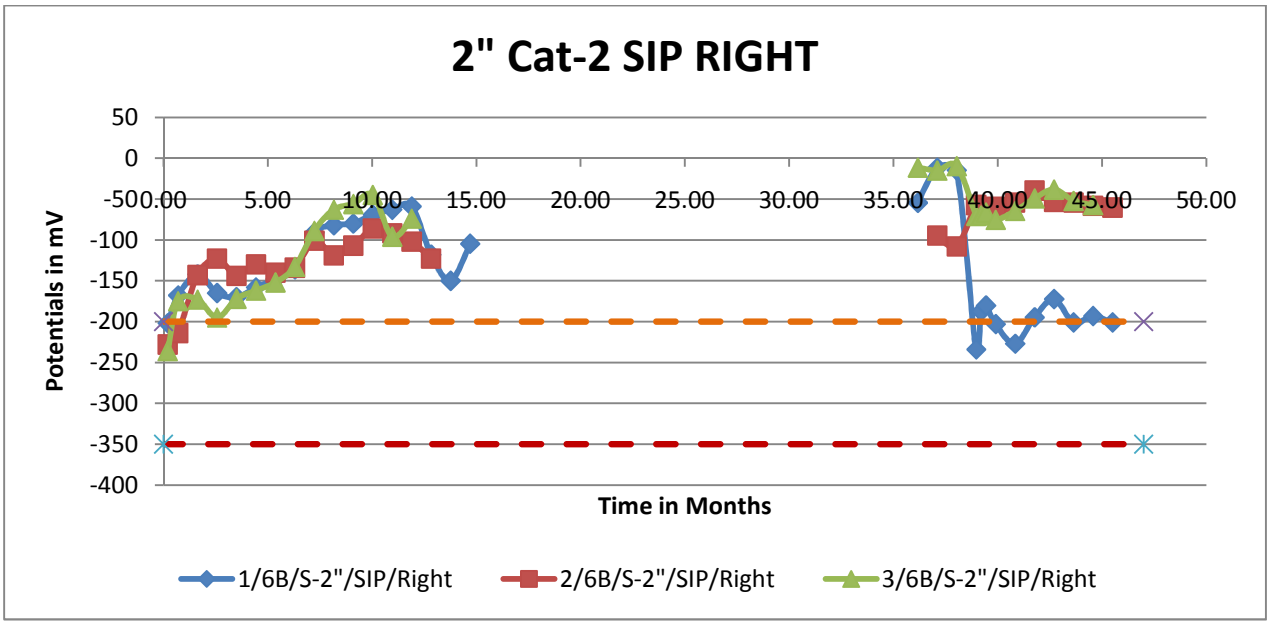

Figure B-22 - Half-Cell Potentials -2" Spacing, 2 Cathode Bars, with SIP, Right Side, Unconnected

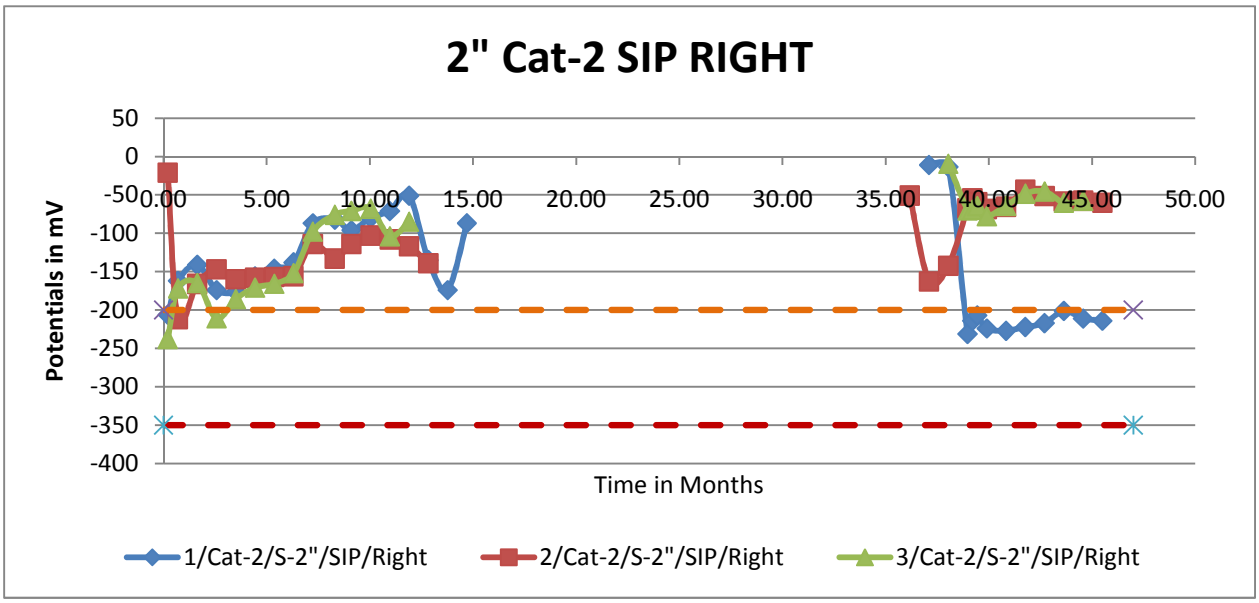

Figure B-23 - Half-Cell Potentials -2" Spacing, 2 Cathode Bars, with No SIP, Right Side, Connected

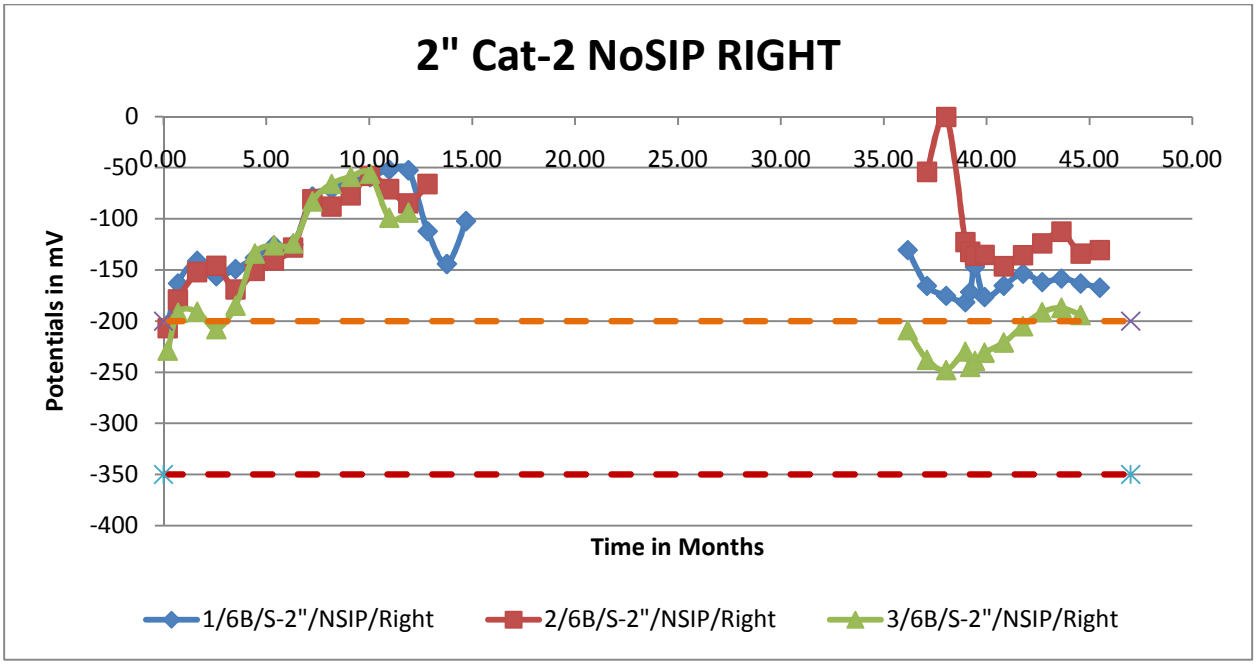

Figure B-24 - Half-Cell Potentials -2" Spacing, 2 Cathode Bars, with No SIP, Right Side, Unconnected

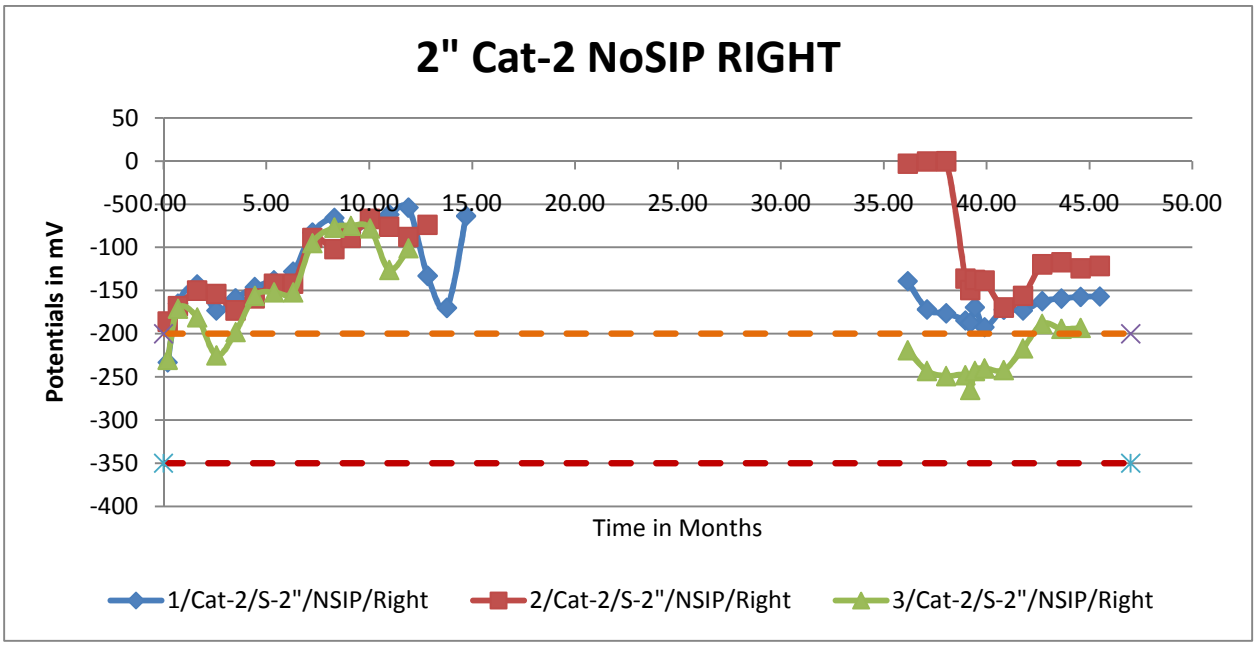

Figure B-25 - Half-Cell Potentials -3" Spacing, 1 Cathode Bar, with SIP, Right Side, Connected

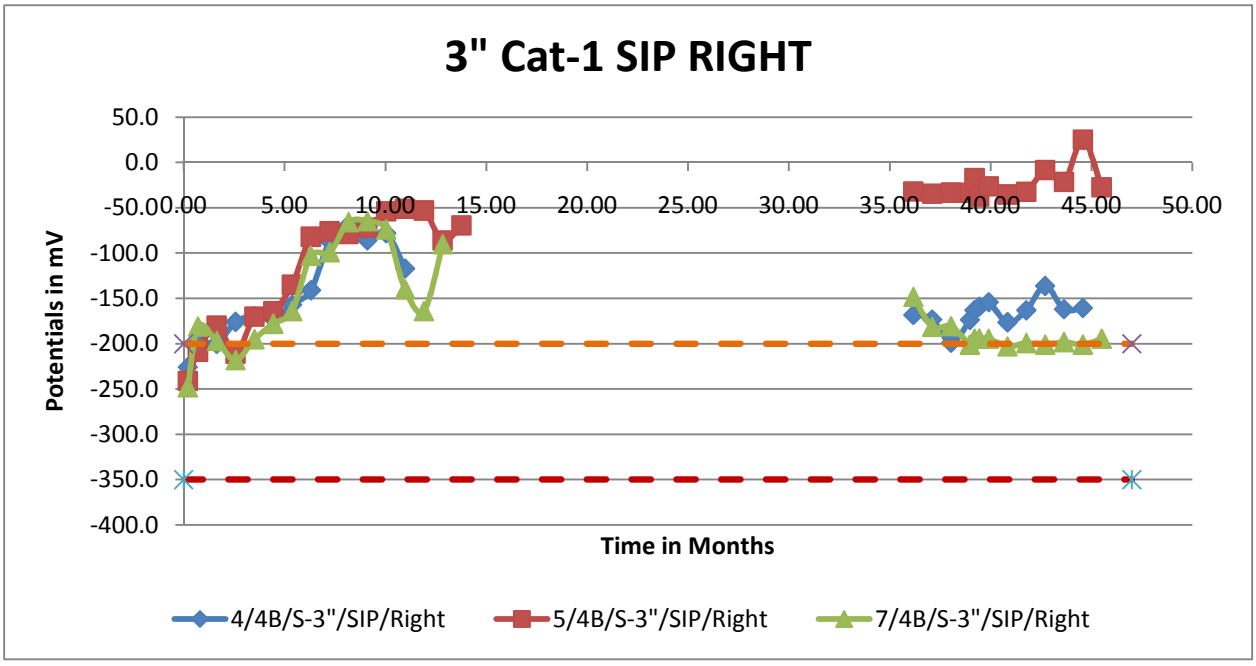

Figure B-26 - Half-Cell Potentials -3" Spacing, 1 Cathode Bar, with SIP, Right Side, Unconnected

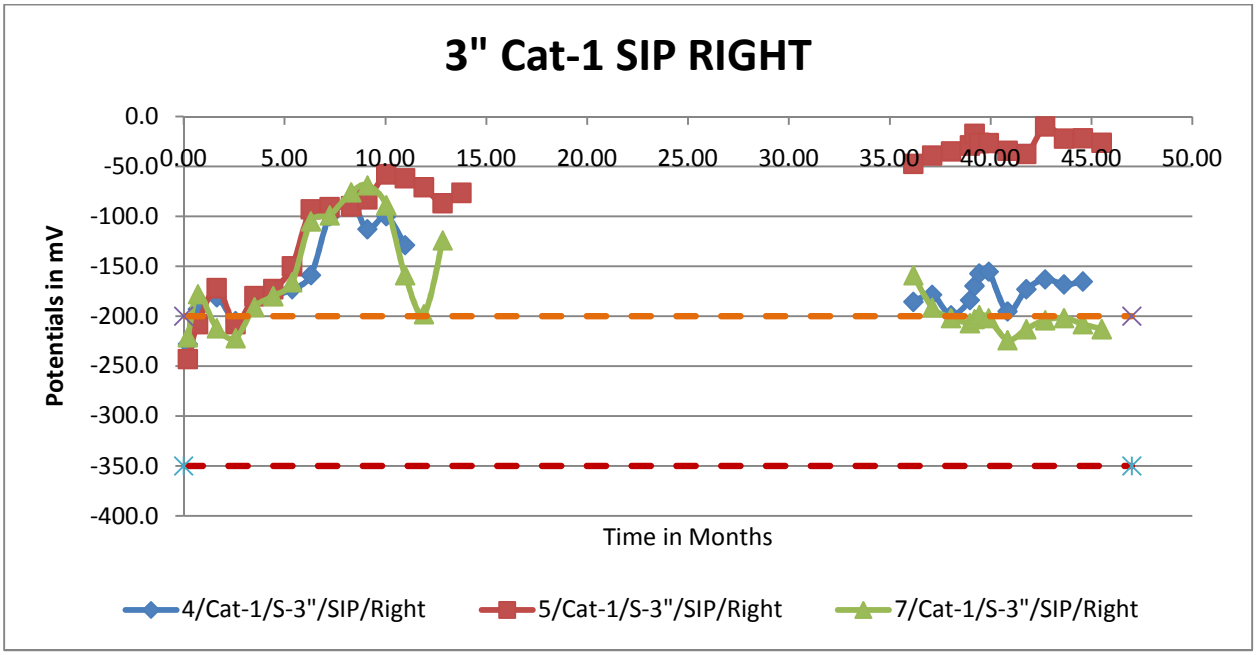

Figure B-27 - Half-Cell Potentials -3" Spacing, 2 Cathode Bars, with SIP, Right Side, Connected

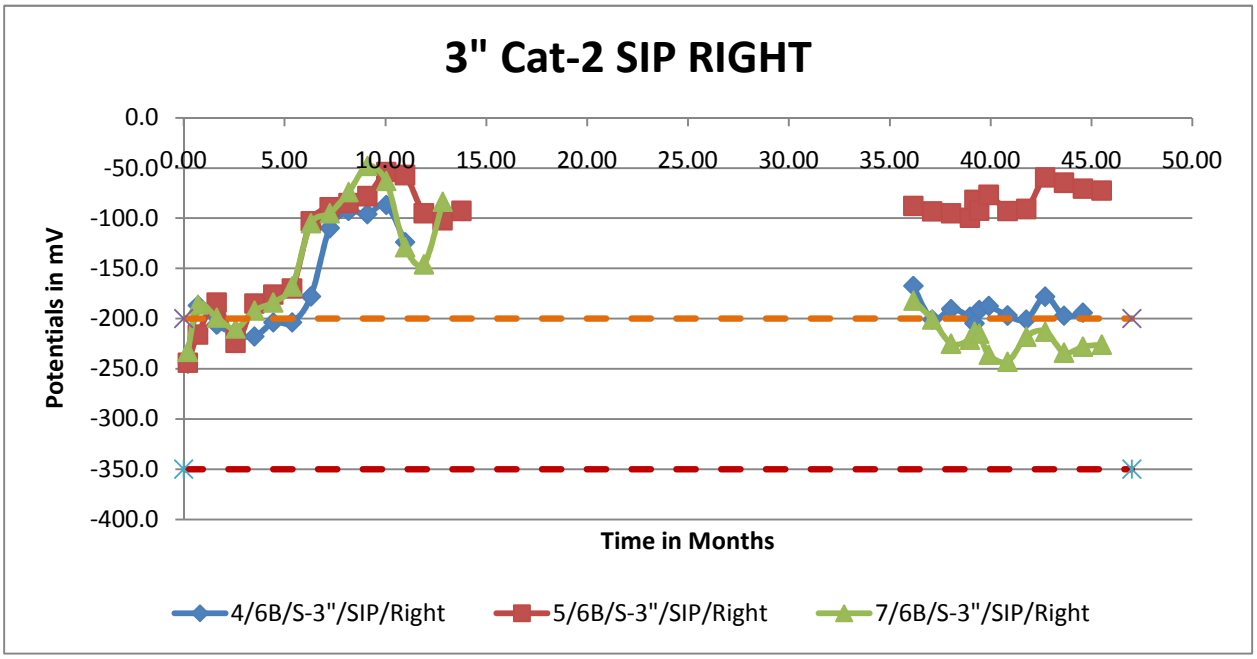

Figure B-28 - Half-Cell Potentials -3" Spacing, 2 Cathode Bars, with SIP, Right Side, Unconnected

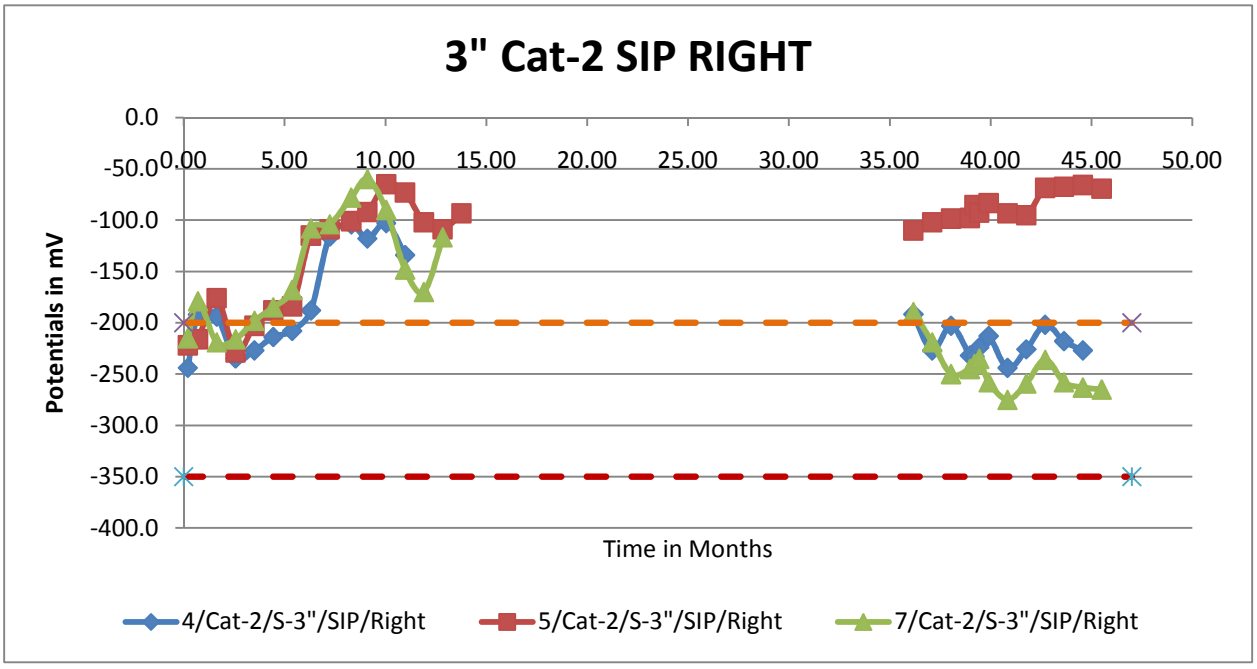

Figure B-29 - Half-Cell Potentials -3" Spacing, 2 Cathode Bars, with No SIP, Right Side, Connected

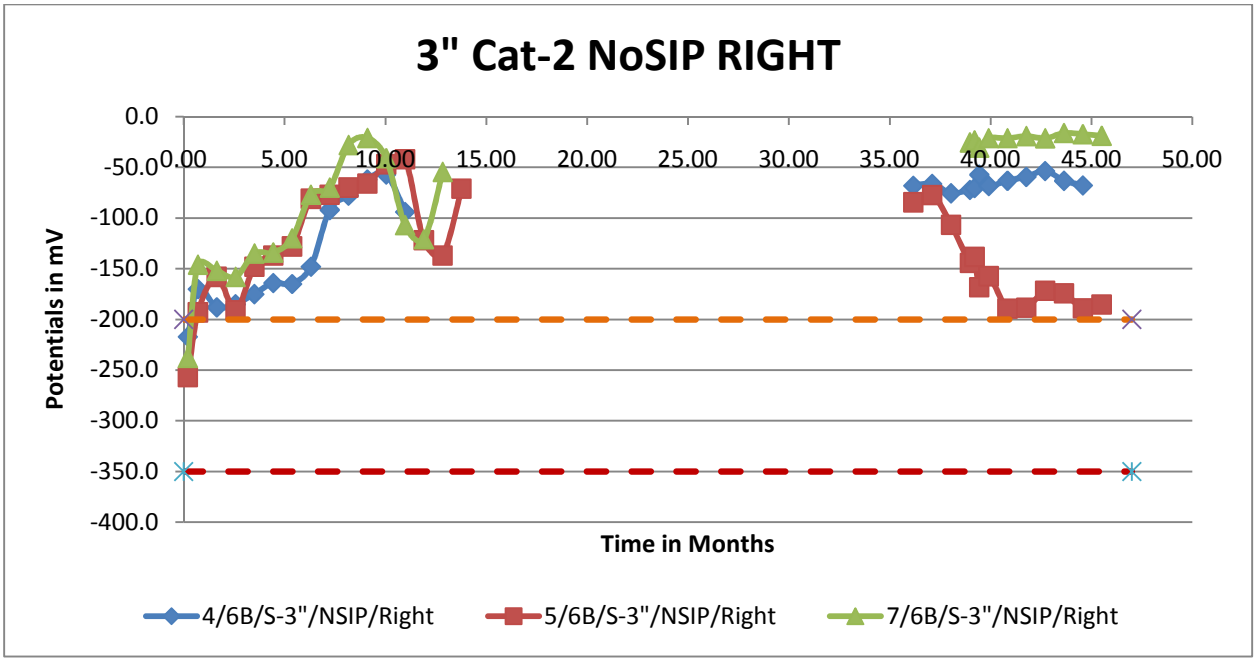

Figure B-30 - Half-Cell Potentials -3" Spacing, 2 Cathode Bars, with No SIP, Right Side, Unconnected

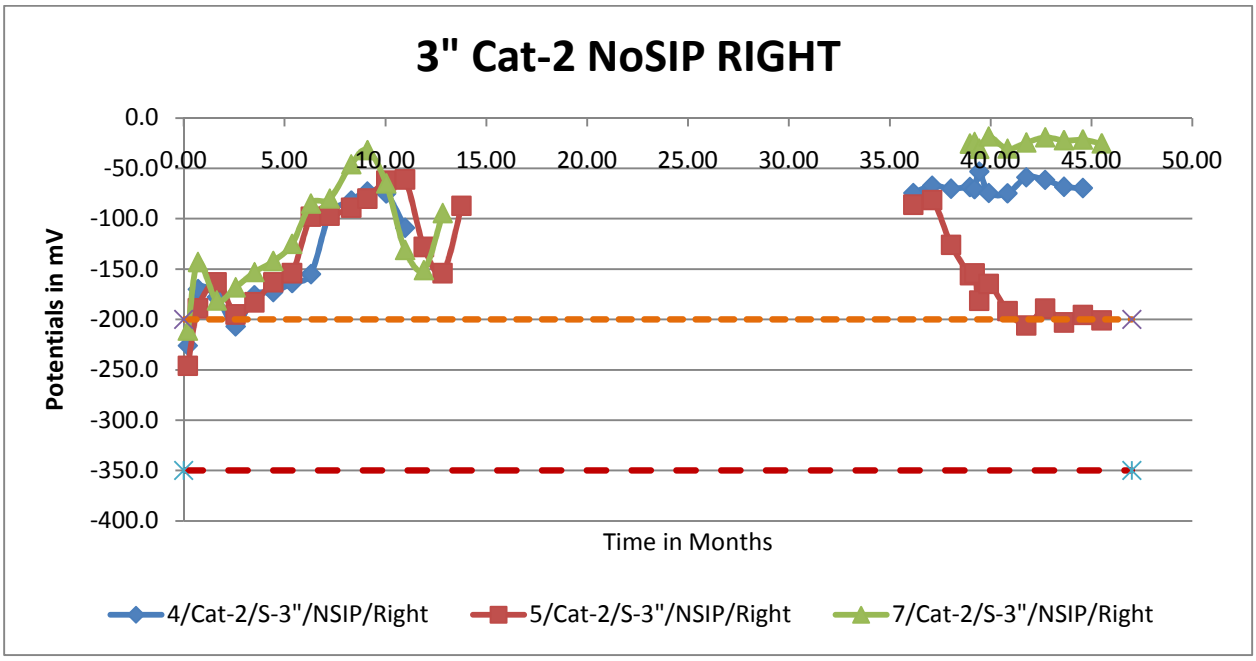

Figure B-31 - Half-Cell Potentials -4" Spacing, 1 Cathode Bar, with SIP, Right Side, Connected

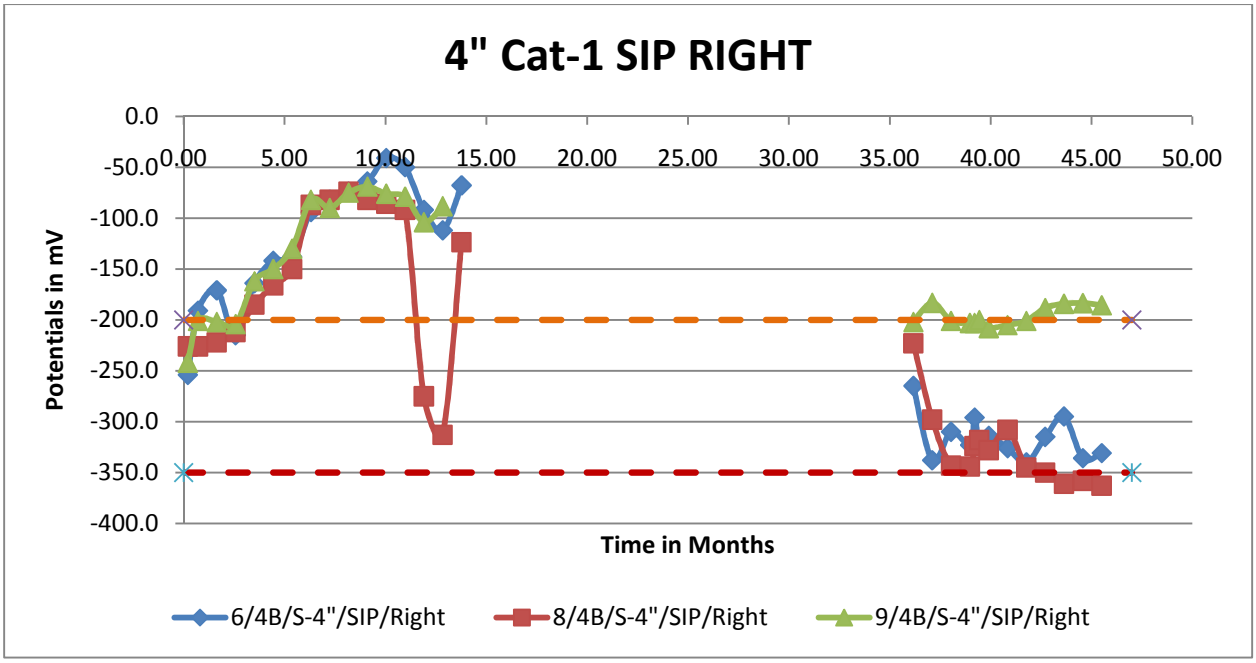

Figure B-32 - Half-Cell Potentials -4" Spacing, 1 Cathode Bar, with SIP, Right Side, Unconnected

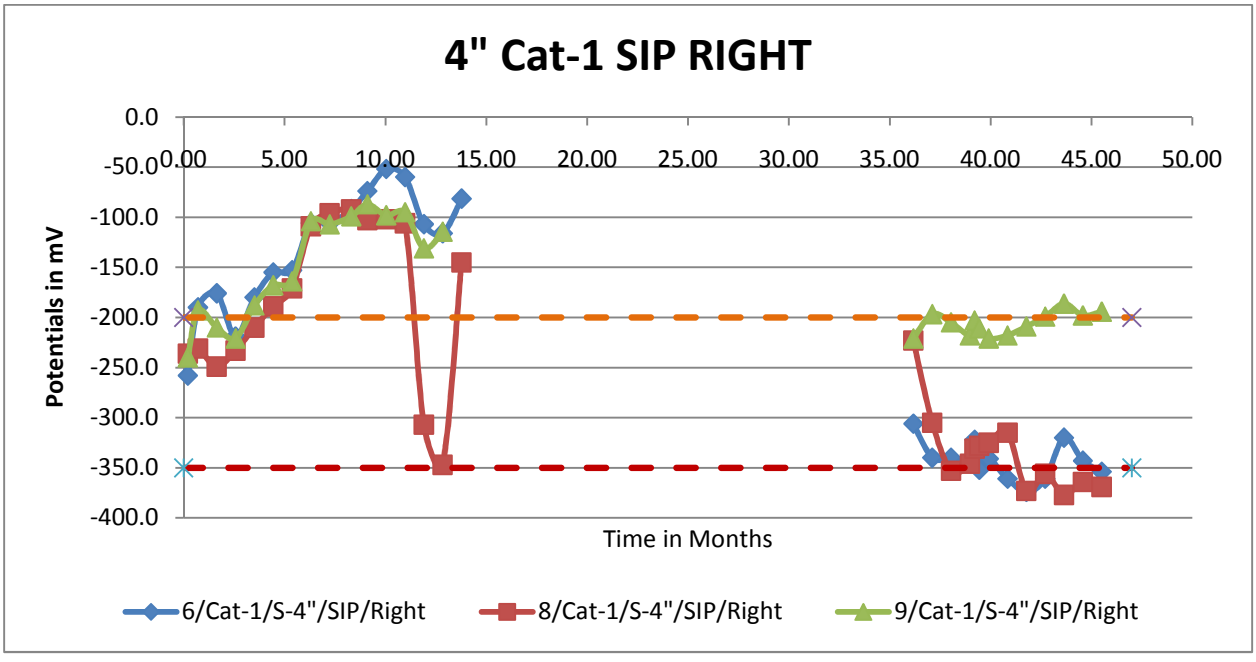

Figure B-33 - Half-Cell Potentials -4" Spacing, 2 Cathode Bars, with SIP, Right Side, Connected

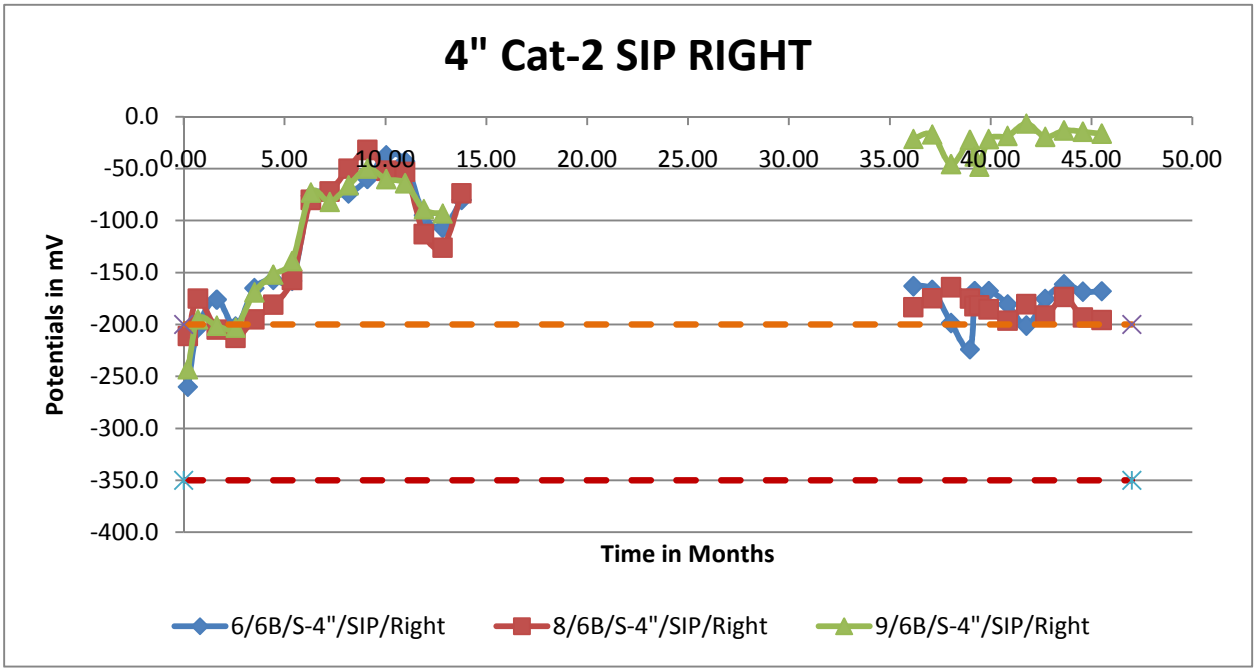

Figure B-34 - Half-Cell Potentials -4" Spacing, 2 Cathode Bars, with SIP, Right Side, Unconnected

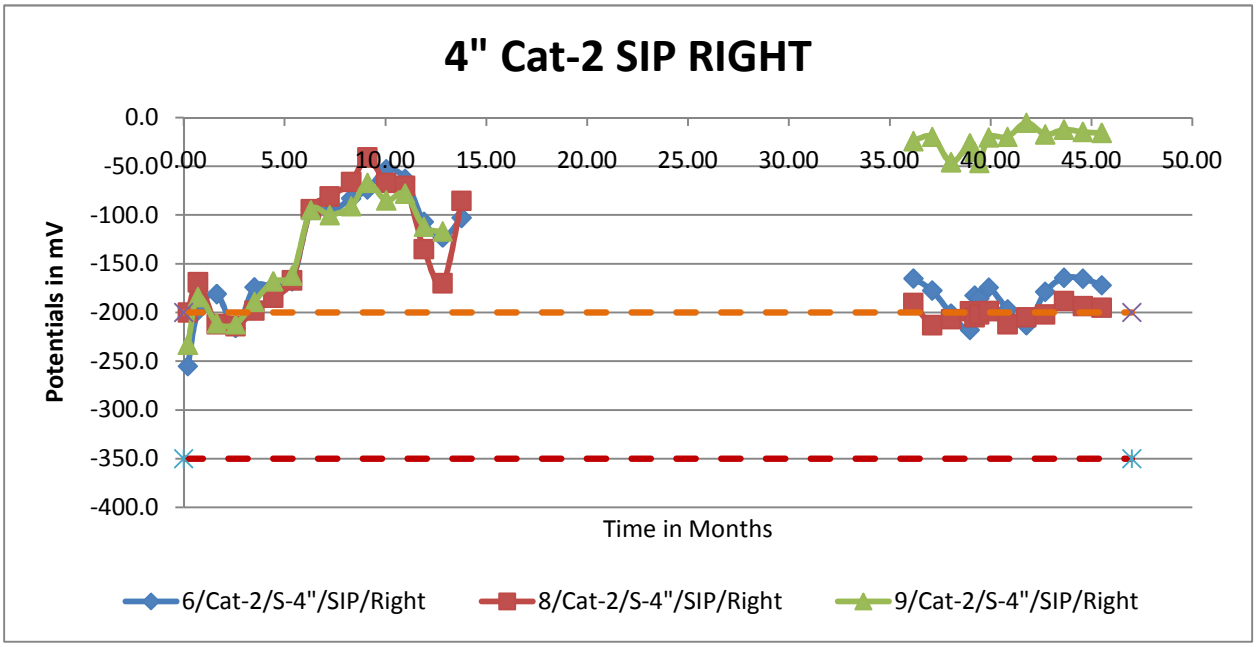

Figure B-35 - Half-Cell Potentials -4" Spacing, 2 Cathode Bars, with No SIP, Right Side, Connected

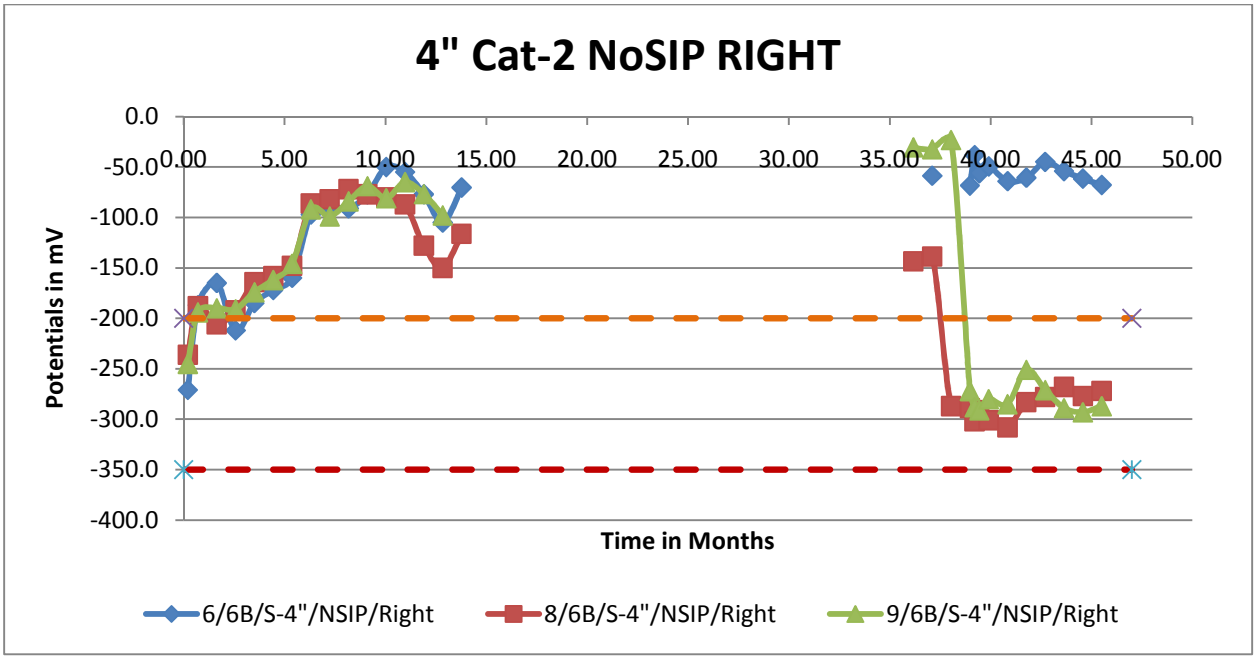

Figure B-36 - Half-Cell Potentials -4" Spacing, 2 Cathode Bars, with No SIP, Right Side, Unconnected

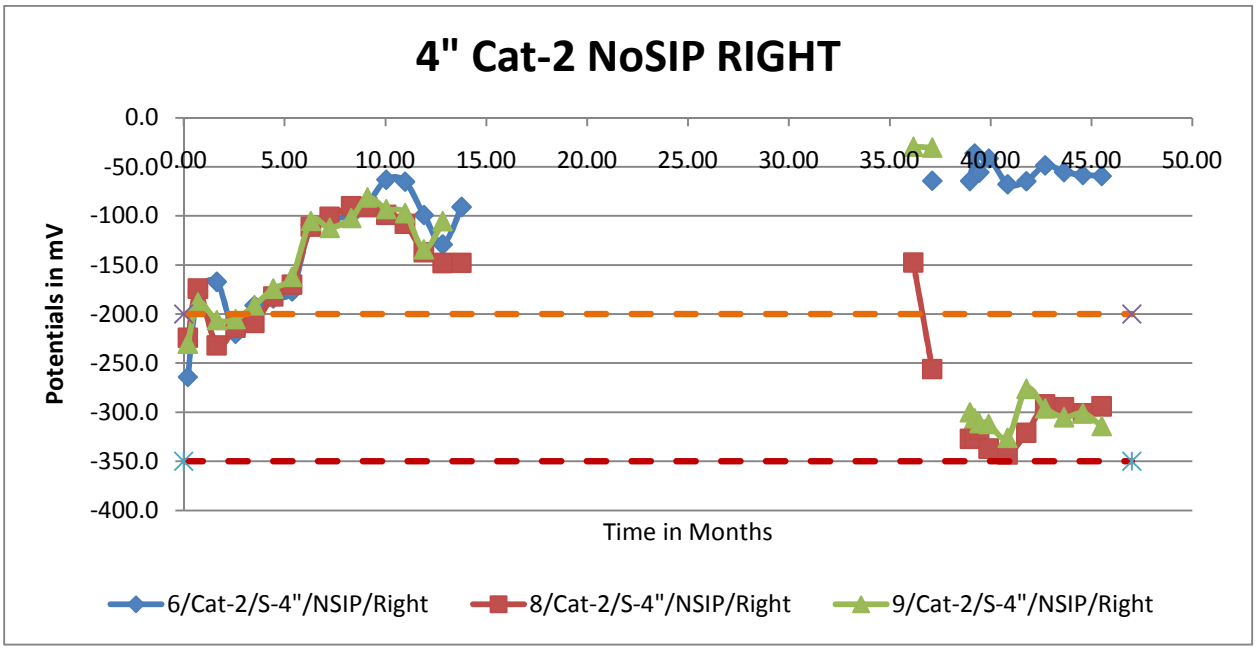

Appendix C – Corrosion Current Density Measurements

Figure C-1 - Corrosion Current Density – 2” Spacing, 1 Cathode Bar, with SIP, Left Side, Connected

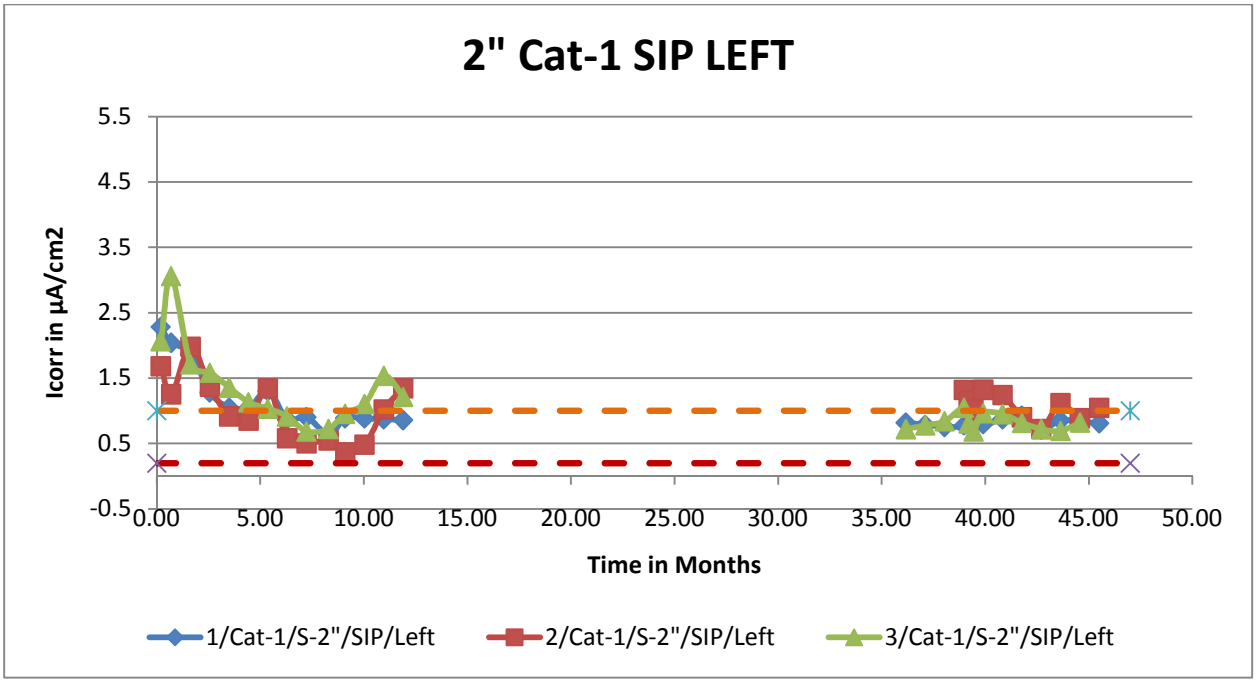

Figure C-2 - Corrosion Current Density – 2” Spacing, 1 Cathode Bar, with SIP, Left Side, Unconnected

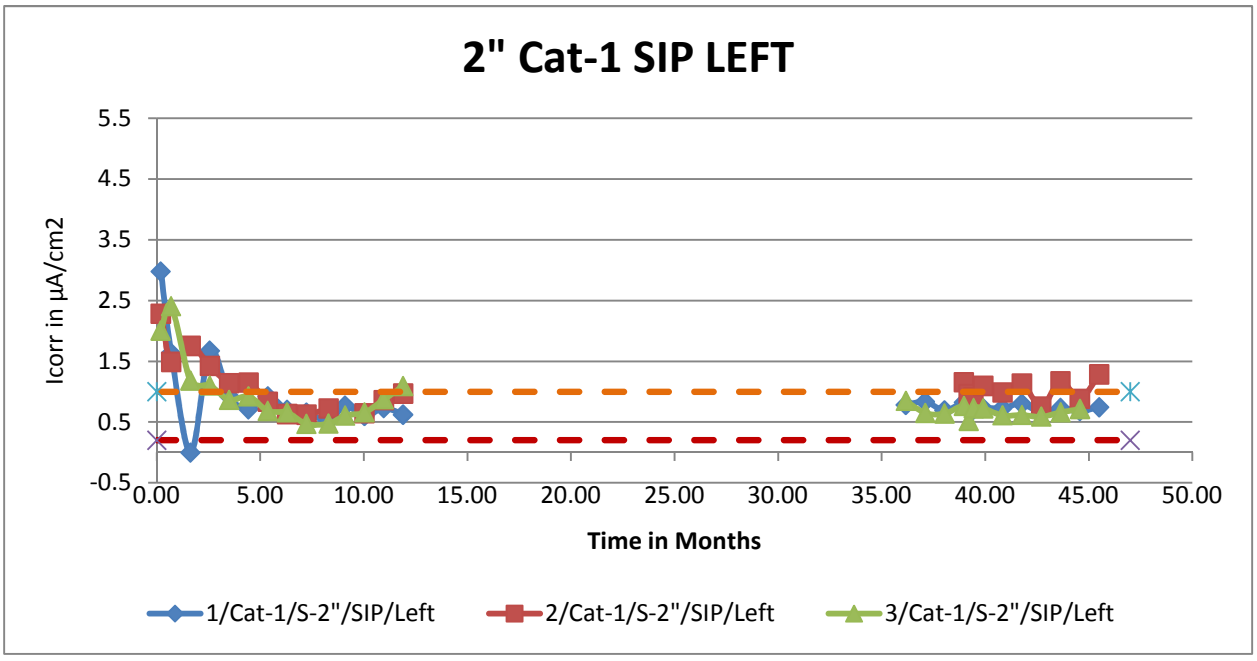

Figure C-3 - Corrosion Current Density – 2” Spacing, 2 Cathode Bars, with SIP, Left Side, Connected

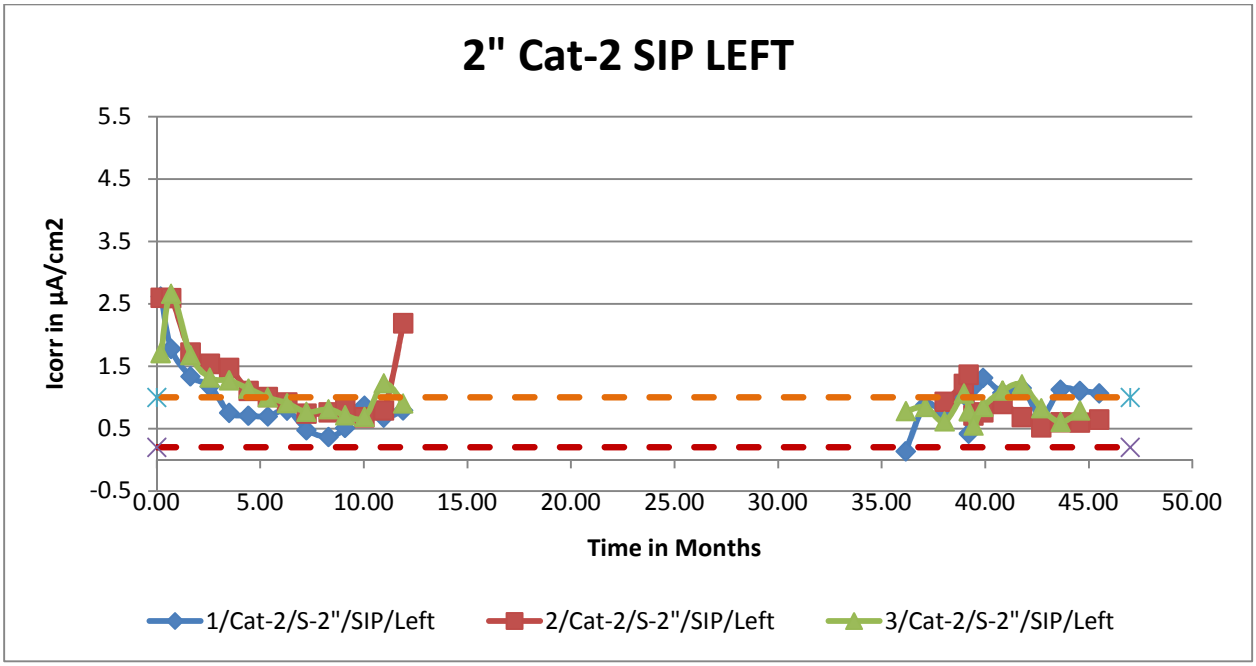

Figure C-4 - Corrosion Current Density – 2” Spacing, 2 Cathode Bars, with SIP, Left Side, Unconnected

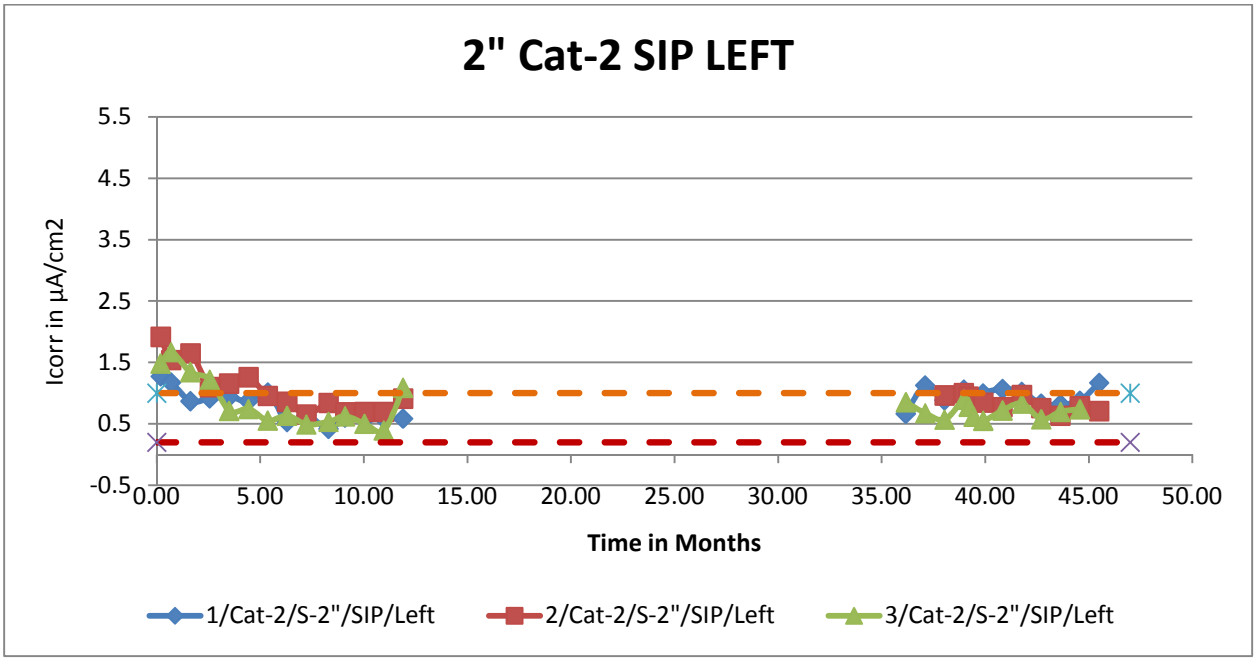

Figure C-5 - Corrosion Current Density – 2” Spacing, 2 Cathode Bars, with No SIP, Left Side, Connected

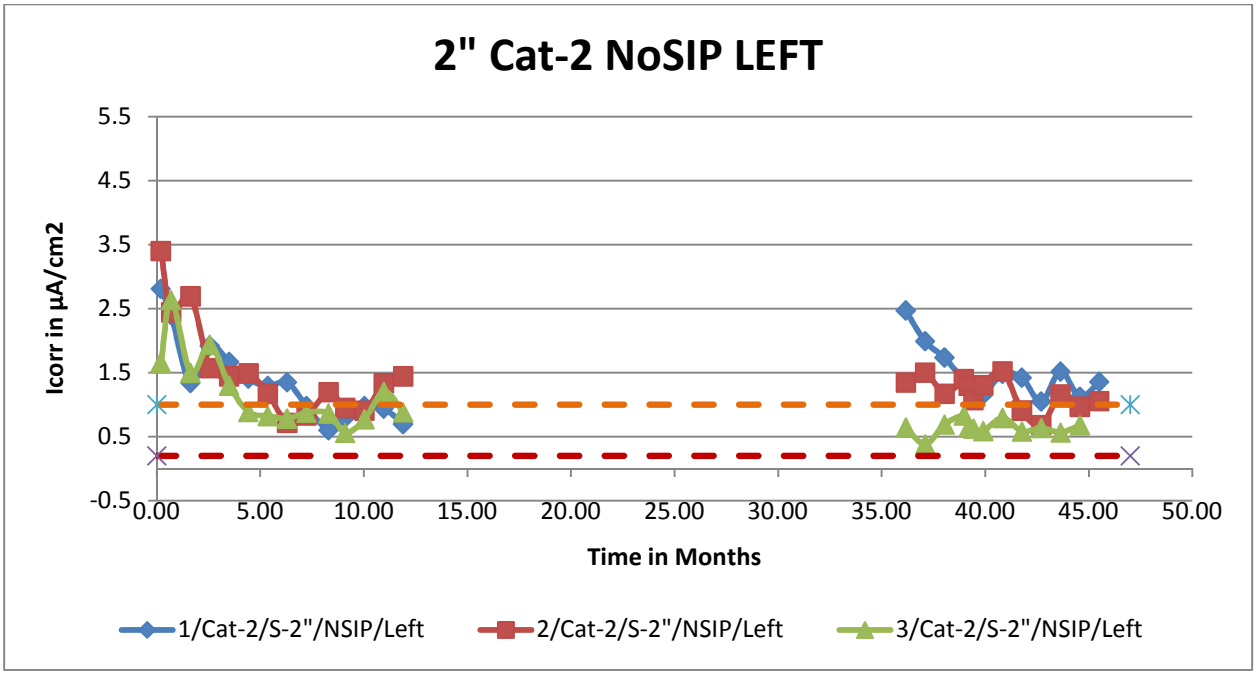

Figure C-6 - Corrosion Current Density – 2” Spacing, 2 Cathode Bars, with No SIP, Left Side, Unconnected

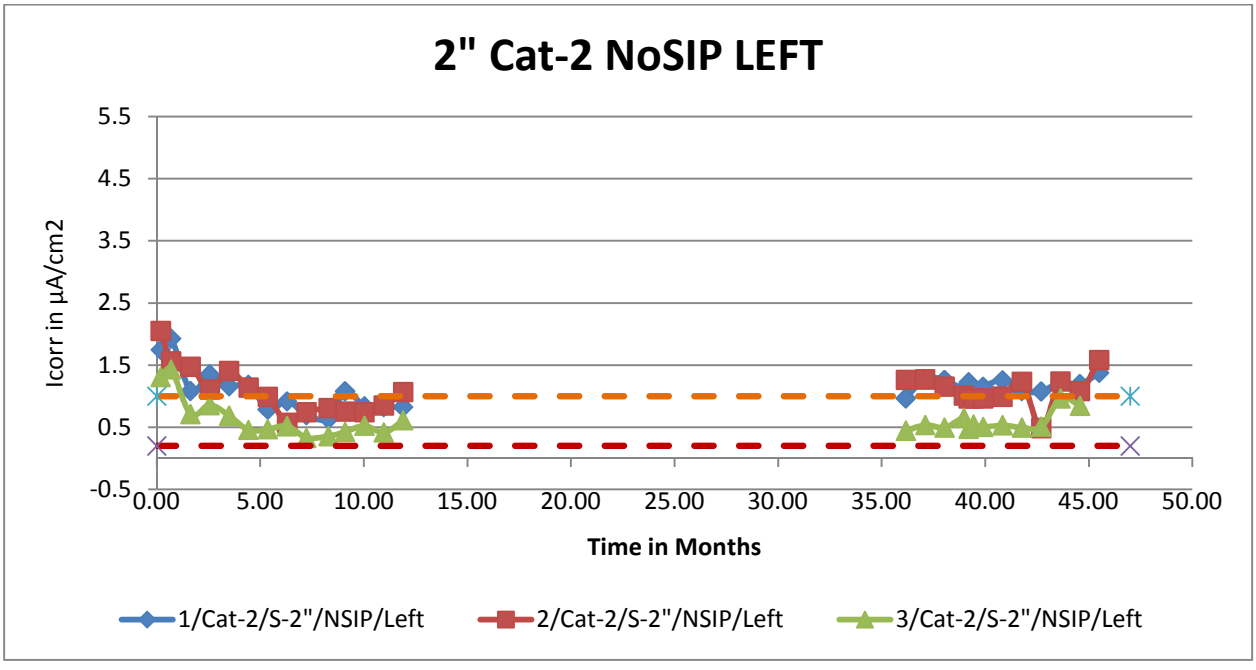

Figure C-7 - Corrosion Current Density – 3” Spacing, 1 Cathode Bar, with SIP, Left Side, Connected

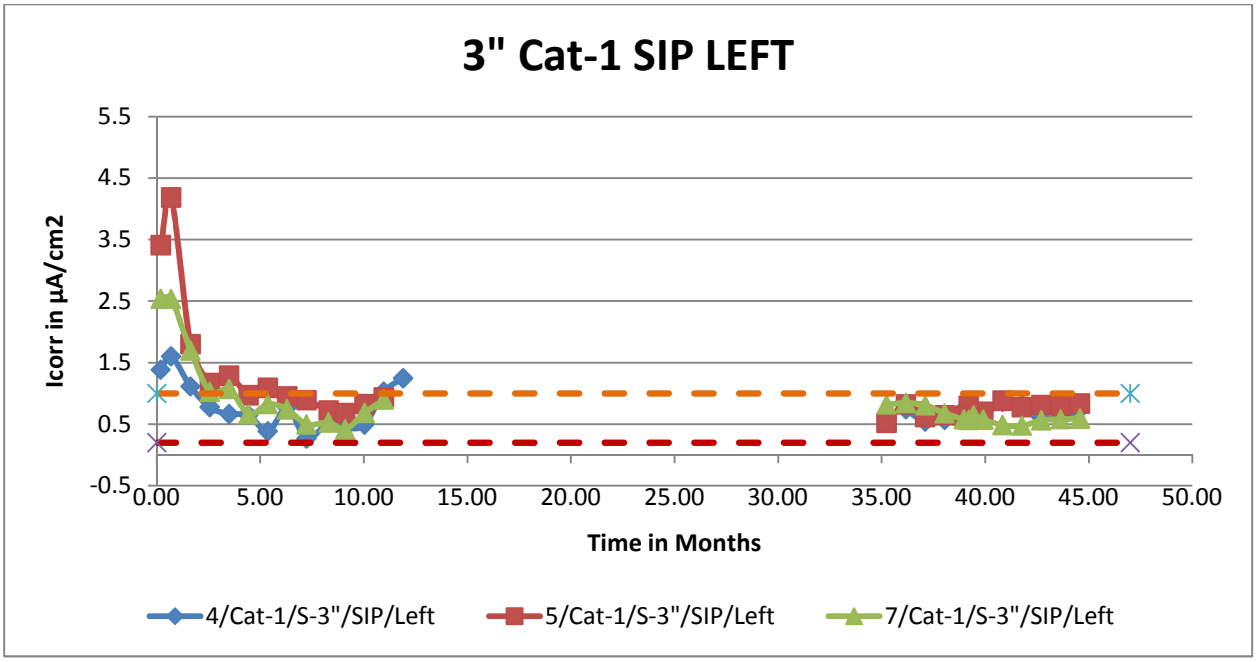

Figure C-8 - Corrosion Current Density – 3” Spacing, 1 Cathode Bar, with SIP, Left Side, Unconnected

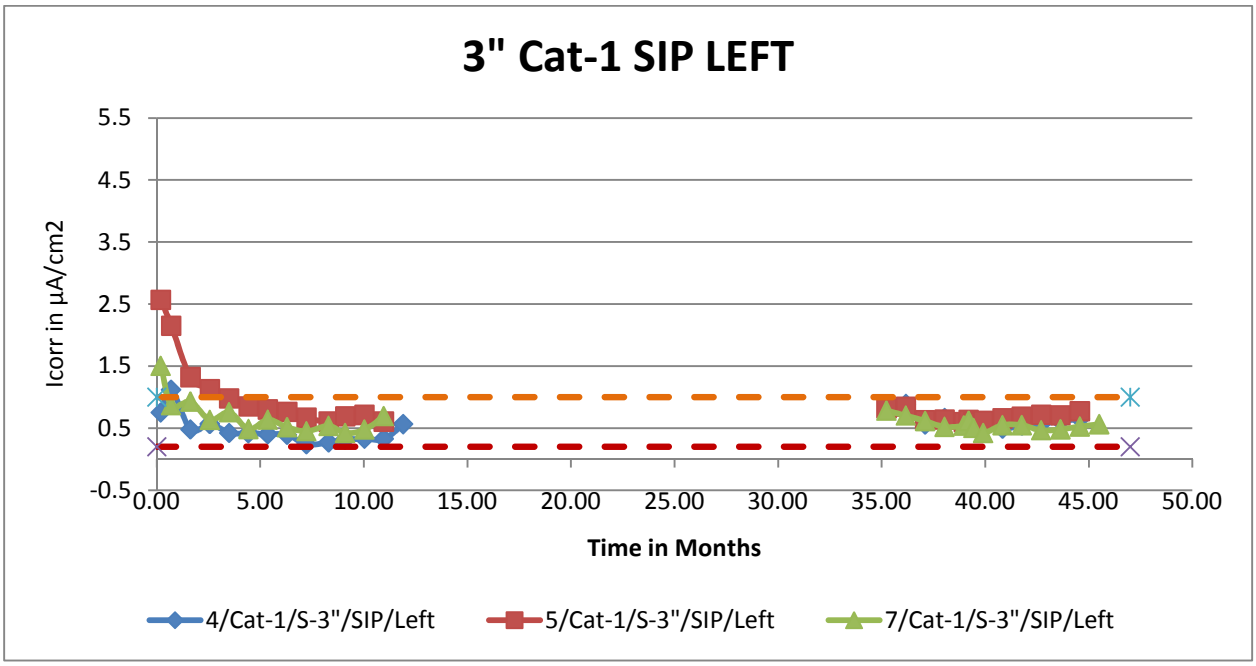

Figure C-9 - Corrosion Current Density – 3" Spacing, 2 Cathode Bars, with SIP, Left Side, Connected

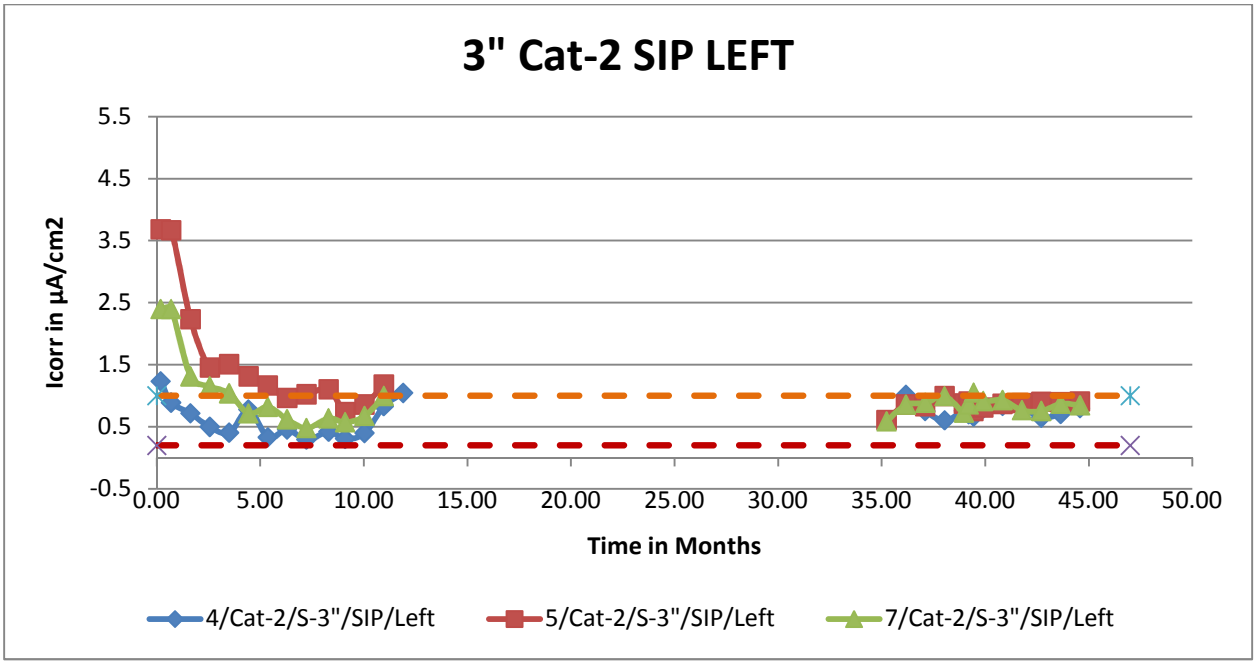

Figure C-10 - Corrosion Current Density – 3" Spacing, 2 Cathode Bars, with SIP, Left Side, Unconnected

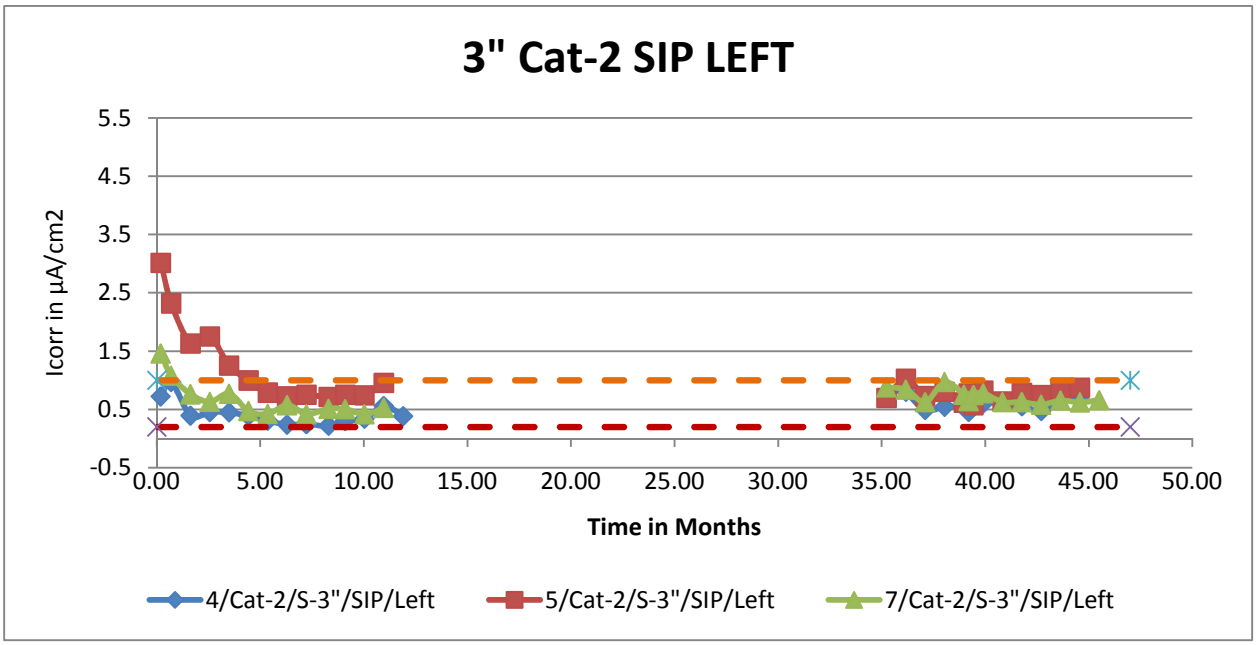

Figure C-11 - Corrosion Current Density – 3” Spacing, 2 Cathode Bars, with No SIP, Left Side, Connected

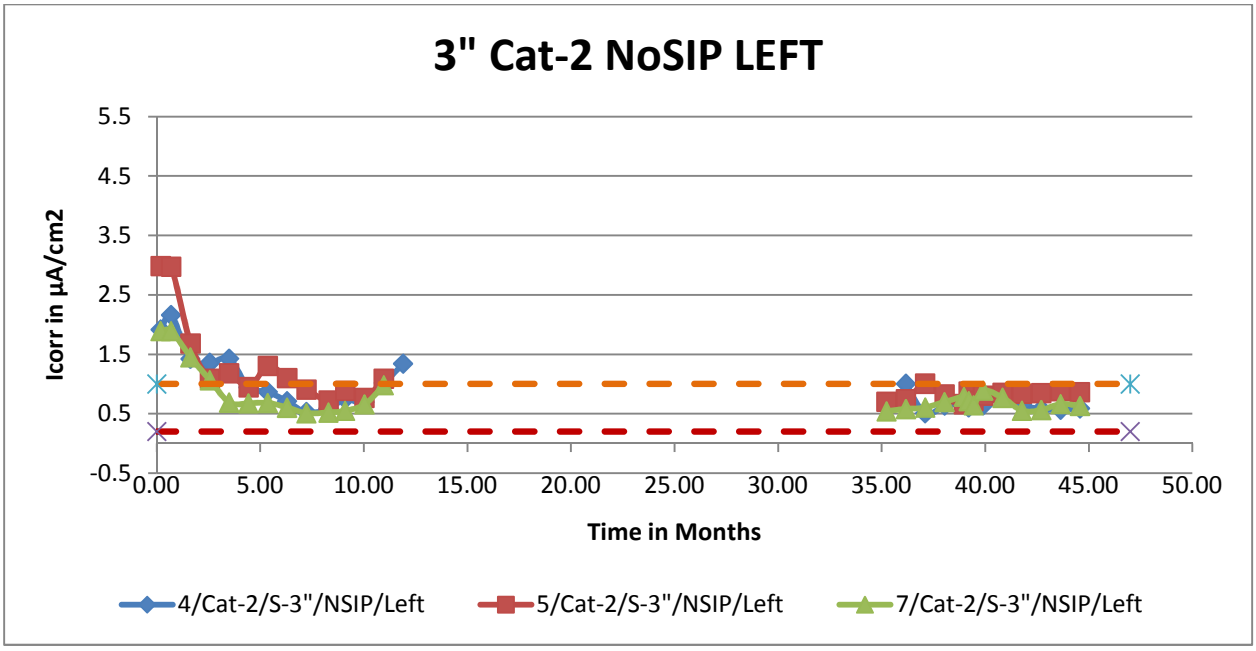

Figure C-12 - Corrosion Current Density – 3” Spacing, 2 Cathode Bars, with No SIP, Left Side, Unconnected

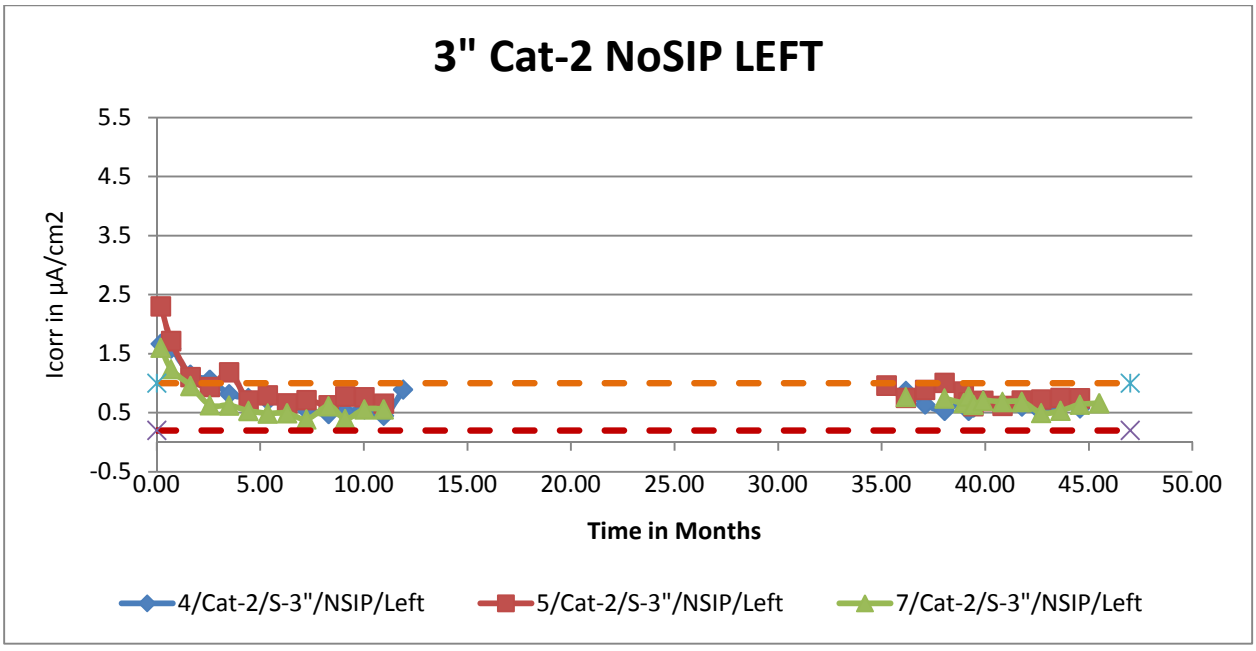

Figure C-13 - Corrosion Current Density – 4” Spacing, 1 Cathode Bar, with SIP, Left Side, Connected

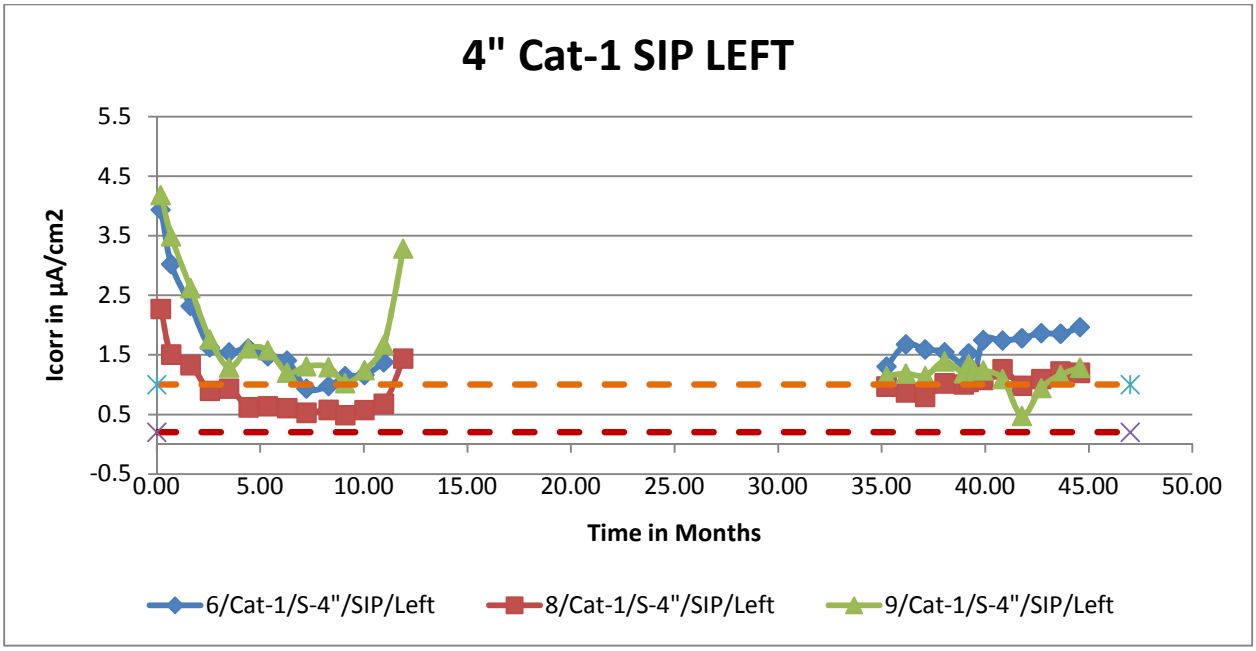

Figure C-14 - Corrosion Current Density – 4” Spacing, 1 Cathode Bar, with SIP, Left Side, Unconnected

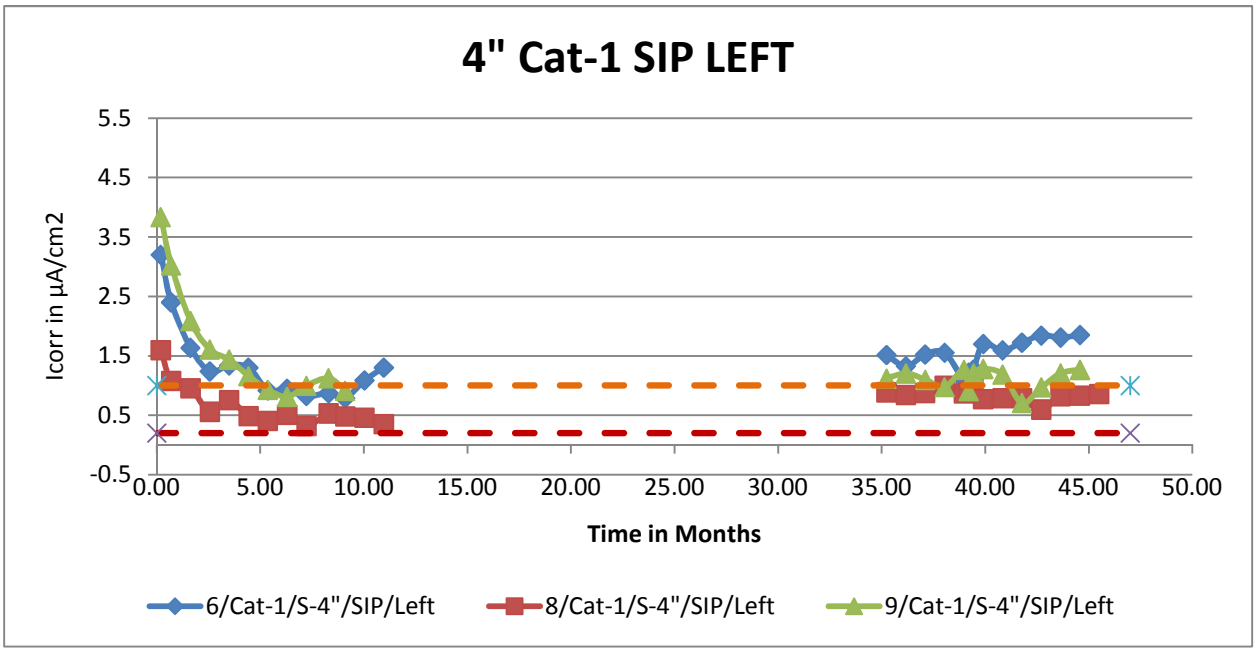

Figure C-15 - Corrosion Current Density – 4” Spacing, 2 Cathode Bar, with SIP, Left Side, Connected

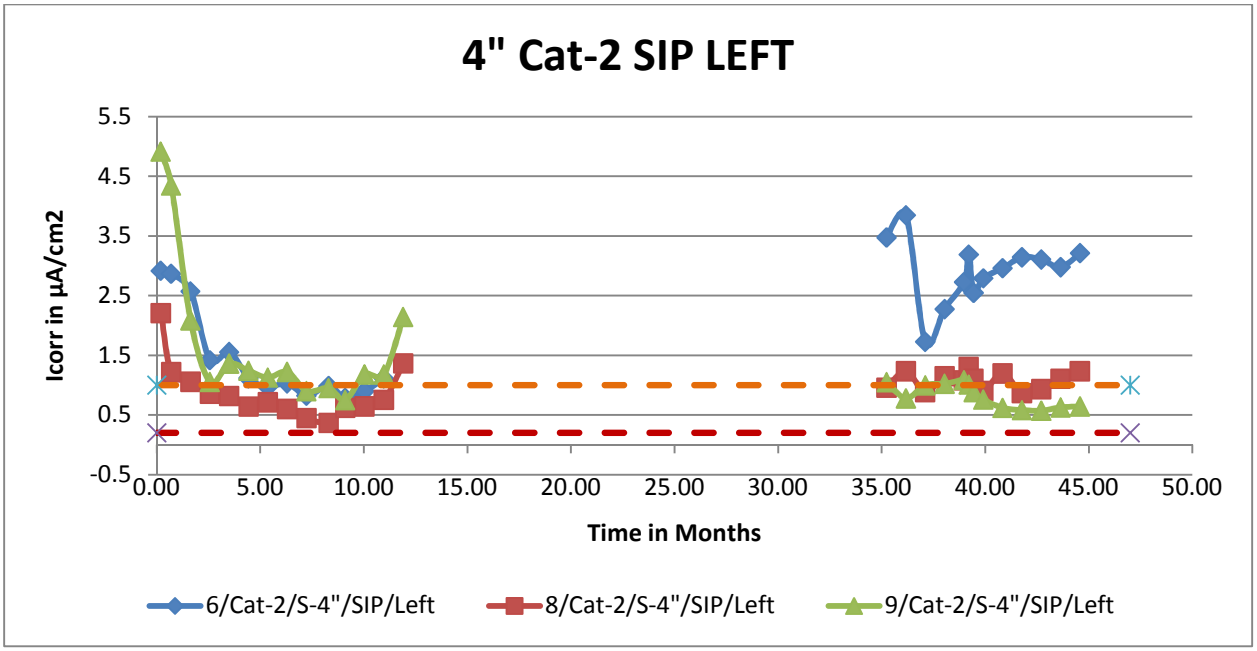

Figure C-16 - Corrosion Current Density – 4” Spacing, 2 Cathode Bar, with SIP, Left Side, Unconnected

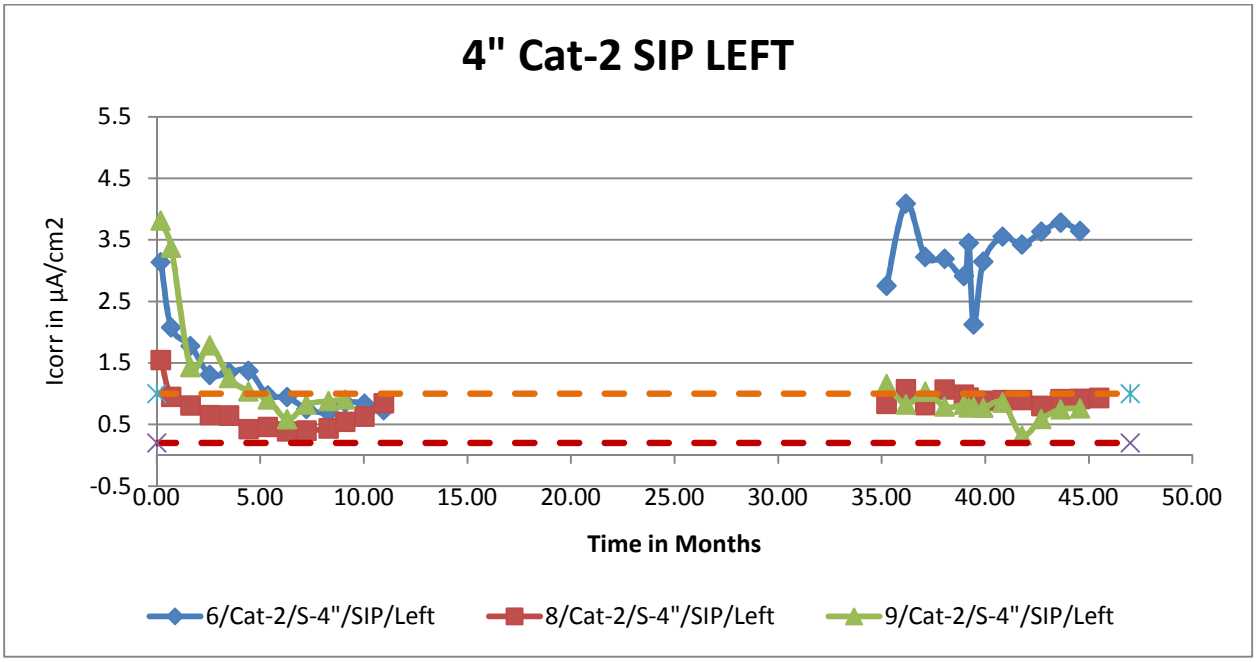

Figure C-17 - Corrosion Current Density – 4" Spacing, 2 Cathode Bar, with No SIP, Left Side, Connected

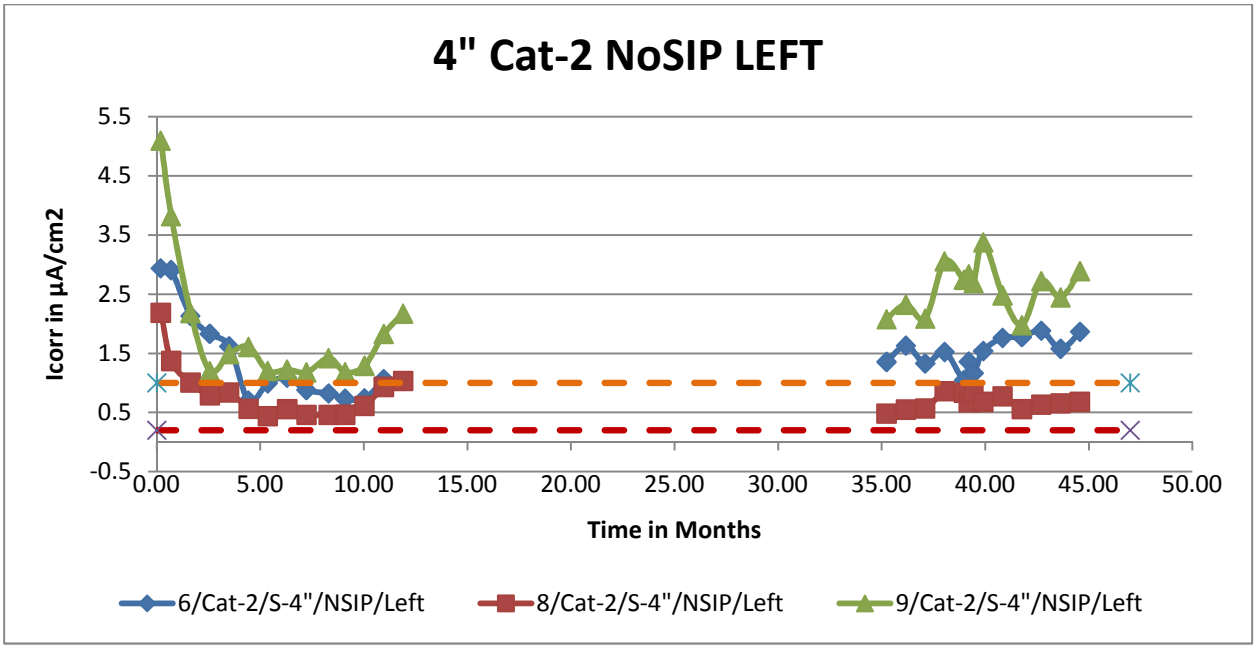

Figure C-18 - Corrosion Current Density – 4" Spacing, 2 Cathode Bar, with No SIP, Left Side, Unconnected

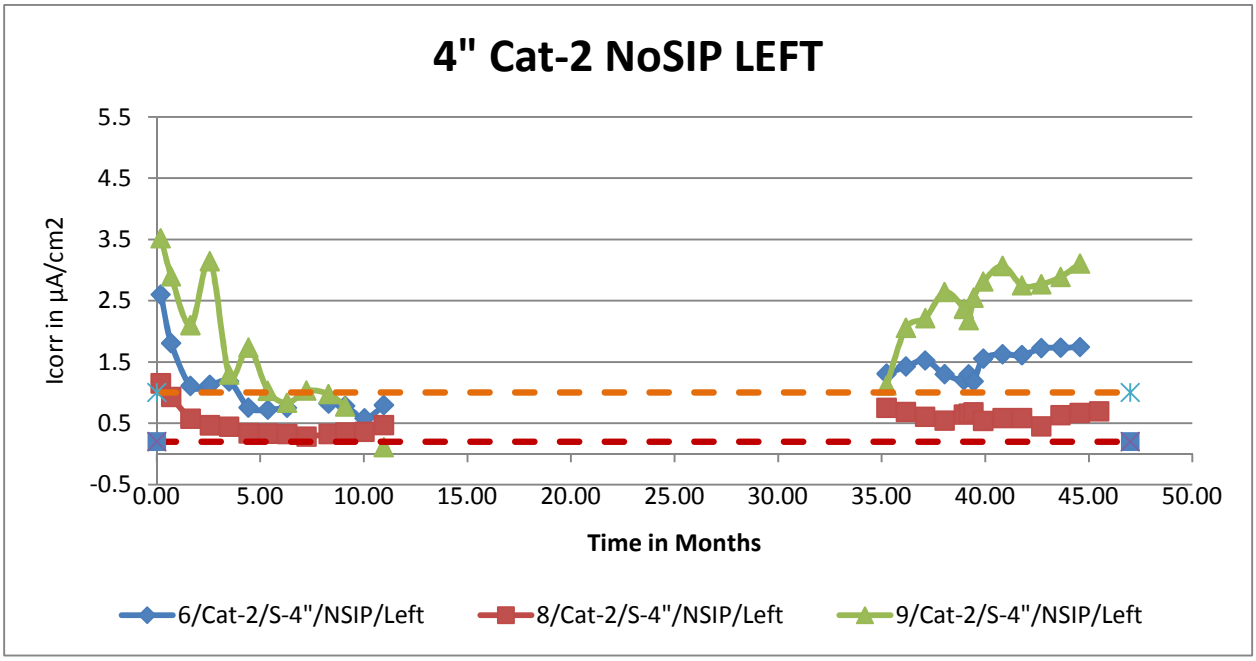

Figure C-19 - Corrosion Current Density – 2” Spacing, 1 Cathode Bar, with SIP, Right Side, Connected

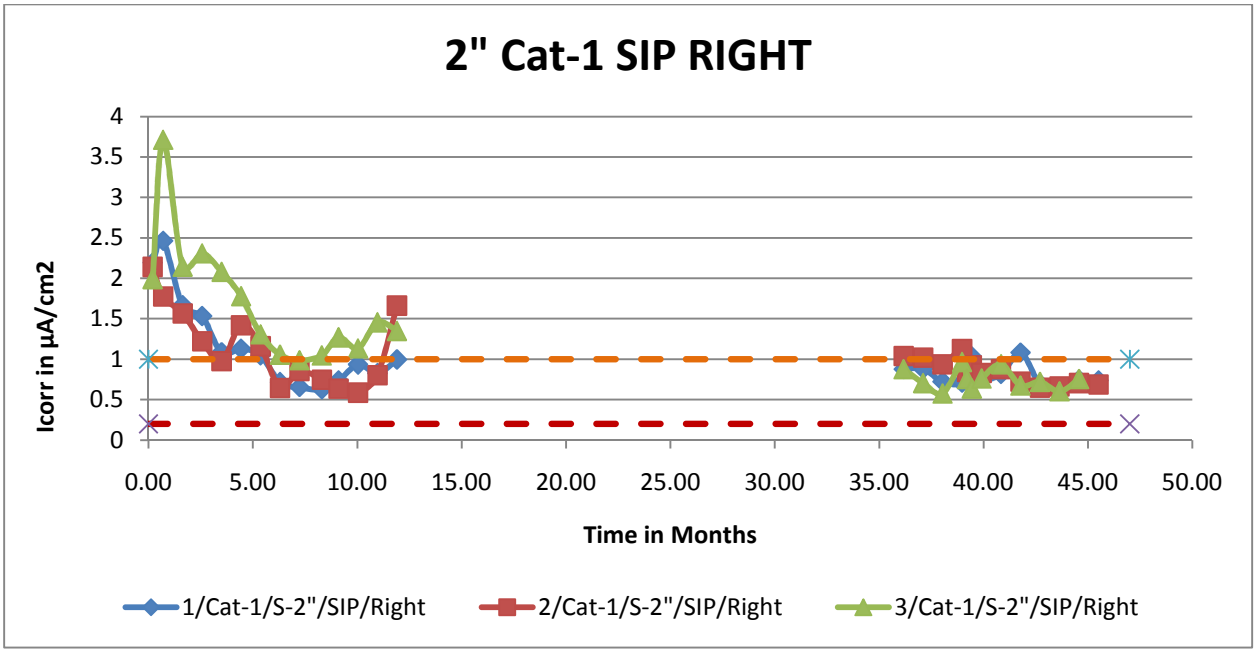

Figure C-20 - Corrosion Current Density – 2” Spacing, 1 Cathode Bar, with SIP, Right Side, Unconnected

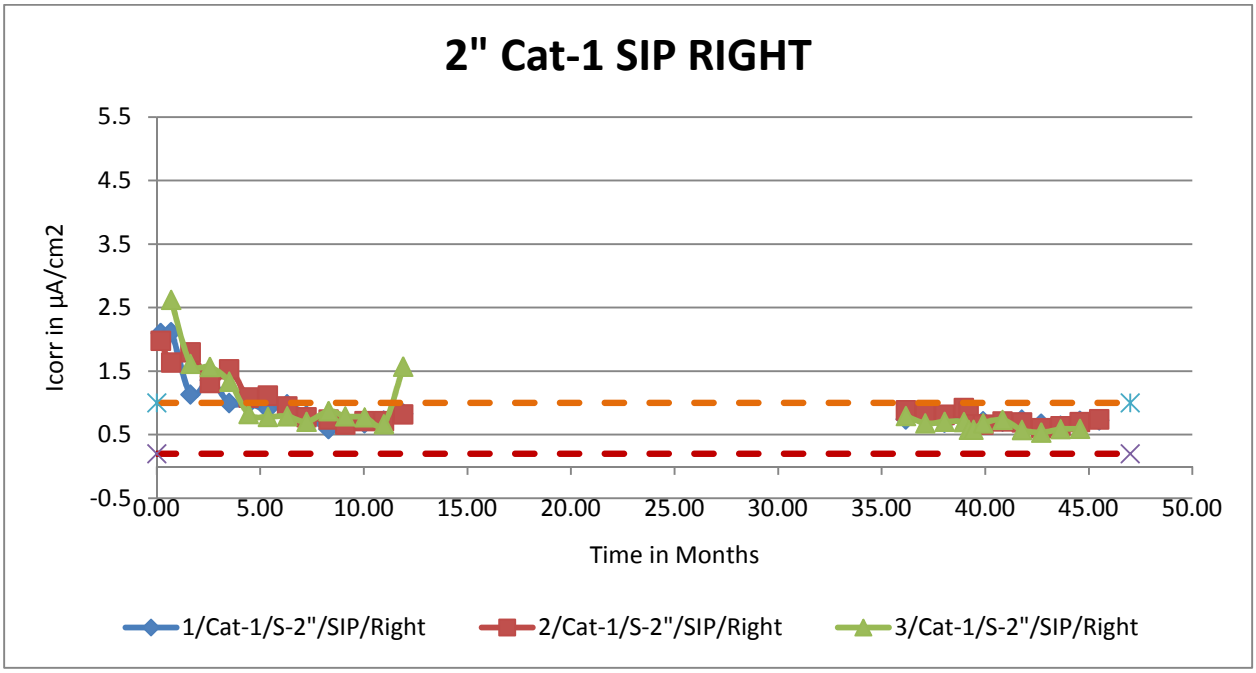

Figure C-21 - Corrosion Current Density – 2" Spacing, 2 Cathode Bars, with SIP, Right Side, Connected

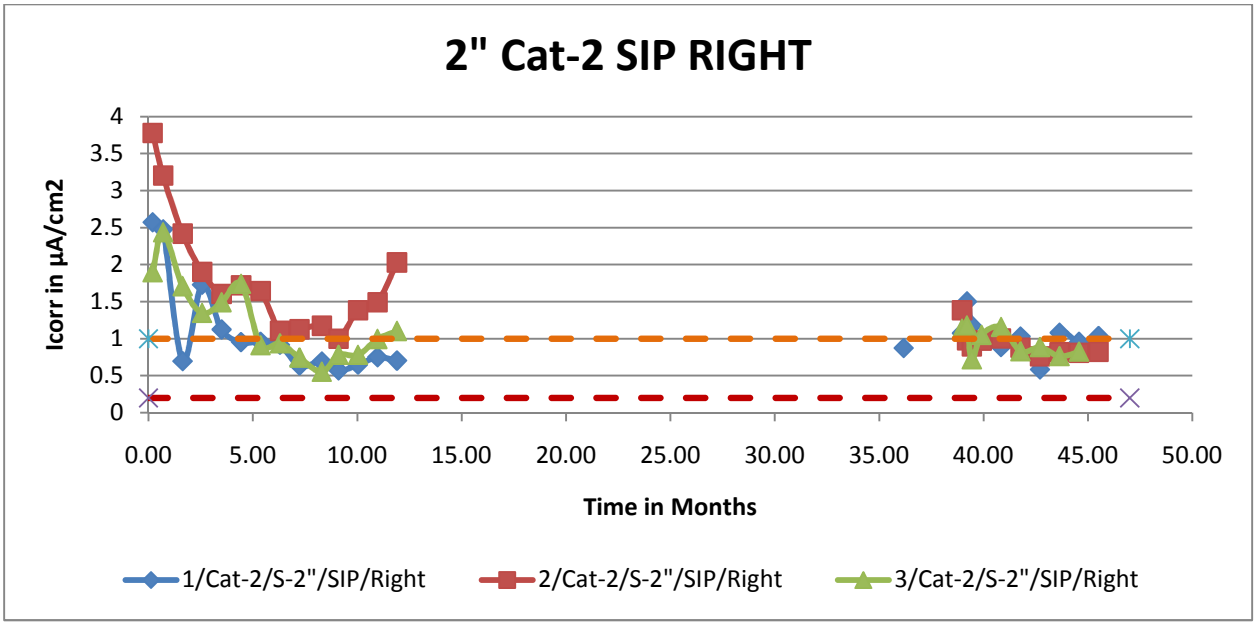

Figure C-22 - Corrosion Current Density – 2" Spacing, 2 Cathode Bars, with SIP, Right Side, Unconnected

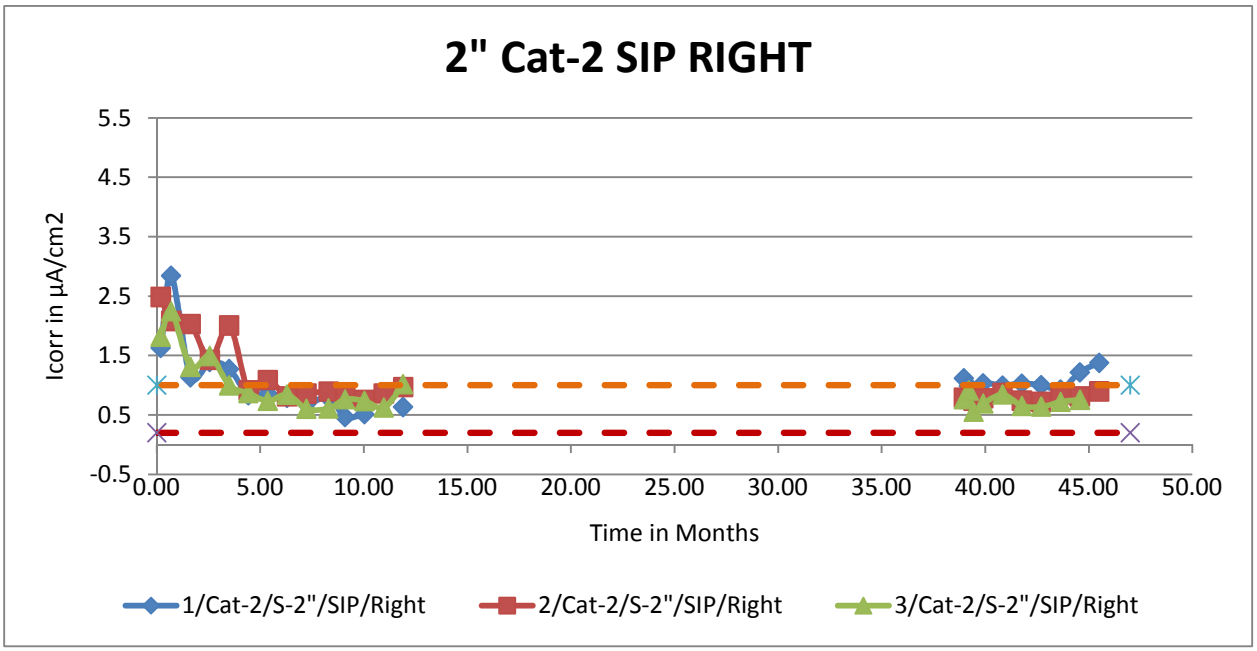

Figure C-23 - Corrosion Current Density – 2” Spacing, 2 Cathode Bars, with No SIP, Right Side, Connected

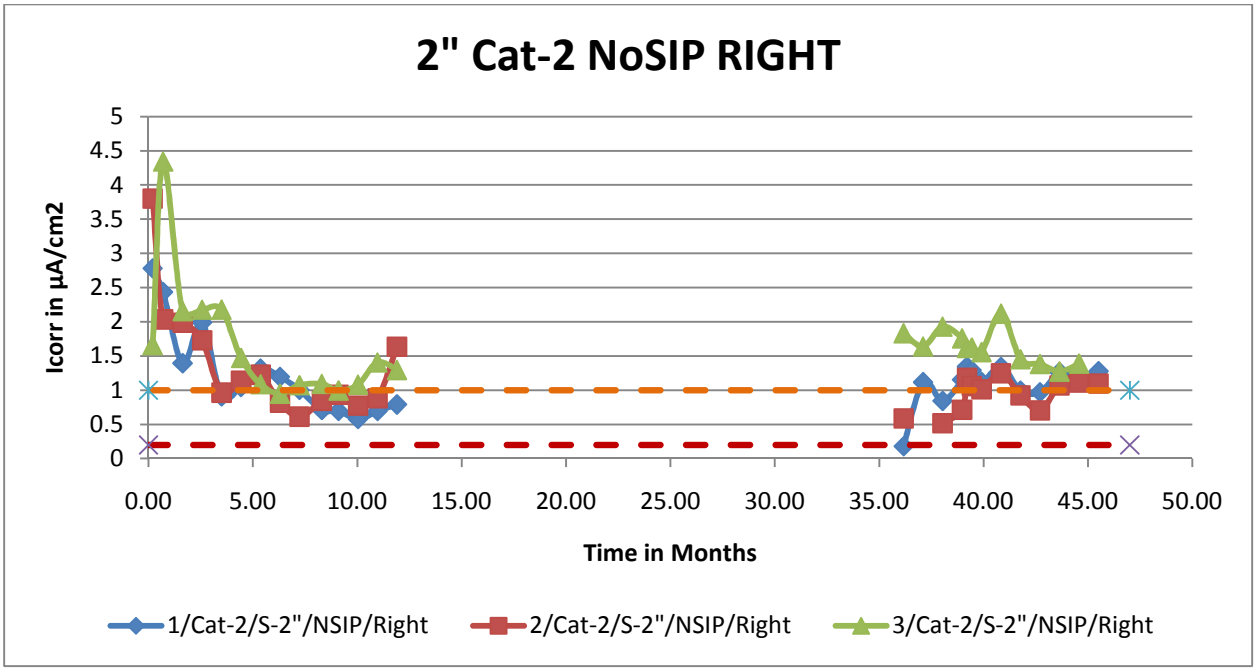

Figure C-24 - Corrosion Current Density – 2” Spacing, 2 Cathode Bars, with No SIP, Right Side, Unconnected

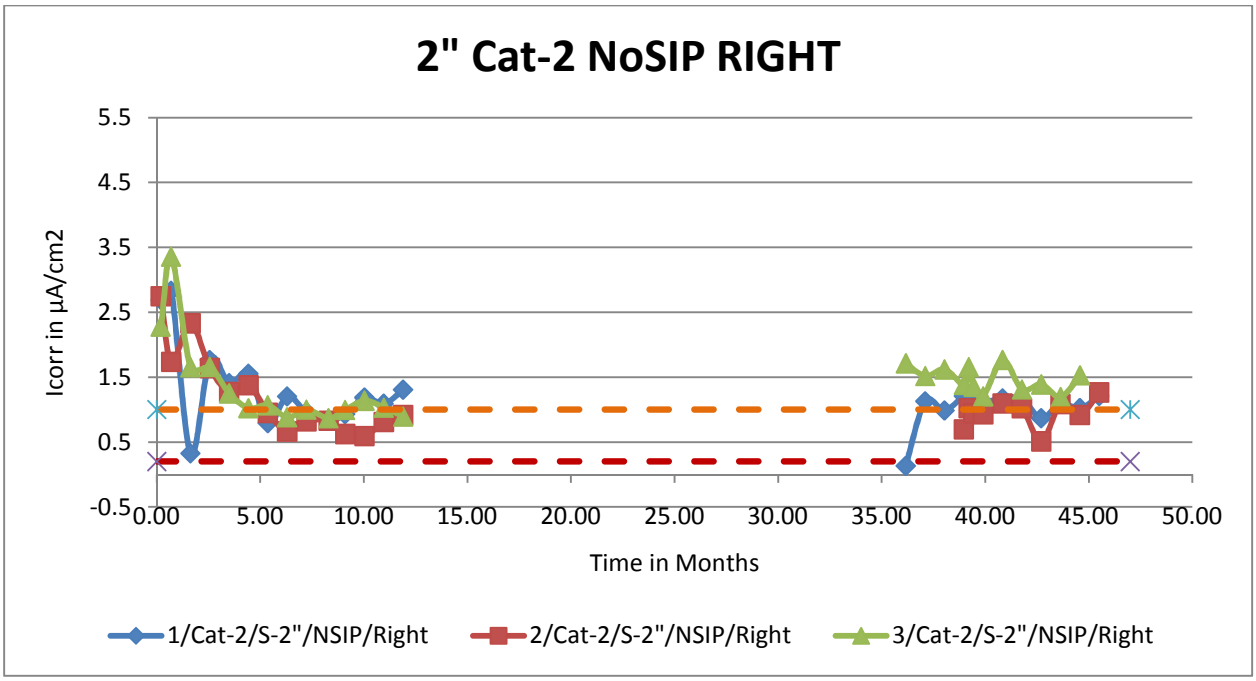

Figure C-25 - Corrosion Current Density – 3” Spacing, 1 Cathode Bar, with SIP, Right Side, Connected

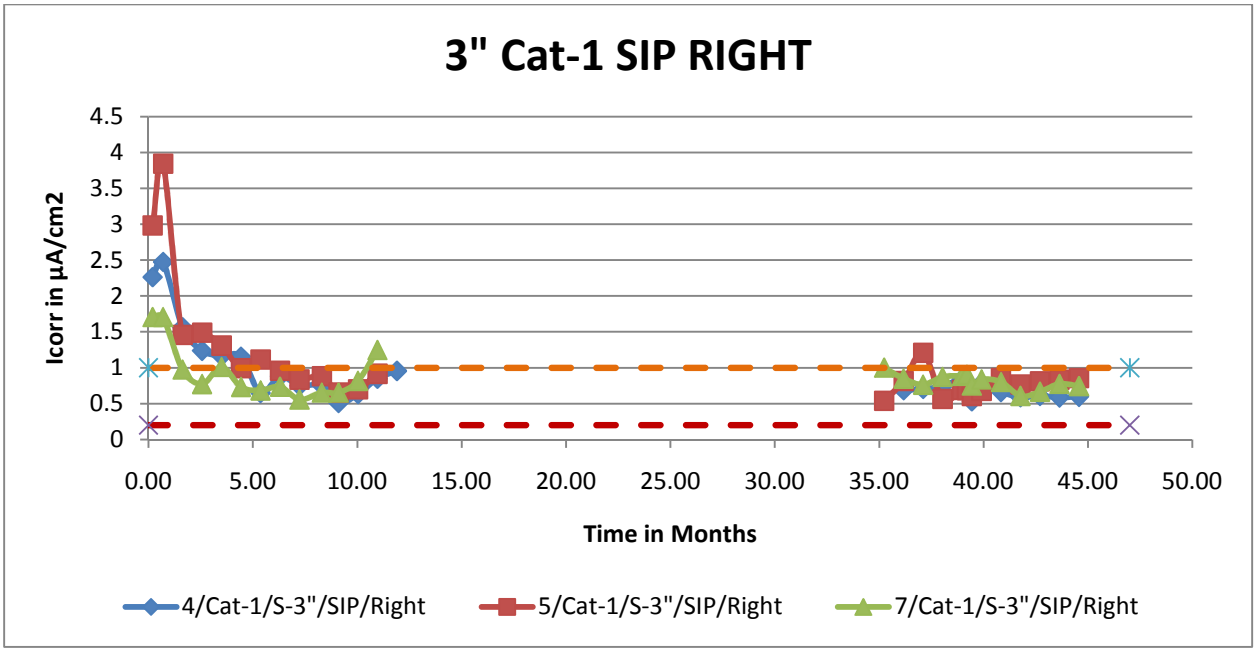

Figure C-26 - Corrosion Current Density – 3” Spacing, 1 Cathode Bar, with SIP, Right Side, Unconnected

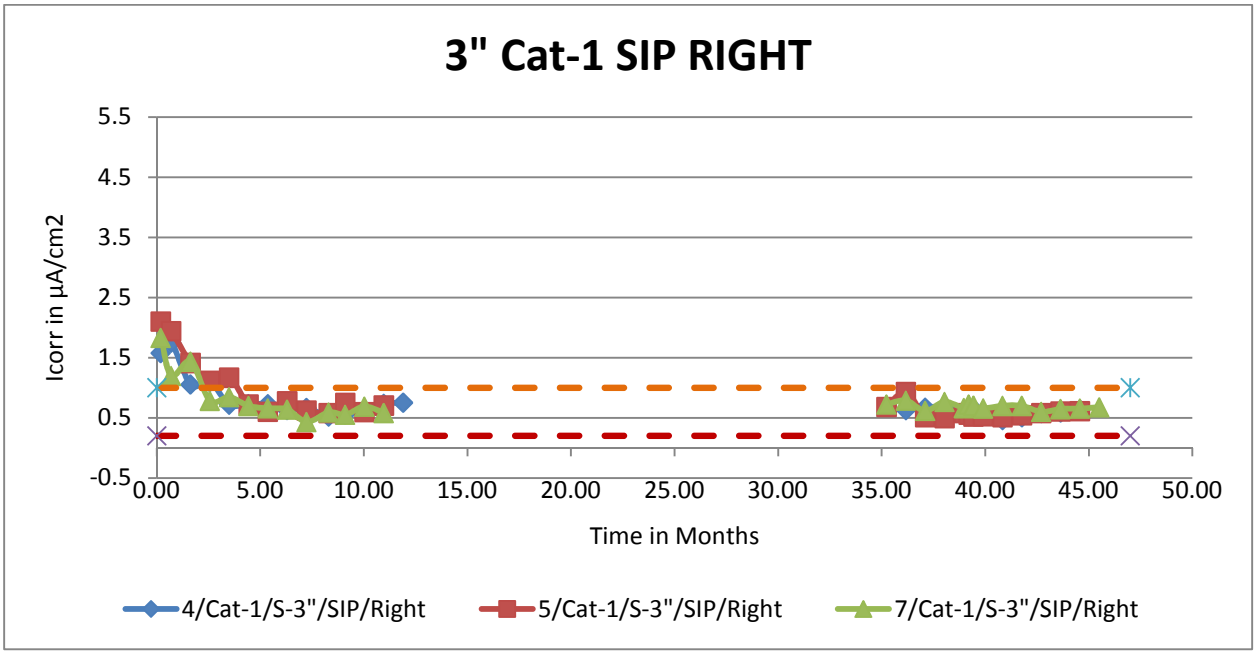

Figure C-27 - Corrosion Current Density – 3" Spacing, 2 Cathode Bars, with SIP, Right Side, Connected

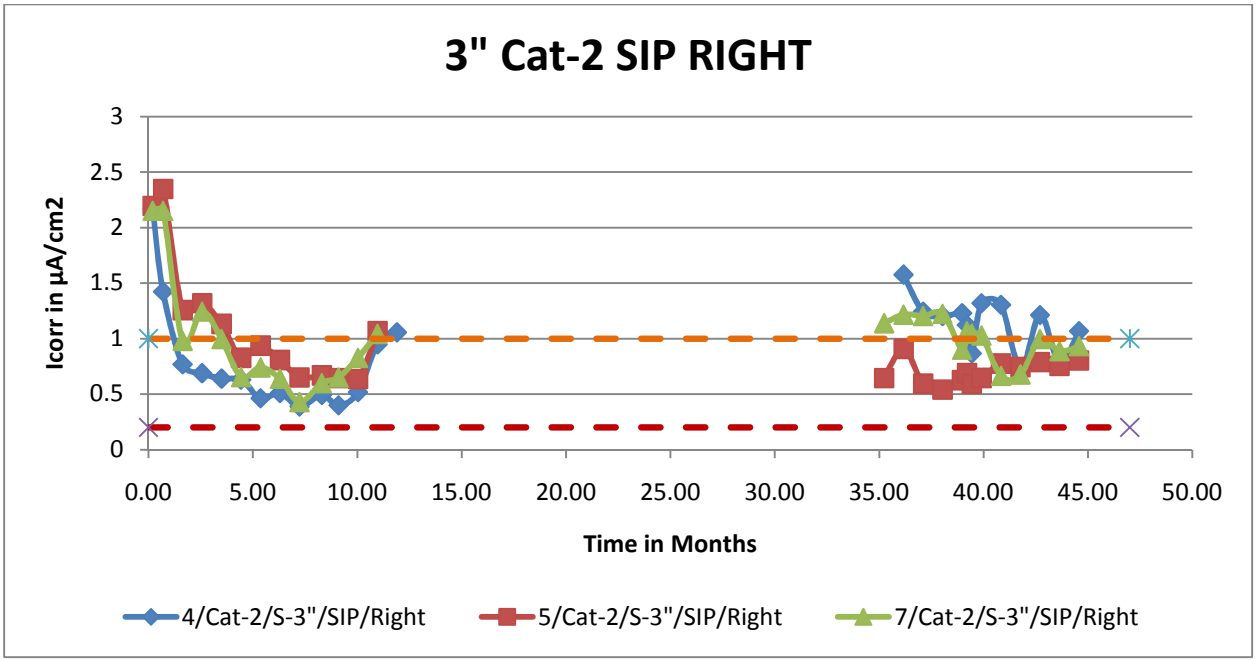

Figure C-28 - Corrosion Current Density – 3" Spacing, 2 Cathode Bars, with SIP, Right Side, Unconnected

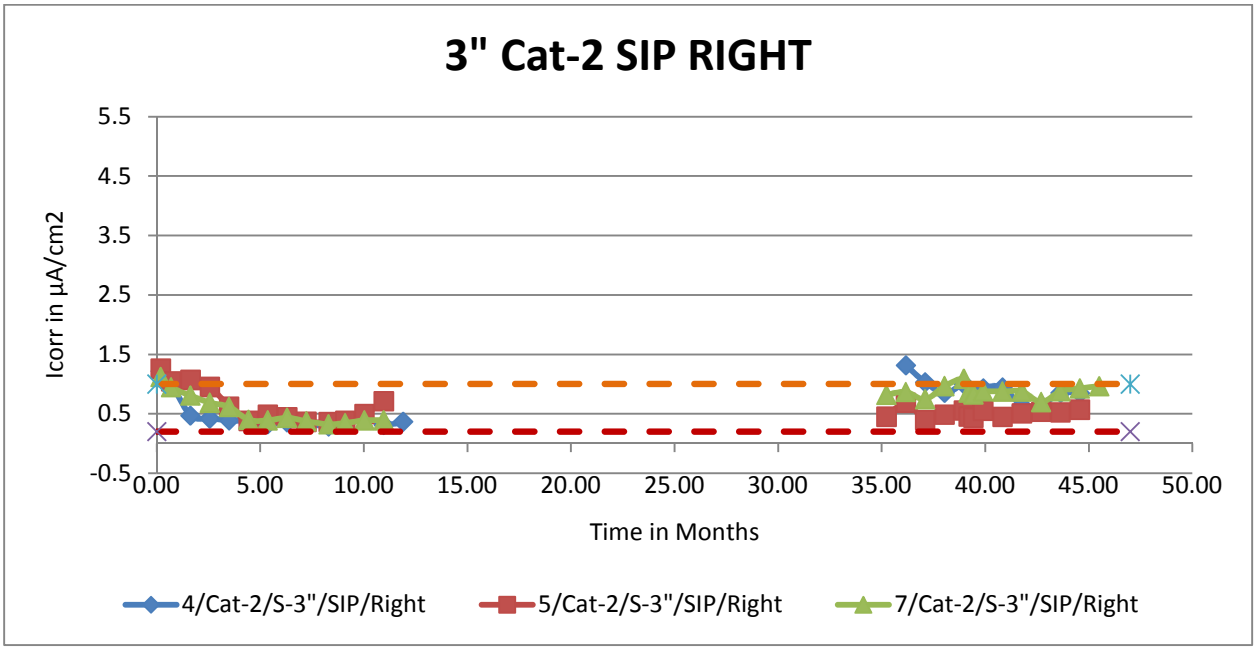

Figure C-29 - Corrosion Current Density – 3” Spacing, 2 Cathode Bars, with No SIP, Right Side, Connected

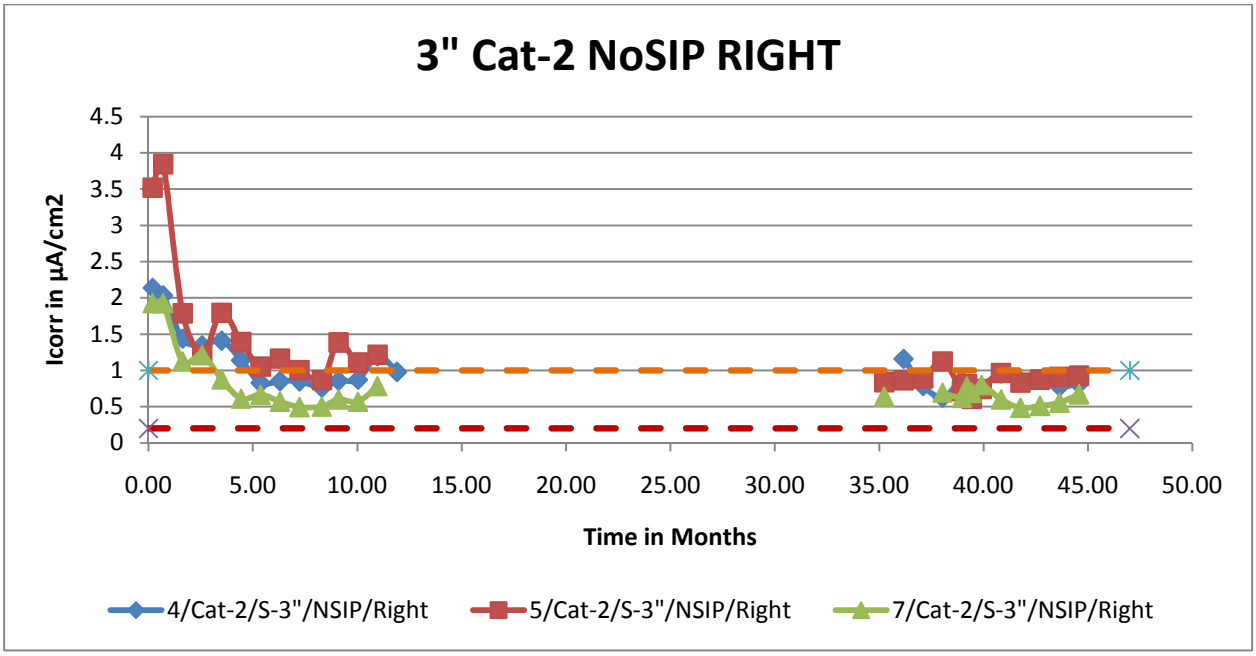

Figure C-30 - Corrosion Current Density – 3” Spacing, 2 Cathode Bars, with No SIP, Right Side, Connected

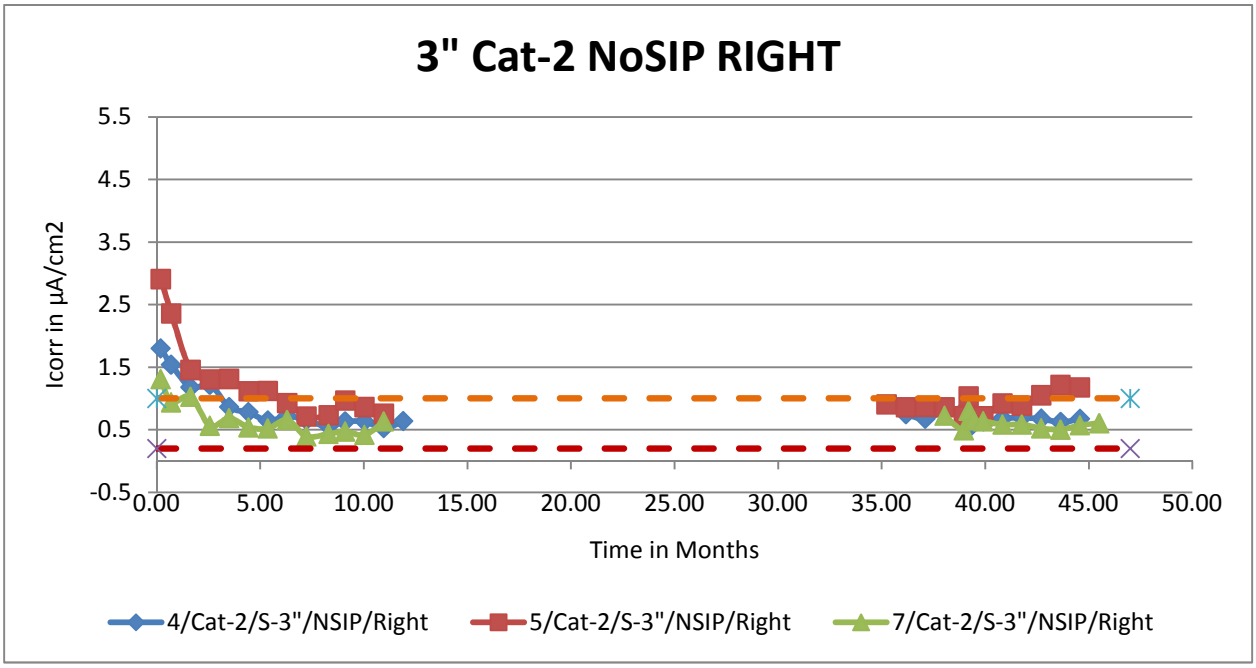

Figure C-31 - Corrosion Current Density – 4” Spacing, 1 Cathode Bar, with SIP, Right Side, Connected

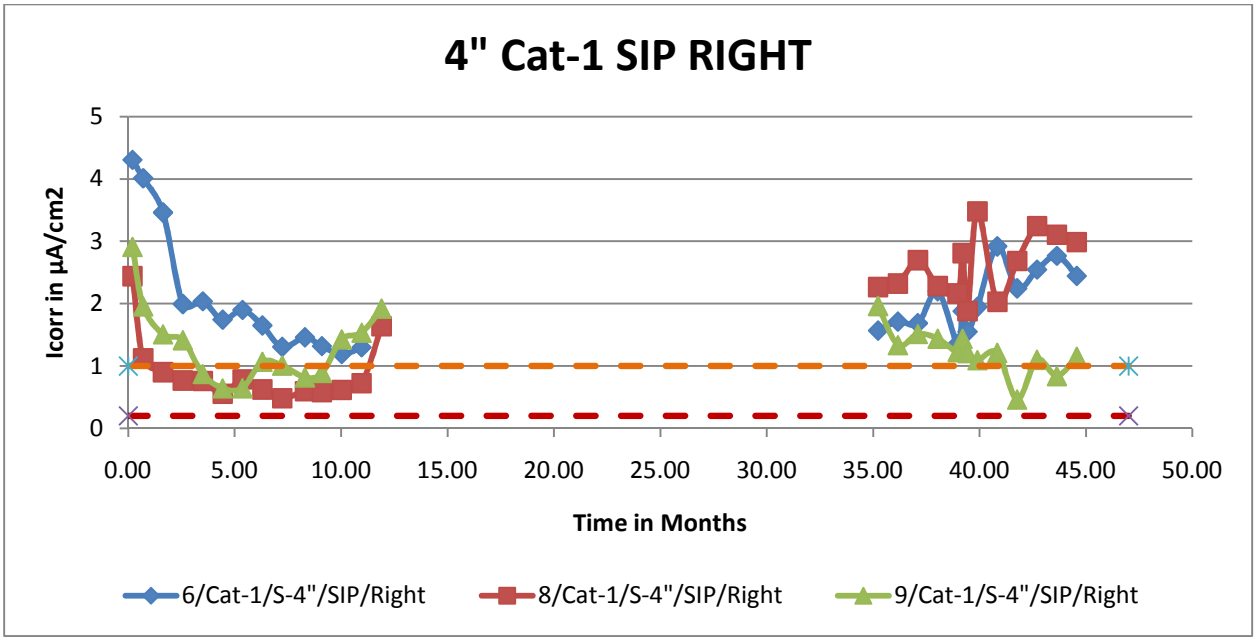

Figure C-32 - Corrosion Current Density – 4” Spacing, 1 Cathode Bar, with SIP, Right Side, Unconnected

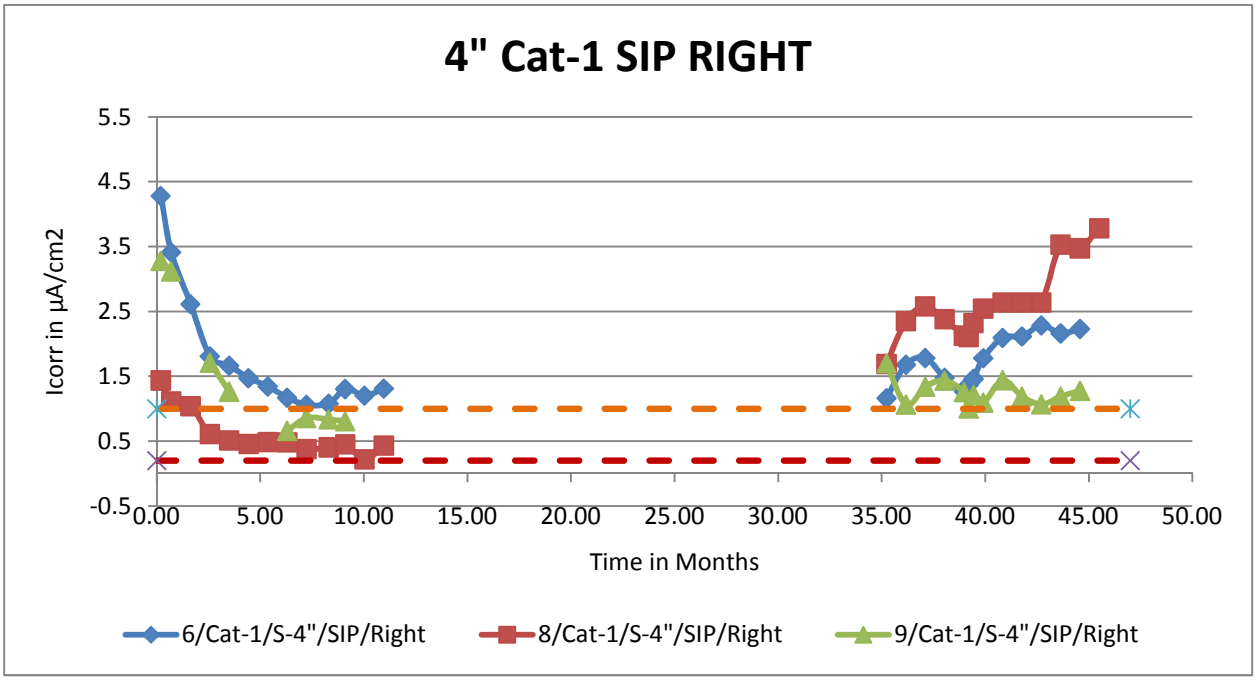

Figure C-33 - Corrosion Current Density – 4” Spacing, 2 Cathode Bars, with SIP, Right Side, Connected

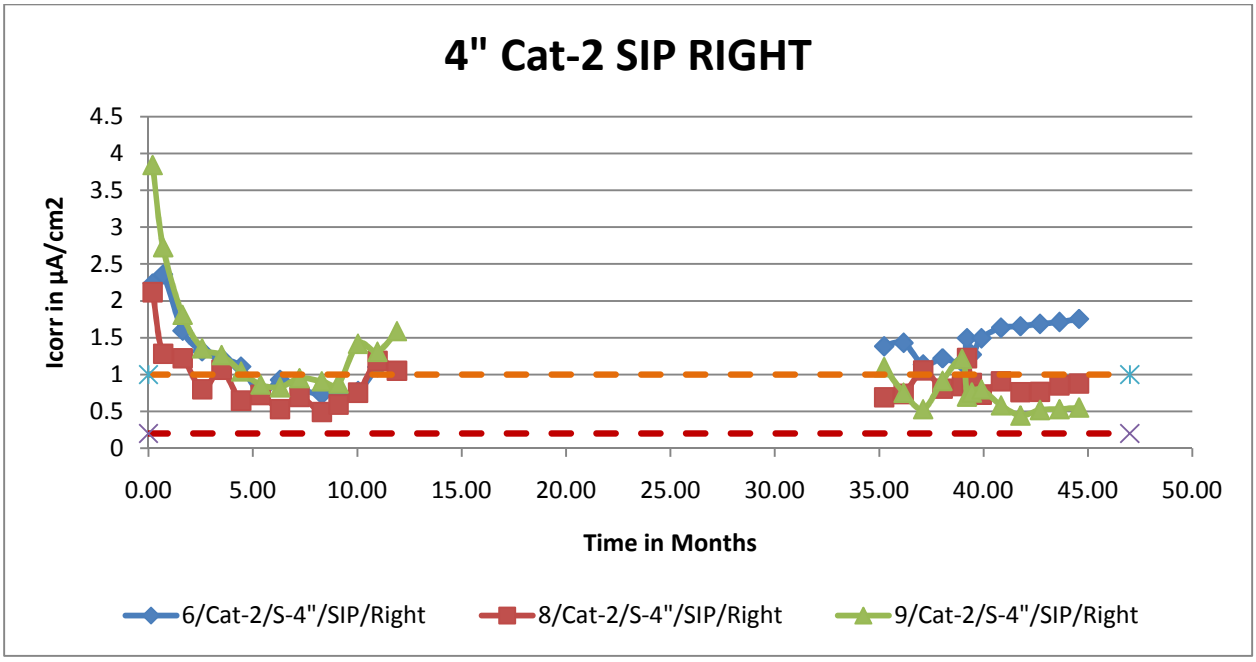

Figure C-34 - Corrosion Current Density – 4” Spacing, 2 Cathode Bars, with SIP, Right Side, Unconnected

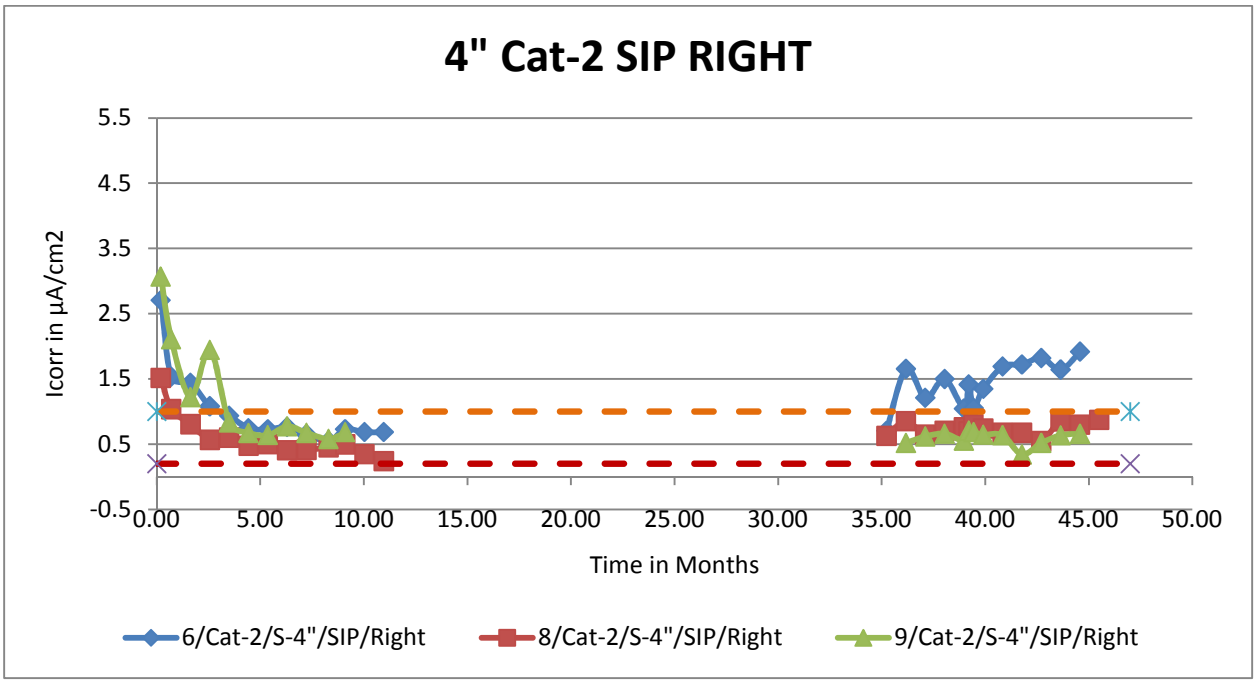

Figure C-35 - Corrosion Current Density – 4” Spacing, 2 Cathode Bars, with No SIP, Right Side, Connected

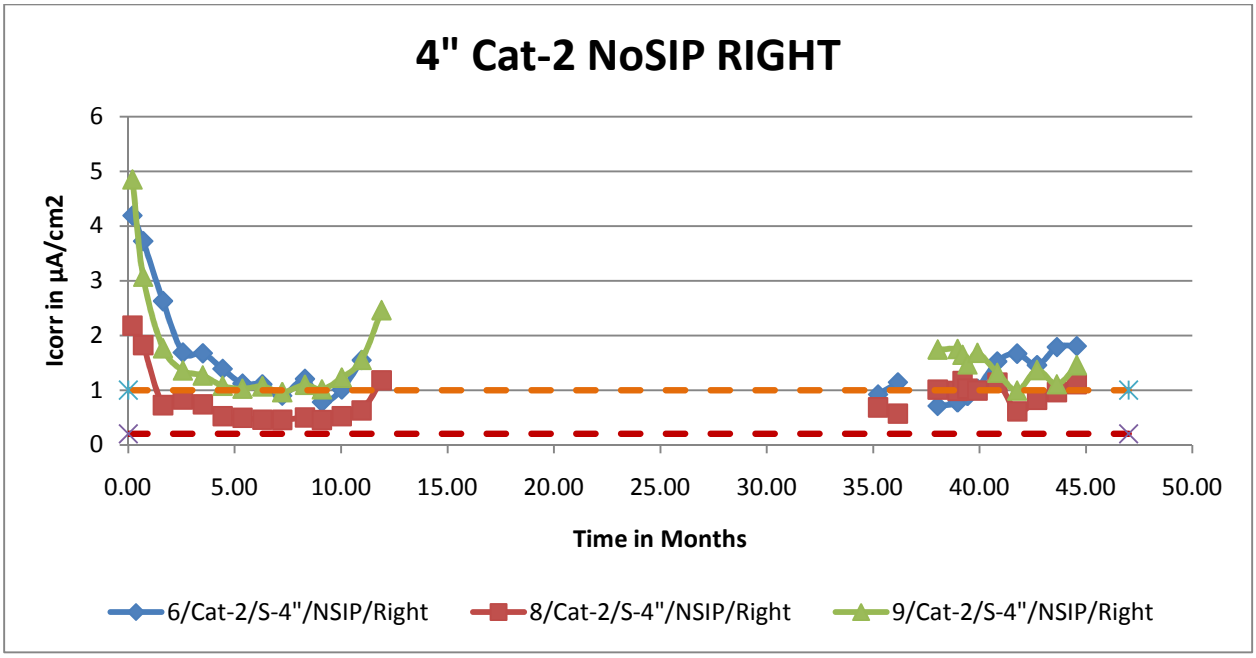

Figure C-36 - Corrosion Current Density – 4” Spacing, 2 Cathode Bars, with No SIP, Right Side, Unconnected

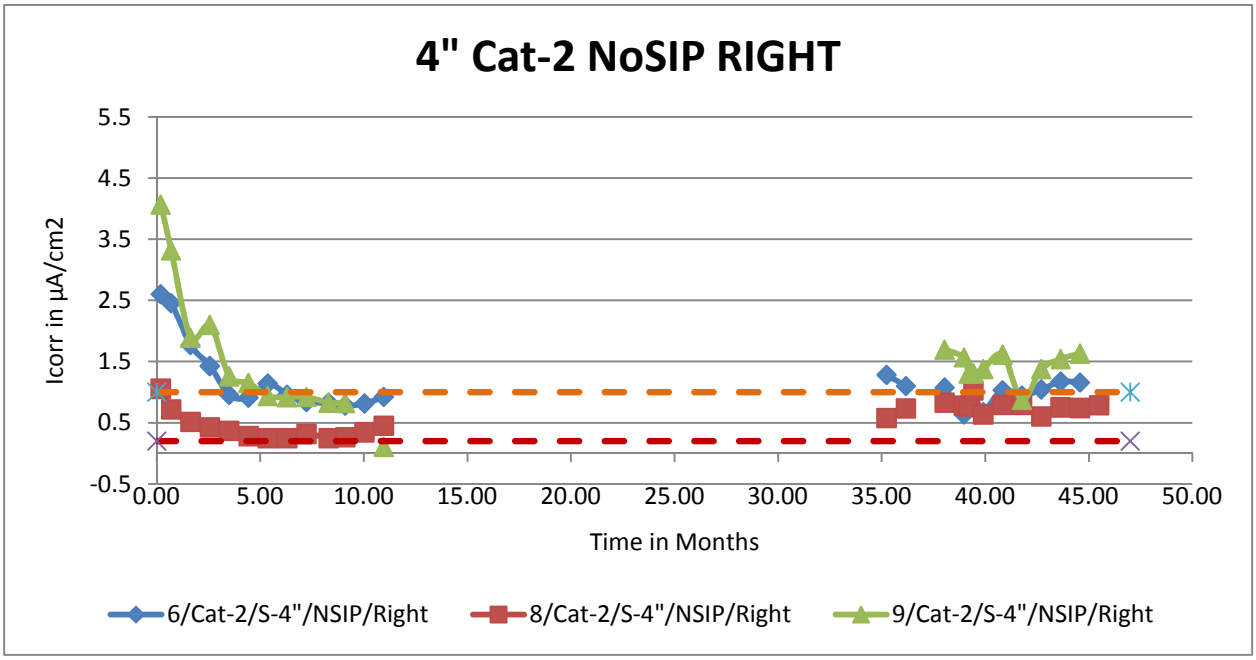

Appendix D – Macro Cell Measurements

Macrocell Currents - Batch – 1

Figure D-1 - Spacing-2”, Cathode-1, SIP

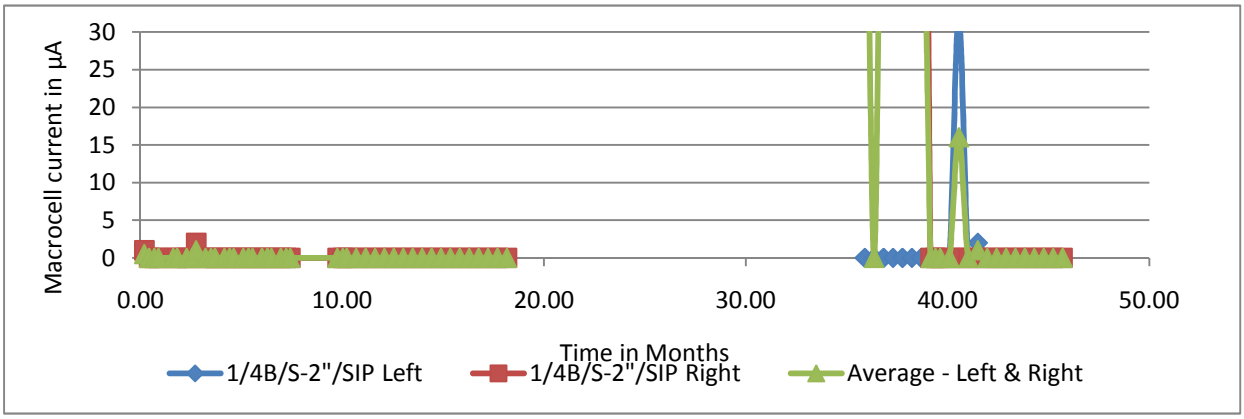

Figure D-2 - Spacing-2”, Cathode-2, SIP

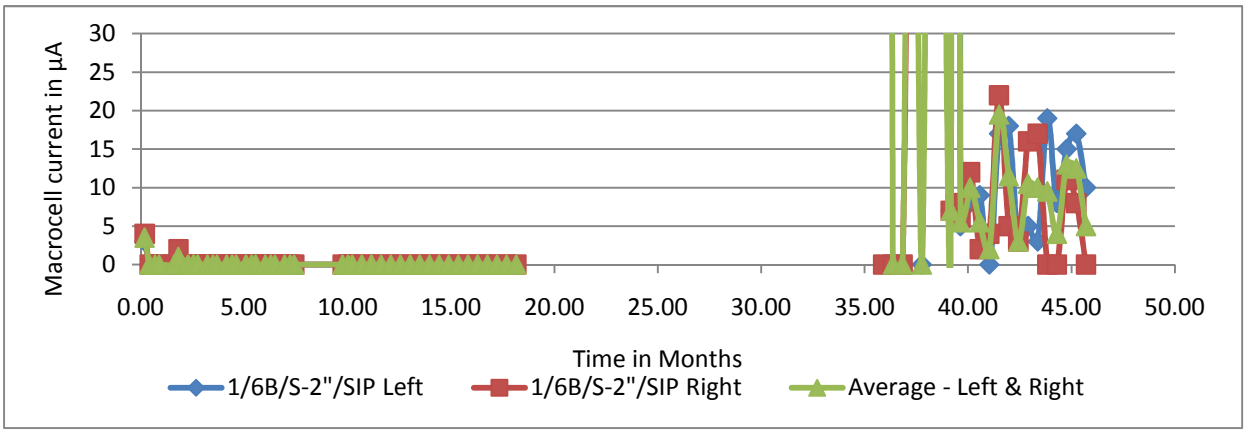

Figure D-3 - Spacing-2”, Cathode-2, NoSIP

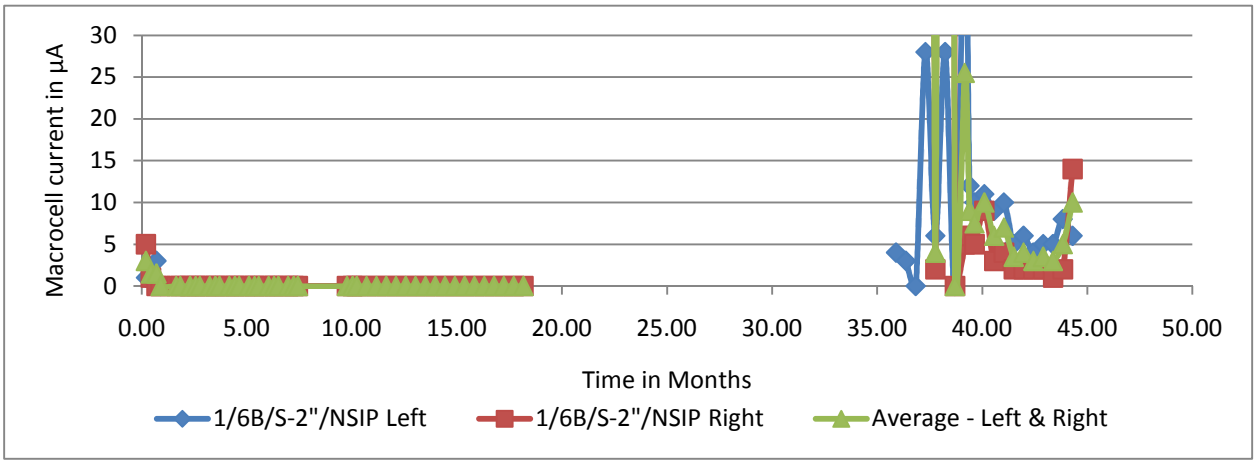

Macrocell Currents - Batch – 2

Figure D-4 - Spacing-2”, Cathode-1, SIP

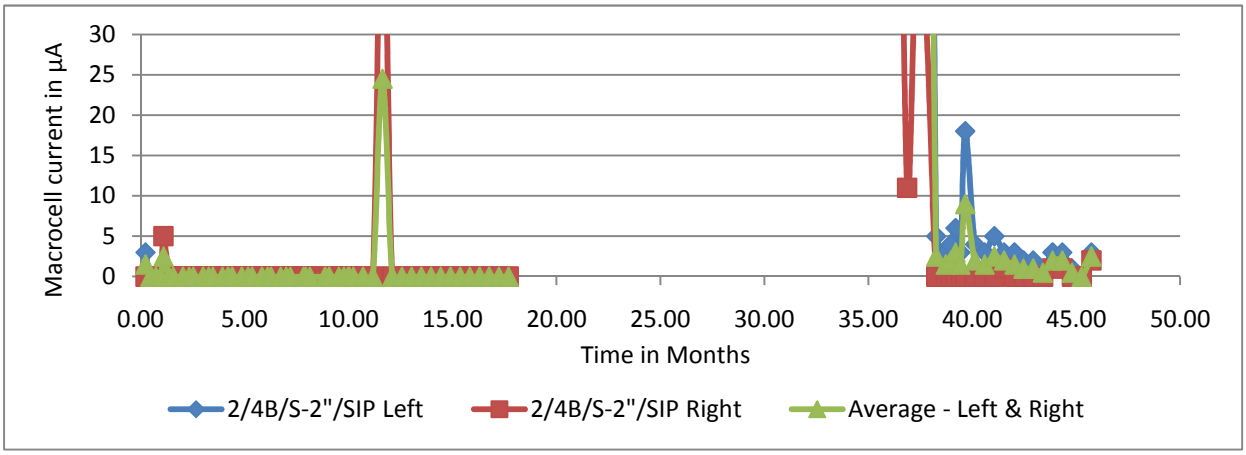

Figure D-5 - Spacing-2”, Cathode-2, SIP

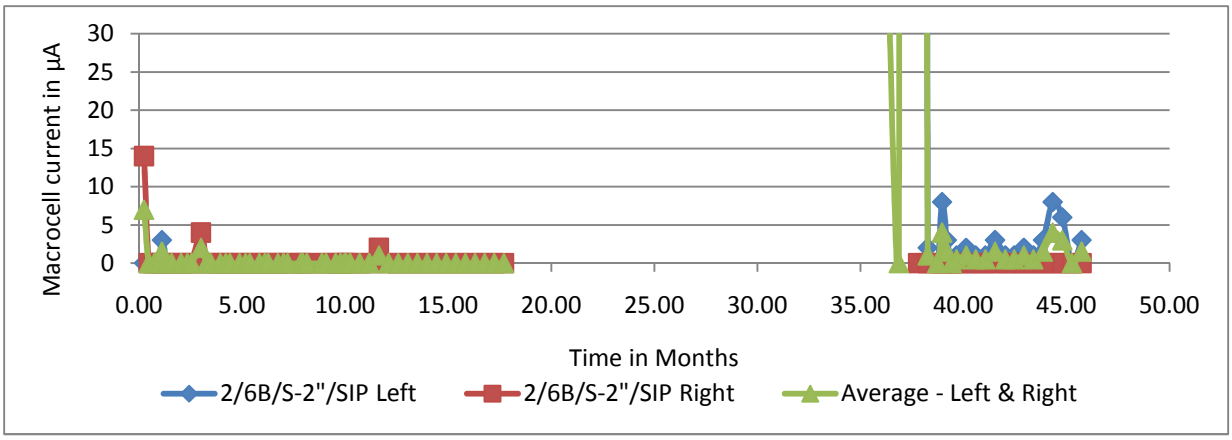

Figure D-6 - Spacing-2”, Cathode-2, NoSIP

Macrocell Currents - Batch – 3

Figure D-7 - Spacing-2", Cathode-1, SIP

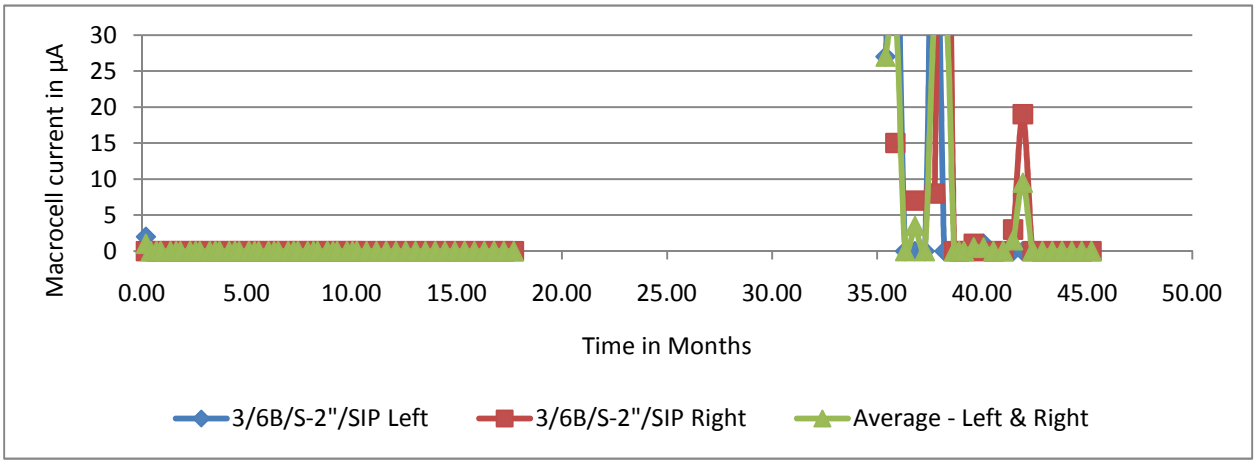

Figure D-8 - Spacing-2", Cathode-2, SIP

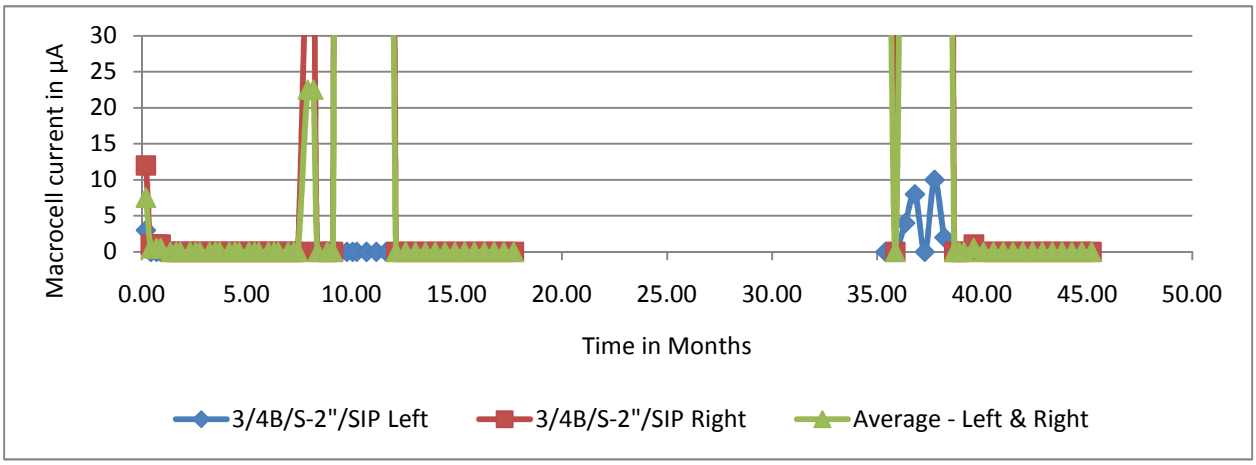

Figure D-9 - Spacing-2", Cathode-2, NoSIP

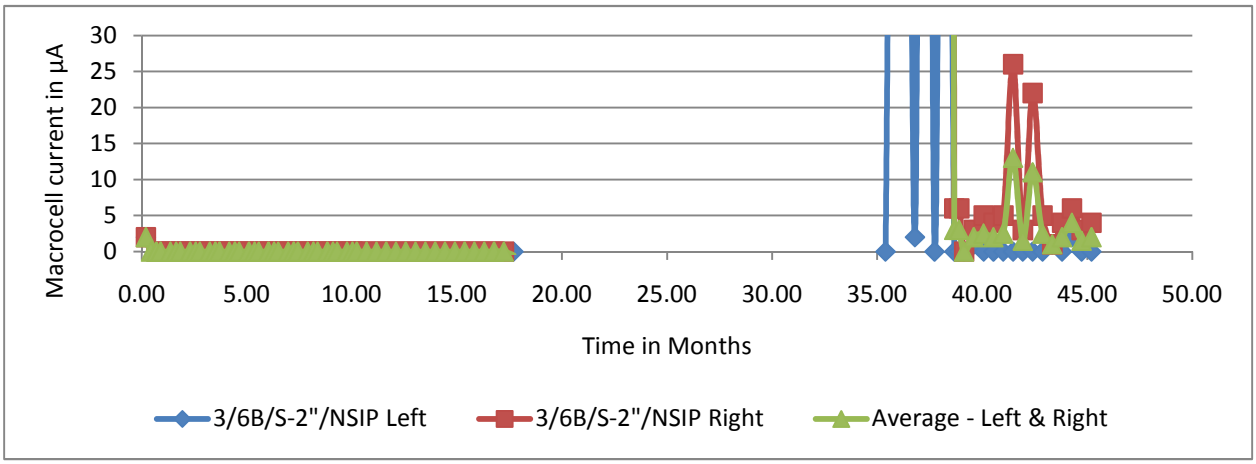

Macrocell Currents - Batch – 4

Figure D-10 - Spacing-3”, Cathode-1, SIP

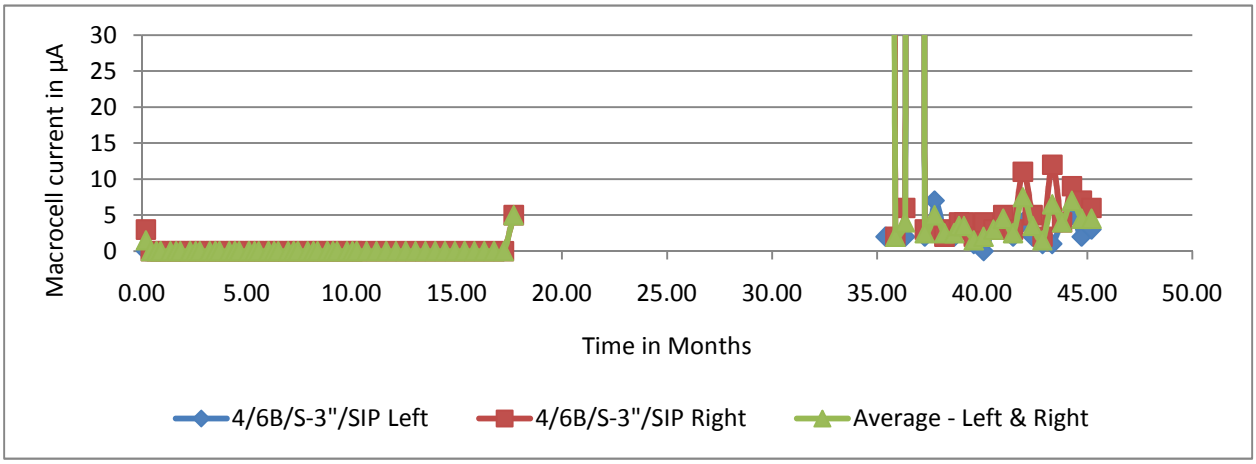

Figure D-11 - Spacing-3”, Cathode-2, SIP

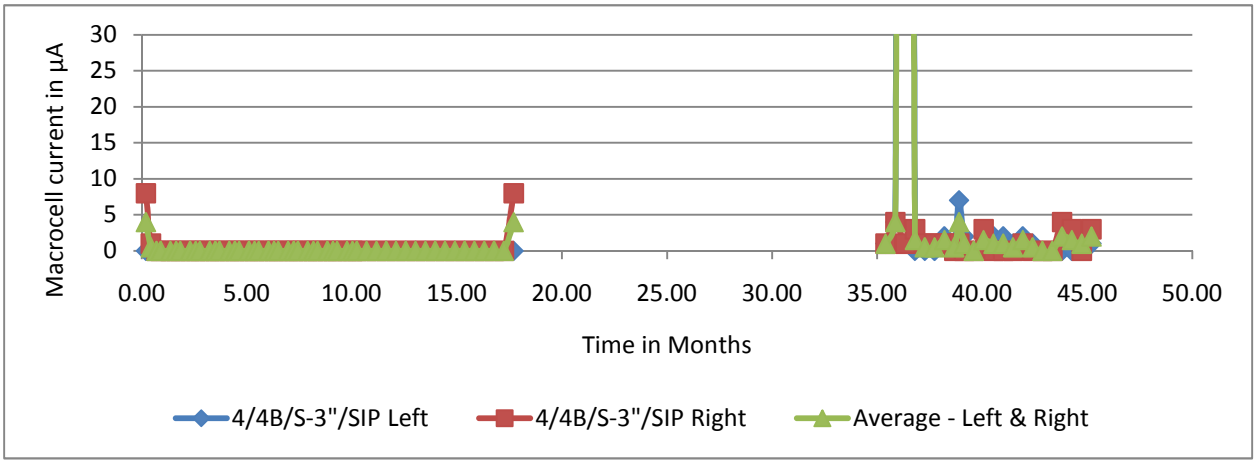

Figure D-12 - Spacing-3”, Cathode-2, SIP

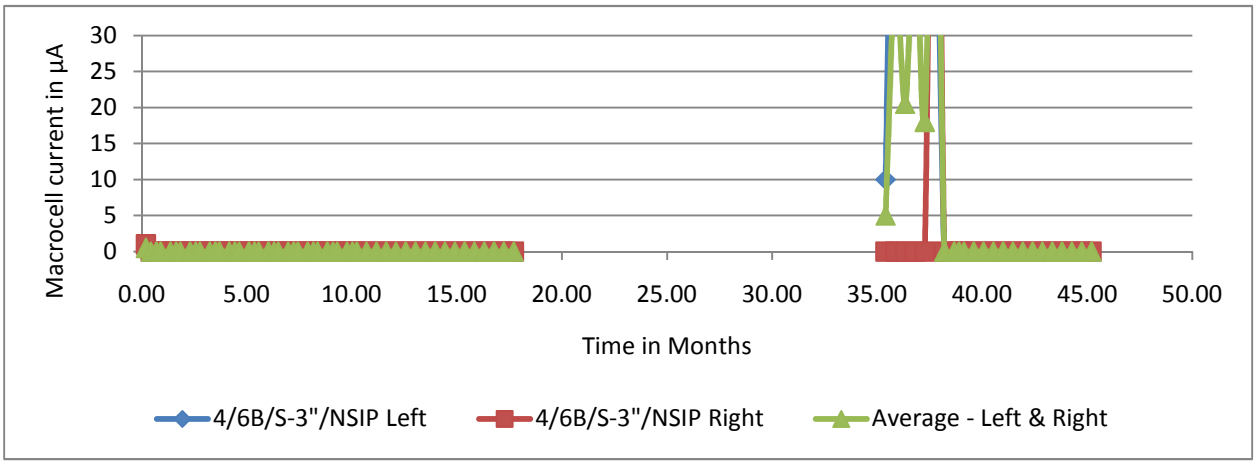

Macrocell Currents - Batch – 5

Figure D-13 - Spacing-3”, Cathode-1, SIP

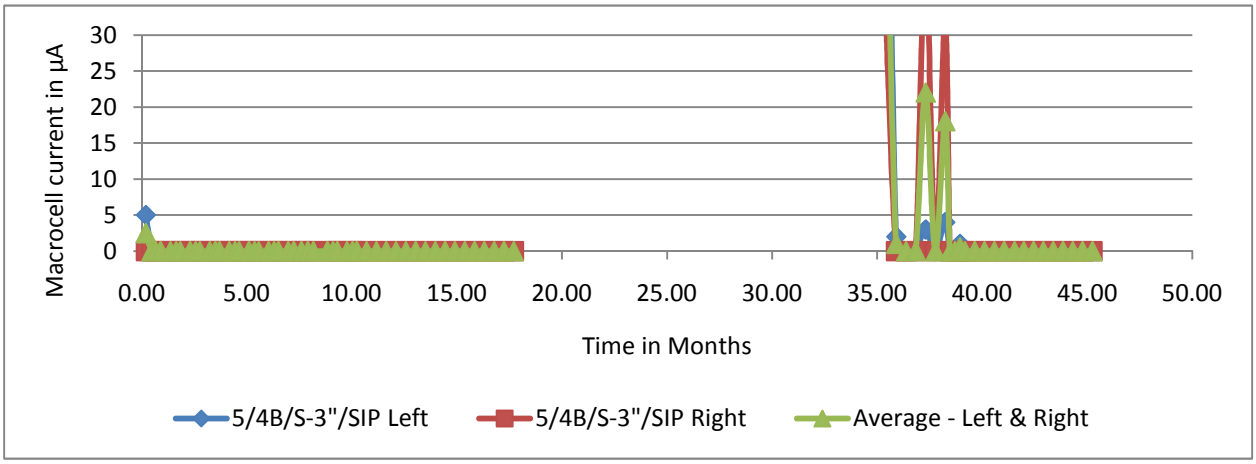

Figure D-14 - Spacing-3”, Cathode-2, SIP

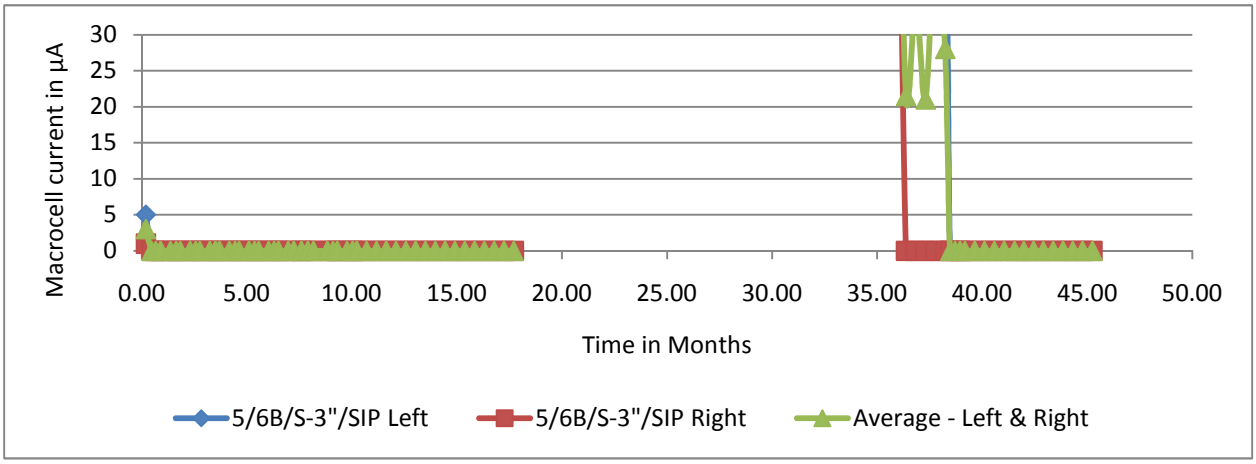

Figure D-15 - Spacing-3”, Cathode-2, NoSIP

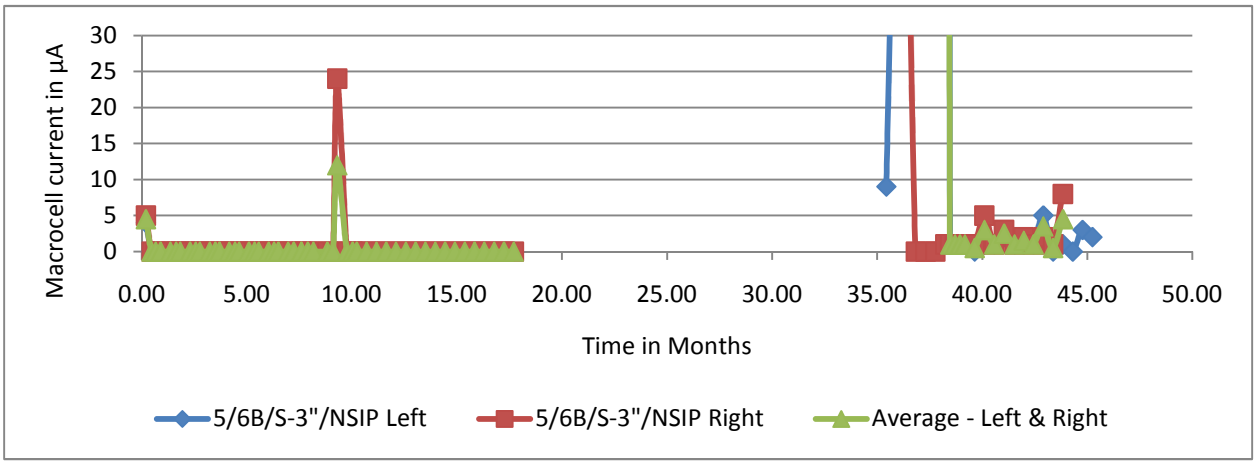

Macrocell Currents - Batch – 6

Figure D-16 - Spacing-4”, Cathode-1, SIP

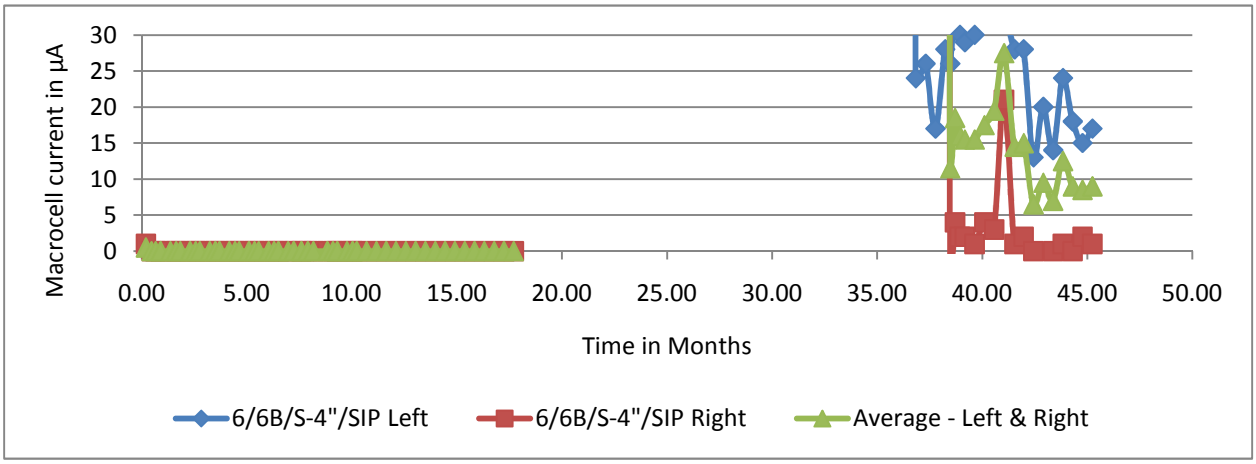

Figure D-17 - Spacing-4”, Cathode-2, SIP

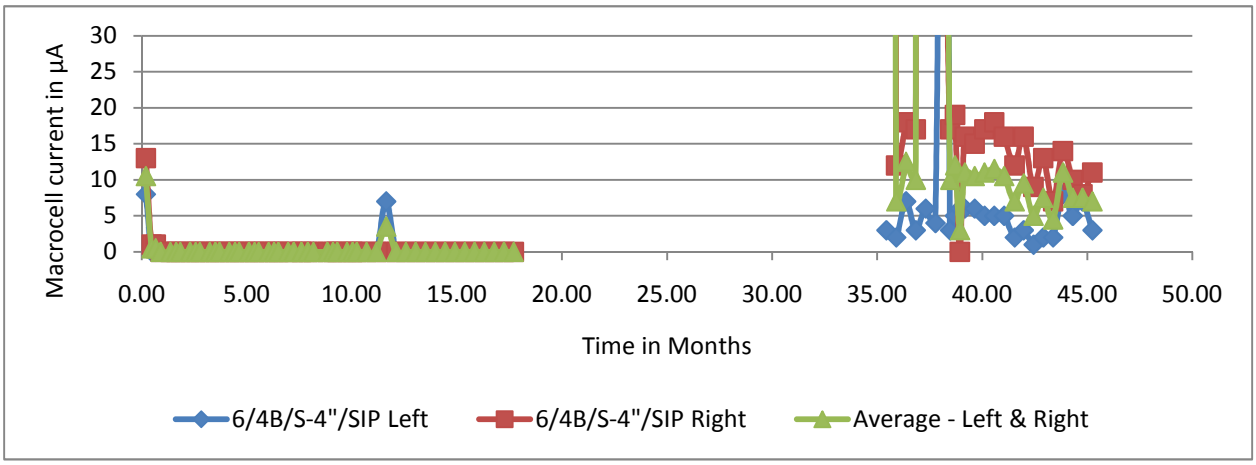

Figure D-18 - Spacing-4”, Cathode-2, NoSIP

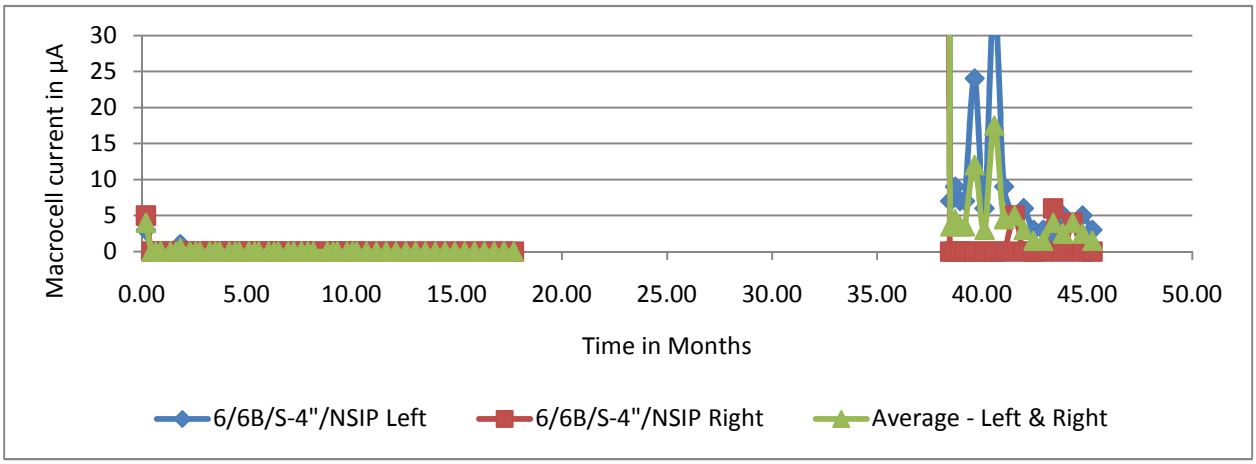

Macrocell Currents - Batch – 7

Figure D-19 - Spacing-3”, Cathode-1, SIP

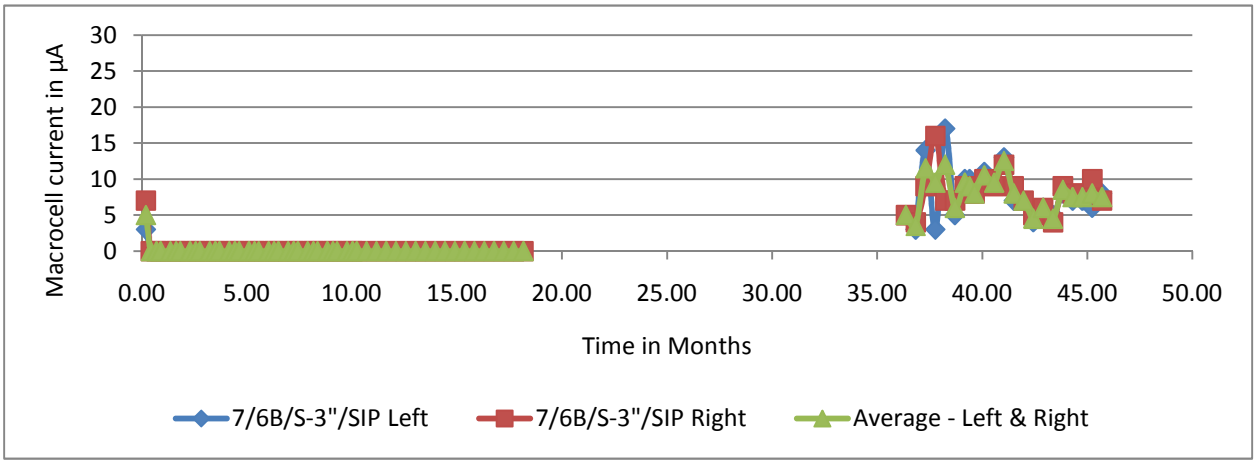

Figure D-20 - Spacing-3”, Cathode-2, SIP

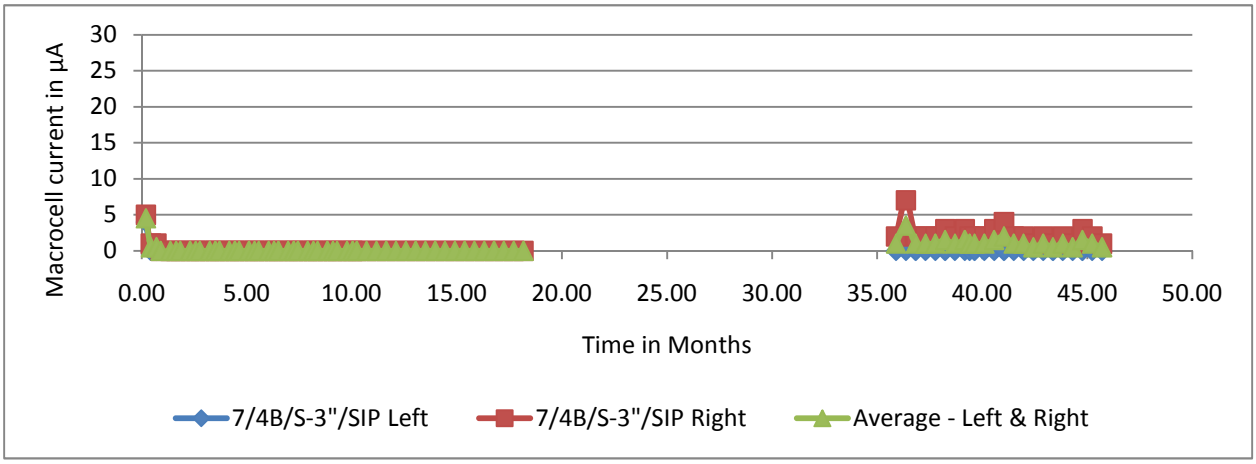

Figure D-21 - Spacing-3”, Cathode-2, NoSIP

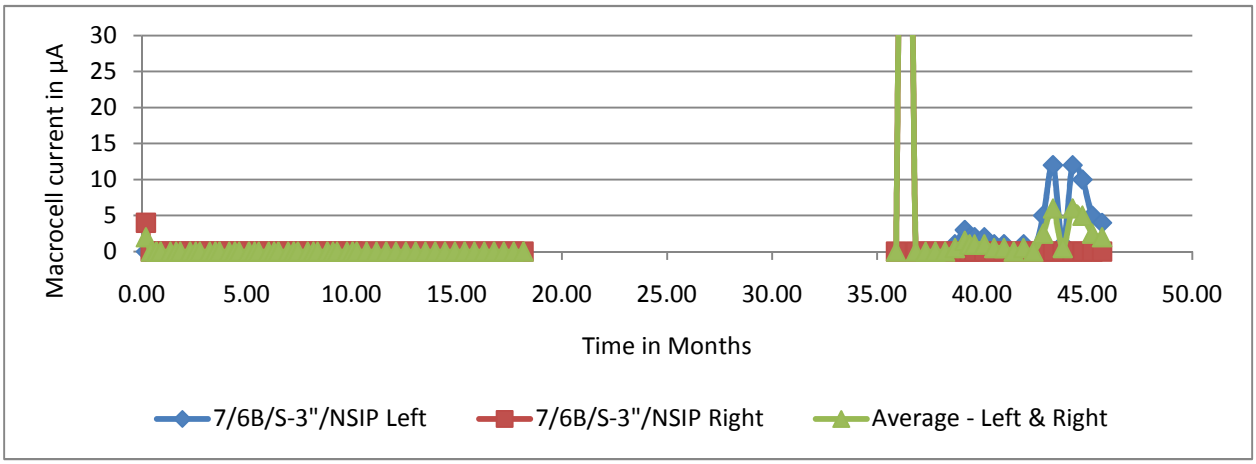

Macrocell Currents - Batch – 8

Figure D-22 - Spacing-4”, Cathode-1, SIP

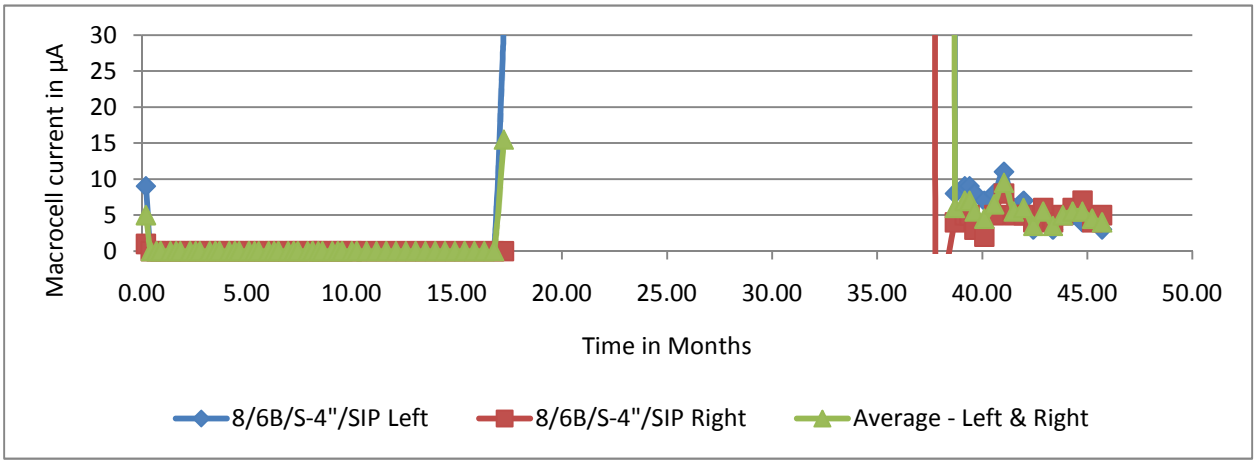

Figure D-23 - Spacing-4”, Cathode-2, SIP

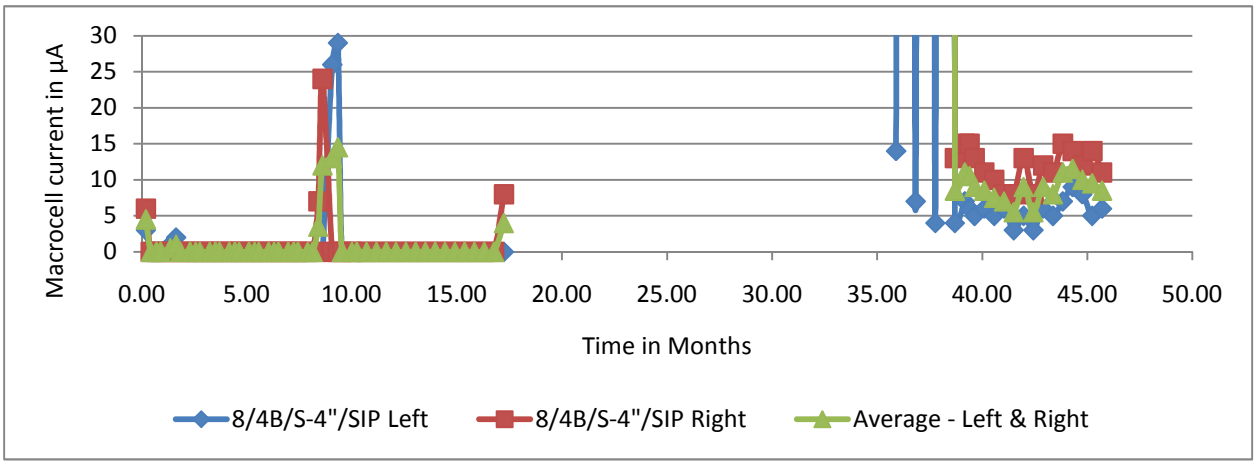

Figure D-24 - Spacing-4”, Cathode-2, NoSIP

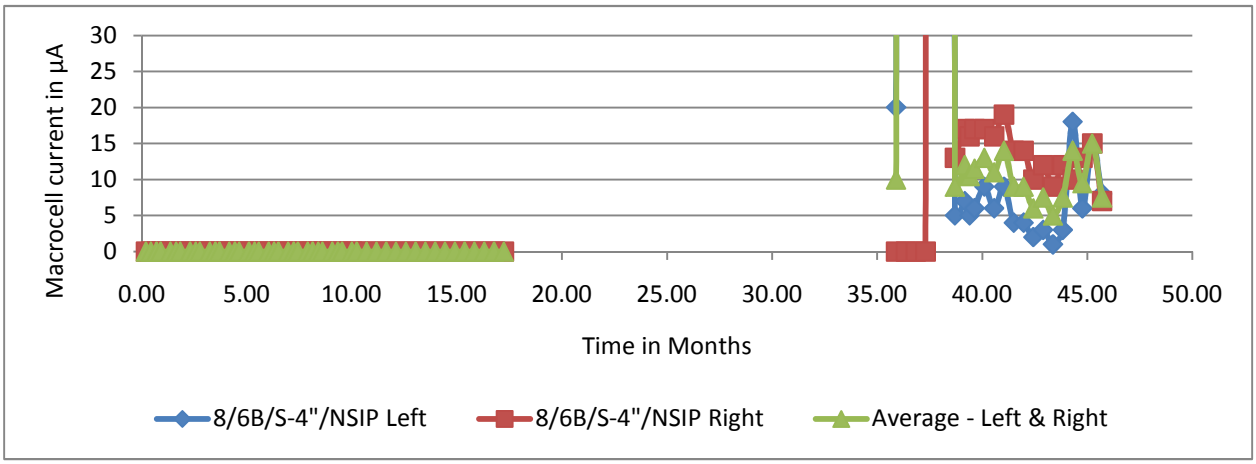

Macrocell Currents - Batch – 9

Figure D-25 - Spacing-4”, Cathode-1, SIP

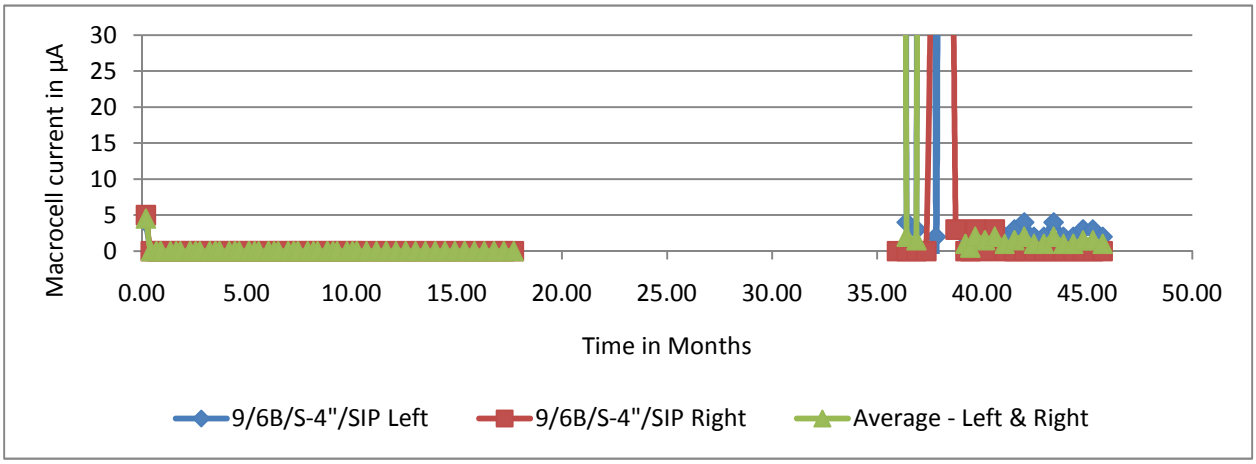

Figure D-26 - Spacing-4”, Cathode-2, SIP

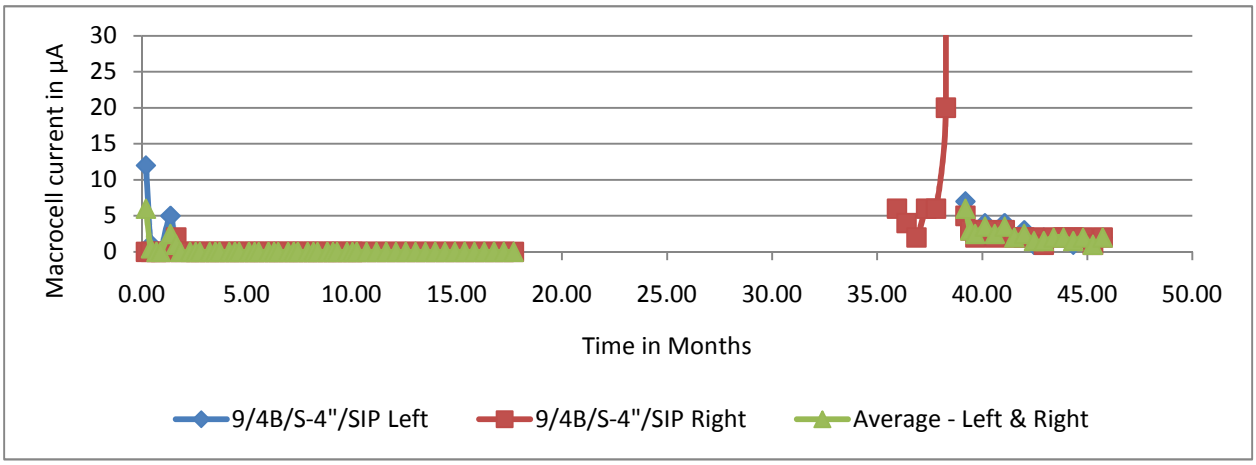

Figure D-27 - Spacing-4”, Cathode-2, NoSIP

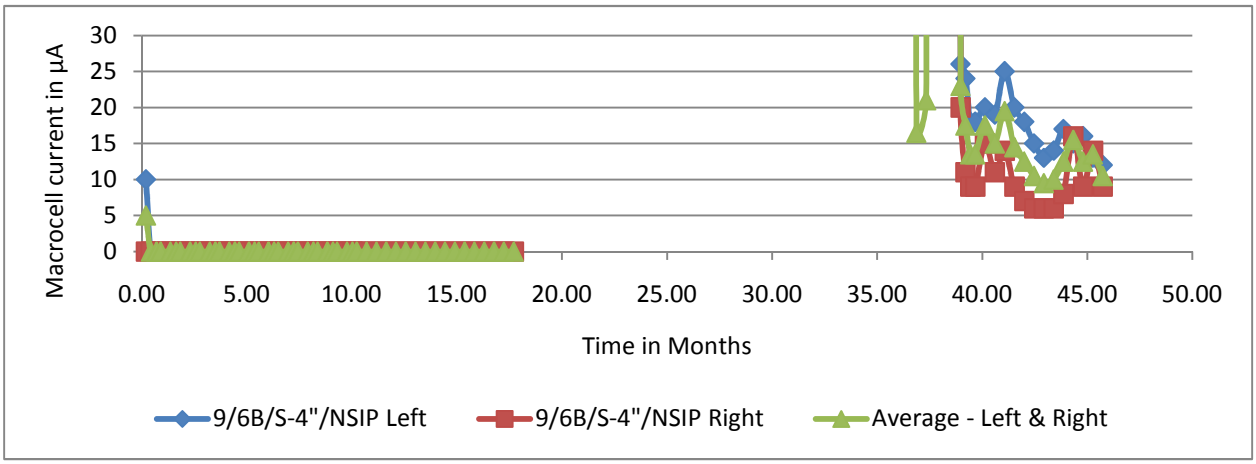

Appendix E – Photographs of Visual Inspection

Figure E-1 – Specimen 6 – C-2 – 4” – SIP – Left – Top Side of both Bars

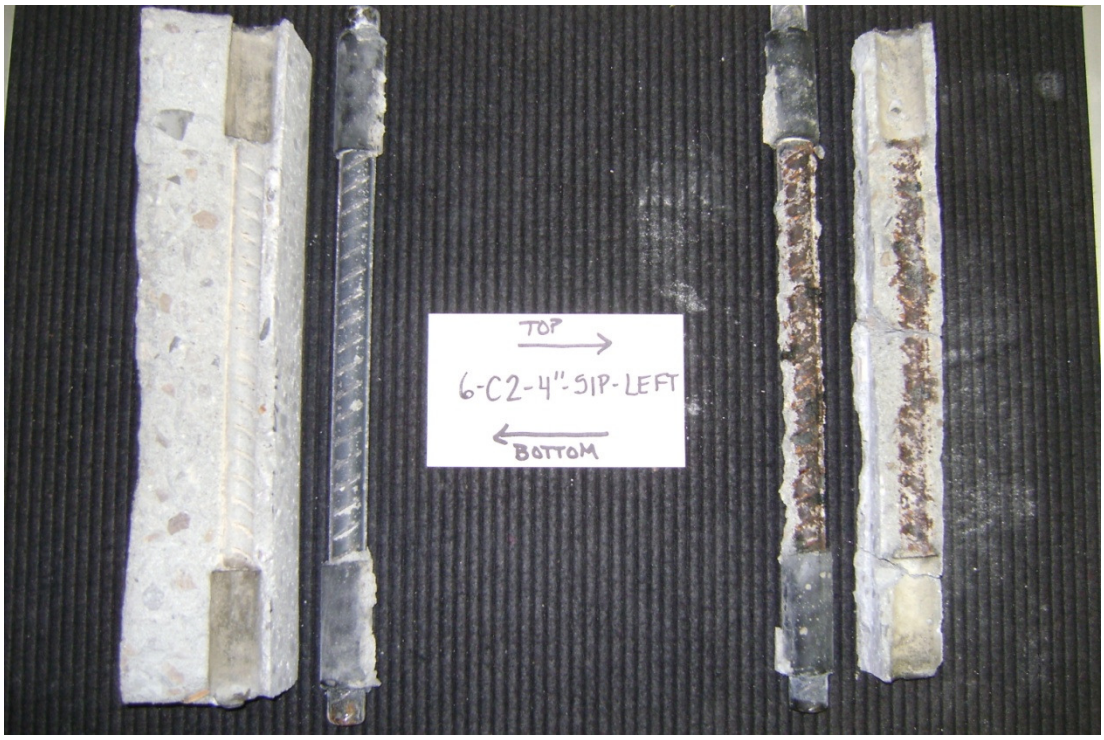

Figure E-2 – Specimen 6 – C-2 – 4” – SIP – Left – Bottom Side of both Bars

Figure E-3 – Specimen 6 – C-2 – 4” – SIP – Left – Top Side of Top Bar

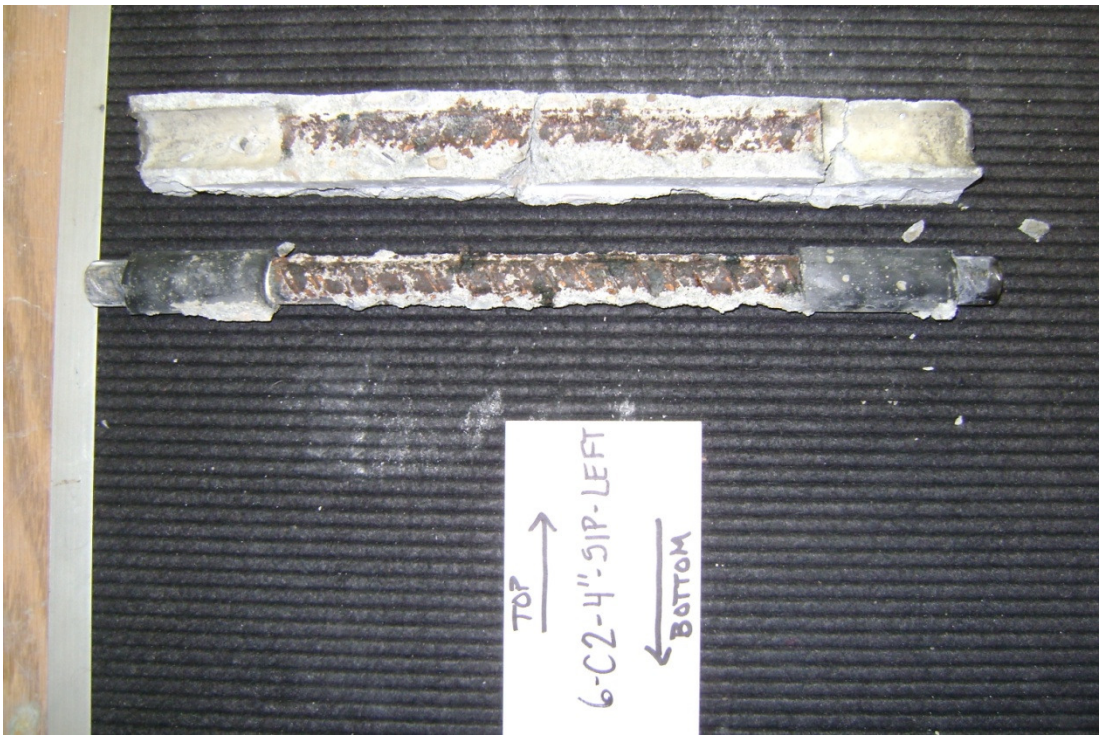

Figure E-4 – Specimen 6 – C-2 – 4” – SIP – Left – Top Side of Bottom Bar

Figure E-5 – Specimen **-** 8 – C-1- 4” – SIP – Right – Top Side of both Bars

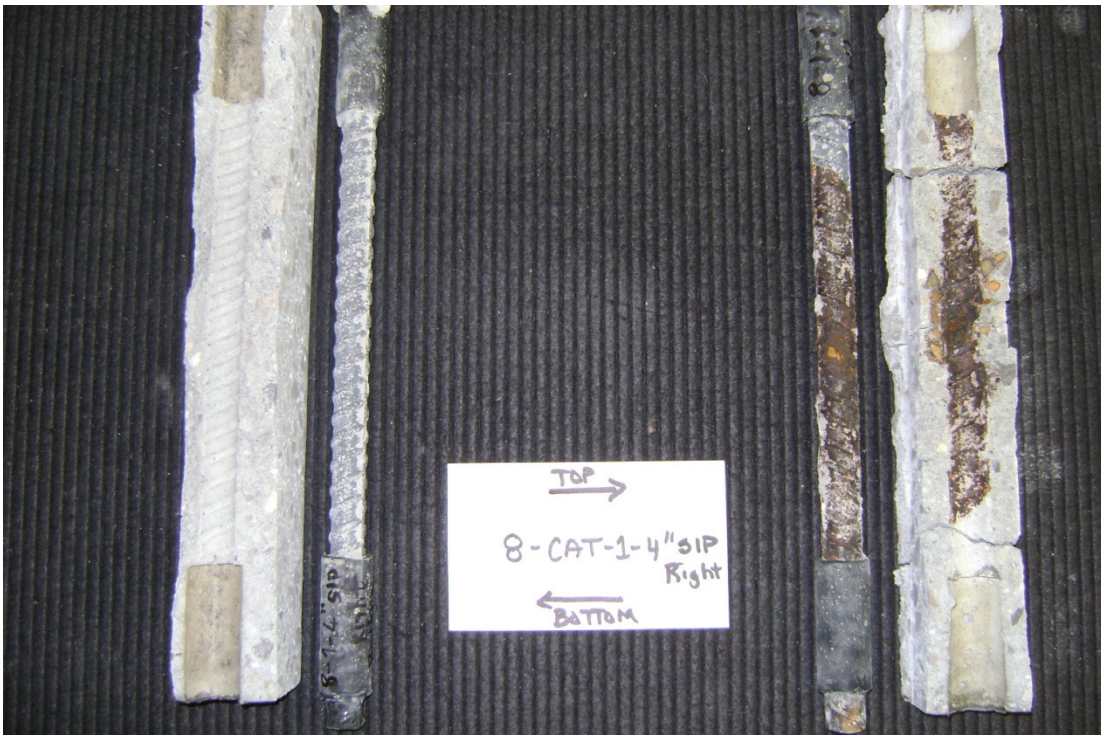

Figure E-6 – Specimen **-** 8 – C-1- 4” – SIP – Right – Bottom Side of both Bars

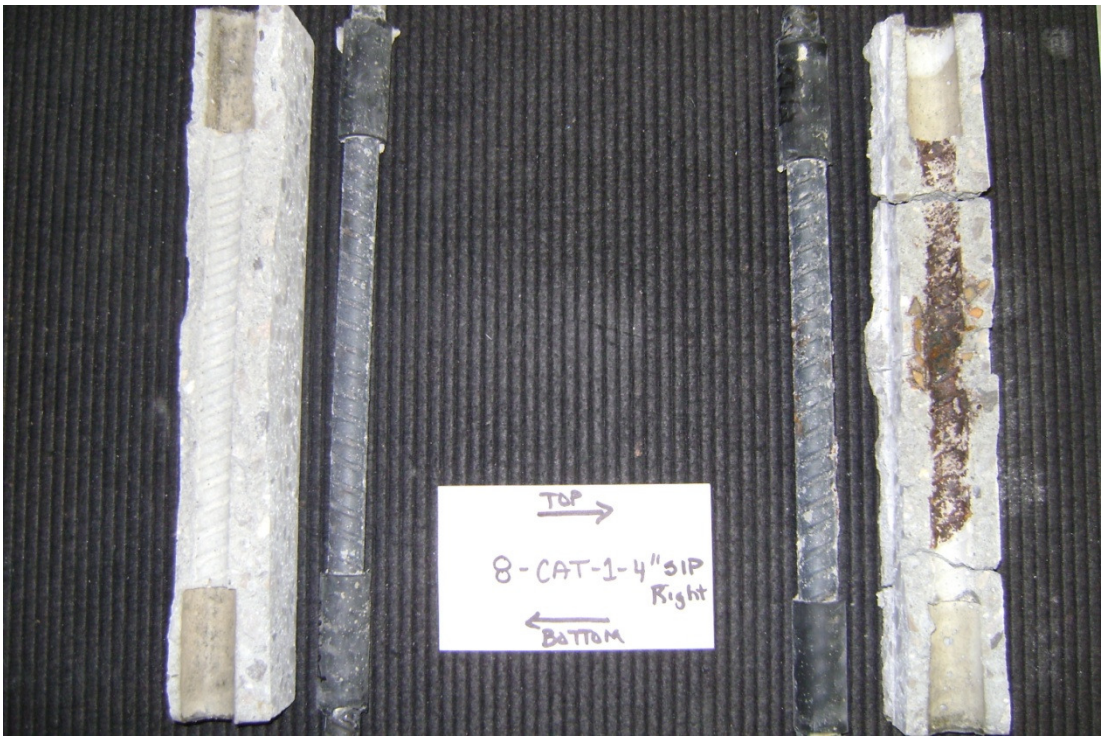

Figure E-7 – Specimen **-** 8 – C-1- 4” – SIP – Right – Top Side of Top Bar

Figure E-8 – Specimen **-** 8 – C-1- 4” – SIP – Right – Top Side of Bottom Bar

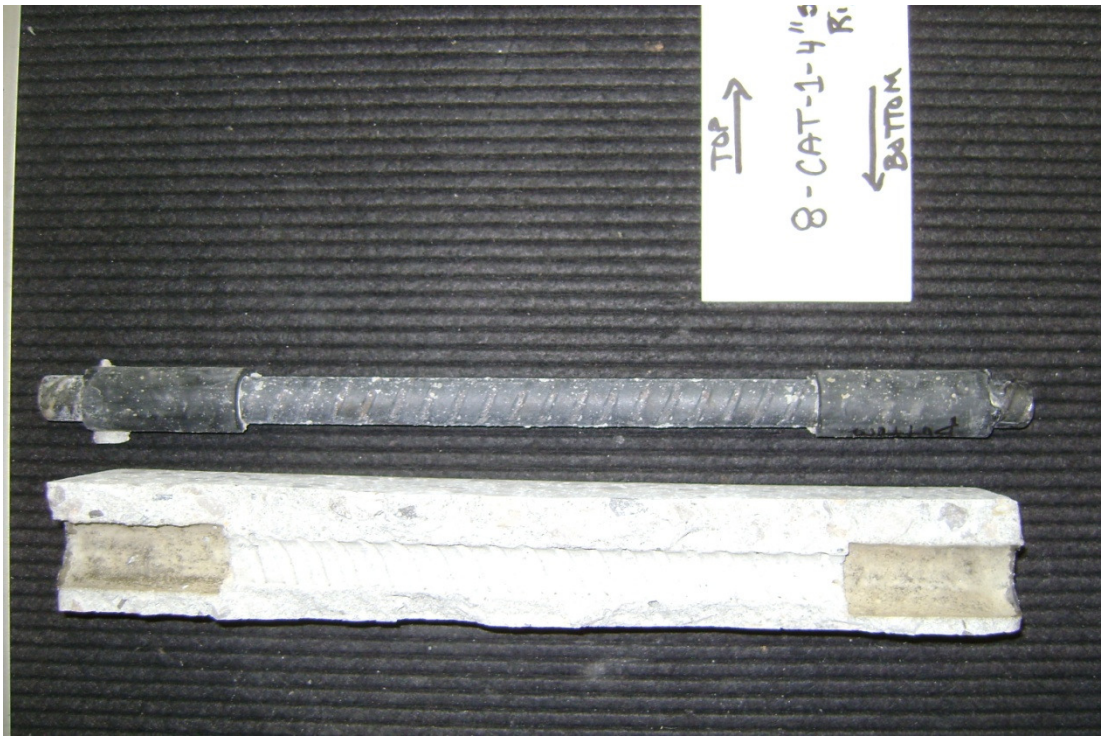

Figure E-9 – Specimen - 9 – C-2 – 4” – NSIP – Right – Top Side of both Bars

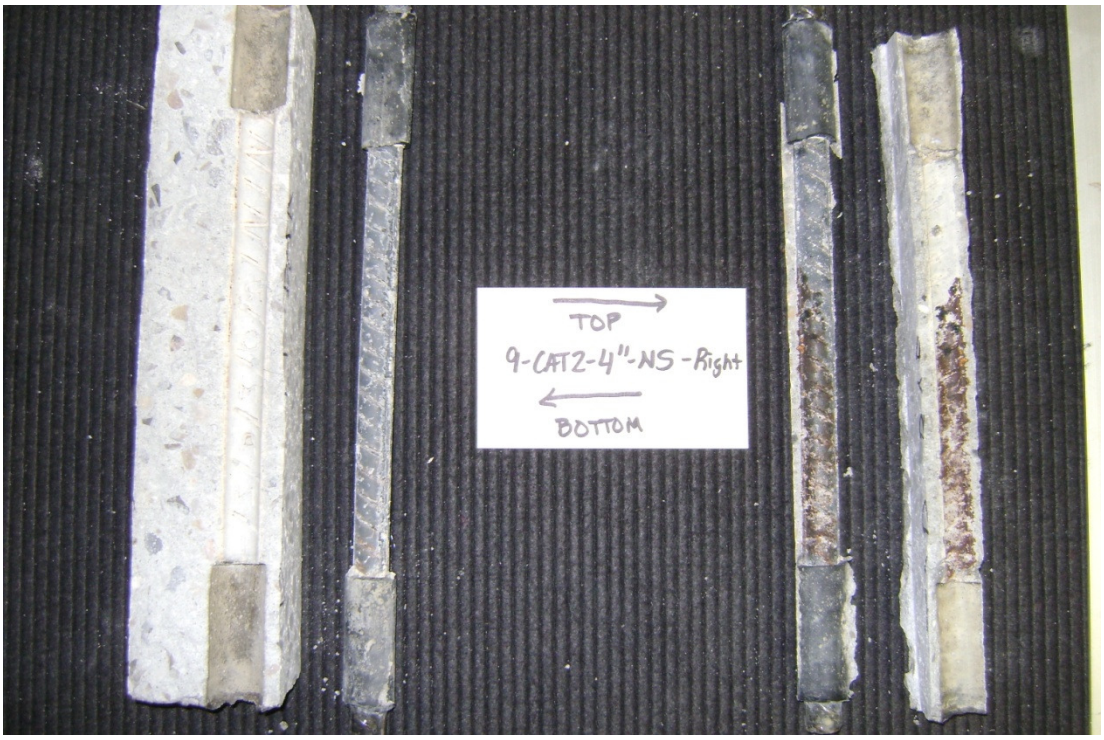

Figure E-10 – Specimen - 9 – C-2 – 4” – NSIP – Right – Bottom Side of both Bars

Figure E-11 – Specimen - 9 – C-2 – 4” – NSIP – Right – Top Side of Top Bar

Figure E-12 – Specimen - 9 – C-2 – 4” – NSIP – Right – Top Side of Bottom Bar

Figure E-13 – Specimen - 3 – C-2 – 2” – NSIP – Right – Top Side of both Bars

Figure E-14 – Specimen - 3 – C-2 – 2” – NSIP – Right – Bottom Side of both Bars

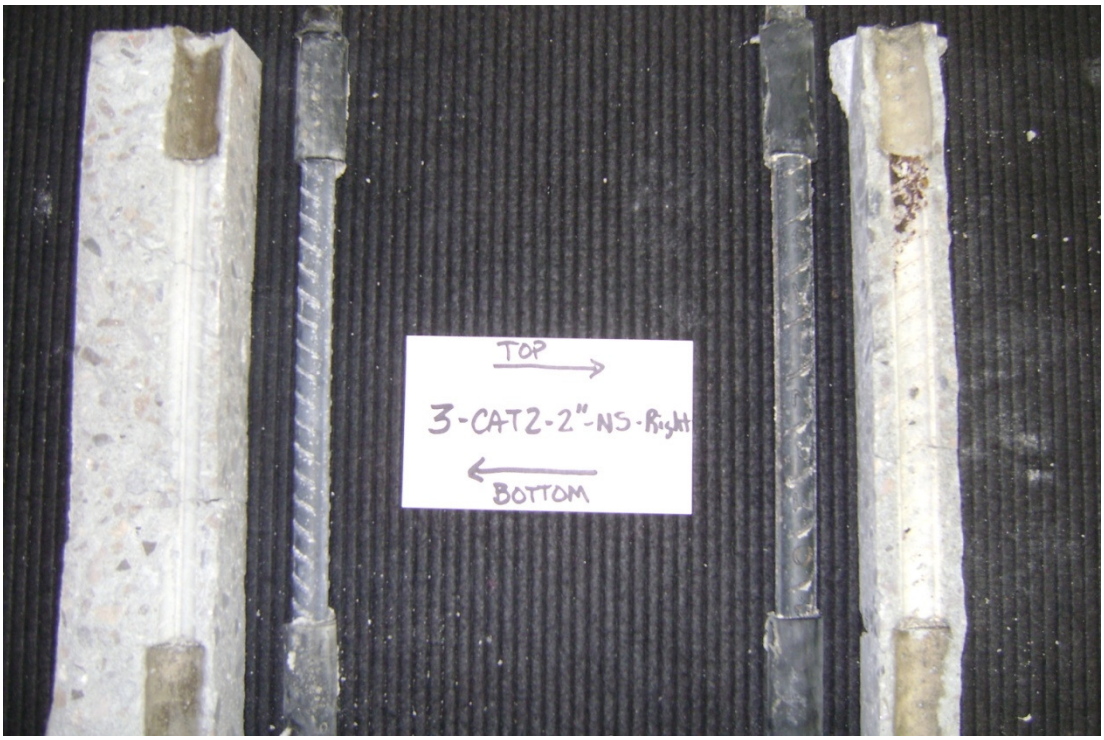

Figure E-15 – Specimen - 3 – C-2 – 2” – NSIP – Right – Top Side of Top Bar

Figure E-16 – Specimen - 3 – C-2 – 2” – NSIP – Right – Top Side of Bottom Bar

Figure E-17 – Specimen - 4 – C-1- 3” – SIP – Right – Top Side of both Bars

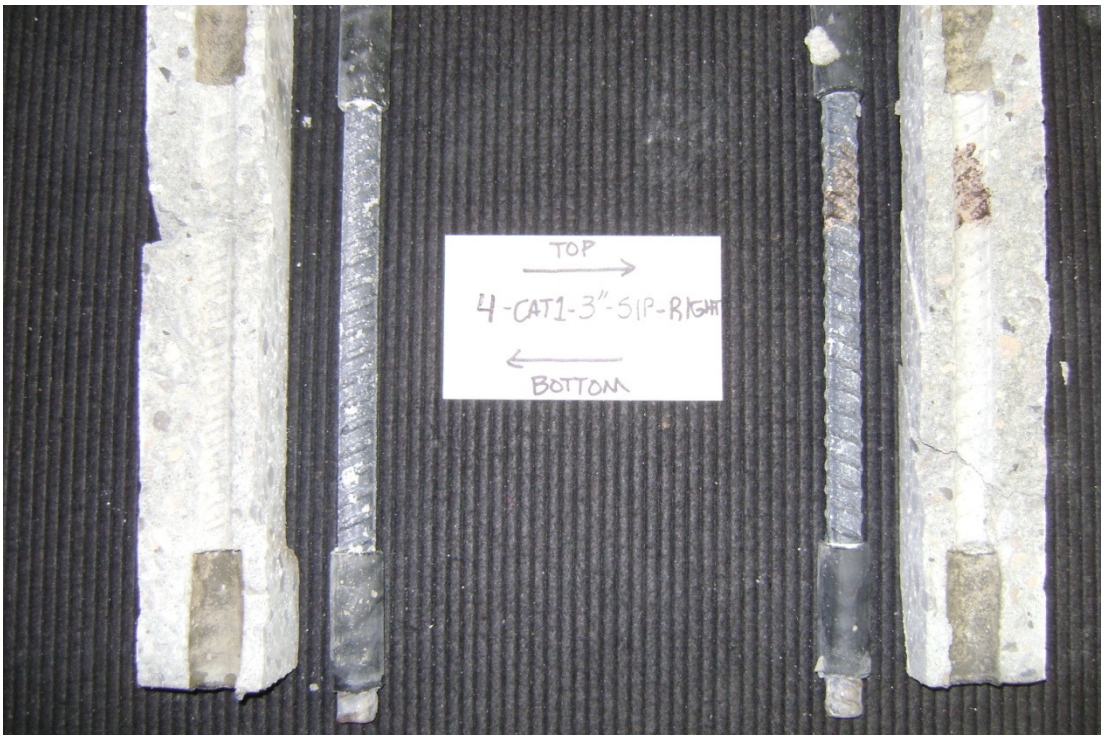

Figure E-18 – Specimen - 4 – C-1- 3” – SIP – Right – Bottom Side of both Bars

Figure E-19 – Specimen - 4 – C-1- 3” – SIP – Right – Top Side of Top Bar

Figure E-20 – Specimen - 4 – C-1- 3” – SIP – Right – Top Side of Bottom Bar

Figure E-21 – Specimen - 9 – C-2 – 4” – SIP – Right – Top Side of both Bars

Figure E-22 – Specimen - 9 – C-2 – 4” – SIP – Right – Bottom Side of both Bars

Figure E-23 – Specimen - 9 – C-2 – 4” – SIP – Right – Top Side of Top Bar

Figure E-24 – Specimen - 9 – C-2 – 4” – SIP – Right – Top Side of Bottom Bar